# UNIVERSITÉ DE STRASBOURG

*ÉCOLE DOCTORALE 414 – SCIENCES DE LA VIE ET DE LA TERRE*
**Institut de Génétique et de Biologie Moléculaire et Cellulaire**
*(CNRS UMR 7104 – INSERM U1258)*

# THÈSE présentée par :

**David PIETRI**

Soutenue le : **18 Décembre 2023**

Pour obtenir le grade de : **Docteur de l'université de Strasbourg**

Discipline/ Spécialité
**Sciences de la vie et de la Santé Aspects moléculaires et cellulaires de la biologie**

# Structure and function of the C9ORF72-SMCR8-WDR41 complex and its implication for Amyotrophic Lateral Sclerosis (ALS)

**THÈSE dirigée par :**
**M CHARLET-BERGUERAND Nicolas** Directeur de Recherche, Université de Strasbourg

**RAPPORTEURS :**
**Mme MARTINAT Cécile** Directrice de Recherche, Université Paris-Saclay
**M KABASHI Edor** Directeur de Recherche, Université Paris

---

**AUTRES MEMBRES DU JURY :**
**M SCHULTZ Patrick** Directeur de Recherche, Université de Strasbourg

# Remerciements

En premier lieu je tiens à remercier mon jury de thèse, Mme MARTINAT Cécile, M KABASHI Edor et M SCHULTZ Patrick, d'avoir accepté de lire et corriger mon travail. Merci notamment à mon comité de suivi de thèse composé de M DUPUIS Luc et M PAPAI Gabor. Merci pour votre temps et expertise sur mon travail durant ces réunions annuelles.

Un grand merci à l'Association pour la Recherche sur la Sclérose Latérale Amyotrophique et autres maladies du motoneurone (ARSLA) de m'avoir fait confiance pour financer cette 4 ème année de thèse.

Je tiens à dire un grand merci à mon directeur de thèse, le Dr. Nicolas Charlet de m'avoir accepté il y a de cela 4 ans pour me lancer dans cette grande aventure que représente la thèse. Merci de m'avoir accueilli et supervisé sur ces différents projets. Ta disponibilité et ton enthousiasme ont été des facteurs importants pour cette thèse.

Je tiens tout particulièrement à remercier Manon. Je suis arrivé quand tu étais encore en thèse et te voilà une post-doc déjà bien accomplie. Merci pour ton aide au laboratoire mais aussi sur mes différents projets ! Ce fut un plaisir d'avoir pu partager des moments avec toi pendant et en dehors du travail. Notre duo de chant restera surement dans les annales ! Je te souhaite pleins de réussite pour la suite même si je n'ai aucun doute sur une belle carrière déjà bien commencée.

Je remercie notamment Véronique, notre infatigable ingénieur, qui a toujours su se démener pour nous faciliter le travail au laboratoire. En espérant que ta retraite se passe bien ! Merci à Léa, notre stagiaire reconverti en ingénieur ! Merci pour ces fous rire en ta compagnie ! Ta bonne humeur constante était un gros plus pour le labo.

Je remercie évidemment mon « petit Nico » comme on l'appelle ! Merci pour ces 4 ans en ta compagnie que ce soit au travail pour ta bonne humeur et ces petites pauses café toujours aussi agréable mais aussi et surtout en dehors du travail. Merci pour tous ces moments à boire des bières, manger un bout mais aussi et surtout pour ces matchs de foot endiablés en ta compagnie. On n'est peut-être pas champion du monde (sacré effrontRerie) mais au moins on est devenu beau et musclé. A l'avenir évite de te prendre les haltères dans la tête ça ne va pas muscler ton cerveau !

Alexia, Alexia que dire, de Strasbourg à Boston pour finalement revenir à Strasbourg, il serait peut-être temps d'arrêter de me suivre partout où je vais. Plus sérieusement, merci pour toutes ces années à tes cotés. Ta présence n'est pas anodine au bonheur quotidien que j'éprouve au travail mais aussi en dehors. Je garde un excellent souvenir de Boston et de nos années de thèse. On se donne rendez-vous d'ici quelques mois dans le sud de la France pour de nouvelles aventures, comme planifié !

Je tiens aussi à remercier Bastien, « Baba » pour les intimes, pour ton expertise sur la protéomique mais aussi et surtout pour toutes ces discussion footballistique (enfin surtout pour toi parce que je suis un beau footix) et ces petites pauses à refaire le monde et savoir ce que l'on a fait de nos week-ends, même si pour toi ce n'était pas très compliqué à deviner ! Merci pour ces moments en dehors du travail que ce soit pour boire une petite bière, faire un five ou encore te chercher dans le festival parce que tes potes t'ont abandonnés !

Mes remerciements vont aussi à notre petit couple préféré, Quentin et Marianne. Même si vous avez des tendances un peu papi avec des dodo aux alentours de 20 h 30, j'ai passé de très bons moments en votre compagnie. Merci pour l'astuce de « WIKIHOW », ça m'a sauvé la vie plus d'une fois (PS : j'ai essayé de taper : comment écrire une thèse mais pas fou, je vous le déconseille). Par ailleurs chatGPT n'est pas fiable je vous le déconseille aussi.

Merci à Marie, Pierre, Camille, Tamara mais ainsi que toutes les personnes que j'ai pu côtoyer de près ou de loin durant ces 4 ans au sein de l'IGBMC. Merci notamment aux différentes plateformes de l'IGBMC, et tout le personnel qui font un travail important afin de nous faciliter la tâche au quotidien.

Merci à Eveline et Maïté pour votre bonne humeur et disponibilité pour nos petits problèmes du quotidien. Vos grands sourires et petites discussions quotidiennes me manqueront à coup sûr.

J’aimerais évidemment remercier Ana, tu m’as connu en début de thèse et nous voilà presque 3 ans plus tard. Merci pour ton soutient, amour et stabilité que tu m’as apportée au quotidien. Ce n’était pas facile tous les jours, mais nous voilà partis pour de nouvelles aventures, à l’autre bout du monde, mais toujours ensemble. *Eu te amo neném*

J’ai failli oublier, (même s’ils s’en fichent un peu), mais merci à nos deux petites terreurs Azul et Aïko. Même si vous passez votre temps à faire n’importe quoi vous avez su me soutenir durant ces longues heures d’écritures.

Merci aussi à ta famille, qui a su m’accueillir à bras ouverts et su me changer les idées quand j’en avais besoin. Vanessa, Charles, félicitations pour votre mariage et votre petite Marie-Louise, je vous souhaite une belle vie pleine de bonheurs.

Mes remerciements vont aussi à tous mes amis, Martin, Evan, Coco, Guillaume mes acolytes Thoréfolléens, mais aussi de l’ESBS : Nikita, Thomas, Capu, Bonnot, Pierre, Lelex, Oliv, Khalid, Claire, Romain, Nico, Francis, Christophe et tous ceux que je pourrais oublier. Vous me créez des souvenirs indélébiles et chaque moment à vos côtés me rappelle la chance que j’ai de vous avoir.

Pour finir je remercie ma famille, tout particulièrement, Papa, Maman, Jessica, merci pour toutes ces années à m’avoir toujours soutenu et encouragé dans mes choix. S’arrêter après un IUT est une solution, finir docteur en est une autre. Jessica, Markus: Herzlichen Glückwunsch zu Ihrem bevorstehenden Baby. Ich kann es kaum erwarten, meine Rolle als Onkel zu erfüllen. Ce fut long mais j’espère vous avoir rendu fière. Tout cela n’aurait jamais été possible sans vous, merci ! *Ma réussite vous appartient (un peu) ...*

*29/04/2020*

*« En souvenir de Pierre, un soldat mais surtout ami partis trop tôt »*

# Contents

# Figures

## Tables

# Abbreviations

**AD** Alzheimer Disease

**ADARB2** Double-Stranded RNA-Specific Editase B2

**ALR** Autophagic Lysosome Regeneration

**ALS** Amyotrophic Lateral Sclerosis

**ALS2** Alsin Rho Guanine Nucleotide Exchange Factor

**ALSFRS-R** ALS Functional Rating Scale Revised

**ALYREF** THO Complex Subunit 4

**AMBRA1** Activating Molecule In Beclin-1 Related Autophagy 1 Protein

**AMPAα** Amino-3-Hydroxy-5-Methyl-4- Isoxazole Propionic Acid

**AMPK** AMP Activated Protein Kinase

**ANG** Angiogenin

**AP** Adaptator Protein

**APP** Aβ and C-Terminal Fragments of the Amyloid Precursor Protein

**ARF** ADP Ribosylation Factors

**ARL** ARF-Like Proteins

**ARNO** ARF Nucleotide-Binding Site Opener

**ASOs** Antisense Oligonucleotides

**ATGS** Autophagy-Related Proteins

**ATXN2** Ataxin 2

**BECN1** Beclin-1

**C9ORF72** Chromosome 9 Open Reading Frame 72

**CAS9** CRISPR Associated Protein 9

**CCNF** Cyclin F

**CHCHD10** Coiled-Coil-Helix-Coiled-Coil-Helix Domain Containing 10

**CHMP2B** Charged Multivesicular Protein 2B

**CMA** Chaperone-Mediated Autophagy

**CNS** Central Nervous System

**CRISPR** Clustered Regularly Interspaced Short Palindromic Repeats

**Cryo**-EM Cryo-Microscopie Electronique

**CSF** Cerebrospinal Fluid

**CSW** C9ORF72-SMCR8-WDR41

**DCTN1** Dynactin Subunit 1

**DENN** Differentially Expressed Normal Versus Neoplastic

**DEPTOR** DEP Domain-Containing Mtor-Protein

**DFCP1** Double FYVE-Containing Protein 1

**DM1** Myotonic Dystrophy Type 1

**DM2** Myotonic Dystrophy Type 2

**DNA** Acide Désoxyribonucléique

**DNM2** Dynamin 2

**DPR** Dipeptide Repeat Proteins

**EAAT2** Excitatory Amino Acid Transporter 2

**ECRTII** Endosomal Sorting Complexes Required For Transport

**ELP3** Elongator Complex Protein 3

**EMA** European Medicines Agency

**ER** Endoplasmic Reticulum

**EURALS** European Als Epidemiology Consortium

**EVs** Extracellular Vesicles

**fALS** Familial Amyotrophic Lateral Sclerosis

**FDA** Food and Drug Administration

**FECD** Fuchs' Endothelial Corneal Dystrophy

**fFTD** Familial Fronto-Temporal Dementia

**FIP200** Focal Adhesion Kinase-Family-Interacting Protein Of 200 Kda

**FLCN** Folliculin

**FNIP** Folliculin Interacting Protein 2

**FTD** Fronto-Temporal Dementia

**FUS** Fused In Sarcoma

**FXTAS** Fragile-X Tremor Ataxia Syndrome

**GABARAP** Γ-Aminobutyric Acid Receptor-Associated Protein

**GABARAPL** Γ-Aminobutyric Acid Receptor-Associated Protein Like

**GDIs** Guanine Dissociation Inhibitors

**GDP** Guanosine Diphosphate

**GEFs** Guanine Nucleotide Exchange Factors

**GFP** Green Fluorescent Protein

**GOF** Gain Of Function

**GRN** Granulin Precursor

**GT1-7** Mouse Hypothalamic Gnrh Neuronal

**GTP** Guanosine Triphosphate

**HA** Human Influenza Hemagglutinin

**HD** Huntington Disease

**HEK-293** Human Embryonic Kidney-293

**hnRNP** Heterogeneous Nuclear Ribonucleoprotein

**HOPS** Homotypic Fusion And Protein Sorting

**Hsc70** Heat Shock Cognate 71 Kda Protein

**HSPs** Hereditary Spastic Paraplegias

**IF5B** Kinesin Family Member 5b

**IPSc** Induced Pluripotent Stem Cells

**IRES** Internal Ribosome Entry Site

**KO** Knock-Out

**LAMP-1** Lysosomal-Associated Membrane Protein 1

**LMN** Lower Motor Neuron

**LOF** Loss Of Function

**MAP1LC3** Microtubule Associated Protein 1 Light-Chain 3

**MAPT** Microtubule Associated Protein Tau

**MATR3** Matrin 3

**MEFs** Mouse embryonic fibroblasts

**mHtt** Pathogenic Mutant Huntingtin

**mLST8** Mammalian Lethal With SEC13 Protein

**MRI** Magnetic Resonance Imaging

**MRNA** Messenger Ribonucleic Acid

**mTOR** Mammalian Target Of Rapamycin

**MTORC1** Mammalian Target Of Rapamycin Complex 1

**MYO1E** Myosin Ie

**Nano LC-MS/MS** Nanoscale Liquid Chromatography Coupled To Tandem Mass Spectrometry

**NBR1** Neighbor Of BRCA1 Gene 1

**NDP52** Nuclear Dot Protein 52

**OPTN** Optineurin

**PD** Parkinson Disease

**PE** Phosphatidylethanolamine

**PET** Positron Emission Tomography

**PFN1** Profilin-1

**PI3KC3** Class III Phosphatidylinositol 3-Kinase Complex 3

**PI4K** Phosphatidylinositol 4-Kinases

**PIPK** Phosphatidylinositol Phosphates Kinases :

**PRAS40** 40 Kda Pro-Rich AKT Substrate

**PS** Phosphorothioate

**PtdIns3P** Phosphatidylinositol-3-Phosphate

**RAB** Ras-Related Proteins In Brain

**Rag** Ragulator-Rag Complex

**RAN** Repeat Associated Non-ATG Translation

**RAPTOR** Regulatory-Associated Protein Of Mtor

**RB1CC1** RB1-Inducible Coiled-Coil Protein 1

**RNA** Ribonucleic Acid

**RNAi** RNA Interference

**ROS** Oxygen Reactive Species

**sALS**, Sporadic Amyotrophic Lateral Sclerosis

**SCA** Spinocerebellar Ataxia

**SCA31** Spinocerebellar Ataxia Type 31

**SCA8** Spinocerebellar Ataxia 8

**SETX** Syntaxin

**sFTD** Sporadic Fronto-Temporal Dementia

**SiRNA** Small Interfering RNA

**SMCR8** Smith Magenis Syndrome Candidate Chromosome Region 8

**SNARE** Soluble N-Éthylmaleimide-Sensitive-Factor Attachment Protein Receptor

**SOD1** Superoxide Dismutase Type 1

**SPG11** Spatacsin

**SPG15** Spastizin

**SQSTM1** Sequestosome 1

**SRSF1** Serine/Arginine-Rich Splicing Factor 1

**SRSF2** Serine/Arginine-Rich Splicing Factor 2

**TAF15** TATA-binding protein-associated factor 2N

**TARDBP** Tar Dna Binding Protein

**TAX1BP1** Tax1 Binding Protein 1

**TBK1** TANK-Binding Kinase 1

**TDP**-43 TAR DNA-Binding Protein 43

**UBQLN2** Ubiquilin 2

**ULK1** Unc-51-Like Kinase 1

**UMN** Upper Motor Neuron

**UPS** Ubiquitin–Proteasome System

**UVRAG** Uv Radiation Resistance Associated

**VAMP** Vesicle-Associated Membrane Protein

**VAPBP** Vesicle-Associated Membrane Protein-Associated Protein B/C

**VCP** Valosin-Containing Protein

**VPS15**, VPS34 Vacuolar Proteins Sorting 15 And 34

**WDR41** WD Repeat Containing Protein 41

**WIPI** WD-Repeat Protein Interacting With Phosphoinositides

**WT** Wild Type

**ZFYVE26** Zinc Finger FYVE-Type Containing 26

# INTRODUCTION

# 1. Amyotrophic Lateral Sclerosis (ALS)

## 1.1 Clinical features

Amyotrophic Lateral Sclerosis (ALS), also called Charcot or Lou Gehrig disease, is the 3rd most common neurodegenerative illness after Alzheimer's and Parkinson's. French physician, Dr. Jean-Martin Charcot (Figure 1), is credited with finding ALS by linking a series of case studies from 1865 to 1869 (Kumar et al., 2011). Charcot coined the term "amyotrophic lateral sclerosis" in 1874. At this time, he stated, "The diagnosis, as well as the anatomy and physiology of the condition amyotrophic lateral sclerosis, is one of the most completely understood conditions in the realm of clinical neurology". Unfortunately, he appears to have misjudged the complexity of this neurodegenerative disease (Turner and Swash, 2015).

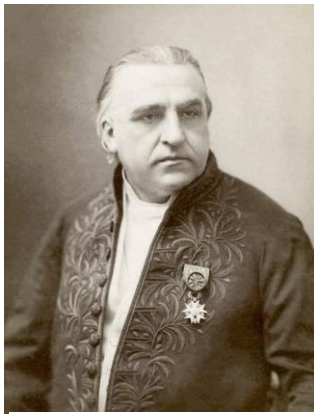

Figure 1 Jean-Martin Charcot (1825-1893)

(National Library of Medicine).

ALS is characterized by the progressive degeneration of both upper motor neurons (projecting from the cortex to the brainstem and the spinal cord) as well as lower motor neurons (projecting from the brainstem or the spinal cord to muscles). This degeneration engenders atrophy and muscle weakness leading to paralysis and death due to a respiratory deficiency in 3 to 5 years after diagnosis. This overall description shows that ALS is highly homogeneous, although clinical genetic postmortem observation studies show significant diversity in the phenotypic expression of ALS. Clinically, there are two principal forms of ALS: the spinal form and the bulbar form (Swinnen and Robberecht, 2014; van Es et al., 2017). More than 70% of patients with classical ALS have one of these two ALS presentations.

- The spinal form accounts for 2/3 of the cases and begins with asymmetric and painless weakness in an upper or lower limb. The spinal form is characterized by a degeneration of lower motor neurons, which results in a clinical examination that reveals muscular atrophy and weakness, fasciculations, and hyperreflexia.

- The bulbar form affects 1/3 of patients and begins in the bulbar muscle due to degeneration of upper motor neurons resulting in dysarthria, dysphagia, and tongue fasciculations.

Currently, Riluzole is the only widely prescribed medication for ALS patients that can extend life expectancy by roughly three months (Bensimon et al., 1994). Another medication, Edaravone, just entered the market and demonstrated a 33% reduction in the rate of illness development (Abe et al., 2017; Ito et al., 2008). Unfortunately, none of these two medications are curative treatments. Further information on treatment and current therapies will be develop in part 3. Besides having no cures, ALS requires a lengthy and challenging diagnosing process.

## 1.2 Diagnosis

As it might be challenging to distinguish ALS from other motor neuron illnesses like Kennedy's disease, or X-linked spinobulbar muscular atrophy, cervical spondylotic myelopathy, or myasthenia gravis, there is currently no precise diagnostic test for ALS. The original El Escorial and later the amended El Escorial (Airlie House) and Awaji criteria are the foundations for the diagnosis of ALS (Brooks, 1994; Brooks et al., 2000; Costa et al., 2012). Based on electrophysiological and neuropathologic evaluation, as well as the progressive spread of symptoms within an area (or to adjacent regions), these criteria are based on definite, probable, plausible, or suspected ALS. The El Escorial criteria and their updates were largely created for research, not for therapeutic use. Current diagnostic criteria, according to ALS experts, are not helpful for patient conversation or the diagnostic procedure (Rutter-Locher et al., 2016). "The Gold Coast criteria" is a simplified version based on earlier criteria, although it has always been formal criteria-focused and may always be excessively restricted (Shefner et al., 2020). Furthermore, the patient had to be there to observe the progression of the illness when these criteria are used, as well as during the neuropathological testing. Unfortunately, the illness can advance quickly, and the majority of patients experience a late diagnosis that prevents them from being eligible for a therapy study.

The majority of the time, the diagnosis is made using an integrative approach that draws on the clinical history (such as the nature of the illness and how its symptoms have changed), the physical examination (such as evaluating reflexes and strength), and confirmation tests (such as electromyography). For an accurate diagnosis of ALS, which is a clinical disease with a diverse phenotypic expression and clinical history, diagnostic and prognostic biomarkers are urgently needed. Though, they have not yet been used on patients, novel diagnostic techniques are actively being researched.

For instance, next-generation sequencing panels and whole-exome sequencing have replaced genetic testing alternatives that previously only tested a single gene. However, the correct use of genetic testing still depends on fundamental clinical abilities such as family history, pedigree analysis, and risk assessment. Indeed, over 40 genes are linked to ALS, but they also have characteristics with other illnesses, which could cause a misunderstanding (Roggenbuck et al., 2017). Modern imaging techniques for the brain and spinal cord include MRI (magnetic resonance imaging) and PET (positron emission tomography). PET is frequently used to rule out structural lesions that influence the motor system since it can provide some diagnostic insight (Kassubek and Pagani, 2019). The ability of biomarkers to be used in therapeutic settings is now very promising, especially for determining the concentrations of neurofilament light polypeptide and phosphorylated neurofilament heavy polypeptide in the cerebrospinal fluid (CSF). In fact, it can tell ALS patients from those with mimics. However, more investigation will be needed to assess their sensitivity and specificity for their integration into clinical practice (Verde et al., 2019).

## 1.3 Front- temporal dementia (FTD)

Fronto-temporal dementia (FTD) disorder is the third most common form of dementia across all age groups, after Alzheimer's disease and dementia with Lewy bodies (Vieira et al., 2013). FTD is caused by progressive atrophy of the frontal and temporal lobes of the brain, causing clinically varied disorders. Frontotemporal dementia is classified into three clinical variants based either on an alteration in behavior or on an alteration in speech (Figure 2) (Bang et al., 2015)

- Behavioral-variant frontotemporal dementia, which is associated with early behavioral and executive deficits. It is also the most common variant with 60-80 % of all FDT.

- Non-fluent variant primary progressive aphasia, with progressive deficits in speech, grammar, and word output.
- Semantic-variant primary progressive aphasia, which is a progressive disorder of semantic knowledge and naming.

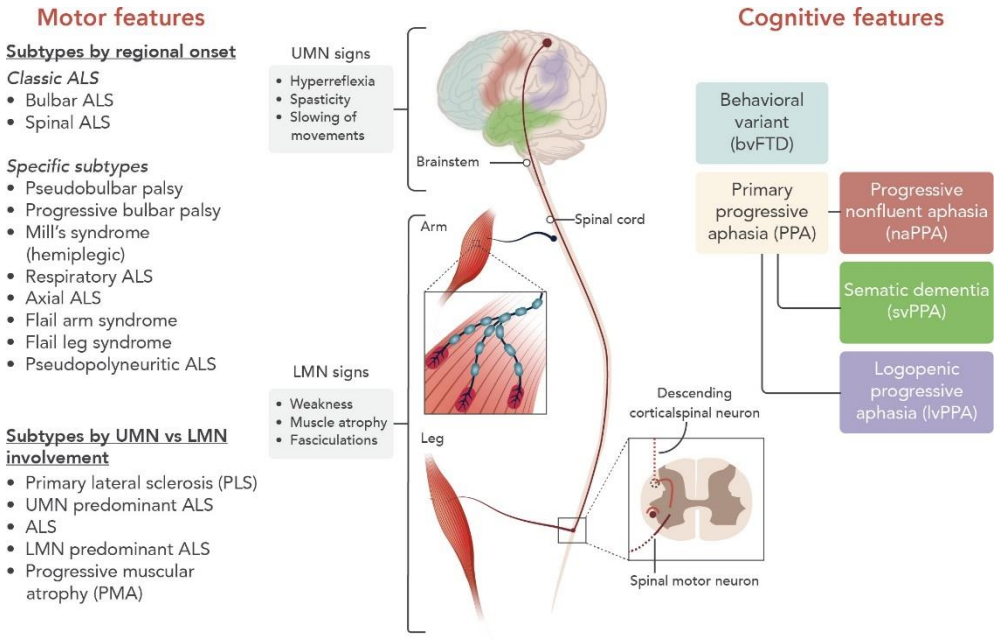


Figure 2 Phenotypic presentations of ALS and different variant in FTD.

Motor features of ALS vary in regional distribution and relative Upper Motor Neuron (UMN) versus Lower Motor Neuron (LMN) involvement. Frontotemporal dementia is classified into three clinical variants based either on an alteration in behavior or on an alteration in speech (Masrori and Van Damme, 2020).

## 1.4 ALS and FTD, a same continuum

Frontotemporal dementia (FTD) and Amyotrophic lateral sclerosis (ALS) are two fatal neurodegenerative disorders that exist within a same clinical and pathological spectrum. One of the earliest hints of this overlap came from clinical observation that both disorders can be present within the same family or even within the same individual. According to estimates, up to 48% of ALS patients exhibit cognitive impairment consistent with FTD, and 15–30% of FTD patients will acquire ALS symptoms (Ringholz et al., 2005).

Recent considerable progress in understanding the genetics of ALS and FTD highlight genetical overlaps: *Tar DNA Binding Protein* (*TARDBP*) which aggregation is a recurrent pathological hallmark in almost all ALS patients and will be discussed more deeply in part 1.7 and 1.8, *Sequestosome 1* (*SQSTM1,* coding for the p62), *Valosin-Containing Protein* (*VCP*), *TANK-binding kinase 1* (*TBK1*), *Coiled-Coil-Helix-Coiled-Coil-Helix Domain Containing 10* (*CHCHD10*) and most importantly *Chromosome 9 Open Reading Frame 72* (*C9ORF72*) are the critical genetic players. Their discoveries have implicated autophagy, RNA processing, vesicle and inclusion formation as the central pathways involved in these forms of neurodegeneration (Figure 3) (Abramzon et al., 2020).

As a result, in chapter 1.8, I will list a few of them and explain how they contribute to ALS and FTD. However, let's first examine the incidence and sex-based distribution of these disorders.

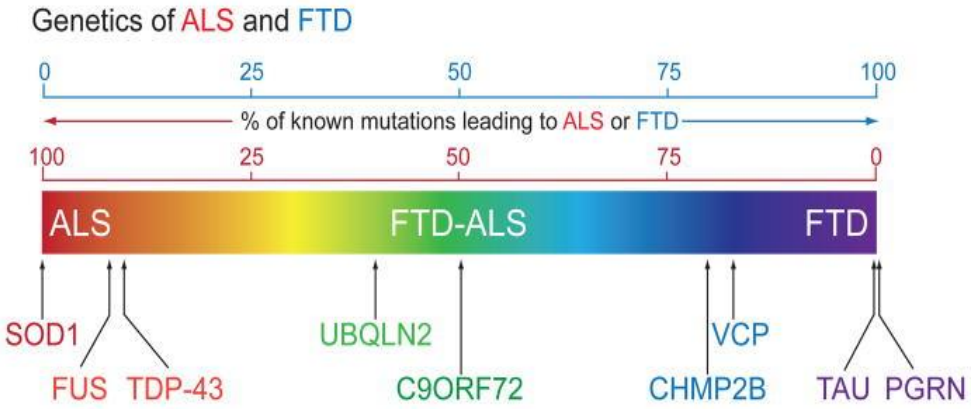


Figure 3 Graphical representation of genetic overlap of ALS and FTD

Some gene are involved in “pure ALS” like *SOD1* or “pure FTD” like PGRN mutation were other gene like *C9ORF72* will most likely lead to ALS and/or FDT (adaptation from (Ling et al., 2013)).

## 1.5 Epidemiology

Epidemiological studies are complex in ALS/FTD due to several factors, including determination of the precise onset, low incidence, high variability in causative mechanisms and hence in symptoms of the disease. These factors make it essential to design rigorous inclusion criteria to get unbiased patient cohorts.

Most population-based epidemiological studies of ALS have come from high-quality European patient registers that have been combined to form the European ALS Epidemiology Consortium (EURALS), which has provided data comparing the incidence of ALS between European countries (Logroscino et al., 2010). According to these data, there are 6.22 prevalence rates and 2.31 incidence rates per 100,000 person-years in Europe (Brown et al., 2021; Logroscino et al., 2010). Male sex has long been recognized as a risk factor for ALS, with the male-to-female ratio in recent studies being between 1 and 2 (Ingre et al., 2015).

Additionally, research has indicated that ALS diagnoses are made between the ages of 54 and 69, with the mean or median age of onset falling between 51 and 66 (Longinetti and Fang, 2019). Although, the majority of ALS cases are sporadic (sALS), approximately 10% of patients present a familial form (fALS), usually with autosomal dominant transmission. Interestingly, as patients with family outputs are simpler to diagnose, the peak age at onset for sporadic cases is 58–63 years, whereas it is 47–52 years for familial cases (Byrne et al., 2011).

For FTD, prevalence and incidence studies are currently limited, but studies reported a pooled prevalence rates of 15-22 (per 100,000 persons) and incidence rates of 1.6 (per 100,000 person-years) (Coyle-Gilchrist et al., 2016). Studies showed an equal male-to-female ratio with an age onset between 55 to 70 years. About 13% of patient will develop the disease before the age of 50. Finally, between 30 to 50 % of the cases appears to have a genetic cause (familial FDT) (Mercy et al., 2008).

As previously mentioned, important genetic factors play a role in ALS and FTD. As a result, it will be discussed in the following chapter.

## 1.6 Genetic mutations

Today, up to 10% of ALS patients are considered to have familial ALS, which is typically inherited in an autosomal dominant way and affects at least one additional family member (Alsultan et al., 2016). Since they develop the diseases without a family history, the last 90–95 percent are displayed as sporadic cases. According to Rohrer et al. (2009), 50 to 70% of FTD cases are categorized as sporadic, while 30 to 50% of patients indicate a positive family history. (Rohrer et al., 2009). However, the division of ALS patients into "familial" and "sporadic" categories, meanwhile, is oversimplified. In fact, thorough commitment to familial genetic history and accurate disease diagnosis are required in order to designate individuals as familial, which is not the case. In fact, there are gaps in the data on familial history, which causes individuals to be labeled as sporadic when they truly were familial cases. The family ties are further complicated by the fact that numerous novel mutations have been discovered in the last few decades that were undoubtedly not present in earlier patients.

The first gene to disclose a thigh association with familial ALS was identified in 1993, a missense mutation in *Superoxide Dismutase 1* (*SOD1*) (Rosen et al., 1993). Modern tools include genome-wide association studies and "next-generation" sequencing enable large-scale searches for genes related to ALS. Currently, more than 40 putative ALS and/or FDT-related genes have been discovered (Table 1). Only four of them accounted for more than 60 % of familial ALS, namely *SOD1, TARDBP, Fused in Sarcoma (FUS)*, and *C9ORF72* while 50-70% of familial FTD cases are caused by mutation in *C9ORF72*, *Microtubule Associated Protein TAU* (*MAPT*) or *Granulin Precursor* (*GRN*) (Figure 4) (DeJesus-Hernandez et al., 2011; Kwiatkowski et al., 2009; Renton et al., 2011; Rosen et al., 1993; Sreedharan et al., 2008; Vance et al., 2009). However, there are great variabilities as genes identified within patients are dependent on geographical regions and ancestors.

In contrast to other disorders, like schizophrenia that are linked to a high number of common variants, there are an increasing number of genes that have been found and implicated in ALS, showing that the genetic architecture is built predominantly on rare variants (van Rheenen et al., 2016). Moreover, different identified genes variants are specific to individuals and families. Numerous initiatives were launched to address these extreme variations, including Project Mine (https://www.projectmine.com) who "plan to map the full DNA profiles of at least 15,000 people with ALS and 7,500 control subjects, and to perform comparative analyses on the resulting data" to provide better clarity of the genetic architecture of ALS.

Additionally, there is mounting evidence that ALS exhibits oligogenic inheritance, in which a phenotypic trait is influenced by more than one gene, due to the more than 40 genes involved in the disease. When some familial ALS (fALS) patients, with a known causative mutation, were discovered to also have an extra mutation in another ALS risk gene, the idea of oligogenic inheritance in ALS was first put out. For example, fALS patients with *SOD1* mutation and additional rare variants in ALS genes have reduced survival (Pang et al., 2017). Additionally, in 5 cases of fALS, *C9ORF72* repeat expansions were discovered alongside *TARDBP*, *SOD1* and FUS/TLS mutations (van Blitterswijk et al., 2012). Also, many genes involved in ALS are defined has pleiotropic (in which a single gene has multiple phenotypic manifestations).

For instance, some Huntington disorders also have *C9ORF72* expansions, the most common genetic cause of ALS/FTD (Moss et al., 2014). Meta-analysis show the potential link between *C9ORF72* repeats and the risk to develop Alzheimer's Disease (Shu et al., 2016). Another example is *VCP* that is involved in ALS, FTD but also in Body Myopathy with Paget's Disease of Bone (Nalbandian et al., 2011). Finally, heritability can also be difficult to determine in some cases, due to the incomplete penetrance of variants in many ALS-associated genes. For example, *C9ORF72* and *Ataxin 2* (*ATXN2)* variants show incomplete penetrance, with symptoms not always manifesting or appearing at a later stage (Elden et al., 2010; Murphy et al., 2017).

Despite the success in uncovering novel genes in familial ALS forms, the majority of patients are sporadic with unknown etiology, probably involving a combination of genetic and biological pathway that will be discuss in the next chapters.

Table 1 Mutated genes responsible for most cases in ALS, FTD and ALS/FTD

Mutated gene classified by the potential pathway their involved to and their involvement in FDT and/or ALS.

| Involved in | Gene | Protein | Functions include | References | FTD and/or ALS related |
|---|---|---|---|---|---|
| RNA processing | TARDBP | TAR DNA-Binding Protein, 43-Kd | Splicing regulation, RNA transport, miRNA biogenesis | Rutherford et al., 2008; Sreedharan et al., 2008; Neumann, 2009 | FTD/ALS |
| | FUS | Fused in sarcoma | Splicing regulation, RNA transport, maintenance of genomic integrity, miRNA processing | Kwiatkowski et al., 2009; Vance et al., 2009 | FTD/ALS |
| | ANG | Angiogenin | RNA processing, neurite outgrowth, vascularisation, stress granule formation | Greenway et al., 2006; Wu et al., 2007 | FTD/ALS |
| | SETX | Senataxin | DNA/RNA metabolism and helicase activity | Chen et al., 2004; Hirano et al., 2011 | ALS |
| | MATR3 | Matrin 3 | RNA processing, chromatin organization | Johnson et al., 2014b | FTD/ALS |
| | ATXN2 | Ataxin 2 | RNA processing (interacts with TDP-43), endocytosis, modulates mTOR signaling | Elden et al., 2010; Sproviero et al., 2016 | FTD/ALS |
| | TAF15 | TATA-binding protein-associated factor 2N | transcription initiation; RNA polymerase II | Couthouis et al., 2011; Ticozzi et al., 2011 | ALS |
| | EWSR1 | EWS RNA Binding Protein 1 | RNA splicing, transcriptional repressor, | Couthouis et al., 2012 | ALS |
| | hnRNPa1 | Heterogeneous nuclear ribonucleoprotein A1 | mRNA processing, splicing, and transport | Kim et al., 2013; Naruse et al., 2018 | ALS |
| | hnRNPA2B1 | Heterogeneous nuclear ribonucleoproteins A2/B1 | mRNA processing, splicing, and transport | Kim et al., 2013; Fifita et al., 2017 | ALS |
| | ELP3 | Elongator complex protein 3 | Protein synthesis, maturation of projection neurons | Simpson et al., 2009 | ALS |

| | | | | | |
|---|---|---|---|---|---|
| Protein Trafficking and degradation | C9ORF72 | Guanine nucleotide exchange C9orf72 | Transcription, splicing regulation, endosomal trafficking, autophagy | DeJesus-Hernandez et al., 2011; Renton et al., 2011 | FTD/ALS |
| | ALS2 | Alsin | Endosomal dynamics and trafficking, neurite outgrowth | Hadano et al., 2001; Yang et al., 2001 | ALS |
| | VAPB | Vesicle-associated membrane protein-associated protein B/C | Vesicle trafficking | Nishimura et al., 2004; Sanhueza et al., 2013 | ALS |
| | CHMP2B | Charged multivesicular body protein 2b | Multivesicular body formation, protein trafficking to lysosomes | Parkinson et al., 2006; Cox et al., 2010 | FTD/ALS |
| | FIG4 | Polyphosphoinositide phosphatase | Endosomal trafficking to Golgi network, autophagy regulation | Chow et al., 2009; Osmanovic et al., 2017; Bertolin et al., 2018 | ALS |
| | UBQLN2 | Ubiquilin-2 | Protein degradation via UPS | Deng et al., 2011; Gellera et al., 2013 | FTD/ALS |
| | SQSTM1 | Sequestosome-1 (p62) | Protein degradation via UPS and autophagy | Fecto et al., 2011; Rubino et al., 2012; Hirano et al., 2013 | FTD/ALS |
| | SIGMAR1 | Sigma non-opioid intracellular receptor 1 | Lipid transport from ER, mitochondrial axonal transport, BDNF and EGF signaling | Luty et al., 2010; Al-Saif et al., 2011; Ullah et al., 2015 | FTD/ALS |
| | OPTN | Optineurin | Golgi maintenance, membrane trafficking, exocytosis, autophagy | Maruyama et al., 2010; Tümer et al., 2012; Pottier et al., 2018 | FTD/ALS |
| | VCP | Valosin Containing Protein | Protein degradation via UPS, autophagy, membrane fusion | Forman et al., 2006; Johnson et al., 2010 | FTD/ALS |
| | TBK1 | Tank Binding Kinase 1 | Autophagy, innate immunity signaling | Borghero et al., 2015; Cirulli et al., 2015; Oakes et al., 2017 | FTD/ALS |
| | MAPT | Microtubule-associated protein tau | Trafficking of autophagic vesicles and autolysosome fusion | Hutton et al,.1998 | FTD |
| | GRN | Progranulin | Lysosome homeostasis; Hydrolase trafficking and function | Baker et al,. 2006 | FTD |
| Cytoskeletal and axonal dynamics | DCTN1 | Dynactin subunit 1 | Axonogenesis, microtubule anchoring, ER to Golgi transport, spindle formation, vesicle transport, cilia formation | Münch et al., 2004, 2005; Takahashi et al., 2008; Liu et al., 2014 | FTD/ALS |
| | PFN1 | Profilin 1 | Cytoskeletal signaling, regulates actin polymerization | Wu et al., 2012; Smith et al., 2015 | ALS |
| | SPG11 | Spatacsin | Cytoskeletal stability, regulating synaptic vesicle transport | Orlacchio et al., 2010; Daoud et al., 2012 | ALS |
| | TUBA4A | Tubulin α-4A chain | Component of microtubules | Smith et al., 2014; Pensato et al., 2015 | FTD/ALS |
| | NEFH | Neurofilament heavy polypeptide | Maintenance of neuronal caliber, intracellular transport | Figlewicz et al., 1994; Al-Chalabi et al., 1999 | ALS |
| | PRPH | Peripherin | Cytoskeletal protein, neurite elongation, axonal regeneration | Gros-Louis et al., 2004; Leung et al., 2004; Corrado et al., 2011 | ALS |
| | NEK1 | NIMA (Never In Mitosis Gene A)-Related Kinase 1 | Cilia formation, DNA-damage response, microtubule stability, neuronal morphology, axonal polarity | Brenner et al., 2016; Kenna et al., 2016; Nguyen et al., 2018; Shu et al., 2018 | ALS |
| Mitochondria | CHCHD10 | Coiled-Coil-Helix-Coiled-Coil-Helix Domain Containing 10 | Mitochondrial protein, cristae morphology, oxidative phosphorylation | Bannwarth et al., 2014; Chaussenot et al., 2014; Johnson et al., 2014a | FTD/ALS |
| | C19ORF12 | Protein C19orf12 | Mitochondrial protein | Deschauer et al., 2012 | ALS |
| Other | SOD1 | Superoxide dismutase [Cu-Zn] | Cytosolic Antioxidant | Rosen et al., 1993 | ALS |
| | ERBB4 | Receptor tyrosine-protein kinase erbB-4 | Neuronal cell mitogenesis and differentiation | Takahashi et al., 2013 | ALS |
| | SS18L1 | Calcium-responsive transactivator | Neuron specific chromatin remodeling | Teyssou et al., 2014 | ALS |
| | PNPLA6 | Neuropathy target esterase | Regulation of neuronal membrane composition | Rainier et al., 2008 | ALS |
| | PON1-3 | Paraoxonase 1-3 | Enzymatic breakdown of nerve toxins | Saeed et al., 2006; Wills et al., 2009; Ticozzi et al., 2010 | ALS |
| | DAO | D-amino-acid oxidase | Regulates D-serine levels, N-methyl-D-aspartate receptor regulation | Mitchell et al., 2010; Morgan et al., 2017 | ALS |
| | CHRNA3,4,B4 | Neuronal acetylcholine receptor subunit α-3, α-4, β-4 | Cholinergic Neurotransmission | Sabatelli et al., 2009, 2012 | ALS |
| | ALS3 | ALS3 | Disulfide redox protein | Hand et al., 2002 | ALS |
| Unknown | ALS7 | Unknown | Unknown | Sapp et al., 2003 | ALS |
| | ALS6-21 | Unknown | Unknown | Butterfield et al., 2009 | ALS |
| | ALS-FTD | Unknown | Unknown | Dobson-Stone et al., 2013 | ALS |

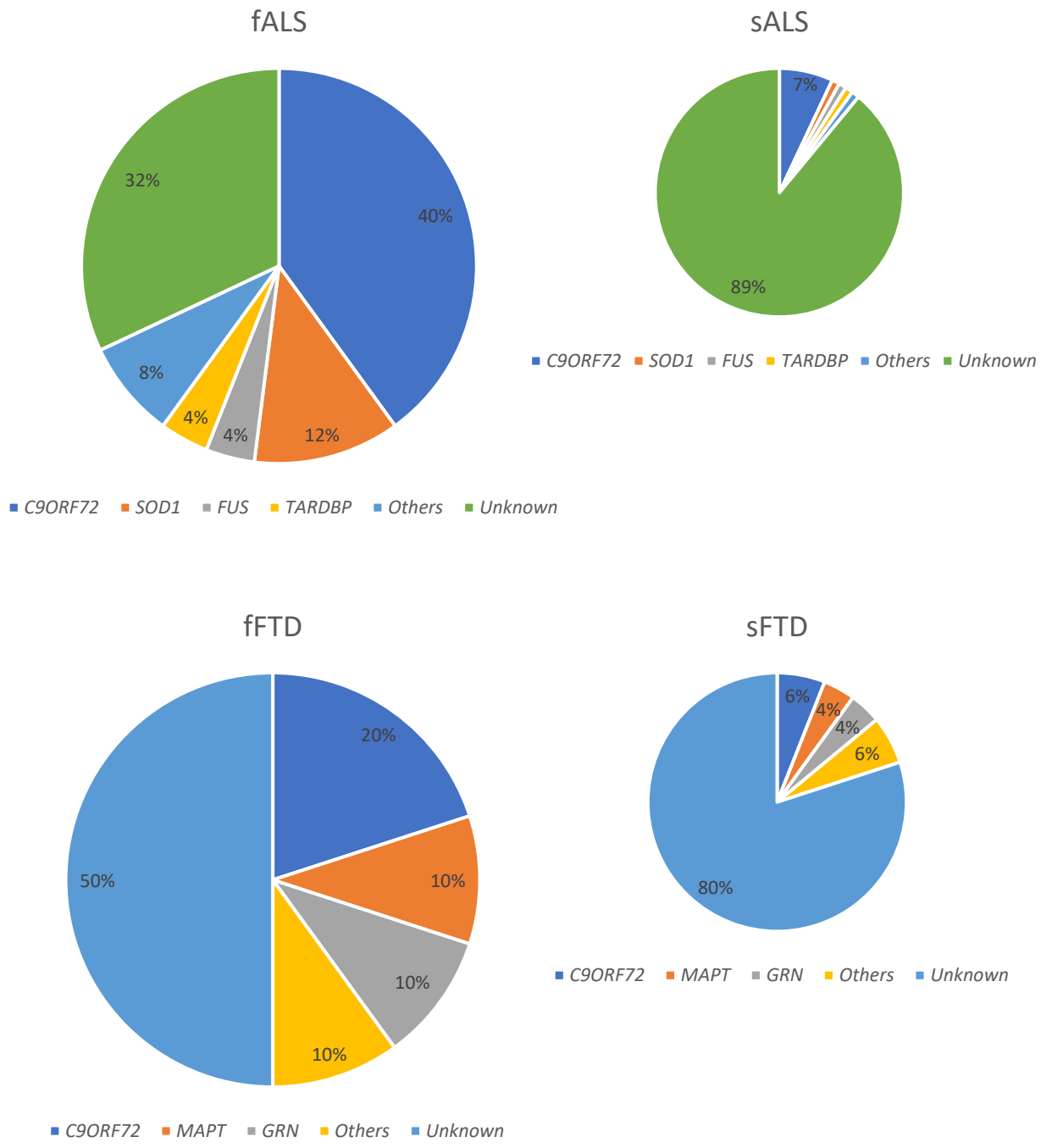


Figure 4 Representation of genes involved in ALS and FDT

*SOD1*, *TARDBP*, *FUS*, and *C9ORF72* count for more than 60 % of fALS were *C9ORF72*, *MAPT* and *GRN* count for more than 50 % of FTD patient. Familial ALS (fALS), Sporadic ALS (sALS), Familial FTD (fFTD), Sporadic FDT (SFTD) (Rohrer et al., 2009; Turner et al., 2017; Zou et al., 2017).

## 1.7 Histopathology

Post-mortem examinations revealed that ALS patients exhibit a loss of motor neurons in the motor cortex and in the ventral horn of the spinal cord, as well as a neuroinflammatory reaction consisting of diffuse astrocytic activation, microglial proliferation and infiltration and muscle denervation visible by histological labelling (Figure 5) (Haidet-Phillips et al., 2011). For FTD patient (Magnetic Resonance Imaging) MRI reveal an atrophy of the frontal lobe and/or temporal.

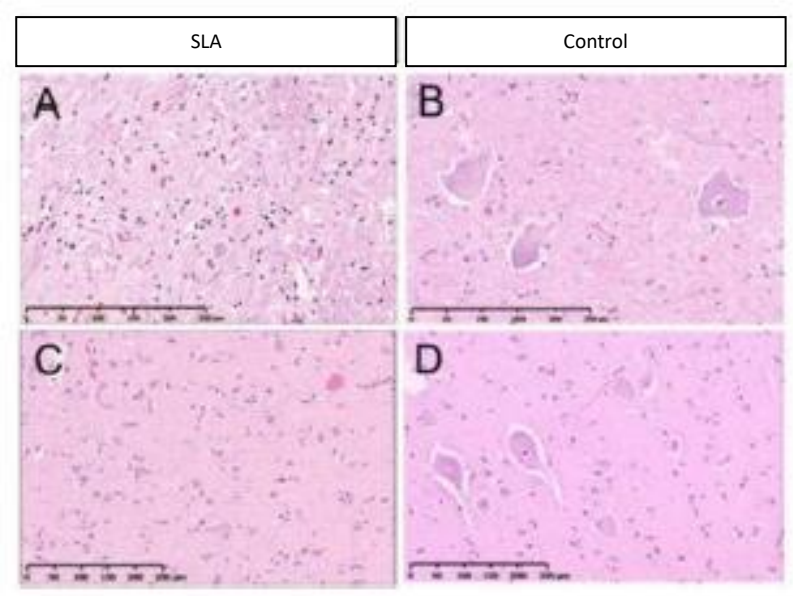


Figure 5 Loss of motor neurons in ALS patient

Loss of motor neurons is shown in an anterior horn of the spinal cord (**A**) and motor cortex (**C**) of ALS and compared to control (**B**, D) [Hematoxylin and eosin (**A-D**)] (Adaptation from Saberi et al., 2015).

In addition, aberrant TAR DNA-binding protein 43 (TDP-43) aggregation is a recurrent pathological hallmark in almost all ALS patients, suggesting that altered TDP-43 function is a significant disease-causing component among the various pathways that appear to contribute to ALS. Indeed, 97% of patients with ALS and 50 % of FTD patients have features of a TDP43 proteinopathy (Figure 6) with depletion of TDP43 in the nucleus and the formation of cytoplasmic aggregates with skein-like or compact morphology in residual motor neurons. (Arai et al., 2006; Neumann et al., 2006). Interestingly, the gene encoding for *TDP-43* (*TARDBP*) is mutated in only 4% of ALS patient (Kabashi et al., 2008; Sreedharan et al., 2008).

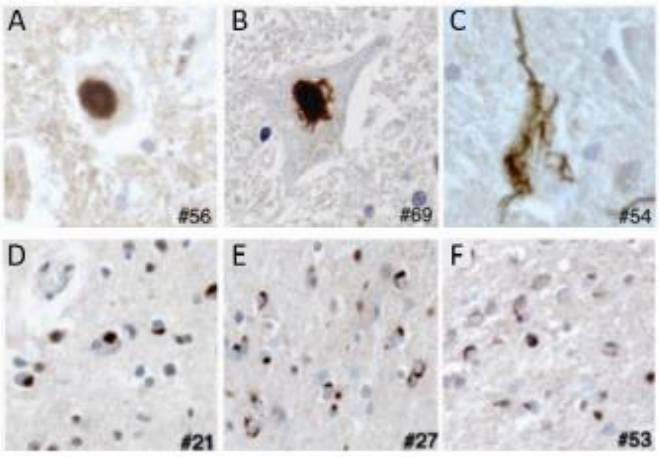


Figure 6 Immunostaining of positive TDP-43 aggregates in ALS and FTD patients

Immunostaining with anti–TDP-43 labeled Lewy body–like (**A**), round (**B**), and skein like inclusions (**C**) in motor neurons of the spinal cord. Same TDP-43 aggregates were observed in affected cortical regions of FTD patients (**D**,**E**,**F**) (Adaptation from Neumann et al., 2006).

Moreover, TDP-43 is also found to accumulate in Alzheimer's disease, Lewy body disease and Spinocerebellar Ataxia Type 2 (SCA2), secondary to other molecules and show their broad implication in neurodegenerative diseases (Amador-Ortiz et al., 2007; Arai et al., 2009). In specific subtypes of ALS, other types of protein aggregates might be observed, such as misfolded superoxide dismutase 1 (SOD1) and hyaline proteins in patients carrying a mutation in *SOD1* gene (Deng et al., 2010; Kato et al., 1999). It is also possible to find fused in sarcoma (FUS) aggregates in cytoplasm, spreads in a prion-like manner through neuronal tissues (Armstrong, 2017). However these inclusions represents respectively less than 2% (SOD1) and 1% (FUS) of patients cases (Ling et al., 2013). Moreover, for patient with mutation in the *C9ORF72* gene, sequestosome 1 (SQSTM1/p62) positive, ubiquitin-positive and TDP43-negative inclusions are caused by dipeptide repeat proteins (DPR) which are translated from the GGGGCC repeats in the *C9ORF72* gene (Al-Sarraj et al., 2011; Mackenzie et al., 2015). Interestingly, protein aggregates combine with dysfunctional proteins disrupt many pathways potentially involved in ALS/FTD and will be discuss in the next chapter 1.8.

## 1.8 Pathophysiology

Despite enormous advancement in recent years, our understanding of the molecular mechanisms underlying ALS remains limited. In fact, a number of genes are connected to the diseases, and in certain cases, a patient will have many altered genes, which will disrupt numerous cellular functions. However, increased knowledge of the genetics architecture allows the discovery of multiple molecular pathways, in different mutations, that seems to converge on recurrent dysregulated nervous system pathways like impaired protein homeostasis, aberrant RNA metabolism, perturbated endosomal and vesicle transport or also disrupted axon structure and function (Figure 7).

***Impaired protein homeostasis***

Maintaining intracellular protein homeostasis ("proteostasis") by balancing protein biogenesis is crucial. Indeed, since the integrity of the proteome is critical for cellular functionality and viability, numerous quality control pathways act together to maintain proteostasis (Balchin et al., 2016). Interestingly, numerous genes mutated in ALS encoded for protein directly involved in protein degradation like the Ubiquitin–Proteasome System (UPS), autophagy and Endoplasmic Reticulum (ER) stress.

*Ubiquitin–Proteasome System (UPS)*

According to Hershko and Ciechanover (1998), the UPS is the primary pathway for the removal of short-lived, damaged, and misfolded proteins from the nucleus and cytoplasm. This pathway is controlled by two independent, subsequent steps: ubiquitylation (covalent attachment of multiple ubiquitin molecules) and proteasomal degradation (Hershko and Ciechanover, 1998). Since 1975, patients have been reported to have protein inclusions; further research revealed that these inclusions were ubiquitin positive (LEIGH et al., 1991; Sun et al., 1975). As developed in part 1.7, abnormal aggregation of TAR DNA-binding protein 43 (TDP-43) (or other protein like SOD1 and FUS) is a pathological hallmark of ALS (Arai et al., 2006; Neumann et al., 2006). Misfolded protein, with an abnormal cellular localization or aberrantly formed, correlates directly or indirectly with an impairment of the proteasomal or autophagic machinery of the cell.

A disruption of the UPS in ALS patients was strongly hypothesized following the discovery of mutations in the genes encoding for the proteins ubiquilin-2 (encoded by *UBQLN2*) and VCP, both implicated in protein clearance via the ubiquitin-proteasome pathway (Johnson et al., 2010; Teyssou et al., 2017). Furthermore, mutations in *Optineurin* (*OPTN*) (Ryan and Tumbarello, 2018), *SQSTM1* (Katsuragi et al., 2015), *SOD1* (Nishitoh et al., 2008), *Vesicle-associated membrane* protein-*associated* protein *B/C* (*VAPB*) (Chen et al., 2010), *C9ORF72* (Yingying Zhang et al., 2018) and *Cyclin F* (*CCNF*) (Tsai et al., 2018) were then all reported to reduce UPS activation and strengthen its role in disease.

*Autophagy*

Autophagy is a self-degradative process, crucial for balancing sources of energy at critical times in development and in response to nutrient stress. Autophagy, also plays a housekeeping role in removing misfolded or aggregated proteins, clearing damaged organelles, such as mitochondria, endoplasmic reticulum and peroxisomes, as well as eliminating intracellular pathogens (Glick et al., 2010). Autophagy and UPS are two tight regulated mechanism where their dysregulation can lead to massive change. It has been shown that mutations in *C9ORF72* (Webster et al., 2016), *SQSTM1* (Katsuragi et al., 2015), *OPTN* (Wong and Holzbaur, 2014) or *TBK1* (Oakes et al., 2017) are all associated with autophagy dysregulation. As autophagy defects contribution to ALS is a main subject and especially for *C9ORF72,* I will develop this part through chapter 2.4.2.

***RNA metabolism alteration***

Two RNA-binding proteins, FUS and TDP-43, have diverse roles in RNA metabolism, including translation, miRNA processing, RNA transport and transcription (Buratti and Baralle, 2001; Schwartz et al., 2012). These genes are mutated in ALS, which causes their proteins to be mislocalized from the nucleus to the cytoplasm, affecting the RNA-processing machinery (Amlie-Wolf et al., 2015; Hiji et al., 2008). Indeed, *Tdp-43* knockdown in mice results in in the alternate splicing dysregulation of numerous mRNA transcripts, and the loss-of-function (LOF) of *Fus* also induces many splicing defects, suggesting important alternate splicing events in ALS patients (Lagier-Tourenne et al., 2012; Polymenidou et al., 2011).

Furthermore, TDP-43 is capable of binding directly to several proteins of the heterogeneous nuclear ribonucleoprotein (hnRNP) family with well-known splicing inhibitory activity, in particular, hnRNP A2/B1 and hnRNP A1 LS patients. (Buratti et al., 2005). It has also been reported that TDP-43 interact with Matrin 3 (MATR3) resulting in altering the global nuclear export of mRNA (Johnson et al., 2014). Other mutation in *ANG* (encoding *angiogenin*) (Pizzo et al., 2013), *SETX* (encoding *senataxin*) (Skourti-Stathaki et al., 2011), *ELP3* (encoding *elongator complex protein 3*) (Simpson et al., 2009) or *TAF15* (encoding *TATA-binding protein-associated factor 2N)* (Kapeli et al., 2016, p. 15) have are all involved in the regulation of RNA and been associated with ALS.

Last but not least, G4C2 sense and antisense RNA for *C9ORF72* caused a toxic gain of function in ALS by forming RNA foci (formation of stable parallel unimeric and multimeric G-quadruplex structures), which sequester various RNA-binding proteins and thereby disrupt RNA metabolism (DeJesus-Hernandez et al., 2011; Reddy et al., 2013). As *C9ORF72* mutation in ALS/FTD is the main cause of ALS and has different potential mechanisms of toxicity, there will be details in chapter 2.3.

***Axonal transport deficit***

Axonal transport is an essential process in neurons which allow the transports of proteins mitochondria, lipids synaptic vesicles and other organelles to and from neurons. They are also responsible for the movement of molecules destined for degradation (Perlson et al., 2010). Thanks to ultrastructural investigation first presentation of axonal deficit in ALS patient was describe in the 90's which shows impaired communication with perturbated organelle traffics or mitochondria and lysosome accumulation in motor neurons (Breuer et al., 1987; Sasaki and Iwata, 1996). Furthermore mutation in the *PFN1* (encoding for *profilin-1*) are associated with ALS (Wu et al., 2012). Mutated genes in mice shows an ALS phenotype with dysregulated actin polymerization impacting the attachment of actin to microtubules leading to slow anterograde and retrograde axonal transport (Fil et al., 2017). Interestingly, microtubules (composed of dimers of α- and β-tubulin) shows a mutated gene in ALS, coding for the alpha tubulin subtype, *TUBA4A*. In ALS patient, it seems to negatively alter microtubule dynamics and stability (Smith et al., 2014).

Moreover, mutation in *DYNACTIN SUBUNIT 1 (DCTN1)* is affecting the tertiary structure of the dynactin protein which has a primary role in anterograde and retrograde movement of diverse cargoes along the microtubule's cytoskeleton. Furthermore, several *Sod1* transgenic mice have shown motor neuron degeneration due to defects in anterograde and/or retrograde transport (Warita et al., 1999).

***Oxidative stress***

Oxidative stress is a phenomenon caused by an imbalance between production and accumulation of oxygen reactive species (ROS) in cells and tissues and the ability of a biological system to detoxify these reactive products (Pizzino et al., 2017). Since the *SOD1* gene mutation in ALS was discovered, researchers studied the potential contribution of oxidative stress to the physiopathology of the disease. Indeed, *SOD1* is a superoxide dismutase that is able to control the levels of a variety of ROS and thus limiting their potential toxicity (Wang et al., 2018). Thus, it has been possible to see an increased level of oxidized proteins, RNA DNA and lipids in post-mortem tissue in *SOD1* ALS cases (Chang et al., 2008; Kikuchi et al., 2002; Strong, 2010). However, *Sod1* KO mice showed slightly increased neuronal cell death following axonal injury, but normal motor neuron development (Reaume et al., 1996). Furthermore *in-vitro* studies of *SOD1* mutants found no correlation between relative enzymatic activity and clinical pathology (Ratovitski et al., 1999). Together, these findings suggest that *SOD1* mutations are more likely to result in a gain of toxic function (misfolding and aggregation of SOD1) rather than a loss-of-function mechanism. However, *Sod1* mice also exhibit a wide range of symptoms, some of which are pertinent to ALS, such as a slowly progressing motor impairment and loss of functional innervation (Fischer et al., 2012; Flood et al., 1999; Larkin et al., 2011).

As ROS are controlling broad aspects of cellular life, increased oxidative stress may affect many signaling pathway like mitochondrial function, exacerbate endoplasmic reticulum stress and impact protein homeostasis mechanisms ultimately leading to cell damage and neuronal loss and thus leading to various neurodegenerative diseases including ALS (Guo et al., 2013; Niedzielska et al., 2016).

***Mitochondrial dysfunction***

Mitochondria is a key organelle generating most of the chemical energy needed to power the cell's biochemical reactions. They have a significant role in ion homeostasis, several metabolic pathways, apoptosis and in ROS production and consumption (Brand et al., 2013).

Mice with *Sod1* mutations exhibit mitochondrial dysfunctions and abnormalities in morphology similar to those seen in ALS patients (Magrané et al., 2014; Velde et al., 2011). Indeed, *Sod1* mutated mice shows mitochondrial degeneration by inducing vacuole formation by extension and leakage of the outer mitochondrial membrane, and expansion of the intermembrane space (Higgins et al., 2003). Moreover, impaired calcium buffering capacity has been observed in mutated *SOD1* ALS patient leading to oxidative damage to mitochondria (Parone et al., 2013). Furthermore, the coiled-coil helix domain-containing protein 10 (*CHCHD10*) has been identified in ALS patient. CHCHD10 seems to interact or being part of the MICOS complex, a large protein complex of the mitochondrial inner membrane that plays crucial roles in the maintenance of crista junctions, inner membrane architecture and formation of contact sites to the outer membrane. Consequently, mutation in *CHCHD10* ALS patient result in mitochondria dysfunction (Genin et al., 2016; Zhou et al., 2019).

Moreover TDP-43 accumulates in the mitochondria of ALS patient where it preferentially binds to mRNAs encoding respiratory chain complex 1 subunits, causing complex 1 disassembly (W. Wang et al., 2016). Similarly, normally localized in the nucleus, FUS accumulate in the cytosol and possibly become toxic by affecting the mitochondrial function (Deng et al., 2018; Vance et al., 2009).

***Excitotoxicity***

Excitotoxicity is a neuronal degeneration induced by overstimulation of glutamate receptors This mechanism is thought to contribute to the neuronal damage in stroke, neurotrauma, epilepsy and many neurodegenerative disorders including multiple sclerosis, Parkinson's disease and ALS (Pitt et al., 2000; Shaw et al., 1995; Vaarmann et al., 2013). In ALS patient, α-amino-3-hydroxy-5-methyl-4- isoxazole propionic acid (AMPA) receptors are more calcium permeable (due to diminution of GluA2 subunit) leading to motor neurons toxicity induced by calcium entry and the downstream susceptibility to excitotoxicity in ALS (Laslo et al., 2001).

Moreover, the excitatory amino acid transporter 2 (EAAT2) is impaired and engender dysfunctional glutamate transport mechanisms in ALS patient. Indeed, localized at the synaptic cleft, EAAT2 normally permit to maintain a low level of glutamate and thus neuron toxicity which is not the case for ALS patient (Medina et al., 1997; Rothstein et al., 1996). Excitotoxicity is a mechanism present in all form of ALS but the mechanism leading to the specific deterioration of motor neurons remain unclear. Interestingly, riluzole, one of the very few drug prescribed for ALS patient, attenuate disease progression notably by inhibiting glutamate release (Kretschmer et al., 1998; Wang et al., 2004).

***Endosomal Pathway and Vesicle Secretion***

Endocytosis is the process by which cells internalize macromolecules and surface proteins. It allows the formations of exosomes (type of extracellular vesicle that contain constituent's protein, DNA, and RNA) and allow the communication between cells and affect the functionality of the recipient cells. Interestingly, intercellular communication through exosomes seems to be involved in the pathogenesis of various disorders, including cancer, neurodegeneration, and inflammatory diseases (Elkin et al., 2016; Kalluri and LeBleu, 2020).

Proteomics analysis comparing brain-derived Extracellular Vesicles (EVs) from WT mice and transgenic amyotrophic lateral sclerosis *Sod1* mutated mice shows that they are enriched in synaptic and RNA-binding proteins and be responsible for neuronal cell death (Silverman et al., 2019). Furthermore, G4C2 repeats expansion in *C9ORF72* affect intracellular localization of *C9ORF72* mRNA leading to production of dipeptide repeat proteins (DPR) causing neuronal cell-death. Interestingly, theses DPR's seems to be spread via EVs (Extracellular vesicles) and that theses DPR could also be a contributor to nucleocytoplasmic trafficking defects (Westergard et al., 2016; Zhang et al., 2015). Also, the C9ORF72 protein structure presents some similarities with the Differentially Expressed Normal versus Neoplastic (DENN) guanine nucleotide exchange factor and may activate RAB proteins such as RAB8A, RAB39B, RAB1a or RABs 1, 7 and 11. Theses RAB's are key regulator of autophagy and/or vesicle-trafficking process (Farg et al., 2014; Sellier et al., 2016; Webster et al., 2016). As *C9ORF72* mutation in ALS/FTD is the main cause of ALS and has different potential mechanisms of toxicity there will be details in section 2.4.2

Other ALS-associated gene variants such as *Alsin Rho Guanine Nucleotide Exchange Factor* (*ALS2*) variants is also known to affect endosomal and vesicle transports. Indeed, *ALS2* is a guanine nucleotide-exchange factor for the small GTPase RAB5 widely studied for it role in endosome trafficking and fusion (Devon et al., 2006; Topp et al., 2004). Furthermore, charged multivesicular protein 2B (CHMP2B), a component endosomal sorting complexes required for transport (ESCRT-III) involved in the processing of cargo into intraluminal vesicles, is associated with ALS (Parkinson et al., 2006). Finally, there is also valosin-containing protein (VCP), an ubiquitous AAA+ ATPase that interacts with clathrin to form early endosomes and also is involved in the autophagic pathways (Bug and Meyer, 2012).

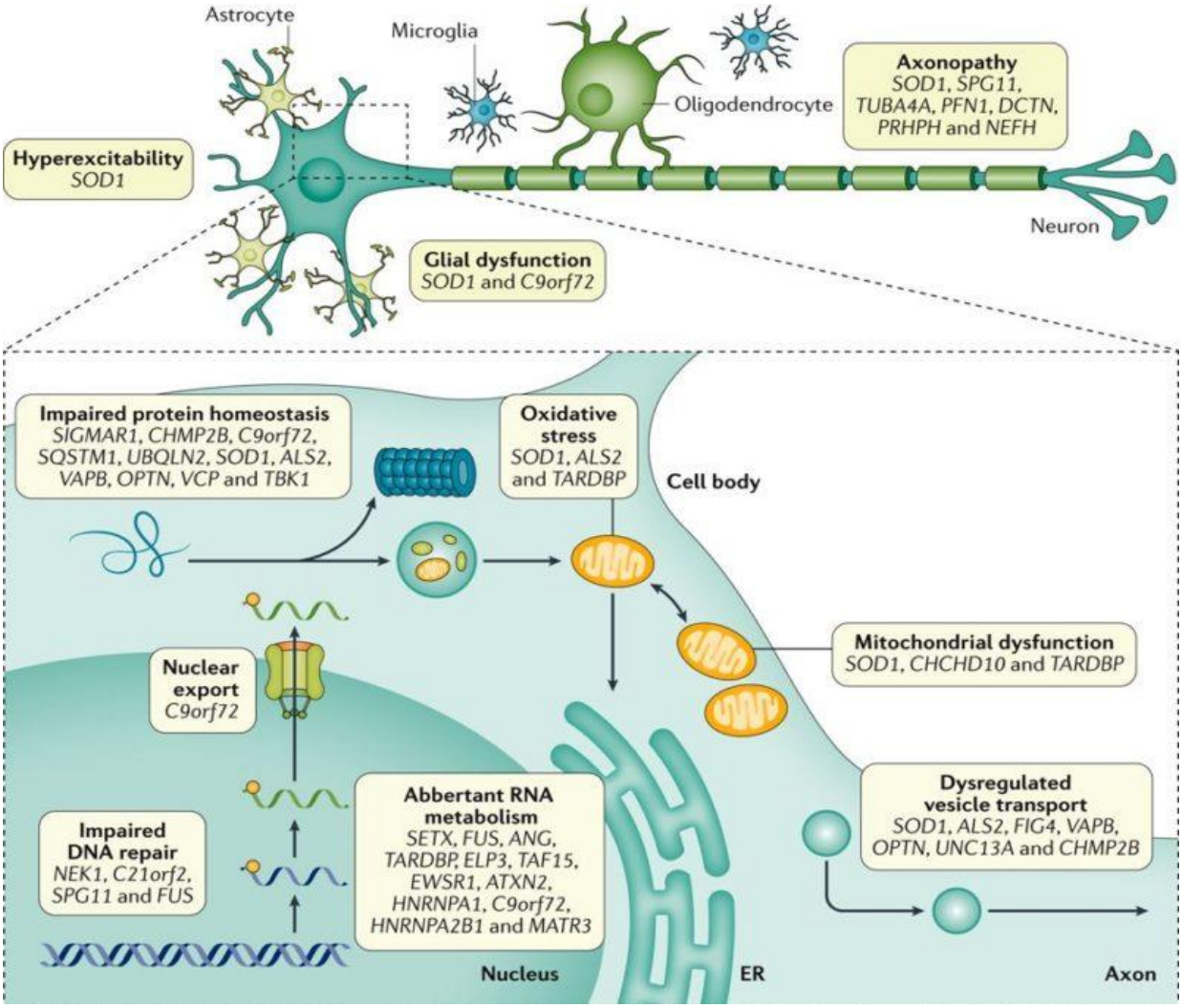


Figure 7 Pathophysiology of ALS

Schematic representation of the different mechanisms and cellular pathways potentially involved in ALS. Various genes that have direct or indirect link with the concerned pathway are also indicated (From (Hardiman et al., 2017)).

This small overview shows the multiple cellular pathway and gene involved in ALS. Interestingly, the fact that ALS patient present oligogenic inheritance (in which a phenotypic trait is determined by more than one gene) and that some ALS gene mutation are pleiotropic (in which a single gene has multiple phenotypic manifestations) complexify even more the determination of typical pattern for ALS patient. Among all this data, these different pathways can be linked to each other and sometimes lead to a pathway cascade. For example, disrupted axonal transport can lead to an accumulation of nonfunctional mitochondria, while ATP deficiency and increased oxidative stress may damage proteins and DNA, which, in turn, could exacerbate the disruption of cellular homeostasis, leading to motor neuron death.

However, some mutations are often found in ALS patient. Indeed, more than 60 % of familial ALS, namely *SOD1, TARDBP, FUS*, and *C9ORF72* accounted for familial ALS where *C9ORF72* mutation represent more than 40 % of all fALS (DeJesus-Hernandez et al., 2011; Kwiatkowski et al., 2009; Renton et al., 2011; Rosen et al., 1993; Sreedharan et al., 2008; Vance et al., 2009). Moreover, among the 40+ identified ALS related genes, more than 50 % have direct implications in proteostasis and/or autophagy, including *C9ORF72,* supporting the major role of these processes in ALS pathogenesis. During my thesis we mainly focused on C9ORF72 pathogenicity in ALS and especially its role in autophagy. The next part 2 will be dedicated to it.

# 2. Implication of C9ORF72 in ALS/FTD

## 2.1 GGGGCC hexa-nucleotide expansion in the *C9ORF72* gene

In 2011, the identification of GGGGCC hexa-nucleotide expansion in the first intron of *C9ORF72* gene was identified as the most common genetic cause of ALS and FTD (DeJesus-Hernandez et al., 2011; Renton et al., 2011). Indeed, in Europe and North America, C*9ORF72* expansion are found in 80 % to 90 % of all familial ALS/FTD (20 to 50 % of familial ALS and 10 to 30 % of familial FTD). However, it represents only 5 to 10 % of sporadic cases. Interestingly, this mutation is exceedingly rare in Asia and the Middle East, indicating that the genetic architecture underlying FTD and ALS may differ in these populations (Majounie et al., 2012).

The size of the hexanucleotide expansion in control healthy subjects ranges between 2 and 24, with a median count of 2 to 8 repeats. In most of the studies, expansion above 30 is considered as pathological. However, only a small proportion of patients present 30 to 100 repetitions. In reality, vast majority of the patient present many hundreds of thousands of repeats (DeJesus-Hernandez et al., 2011; Fournier et al., 2019). Currently, there is heterogeneity in the correlation between repeats expansion, size age at onset and disease severity. Indeed, within a same patient, different expansions size can be measured in different part of the CNS and in the blood (van Blitterswijk et al., 2013; Van Mossevelde et al., 2017; Waite et al., 2014).

This variability between the studies could be explained by the somatic instability of the GGGGCC repeat number in several tissues and among central nervous system regions (Van Mossevelde et al., 2017). Additionally, the repeat number fluctuates over time in subsequent blood collections from *C9ORF72* mutation carriers as well as with age at the time of collection (Fournier et al., 2019; Suh et al., 2015). Instability and mosaicism of expansions can be an explanation underlying the clinical heterogeneity observed in patient. However, clear explanation is still lacking with conflicting results among literatures (Beck et al., 2013; Gijselinck et al., 2016; Nordin et al., 2015; van Blitterswijk et al., 2013; Van Mossevelde et al., 2017).

## 2.2 *C9ORF72* structure, transcript variants and protein isoforms

The *C9ORF72* gene, for "*Chromosome 9 Open Reading Frame 72 locus*", consists of 11 exons, with ten coding exons (exons 2 to 10) and two non-coding exons (exon 1a and 1b). The *C9ORF72* gene contain two distinct promoter regions between these two non-coding exons leading to three coding variants. The variant 1, is a short transcript containing non-coding exon 1a and coding exons 2-5. Variant 2 and 3 differ only on the inclusion or not of non-coding exons 1a (variant 3) or 1b (variant 2) but both contain exons 2-10. Alternative splicing of intron 5 of these three RNA variants, results in the production of two different isoforms: one long form of the protein and one short. The short form (*C9ORF72-S*), encoded by the variant 1, is composed of 222-amino acid with a molecular weight of 24 kDa. Short isoform is unstable and rapidly degraded by the cell. The long form (*C9ORF72-L*), encoded by the variant 2 and 3, is composed of 481- amino acid with a molecular weight of 54 kDa and is the most abundant (Figure 8) (DeJesus-Hernandez et al., 2011; Renton et al., 2011).

Interestingly, the *C9ORF72* human gene is highly conserved in primates and other model system (chimpanzee (gene LOC465031, 99.58%), rat (gene RGD1359108, 97.71%), rabbit (gene *C9ORF72*, 98.54%), suggesting that the protein(s) encoded by *C9ORF72* have fundamental biological functions (http://www.ensembl.org).

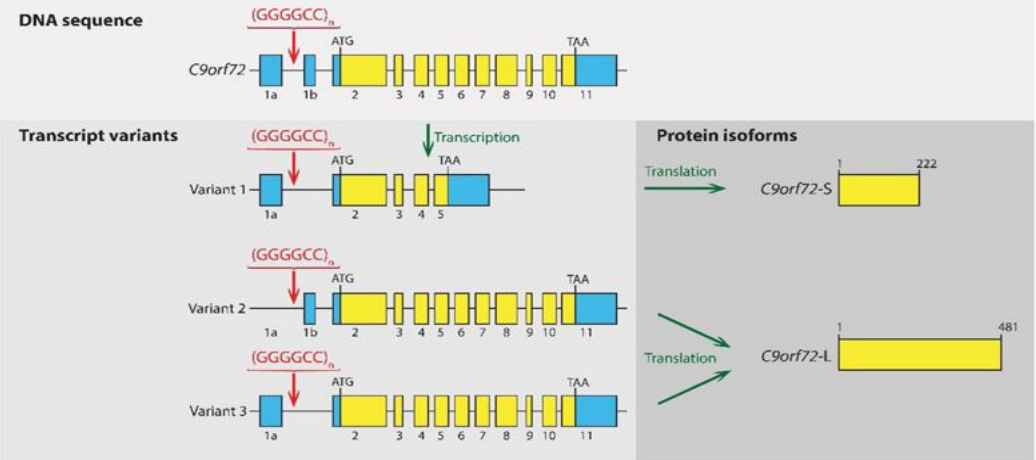


Figure 8 *C9ORF72* structure, variants and protein isoforms

The *C9ORF72* gene in composed of 10 coding exons (in yellow) and 2 non-coding exons (in blue). The GGGGCC hexanucleotide repeat expansion mutation is located in the first intron of variants 1 and 3 and within the promoter region of variant 2. The short form (*C9ORF72*-S), encoded by the variant 1 and the long form (*C9ORF72*-L) encoded by the variant 2 and 3 (From Balendra and Isaacs, 2018).

## 2.3 Mechanism of pathogenicity of C9ORF72 in ALS/FTD

There are three possible pathogenic mechanisms explaining *C9ORF72* ALS phenotype (Figure 9):

- First, transcripts containing expanded repeats accumulate in RNA foci that recruit various RNA-binding proteins (RBP), potentially altering their localization and functions.
- Second, sense G4C2 and antisense C4G2 expanded repeats are repeat-associated non-AUG (RAN) translated into dipeptide repeat (DPR)-containing proteins, which form inclusions throughout the brain of patients with C9-ALS/FTD, as well as in mice expressing expanded G4C2 repeats.
- Third, expanded G4C2 repeats promote DNA epigenetic changes that lead to decreased expression of C9ORF72 mRNA and protein levels in C9-ALS/FTD individuals.

I will now go through these three main mechanisms in the next part.

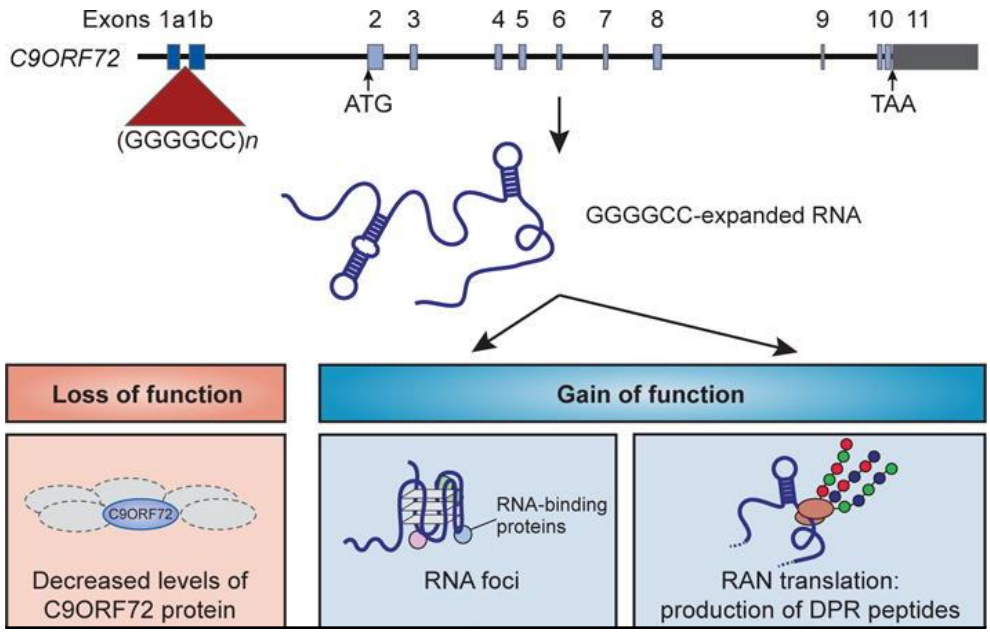


Figure 9 Three possible pathogenic mechanisms in *C9ORF72* ALS patients

GGGGCC hexa-nucleotide expansion in the *C9ORF72* gene can either lead to a loss of function mechanism with (1) abolition of expression and thus decreased levels of protein, and/or gain of function mechanism with (2) the formation of RNA foci that sequester RBP and (3) unconventional translation to produce dipeptide repeat proteins, some of which may be toxic (Adaptation from Taylor et al., 2016).

### 2.3.1 Gain of function (GOF) mechanisms

#### 2.3.1.1 RNA foci

The toxicity of *C9ORF72* repetitions is explained by two gain of function mechanisms. First one, the GGCCCC repeats are transcribed into RNA species and accumulate in nuclear RNA foci (Figure 10). Presence of sense and antisense RNA foci have been observed in *C9ORF72* -ALS patient concomitant with the discovery of the expanded GGGGCC repeat (DeJesus-Hernandez et al., 2011; Greco et al., 2002; La Spada and Taylor, 2010).

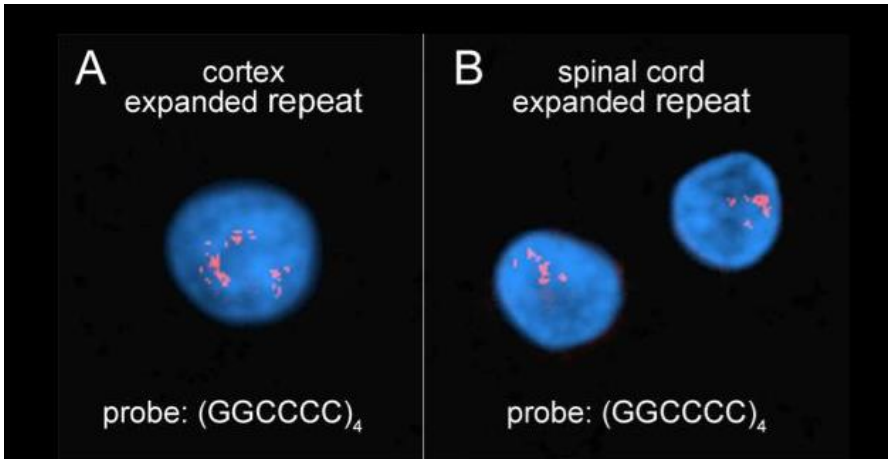


Figure 10 RNA foci composed of GGGGCC hexanucletotide repeats

Multiple RNA foci in the nucleus (stained with DAPI, blue) of a frontal cortex neuron and spinal cord using a Cy3-labeled $(GGCCCC)_4$ oligonucleotide probe (red) (Adaptation from (DeJesus-Hernandez et al., 2011)).

Further studies will show ARN foci in lymphoblast, fibroblast and induced pluripotent stem cell-differentiated neurons from *C9ORF72* expanded cases (Almeida et al., 2013; Conlon et al., 2016.; Cooper-Knock et al., 2014; Donnelly et al., 2013; Fratta et al., 2013; Haeusler et al., 2014; Xu et al., 2013). *In-vitro*, the sequences transcribed forms secondary structures, like hairpins and highly stable DNA and RNA structures called G-quadruplex and R-loops (Fratta et al., 2013; Haeusler et al., 2014; Zhou et al., 2018). Consequently, *in-vivo* and *in-vitro* studies have shown that such secondary structures mediate sequestration of RNA-bindings proteins (RBPs). RBPS have various roles in splicing, translational regulation, RNA transport and degradation and their titration could dysregulate all these pathways.

Most frequently identified RBPs, that interact *C9ORF72* RNA foci, are the *heterogeneous nuclear ribonucleoprotein* (*hnRNPs*), in particular, *hnRNP H*, although *hnRNP A1* and *hnRNP A3* are also detected, as well as *ADARB2* (*double-stranded RNA-specific editase B2*), *Pur-α*, *SRSF1* (*serine/arginine-rich splicing factor 1*), *SRSF2* (*serine/arginine-rich splicing factor 2*) and *ALYREF* (*THO complex subunit 4*) (Conlon et al., 2016; Cooper-Knock et al., 2014; Davidson et al., 2017; Donnelly et al., 2013; Lee et al., 2013; Xu et al., 2013).

#### 2.3.1.2 Dipeptide repeat proteins (DPR)

Second, gain of function mechanism is based on the findings that the bidirectionally transcribed repeat expansions can escape the nucleus and be translated in DPR (Dipeptide repeat). DPR are type of protein fragment that is produced through a non-canonical translation, called Repeat Associated Non-ATG translation (RAN) of expanded hexanucleotide repeats in the *C9ORF72* gene (Ash et al., 2013; Mori et al., 2013b; Zhang et al., 2014; Zu et al., 2013).

RAN translation was first discovered while studying CAG-CTG expansion mutations in spinocerebellar ataxia 8 (SCA8) and myotonic dystrophy type 1 (DM1). They showed, in transfected cells, that both CAG and CUG expansion transcripts are translated in polyGln, polyAla and polySer expressed from CAG expansions and polyLeu, polyAla and polyCys proteins expressed across CUG expansion without any AUG codon. Since the discovery of "RAN" translation, the accumulation of "RAN protein" has been escribed in many neurodegenerative and neuromuscular disease like fragile-X tremor ataxia syndrome (FXTAS) (Todd et al., 2013), Huntington disease (HD) (Bañez-Coronel et al., 2015), myotonic dystrophy type 2 (DM2) (Zu et al., 2017), Fuchs' endothelial corneal dystrophy (FECD) (Soragni et al., 2018), and spinocerebellar ataxia type 31 (SCA31) (Ishiguro et al., 2017).

RAN translation has been largely discussed among the scientific community and especially on its mechanism. One explanation can be that expansion of RNA-level repeats would be able to form hairpin-like structures and thus to potentially recruit certain eIF factors and/or the ribosome directly, while viral Internal ribosome entry site (IRES) sequence (Cleary and Ranum, 2013).

In this aspect, the five DPRs that are translated from C9 GGGGCC (sense) or CCCCGG (anti-sense) repeats are poly-(Gly-Ala) (GA) and poly-(Gly-Arg) (GR) from sense transcripts, poly-(Pro-Arg) (PR) and poly-(Pro-Ala) (PA) from antisense transcripts, and poly-(Gly-Pro) (GP) from both the sense and antisense transcripts (Figure 11) (Ash et al., 2013; Mori et al., 2013b; Zhang et al., 2014; Zu et al., 2013).

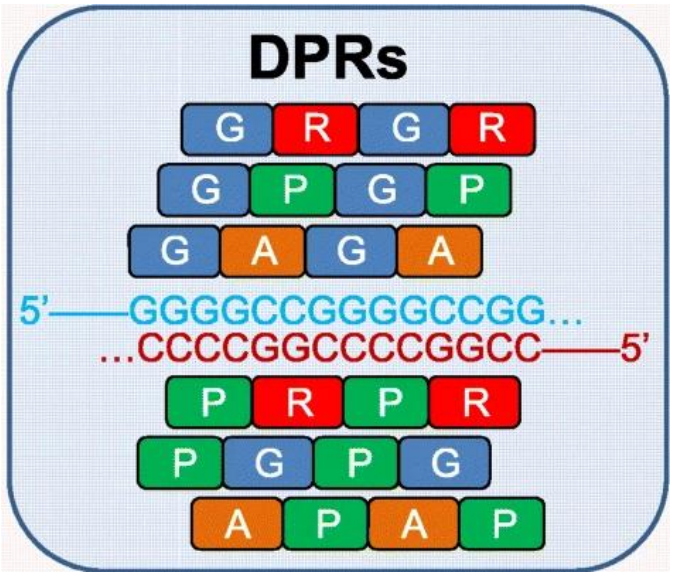


Figure 11 Sense and anti-sense RNA traduction into DPRs

C9 GGGGCC repeats translated into poly-(Gly-Ala) (GA) and poly-(Gly-Arg) (GR) from sense transcripts, poly-(Pro-Arg) (PR) and poly-(Pro-Ala) (PA) from antisense transcripts, and poly-(Gly-Pro) (GP) from both the sense and antisense transcripts (Adaptation from (X. Tang et al., 2020)).

Thanks to antibody, presence of these DPR have been confirmed and visualized as cytoplasmic inclusions in neurons of C9 ALS/FTD patients which colocalize with autophagic proteins like p62 and ubiquitin but are negative for TDP-43 (Gendron et al., 2013; Mackenzie et al., 2013; Mori et al., 2013a; Zu et al., 2013). Several histopathological studies reveal that there seems to be no correlation between DPR inclusions and neurodegeneration. Indeed, TDP-43 are prominent in degenerating regions of the brain and the spinal cord while DPR inclusions have been identified in the hippocampus, basal ganglia, frontal cortex, cerebellum and motor cortex in patients with ALS/FTD (Al-Sarraj et al., 2011; Cooper-Knock et al., 2014; Gomez-Deza et al., 2015; Schipper et al., 2016).

However, post-mortem studies focus on the final stage of the diseases and do not consider the early pathogenicity of DPRs and especially if soluble DPRs could mediate neurotoxicity. It has thus been proposed that DPR proteins could be extremely toxic to motor neurons in a soluble form, resulting in an absence of inclusion in these cells (Quaegebeur et al., 2020).

It's interesting to note that various *in-vitro* and *in-vivo* models demonstrated the potential toxicity of DRPs and/or RNA foci; these models will be discussed in the following section.

#### 2.3.1.3 Gain of functions models

***RNA foci toxicity***

Many *in-vitro* and *in-vivo* models have been created to evaluate the toxicity of repetitive RNA and/or DPR. Expanded GGGGCC repeats transfected into primary cortical and motor neurons showed lower survival and presence of nuclear RNA foci. In these cells, no DPRs were discovered (Wen et al., 2014). Similarly, RNA toxicity has also been implicated in eyes and motor neurodegeneration with low or non-detectable levels of DPRs (Xu et al., 2013; Zhang et al., 2015). Furthermore, motor axonopathy has been observed when both sense and antisense RNA repeats were expressed in *zebrafish* model without the presence of DPRs (Swinnen et al., 2018). However, same expression of sense and antisense repeats in a *Drosophila* model didn't lead to neurodegeneration (Moens et al., 2018).

***DPRs toxicity***

The absence of DPRs does not rule out a role for these proteins. To determine the relative contributions of RNA and DPRs in these models, more sensitive detection tests for DPRs would be needed (Figure 12).

Indeed, other studies shows that neurotoxicity caused by overexpression of GGGGCC repeats in *Drosophila* models is attributable to DPR's rather than repeat RNA (Mizielinska et al., 2014; Tran et al., 2015). The first study showed that neurodegeneration was reduced when a stop codon, preventing the translation of DPRs, was inserted. The second one show that their construct allowed the formation of RNA foci without production of DPRs with no clear evidence of neurodegeneration.

However, when increasing the expression of transgene, in this same model, DPRs where produce and engender lifespan reduction, although the frequency of sense foci remained the same. Both of these studies, support the idea that DPR mediate neurotoxicity rather that RNA repeats. Further studies confirmed toxicity of these DPRs in *in-vitro* models but also *Drosophila*, *zebrafish* and mice (Boeynaems et al., 2016; Chang et al., 2016; Freibaum et al., 2015; Li et al., 2020; Maor-Nof et al., 2021; Schludi et al., 2017; Swaminathan et al., 2018; Swinnen et al., 2018; Tran et al., 2015; Wen et al., 2014; Zhang et al., 2016, 2014; Zu et al., 2013).

Among all the DPRs*, in-vitro* and *in-vivo* studies have shown that poly(GR) and poly(PR) are the most toxic. These DPRs are both highly charged and polar. The poly(GR) DPR is unstable under cell culture conditions (half-life < 30 min), whereas the poly(PR) DPR is relatively stable (half-life ~72 h) (Kwon et al., 2014). Poly(PR) DPRs are almost exclusively localized within the nucleolus, whereas poly(GR) DPRs are observed both in the nucleolus and within the cytoplasm. Toxicity of these DRPs has been explained by their possible role in influencing the formation of membrane-less organelles and their liquid–liquid phase separation dynamics. These studies show that these DPR proteins are toxic by altering nucleocytoplasmic transport and/or by altering the mechanisms of protein degradation, in particular the proteasome and tend to interact with several proteins inducing perturbation of their downstream pathway (Lee et al., 2016; Lin et al., 2016). Finally, they induced developmental problems, locomotor and survival deficit in mice, *Drosophila* and *zebrafish* (Boeynaems et al., 2016; Cook et al., 2020; Freibaum et al., 2015; Lee et al., 2016; Li et al., 2020; Maor-Nof et al., 2021; Mizielinska et al., 2014; Riemslagh et al., 2021; Tao et al., 2015; Wen et al., 2014).

Of the five DRP, the poly(GA) DPR is the most readily visible in p62/ubiquitin positive inclusions in the brain and spinal cord of patients with ALS/FTD (May et al., 2014; Zhang et al., 2014). Poly(GA) has a strong ability to aggregate and thus forming amyloidogenic parallel β-sheet structure fibrils that tend to remember the structure of the amyloid-beta peptide present in Alzheimer's disease (Chang et al., 2016; Edbauer and Haass, 2016).

Furthermore, the poly(GA) DPR tends to binds Unc119, ubiquilin-1 and -2, and some proteasomal subunits engendering direct proteasomal impairment. Cryo-EM resolution of cellular aggregates of poly(GA) confirms the presence of many proteasome subunits 26S in these inclusions (Guo et al., 2018). Similarly to poly(GR) and poly(PR) inclusions, poly(GA) overexpression induce toxicity in various models like mice, *zebrafish*, primary neurons and cultured cells (Schludi et al., 2017; Zhang et al., 2016).

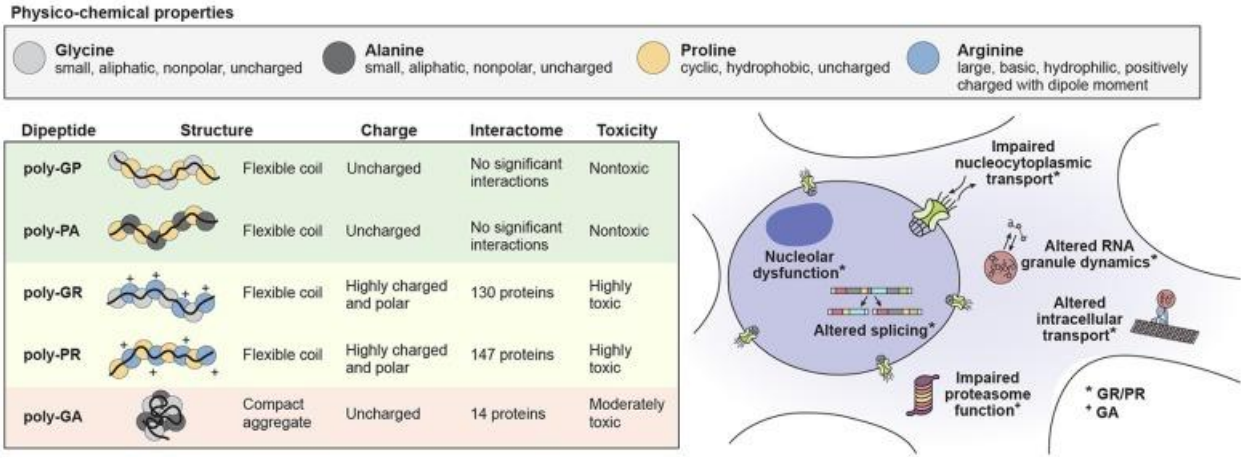


Figure 12 Physico-chemical properties of individual DPR species influence

Properties of the five DPRs from C9 repeats and their potential involvement in different pathways (Freibaum and Taylor, 2017).

Finally, studies shows no toxicity induce by poly(GP) and poly(PA) in *Drosophila* (Freibaum et al., 2015; Lee et al., 2016; Mizielinska et al., 2014; Wen et al., 2014). Indeed, transfection in culture of immortalized cells showed that the poly(GP) protein aggregates less than other DPR proteins and could explain their absence of toxicity (Yamakawa et al., 2015). However, poly(GP) are the most expressed DPR and can be used to discriminate patients and healthy patients. Thus, the poly(GP) protein assay could serve as early biomarker to identify potential patients (Gendron et al., 2017; Lehmer et al., 2017; Meeter et al., 2018).

Animal and cellular studies highlight a neurotoxic role of poly(GR) and poly(PR) and to a lesser degree of poly(GA). Human post-mortem studies in contrast have been much less clear on a potential role of DPR toxicity. Interestingly, our team recently show that the sole expression of DPR proteins under their native sense or antisense sequences is not sufficient to be pathogenic in isolation.

In contrast, neuronal cell loss in ALS/FTD may result from a double-hit mechanism where the suboptimal autophagy due to the reduced expression of C9ORF72 may synergize toxicity (Boivin, 2020). For RNA foci, titration of binding proteins to RNA appears weak and only leads to subtle splicing alterations in patients obtained from SLA/DFT. Further studies need to be conducted to show their implication in ALS. Next chapter will be focused on the last potential mechanism of toxicity, the loss of function mechanism.

### 2.3.2 Loss of function (LOF) mechanism

#### 2.3.2.1 Haploinsufficiency of *C9ORF72* in patients

When the GGGGCC repeats in the *C9ORF72* gene were discovered, lower *C9ORF72* RNA levels were also described (DeJesus-Hernandez et al., 2011; Renton et al., 2011). Further studies confirmed these results by showing a decreased around 50 % in total sense *C9ORF72* transcript levels in frontal cortex and cerebellum (Belzil et al., 2013; Ciura et al., 2013; Fomin et al., 2018; van Blitterswijk et al., 2015). To explained this decreased expression, epigenetic modification of *C9ORF72* was proposed. Indeed, several studies revealed that in 20–40% of cases, the CpG island in the *C9ORF72* promoter region upstream of the pathogenic repeats was hypermethylated (Belzil et al., 2014; Gijselinck et al., 2016; Xi et al., 2015, 2013). Furthermore, tri-methylation of histone H3 and H4 due to the pathogenic repeats was also demonstrated (Belzil et al., 2014). These hypermethylation is associated with increased repeat length and reduced transcription of *C9ORF72.* Further studies confirmed that these expansion leads to lower *C9ORF72* mRNA level suggesting a reduce expression of the C9ORF72 protein. However, it is important to notice the increased range and specificity of antibody that explained the large panel of confusing results on the protein expression and subcellular localization.

However, it seems that the C9ORF72 protein is mainly expressed in the brain, spinal cord and immune system but, also at lower levels, in the lung, heart, liver, kidney and skeletal muscle. Interestingly, the long form on the protein is the most abundant in human and mouse brain and that its level is reduced in C9ORF72 ALS/FTD patients' cerebellum, frontal cortex as in other part of the cortex in particular in the occipital, motor, and temporal cortices with a decrease between 25 % to 50 % of the protein level (Frick et al., 2018; Saberi et al., 2018; Xiao et al., 2015).

Recently, a new test using mass spectrometry without using any antibody (to eliminate the confusion around their specificity) confirmed that the frontal cortex of C9-FTD patients present a 42 % decreased of C9ORF72 protein (Viodé et al., 2018).

However, haploinsufficiency has been highly contested. Indeed, classical genetic representation of a LOF mechanisms include increased clinical severity in homozygous mutated patient and mutation occurring in the coding region. For *C9ORF72* repeat expansion, only one patient has been reported as homozygous and did not exhibit severe clinical phenotype compared to heterozygous patient (Cooper-Knock et al., 2014; Fratta et al., 2013). Furthermore, no deleterious mutations were reported within patients, except one. This patient presents a splice site mutation disrupting the reading frame leading to a premature stop codon and thus a decrease level of *C9ORF72* mRNA. The patient had no family history of the disease, autopsy could not be performed and assessment of a *C9ORF72* repeat expansion have not been performed which makes the interpretation of this case difficult (Liu et al., 2016).

Altogether, these data show the existence of a LOF mechanism but are difficult to combine together. Indeed, low specificity of antibody, low sample size and clear indication of C9ORF72 functional impairment in ALS/FTD patient is still lacking.

#### 2.3.2.2 *In-vitro* loss-of-functions models

Similarly, to post-mortem findings, most of C9 patient's Induced pluripotent stem cells (iPSC) derived motor neurons (MNs) present a reduction of about 50% in *C9ORF72* transcripts (Almeida et al., 2013; Donnelly et al., 2013; Shi et al., 2018). However, a recent study did not observe any of this change in iPSC-s or fibroblast (Fumagalli et al., 2021). By the way, these studies show that protein level is reduced in fibroblasts, but not in C9 iPSC-derived motor neurons (MNs). There are discrepancies between transcript, protein alteration and also between models. As for patients' post-mortem studies, the increased range and specificity of antibody can explain the large panel of confusing results on the transcript/protein expression. Interestingly, in C9 patient iPSC-derived MNs, different hallmarks of impaired autophagy has been described like p62 aggregation, proteasomal degradation and reduced autophagic flux (Almeida et al., 2013; Shi et al., 2018; Webster et al., 2016). Further information's on autophagy will be discussed in chapter 2.4.2.

In order to clarify the role of *C9ORF72* haploinsuffiency in ALS/FTD patients, several *C9ORF72* loss of functions models have been developed by various knockdown/knockout approaches (i.e. small interfering RNA (siRNA), antisense oligonucleotides (ASO), CRISPR clustered regularly interspaced short palindromic repeats/CRISPR associated protein 9 (CRISPR/Cas9)).

Survival of induced pluripotent stem-cell-derived neurons (iPSNs) and primary cortical neurons do not seem to be affected upon reductions of *C9ORF72* (Sareen et al., 2013; Wen et al., 2014). However, one study shows a decreased survival of iPSNs when a heterozygous and homozygous *C9ORF72* deletion was realized. Interestingly, adding *C9ORF72* rescues the survival of these neurons, indicating importance of *C9ORF72* in neurodegeneration (Shi et al., 2018). Moreover, gene expression alterations in this model correlate with those observed in C9 ALS/FTD patients' postmortem tissues. Overall depletion (90-100%) of *C9ORF72* leads to transcriptome alteration in different cell types and of different pathway's like autophagic, lysosomal and endosomal dysfunction (Farg et al., 2014; Sellier et al., 2016; Shi et al., 2018; Webster et al., 2016).

However, one needs to keep in mind that these models are artificial, hence, impairing disease relevance. That's why in parallel *in-vivo* models were developed.

#### 2.3.2.3 *In-vivo* loss-of-functions models

First *in-vivo* models were generated in lower-order organisms. A null mutation of the *Caenorhabditis elegans C9ORF72* orthologue shows motor neuron degeneration and stress sensitivity (Therrien et al., 2013). Similarly, knockdown of *C9ORF72* was performed in *zebrafish* model, causing both behavioral and cellular deficits related to locomotion without major morphological abnormalities. These deficits were rescued upon overexpression of human *C9ORF72* mRNA transcripts (Ciura et al., 2013). Higher order organism models were also generated. *C9orf72* mouse knockdown engender a 50-70 % *C9orf72* RNA decrease without decreased protein. Importantly, no *C9or72* hallmarks were observed (TDP-43, P62 or ubiquitin aggregates) as no behavioral or motor phenotypes.

Interestingly, mouse *C9orf72* knockout do not present any motor neuron degeneration but an inflammatory phenotype (splenomegaly, enlarged lymph nodes, infiltration of immune cells, increased expression of inflammatory cytokines, presence of auto-antibodies and immune-mediated glomerulonephropathy) (Burberry et al., 2016; Jiang et al., 2016; Koppers et al., 2015; O'Rourke et al., 2016; Shi et al., 2018; Sudria-Lopez et al., 2016; Sullivan et al., 2016). Interestingly, increased levels of autophagy and lysosomal proteins and autophagy defects were detected in both the spleen and liver of *C9orf72* deficient mice, supporting an *in-vivo* role of C9ORF72 in regulating the autophagy/lysosome pathway (O'Rourke et al., 2016).

Unfortunately, the motor phenotype found in *Zebrafish* and *C.elegans* do not correlate with the immunological phenotype in *C9orf72* mouse model. Discrepancy could be explained by a difference in homology of the *C9ORF72* orthologues in the various disease models (i.e. 21% in *C. elegans*, 75% in *zebrafish* and 98% in mice) and differences in RNA and protein processing events. Altogether, these results show that the loss of function mechanism does not seem to be a primary mechanism to precipitate disease but could possibly work in coordination with the other two gain of function mechanism hypotheses. However, one issue still does not seem to be resolved: What is the role of C9ORF72?

## 2.4 Functions of C9ORF72

### 2.4.1 C9ORF72-SMCR8-WDR41 complex

It has been shown that C9ORF72 forms a trimer with SMCR8 and WDR41, named CSW. WDR41 ("WD repeat containing protein 41") is a 52 kDa protein composed of 6 WD40 domains. SMCR8 ("Smith Magenis syndrome Candidate Chromosome Region 8") is a 105 kDa protein that contains, like C9ORF72, two DENN domains. The function of WDR41 and SMCR8 are unknown (Amick et al., 2016; Sellier et al., 2016; Sullivan et al., 2016; Ugolino et al., 2016; Yang et al., 2016). Bioinformatics analysis based on sequence alignment shows that C9ORF72 and SMCR8 contains N-terminal longin domain, followed by DENN, and d-DENN domains characteristic of DENN proteins "Differentially Expressed in Normal and Neoplastic cells", known to regulate the Guanosine Diphosphate/Guanosine Triphosphate (GDP/ GTP) exchange cycle of RAB/ARF (ADP ribosylation factors) proteins (Figure 13) (Levine et al., 2013; Zhang et al., 2012).

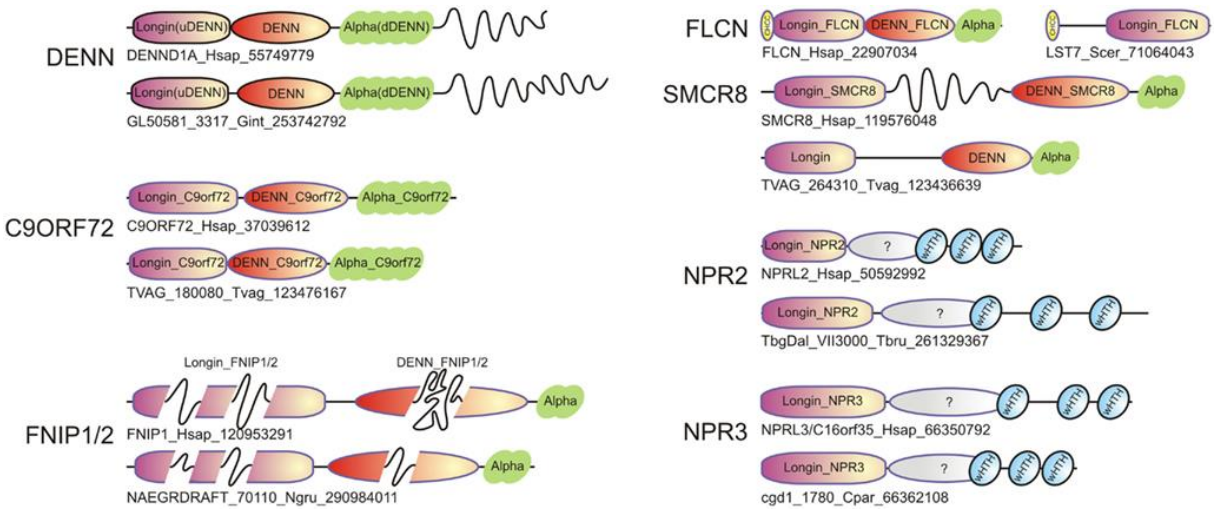


Figure 13 Domain architecture representation of C9ORF72 and SCMR8

Schematic representation of DENN proteins "Differentially Expressed in Normal and Neoplastic cells", including C9ORF72 and SMCR8, with their different longin and DENN domains (Zhang et al., 2012).

RAB/ARF proteins are members of the small GTPase superfamily. To date, there is around 170 small GTPases identified in humans. Thanks to sequence and functional similarity they can be divided into 5 mains families: Ras, Rho, Rab, Arf/Arl and RAs-related Nuclear protein (Ran) (Figure 14). The first family discovered was the Ras family which are known to regulate cell proliferation, differentiation, morphology, and apoptosis. The Rho family, composed of around 20 proteins has a role in actin cytoskeleton remodeling and cell polarity. The largest family is the Rab family with around 60 proteins all having a role in vesicle formation, movement and fusion, and vesicular cargo trafficking. The Arf/Arl family is composed of 30 proteins and is also involved in vesicle trafficking. The Ran subfamily consists of only one protein, which is the most abundant small GTPase in the cell and is involved in nuclear transport.

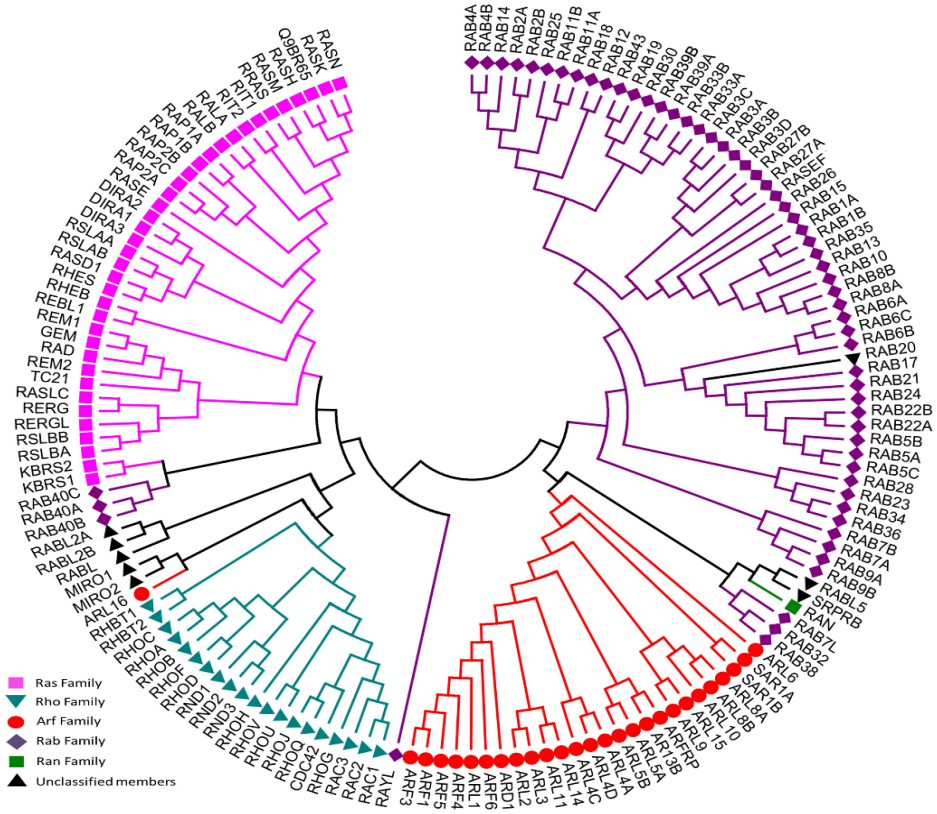


Figure 14 The human small GTPase superfamily

The different human small GTPase separated by color : Ras (lilac), Rho (cyan), Rab (purple), Arf (red), Ran (green), and unclassified members (blank) (Qu et al., 2019).

Despite their different pathway involvement, they are all similarly regulated. Indeed, small GTPases can be either in an inactive GDP-bound form and an active GTP-bound form where it can bind to effector and regulate various cell process. Their cycle is regulated by other protein called GTPase activating proteins (GAPs) that stimulate the hydrolysis of GTP to GDP leading to inactivation of the GTPase and by guanine nucleotide exchange factors (GEFs) catalyzing the dissociation of GDP to allow the binding of the GTP and thus produce the active form of the GTPase (Figure 15). Furthermore, guanine dissociation inhibitors (GDIs) are able to bind and sequester the inactive form of the GTPase away from cellular membranes preventing the interaction with effector molecules. It provides an additional level of control (For review (Qu et al., 2019)).

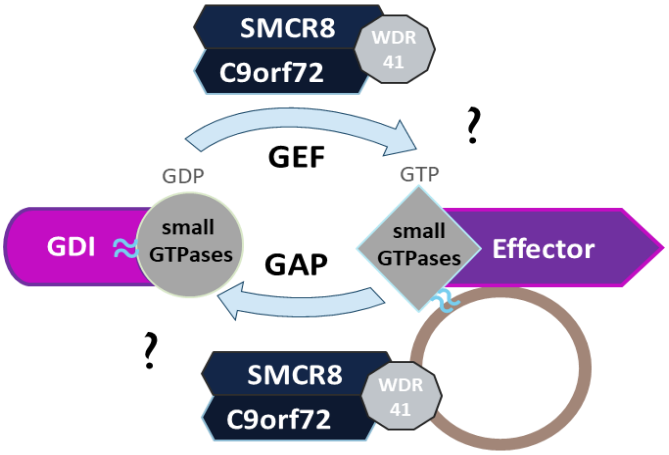


Figure 15 CSW complex is a GAP or a GEF for a small GTPase

CSW complex could regulate small GTPase by either an activator (GEF) by allowing the small GTPase to bind GTP or an inactivator (GAP) by allowing the small GTPase to bind GTP.

Since the discover of C9ORF72-SMCR8-WDR41 (CSW) complex being part of the DENN protein family, several papers showed that CSW could regulate several RAB GTPase like RAB8a and RAB39b (Sellier et al., 2016; Yang et al., 2016), RAB1a (Webster et al., 2016) and/or RAB5 (Farg et al., 2014; Shi et al., 2018) in order to regulate autophagy; RAB7 and RAB11 to regulate endocytosis (Farg et al., 2014) or RAB3 to regulate exocytosis (Frick et al., 2018). Additionally, it has been demonstrated that the CSW complex can form a complex with the Unc-51-like kinase 1 (ULK1) complex, thereby regulating autophagy. This is in accordance with *C9ORF72* deficient *in-vivo* and *in-vitro* models, which exhibit increased levels of autophagy, lysosomal proteins, and autophagy defects (Amick et al., 2016; Sullivan et al., 2016; Yang et al., 2016). Interestingly, in the complex C9ORF72/SMCR8/WDR41, SMCR8 is activated through a phosphorylation mediated by TBK1, which is mutated in some ALS/FTLD cases (Cirulli et al., 2015; Freischmidt et al., 2015; Sellier et al., 2016).

The CSW complex structure will be the main focus of this thesis, as well as its function as a small GTPase regulator and implications in autophagy. Implication of C9ORF72 in autophagy is an active field of research. Indeed, numerous papers shows that C9ORF72 could regulate autophagy and will be described in the next part.

### 2.4.2 Implication of C9ORF72 in autophagy

#### 2.4.2.1 Overview of autophagy

Autophagy (or autophagocytosis; from the Ancient Greek αὐτόφαγος, autóphagos, meaning "self-devouring") is a natural intracellular lysosome-mediated degradation process for nonessential or damaged cellular constituents. It promotes survival in the event of energy or nutrient shortage and responds to various cytotoxic insults. Autophagy was discovered in 1963 by Christian de Duve, when he found that acid phosphatase of rat liver is enclosed within a special type of cytoplasmic granules, later called the lysosomes (De Duve, 1963). This discovery earned him a Nobel Prize in Physiology or Medicine in 1974. However, in the following 30 years the autophagy research remained a relatively small field, mainly due to limited research tools and lack of understanding of its molecular mechanisms. In 1993, the ground-breaking work by Yoshinori Ohsumi identified 15 autophagy-related proteins (ATGs) (originally termed Apgs) essential for autophagic delivery of cargo to lysosome engendering a new field interest and an increase knowledge in the autophagic process (Tsukada and Ohsumi, 1993). Their findings were awarded in 2016 by a Nobel Prize in Physiology or Medicine. Today more than 40 ATGs have been identified and the autophagy filed is still expanding (Mizushima et al., 2021; Nakatogawa et al., 2009).

Autophagy refers not only to one biological process but to three types of autophagy: microautophagy, macroautophagy, and chaperone-mediated autophagy (CMA) (Figure 16).

- Chaperone-mediated autophagy (CMA) involved the recognition by chaperone Heat shock cognate 71 kDa protein (HSC70) and cochaperones of a KFERQ-like motif-bearing proteins leading to the transport of this protein to the lysosome for degradation (Kaushik and Cuervo, 2012).
- Microautophagy refers to the direct uptake of cargo through invagination of the lysosomal membrane (Li et al., 2012).
- Macroautophagy occurs when a double membrane vesicle envelops cytosolic materials, such as proteins and organelles, forming a structure called the autophagosome that fuses with the lysosome, thereby transferring its luminal content for degradation.

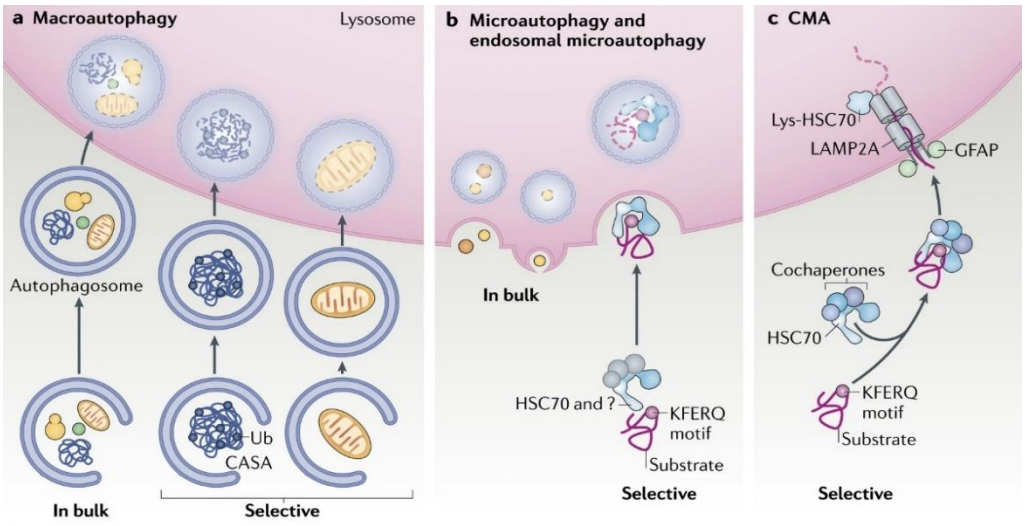


Figure 16 Schematic representation of the three types of autophagy

Autophagy can be divided in three type called macroautophagy (**a**), microautophagy (**b**) and chaperone-mediated autophagy (CMA) (**c**). The protein-mediated autophagy chaperones specifically degrade the proteins containing a KFERQ sequence; micro-autophagy where the lysosome degrades directly cytoplasmic components and macro-autophagy involving a double membrane called autophagosome which encompasses the material to be degraded then, merges with lysosome (Adaptation from (Kaushik and Cuervo, 2018)).

Autophagy will here be related to macroautophagy has it is the most described pathway. Autophagy goes through multiples steps starting with initiation and nucleation leading to the formation of an isolation membrane called “phagophore”. The membrane then begins to extend in the elongation stage to form a double-membrane sequestering compartment. Furthermore, there is the maturation step where the phagophore will fully surrounds its cargo and fuses to form the double-membrane called “autophagosome”. Once the autophagosome is formed the cargo has to be delivered to the lysosome. After the destination is reached the autophagosome and the lysosome fused to form the autolysosome. This last step lead to the autophagosomal contents to be degraded by lysosomal acid hydrolases and the contents of the autolysosome to be released for metabolic recycling (Figure 17).

The concept of autophagy is a tightly regulated signaling pathway with numerous proteins involved and will be described in the next part.

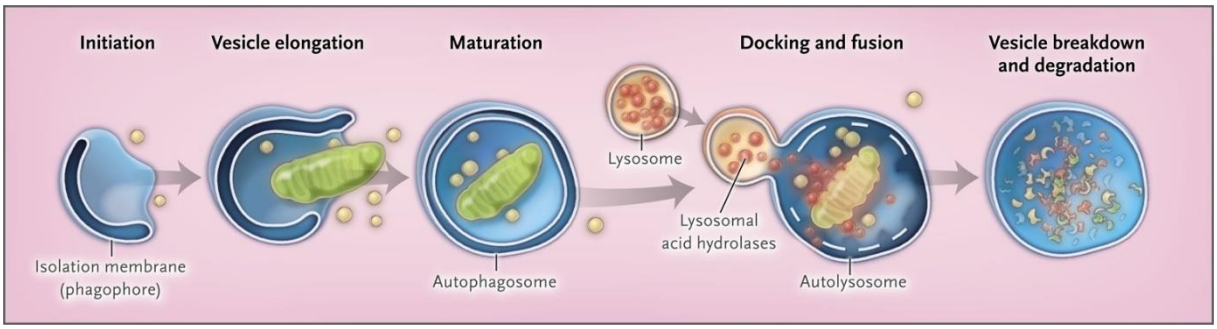


Figure 17 Overview of the different stages of autophagy

Autophagy is divided in four steps : Initiation and nucleation, elongation and maturation, fusion and degradation (Choi et al., 2013).

### 2.4.2.2 Autophagy signaling pathway regulation

#### 2.4.2.2.1 Initiation and nucleation

The membrane-associated ULK complex that contains the UNC51-like Ser/Thr kinases ULK1 (ATG1 orthologues), ATG13 and FIP200 (Focal Adhesion Kinase-family-interacting protein of 200 kDa, ATG 17 orthologue), and ATG101, is forming the autophagy initiation complex. (Ganley et al., 2009; Hara et al., 2008; Hosokawa et al., 2009; Jung et al., 2009). This autophagy initiation complex is regulated by one major regulator of autophagy namely the MTORC1 (mammalian target of rapamycin complex 1) kinase complex that bind with the autophagy initiation complex (Figure 18). The mTORC1 complex is formed by 5 proteins: mTOR (mammalian target of rapamycin), RAPTOR (regulatory-associated protein of mTOR), mLST8 (mammalian lethal with SEC13 protein), DEPTOR (DEP domain-containing mTOR-protein) and PRAS40 (40 kDa Pro-rich AKT substrate) (Saxton and Sabatini, 2017). In basal condition mTORC1 complex is activated and phosphorylate ULK1/2, ATG13, acting as a negative regulator inactivating them. However, under starvation mTORC1 complex dissociates from the ULK1 complex resulting in dephosphorylation at these sites and induction of macroautophagy (Hosokawa et al., 2009; Jung et al., 2009). Part of the complex, ATG101 (encoded by *C12ORF44)*, stabilizes ATG13, protecting it from proteasomal degradation (Mercer et al., 2009).

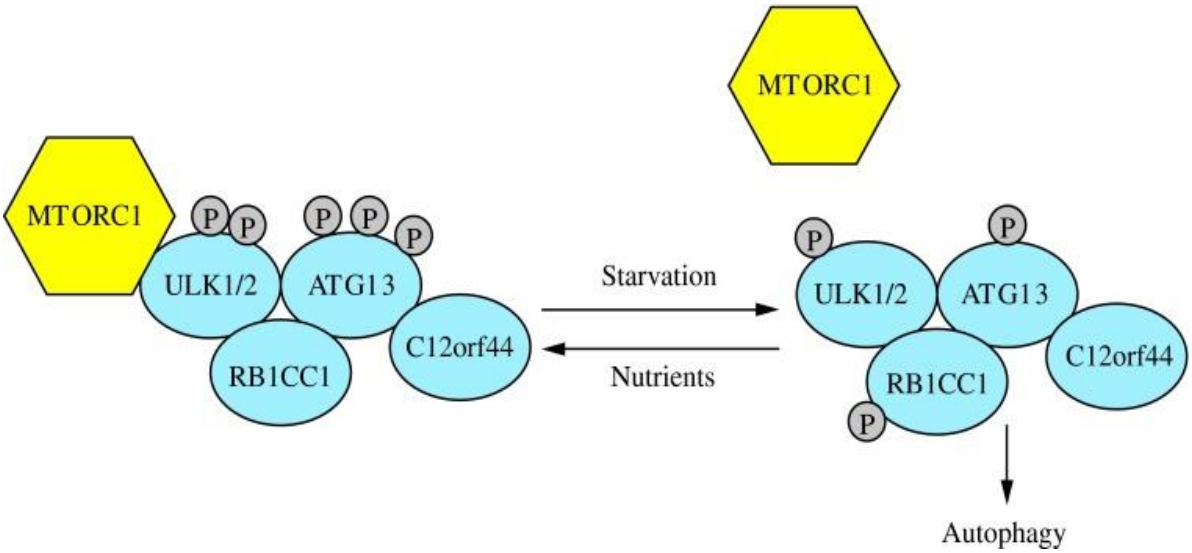


Figure 18 The induction complex consists of ULK1/2, ATG13, RB1CC1 and ATG101.

Under nutrient-rich conditions, MTORC1 associates with the complex and inactivates ULK1/2 and ATG13 through phosphorylation. During starvation, mTORC1 dissociates from the complex and ATG13 and ULK1/2 become partially dephosphorylated by ,as yet, unidentified phosphatases, allowing the complex to induce macroautophagy (Parzych and Klionsky, 2014).

Interestingly, in 2008 two teams identified four small GTPase called Ragulator-RAG complex (RAG), namely RAG A,B,C and D (Kim et al., 2008; Sancak et al., 2008). Briefly, the RAG GTPases sense amino acid levels and form heterodimers, where RAGA or RAGB binds to RAGC or RAGD, to recruit mTORC1 to the lysosome where it becomes activated. In amino acid-rich conditions, the 'active' RAG GTPase heterodimer (GTP-bound RAGA/B and GDP-bound RAGC/D) recruit mTORC1 from an unknown location to the lysosome (Groenewoud and Zwartkruis, 2013). Once at the lysosome mTORC1 encounters the small GTPase Ras homolog enriched in brain (Rheb), Rheb increases the catalytic activity of mTORC1 and results in mTORC1 activation (Long et al., 2005). RAG GTPase act as preliminary amino acids sensors to activate/inactivate mTORC1 and thus initiate autophagy (Figure 19).

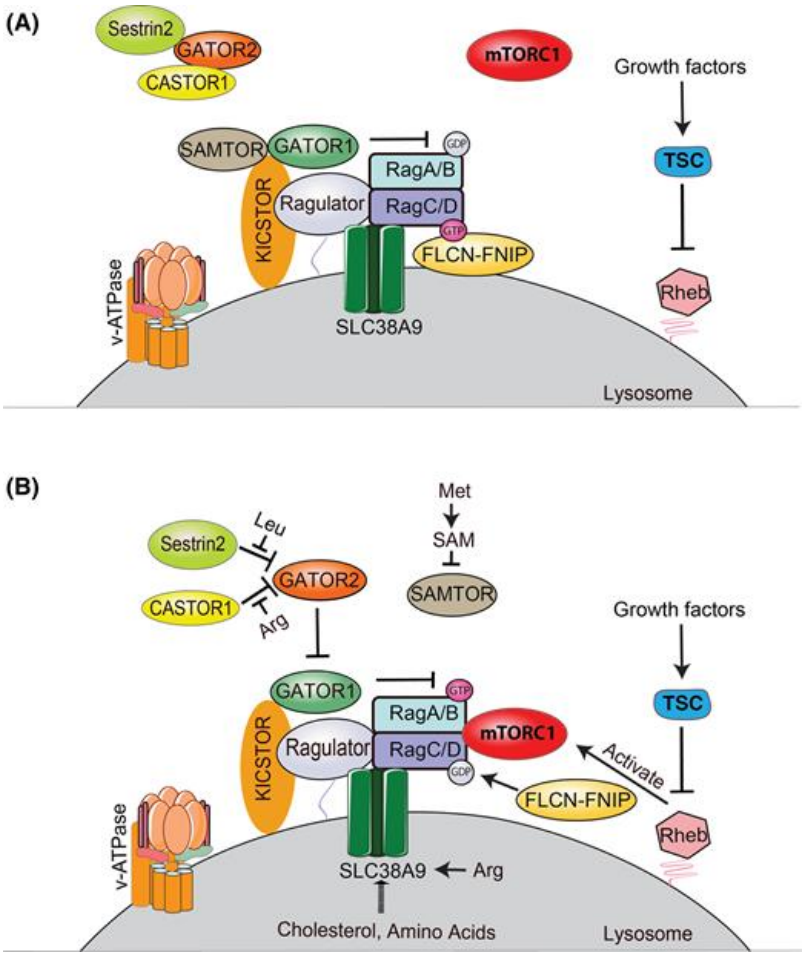


Figure 19 mTORC1 regulation by RAG GTPases

(**A**) In absence of amino acids GATOR1 negatively regulates activation of RAG GTPase. Sestrin2 and CASTOR1 interacts with GATOR2 to prevent its inhibition towards GATOR1. (**B**) In presence of amino acids folliculin and its associated proteins (FLCN–FNIP) acts as a GAP for RAGC/D and GATOR2 inhibits GATOR1 GAP activity for RAGA/B. The active RAG GTPase (when GTP-bound RAGA/B forms a complex with GDP-bound RAGC/D) heterodimer interacts with mTORC1 and recruits it to the lysosome subsequently promoting its activation by Rheb (Lama-Sherpa et al., 2023).

Furthermore, autophagy can also be promoted by AMP activated protein kinase (AMPK), which is a key energy sensor and regulates cellular metabolism to maintain energy homeostasis. For example, under glucose starvation, AMPK promotes autophagy by directly activating ULK1 through phosphorylation of Ser 317 and Ser 777 (Figure 20) (Kim et al., 2011).

After mTORC1 dissociation and ULK1 initiation complex auto-activation, the PI3KC3 nucleation complex (class III phosphatidylinositol 3-kinase complex 3) will be recruited (Figure 20). This complex is composed of VPS15, VPS34 (vacuolar proteins sorting 15 and 34), BECN1 (Beclin 1), ATG14 and AMBRA1 (activating molecule in Beclin-1 related autophagy 1 protein). ULK1 is able to phosphorylate AMBRA1 and BECN1, two interacting protein that will regulate PI3KC3 complex. Indeed, regulation of the PI3KC3 complex occurs largely through proteins that interact with BECN1 like AMBRA1 which is a positive regulator of the complex.

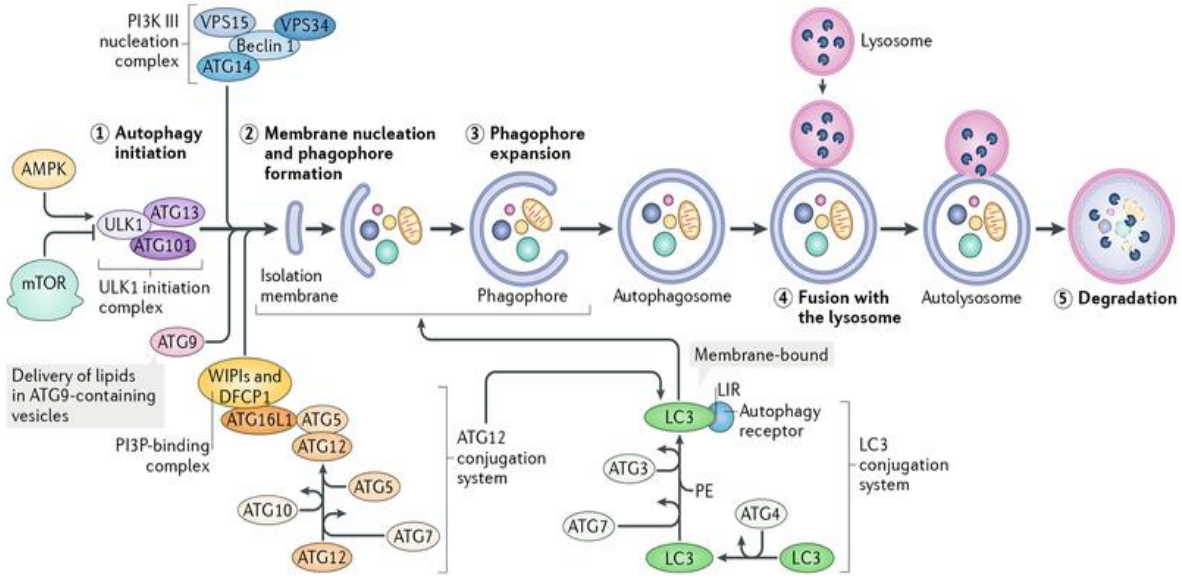


Figure 20 Schematic representation of the protein involved in the autophagic signaling pathway

Initiation involves the ULK1 complex which phosphorylates and activates the PI3KC3 complex which allows the generation of PI3P. These PI3Ps recruit the DFCP1 and WIPI proteins which will allow, via the intervention of the conjugation systems and the anchoring of the LC3 proteins to the autophagosome. This mature autophagosome then fuse to a lysosome where its contents is degraded (Hansen et al., 2018).

A negative regulator of autophagy is the antiapoptotic protein BCL2 that binds BECN1 and prevents its interaction with PIK3C3; thus, inhibiting macroautophagy (Liang et al., 1999; Mercer et al., 2021). Once dissociated and BECN1 phosphorylated, it will activate VPS34 that will generates PtdIns3P (Phosphatidylinositol-3-phosphate) at the membrane of the ER, which is required for initiating the nucleation: the process of autophagosome formation, by generating isolation membrane (Di Bartolomeo et al., 2010; Mercer et al., 2021; Russell et al., 2013). Another protein, UV Radiation Resistance Associated (UVRAG) promotes autophagosome formation in vitro by associating with Beclin-1 and up-regulating class III phosphatidylinositol 3-kinase activity (Liang et al., 2008). However, study found that siRNA knockdown of UVRAG in HeLa cells does not affect macroautophagy (Itakura et al., 2008). Furthermore, very little is known about upstream events regulating the constituents of the various PI3KC3 complexes.

#### 2.4.2.2.2 Elongation and maturation

WD-repeat protein Interacting with PhosphoInositides (WIPI's) and Double FYVE-containing protein 1 (DFCP1) associate with phagophore by binding to PtdIns3P at the omegasome, the site in the ER where the phagophore comes from, engendering the formation of the double membrane and elongation of the phagophore (Figure 20, Figure 21) (Roberts and Ktistakis, 2013). Indeed WIPI4 recruits ATG2 and ATG9 to respectively transports phospholipids from ER to the cytoplasmic leaflet of IM (isolation membrane) and to transports phospholipids between the cytoplasmic and luminal leaflets of IM (Chowdhury et al., 2018; Kotani et al., 2018; Matoba et al., 2020; Sawa-Makarska et al., 2020; Valverde et al., 2019). Altogether this leads to enables IM expansion for autophagosome formation.

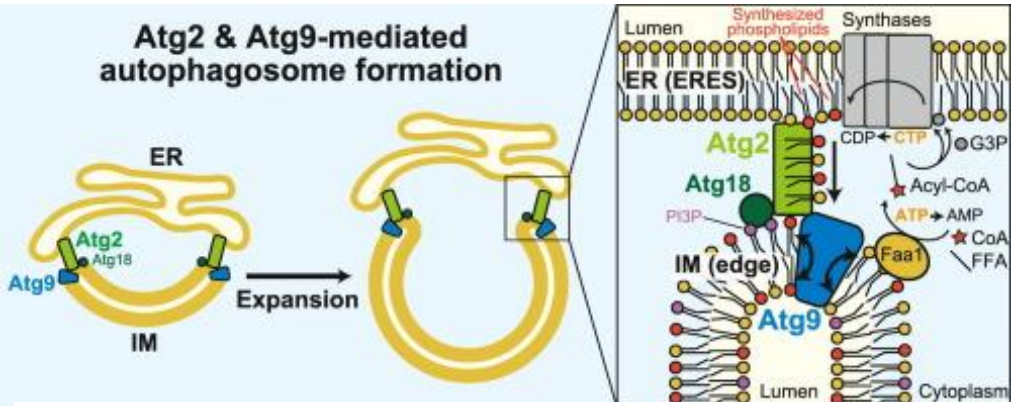


Figure 21 ATG2 and ATG9 role in autophagosome formation

ATG2 and ATG9 respectively transports phospholipids from ER to the cytoplasmic leaflet of IM (isolation membrane) and transports phospholipids between the cytoplasmic and luminal leaflets of IM in order to induce IM expansion for autophagosome formation (Noda, 2021).

Furthermore, two conjugation systems involving ubiquitin-like (UBL) proteins will contribute to the expansion of the phagophore. The first one is the Atg12–Atg5-Atg16L1 complex recruited by WIPI2 by its interaction with ATG16L. ATG12 is bind to ATG5 in an ATG7 an E1 type activator protein and, ATG10, an enzyme of E2-type conjugation dependent manner. Then ATG16L1 dimerizes and allows association with the phagophore, promoting membrane expansion (Figure 20) (Hamasaki et al., 2013; Kim et al., 1999; Mizushima et al., 2003).

The second UBL system involved in phagophore expansion is the Atg8/LC3 system. The Atg8/MAP1LC3 (microtubule associated protein 1 light-chain 3, hereafter referred to as LC3) conjugation system is required for elongation and maturation of the autophagosome. ATG8/LC3 is then cleaved by ATG4 protease to expose a C-terminal glycine residue. Cleaved LC3 is then conjugated to phosphatidylethanolamine (PE) by sequential activation of Atg7 (E1-like enzyme), Atg3 (E2-like enzyme), and the Atg12 complex, to generate LC3-PE (a membrane-bound form of LC3 also referred to as LC-II), the level of which is known to be correlated with the number of autophagosomes (Figure 20). However, it is important to note that there is several mammalian ATG8 orthologs classified into the LC3, GABARAP (γ-aminobutyric acid receptor-associated protein), and GABARAPL (γ-aminobutyric acid receptor-associated protein like) subgroups with LC3 largely studied among the other (Lee and Lee, 2016; Lystad et al., 2019).

#### 2.4.2.2.3 Autophagosome completion and fusion

The last step of autophagy is when the completed autophagosome traffics, with the help of microtubules and RAB GTPases including RAB7, fuse with a lysosome and form the autolysosome (Figure 20) (Gutierrez et al., 2004; Monastyrska et al., 2009). Fusion is mainly mediated by the Homotypic fusion and protein sorting (HOPS) complex composed of six subunits (Vps11, Vps16, Vps18, Vps39, and Vps41) and several SNARE proteins. Indeed, HOPS binds small membrane-associated GTPases and assembles SNAREs for fusion like Syntaxin-17 (STX17), Vesicle-associated membrane protein 3 and 7 (VAM3P, VAM7P), and VTI1P in order to enhance the efficiency of fusion (Fader et al., 2009; Jahn and Scheller, 2006; Jiang et al., 2014; Y. Wang et al., 2016). After fusion, hydrolytic lysosomal enzymes are activated and degrade both the luminal content of the autophagosomes and its inner membrane. This will allow the formations of new metabolites that will be recycle back to the cytoplasm for being reused.

### 2.4.2.3 Selective and non-selective autophagy

There can be a distinction between selective and non-selective autophagy. Nonselective autophagy is used for the turnover of bulk cytoplasm under starvation conditions (privation of nutrient), whereas selective autophagy specifically targets damaged or superfluous organelles, including mitochondria and peroxisomes, as well as invasive microbes (Jin et al., 2013). However selective macro-autophagy utilizes the same core machinery used for nonselective macro-autophagy (Figure 22). Everything starts with ubiquitin, a small protein consisting of 76 amino acids, found in all tissues of eukaryotic organisms. Ubiquitin acts as a modifier by covalent attachment to cellular proteins. This process of tagging a protein with ubiquitin is called ubiquitination and is known to regulate and control physiological and pathological cellular event (Shaid et al., 2013). Under normal (nutrient-rich) conditions basal autophagy serves as an intracellular quality control system: protein aggregates including damaged or redundant organelles are selectively eliminated. However, the exact mechanism of cargo recognition is still poorly understood but is clearly linked to ubiquitination. However, we know that selectivity is ensured by target-specific autophagy receptors that form a bridge between the ubiquitylated cargo and LC3 component of autophagic membranes encouraging the phagophore to expand around autophagic substrates (Turco et al., 2020).

P62, nuclear dot protein 52 (NDP52), Tax1 Binding Protein 1 (TAX1BP1) and OPTN are autophagic receptors that can recognize ubiquitin (Bussi et al., 2018; Koerver et al., 2019; Papadopoulos et al., 2017; Thurston et al., 2012; Yoshida et al., 2017). Recently, TBK1 was identified to play a crucial role by binding and phosphorylates autophagy receptors OPTN and p62. Thus, it enhances the ability of the receptors to bind ubiquitinated residues on target cargo and LC3-II to be recruited to the phagophore for degradation (Oakes et al., 2017).

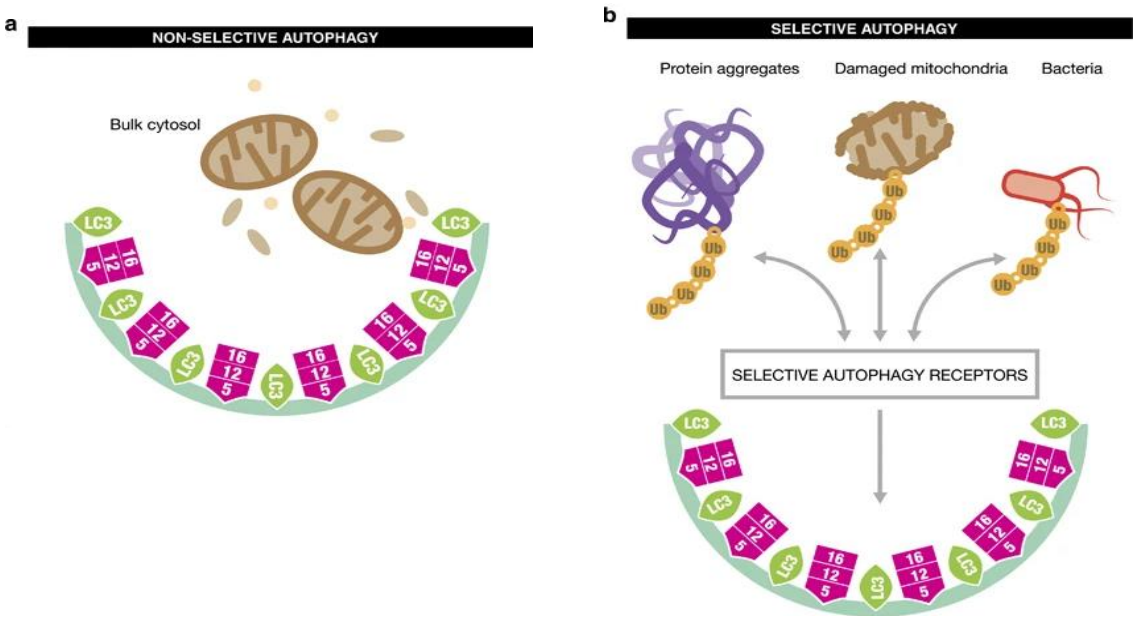


Figure 22 Non-selective autophagy and selective autophagy

(**a**) Non-selective autophagy is used for the turnover of bulk cytoplasm under starvation conditions (privation of nutrient). (**b**) Selective autophagy is dependent of ubiquitinated protein recognize by autophagic receptors that will recruit autophagic machinery (Adaptation from (Shaid et al., 2013)).

Selective autophagy and Ubiquitin–proteasome system (UPS) are two tightly linked degradation process and are often working together despite two different regulation pathways. Indeed, under certain conditions the capacity of the chaperone-mediated refolding machinery and the UPS is overloaded, protein aggregation occurs, which are then targeted for autophagic clearance (Shaid et al., 2013). Furthermore most short-lived proteins and soluble misfolded proteins are degraded by UPS, whereas long-lived proteins, insoluble protein aggregates, whole organelles (such as mitochondria, peroxisomes) and intracellular parasites are mostly destroyed by autophagy (Kocaturk and Gozuacik, 2018).

Interestingly, some mutations in the *OPTN*, *UBIQUILIN* 2 (UBQNL2), *SQSTM1* (coding for the p62 protein), and *TBK1* genes are associated with ALS and FTD (Cirulli et al., 2015; Deng et al., 2011; Fecto et al., 2011; Freischmidt et al., 2015; Maruyama et al., 2010). Accumulation of toxic protein aggregates is a hallmark of several common human diseases, so-called protein misfolding disorders or proteinopathy. Autophagy malfunction has currently been found in a number of human disorders, such as cancer and neurodegenerative illnesses like ALS. Its modulation has great promise as a therapeutic strategy. There will be described in 3.2.

In the past few years early stages of the autophagy have been largely studied and described. However, the molecular mechanisms underlying the function of lysosomes, for example lysosome consumption and regeneration after autolysosome formation, have received less attention.

#### 2.4.2.4 Autophagic Lysosome Reformation (ALR)

##### 2.4.2.4.1 Overview of ALR

Quite recently Yu et al discover that the number of lysosomes were reduced after 4h of starvation but slowly recovered after 12 h in different cell lines (Yu et al., 2010). Thanks to microscopy analyses they found that long tubular structure extended from autolysosomes and formed new vesicles. Theses vesicles were positive for LAMP-1 and negative for autophagosome marker LC-III. This new process of lysosome regeneration has been called ALR (Autophagic Lysosome Regeneration).

#### 2.4.2.4.2 Regulation of ALR

Previous chapter described that in basal condition mTORC1 complex is activated and phosphorylate ULK1/2 and ATG13, acting as a negative regulator inactivating them. However, under starvation mTORC1 complex dissociates from the ULK1 complex resulting in dephosphorylation at these sites and induction of macroautophagy (Hosokawa et al., 2009; Jung et al., 2009). But after prolonged starvation and multiple release of metabolites due to degradation of the autophagosome, the levels of amino acids will rise and thus reactivate mTORC1 to avoid excessive degradation and maintained the number of cellular lysosomes by ALR (Figure 23) (Yu et al., 2010).

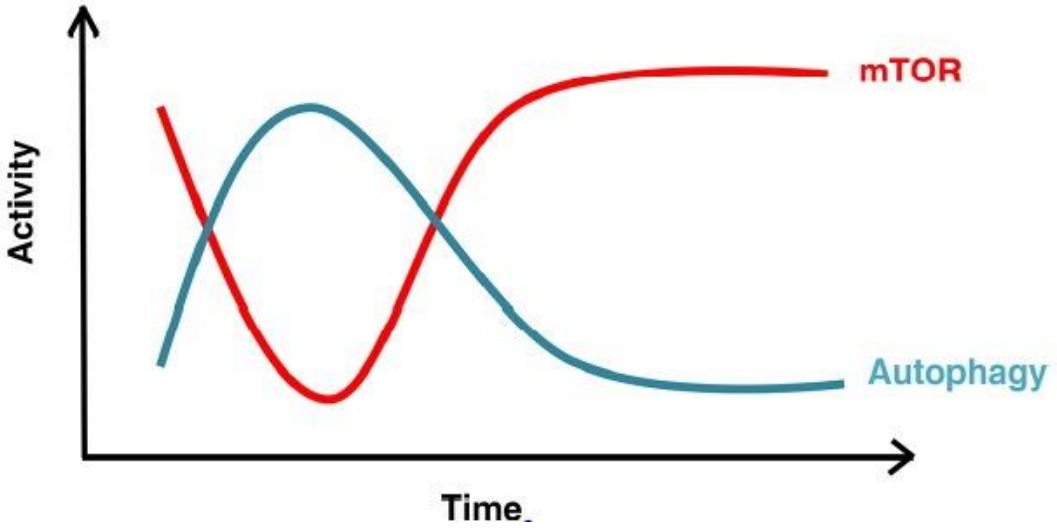


Figure 23 Correlation between mTOR activity and autophagy during starvation

During amino acids deprivation mTOR dissociate from ULK1 complex to induce autophagic pathway. After prolonged starvation mTOR is reactivated and thus prevent excessive degradation and promote ALR (Chen and Yu, 2018).

#### 2.4.2.4.3 Molecular pathways of ALR

Autolysosome membrane remodeling during ALR is controlled by the transient and reversible generation of a suite of membrane-bound phosphoinositide's (Figure 24-A). Indeed, PtdIns3P is generated from PtdIns by the class III phosphoinositide 3-kinase complex that includes PIK3C3/VPS34 (Hirst et al., 2021; Munson et al., 2015). PtdIns4P from PtdIns is controlled by the phosphatidylinositol 4-kinases PI4K2A (Khundadze et al., 2021) or PI4KB/PI4K3B (Sridhar et al., 2013). In turn, PtdIns4P serves as a substrate for the synthesis of PtdIns(4,5)$P_2$ by the PtdIns4P-5kinases, PIP5K1A or PIP5K1B (Du et al., 2016; Rong et al., 2012).

Interconversion between PtdIns(4,5)$P_2$ and PtdIns4P on autolysosome membranes is important for ALR, whereby PtdIns(4,5)$P_2$ is hydrolyzed by the inositol polyphosphate 5-phosphatase INPP5K to form PtdIns4P (Eramo et al., 2021).

Membrane dynamics control by these phosphoinositide's will allow structural changes and thus the recruitment of specific effector proteins. First the Adaptator protein 2 (AP-2) Clathrin complex will stimulate membrane budding (Traub et al., 1996). Then, Kinesin Family Member 5B (KIF5B) mediated the generation of the reformation tubules at the sites of the clathrin buds by providing a pulling force along microtubules (Du et al., 2016). Finally, when the tubules has reach the proper size, Dynamin 2 (DNM2) will be recruited and will drive the scission of the tubule to form the protolysosome (Schulze et al., 2013). The hereditary spastic paraplegia protein complex AP-5-SPG11-SPG15-ZFYVE26, is also recruited to autolysosomes via ZFYVE26 binding to PtdIns3P and is required for ALR (Figure 24-B) (Chang et al., 2014).

Interestingly, various diseases notably neurodegenerative disorders showed alteration of autophagic lysosome reformation. For example, in Parkinson Disease (PD) a single nucleotide polymorphism at the GAK locus has been reported as a risk factor for Parkinson's disease (PD) and that GAK knockout (KO) in A549 cells impaired autophagosome-lysosome fusion and autophagic lysosome reformation resulting in accumulation of enlarged autophagosome and autolysosome. Furthermore lysosome recycling by ALR was impaired in neurons so that there were not enough functional lysosomes to sustain autophagic clearance of α-synuclein causing PD (Miyazaki et al., 2021). It has also been reported in Hereditary Spastic Paraplegias (HSPs), disease that involves weakness and spasticity, which is stiffness of the legs. SPG11 and SPG15 have a similar clinical course and together are the most prevalent autosomal recessive HSP entity (Pensato et al., 2014).

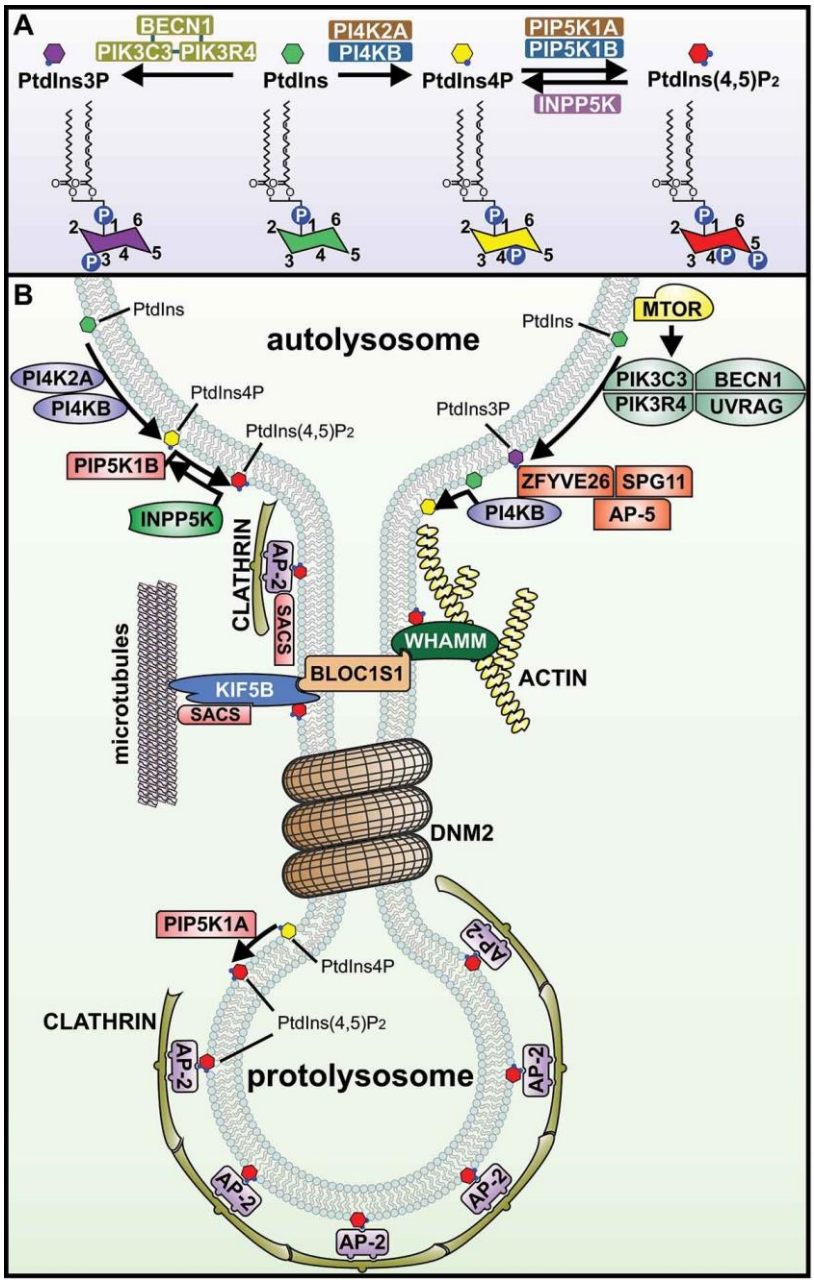


Figure 24 Membrane-bound phosphoinositides pathway and schematic representation of ALR

(**A**) Autolysosome membrane remodeling during ALR is controlled by the transient and reversible generation of a suite of membrane-bound phosphoinositides. (**B**) The formation of new lysosome is regulated by various proteins and is so called Autophagic Lysosome Regeneration (ALR) (Nanayakkara et al., 2023).

These two respective proteins play a role for macroautophagy/autophagy and autophagic lysosome reformation (ALR). Indeed, mutation in these two proteins engender various molecular disorder. For example, it will prevent ALR initiation downstream of mTOR reactivation, has an effect on PtdIns3P-dependent ALR functions and also impaired regulation of PtdIns4P, altering CLATHRIN and DNM2 association with autolysosome reformation tubules during ALR. Furthermore, *Spg11* and (*zinc finger FYVE-type containing 26*) *Zfyve26* KO mice developed motor impairments (Chang et al., 2014; Khundadze et al., 2021; Maruyama et al., 2010; Oakes et al., 2017; Stevanin et al., 2007; Varga et al., 2015).

#### 2.4.2.5 Potential role of C9ORF72 in autophagy

##### 2.4.2.5.1 Autophagy defect in neurodegenerative diseases

As previously described, the accumulation of cytoplasmic aggregates is one the pathological hallmarks of various neurodegenerative diseases including mutant α-synuclein in Parkinson disease (PD), Aβ and C-terminal fragments of the amyloid precursor protein (APP) in Alzheimer disease (AD), pathogenic mutant huntingtin (mHtt) in Huntington disease (HD), and mutant SOD1 (superoxide dismutase 1) as well as TDP-43/TARDBP (TAR DNA binding protein) in amyotrophic lateral sclerosis (ALS) (Deng et al., 2017; Menzies et al., 2017). These aggregates impair diverse neuronal functions like axonal transport, synaptic integrity, mitochondrial bioenergetic machinery or the regulation of transcription (Batool et al., 2019; Dugger and Dickson, 2017; Ruegsegger and Saxena, 2016). Aggregates should typically be removed by the autophagy-lysosome pathway, but this is frequently not the case. This raises the possibility that autophagy malfunction plays a part in neurological disorders. Indeed, in this instance, protein aggregation is simply a direct consequence of a malfunction in a process that regulates the clearance of proteins, including autophagy (Levine and Kroemer, 2008). Furthermore, not only the proteinopathy of the abnormal proteins has been identified as a major pathological feature in ALS, but also the abnormal accumulation of functional proteins like TDP-43 (Arai et al., 2009; Neumann et al., 2006), SOD1 (Forsberg et al., 2010; Paré et al., 2018; Watanabe et al., 2001) and SQSTM1/P62 (Arai et al., 2003; Hiji et al., 2008; Mizuno et al., 2006) reinforcing the idea that one or multiple clearing mechanisms are faulty (Menzies et al., 2017).

Consistent with previous explanations, gene mutations in various autophagic receptors are closely associated with neurodegenerative diseases e.g., *SQSTM1* (*sequestosome 1*), *OPTN* (*optineurin*), *NBR1* (*neighbor of BRCA1 gene 1*), *TANK binding kinase 1* (*TBK1*) (Deng et al., 2017; Oakes et al., 2017; Rayner et al., 2021; Renton et al., 2014).

#### 2.4.2.5.2 Is C9ORF72 ALS caused by a defect of autophagy?

C9ORF72 and more precisely C9ORF72-SMCR8-WDR41 complex has been largely described to potentially regulate membrane trafficking and autophagy at various steps.

The first autophagic function of C9ORF72 was described in *C9orf72* KO mice which exhibited increased levels of autophagic components like LC-III but also dysregulation of mTORC1 (O'Rourke et al., 2016; Sullivan et al., 2016; Ugolino et al., 2016). Furthermore, a systematic proteomic analysis of the human autophagy system or co-IP revealed SMCR8 as an interacting protein of FIP200 (Behrends et al., 2010; Sullivan et al., 2016; Webster et al., 2016). FIP200 is part of the ULK1 kinase complex and is currently one of most upstream regulators of the autophagic pathway. Furthermore, C9ORF72-SMCR8-WDR41 complex shows an interaction with ULK1 which was enhanced during starvations (Sellier et al., 2016; Webster et al., 2016; Yang et al., 2016). The activity of the CSW complex appears to be regulated, after the initiation of autophagy, in particular by phosphorylation. Indeed, the SMCR8 protein is phosphorylated on many amino acids by various kinases involved in autophagy including ULK1 ( (Behrends et al., 2010; Sellier et al., 2016), TBK1 (Sellier et al., 2016), mTOR (Hsu et al., 2011) and AMPK (Hoffman et al., 2015).

In addition, numeral studies observed that CSW complex colocalize at the lysosomes and that the colocalization is enhanced during starvation (Amick et al., 2020, 2018, 2016; Sullivan et al., 2016). Interestingly, multiple alterations of lysosomes have been described after depletion of *C9ORF72*, including alterations of their biogenesis in motor neurons differentiated from iPS cells of C9-ALS/FTD patients (Shi et al., 2018), alterations in their size and localization in HeLa cells (Amick et al., 2016), in their number in mouse embryonic fibroblasts (MEFs) developed from knockout mice for *C9orf72* (Ugolino et al., 2016) and their acidification into macrophages purified from *C9orf72* or *Smcr8* KO mice (Shao et al., 2020).

Interestingly, recent paper also show the potential role of C9ORF72 which associate with RAG GTPases and thus regulates mTORC1 who himself interact with ULK1 kinase complex (Wang et al., 2020). Interestingly, folliculin and its associated proteins (FLCN–FNIP), which present same characteristic DENN domain as C9ORF72 and SMCR8, also interact with RAG GTPase mainly acting as a GAP for RAGC/D (Tsun et al., 2013). Thus, several studies have reported that depletion of C9ORF72 or SMCR8 does not modify the localization of mTOR but modifies its activity. Indeed, the CSW complex appears to be required for mTOR activation, suggesting that C9ORF72 is a negative regulator of autophagy (Amick et al., 2018; Ugolino et al., 2016; Wang et al., 2020). As described before, bioinformatics analysis based on sequence alignment shows that C9ORF72 and SMCR8 contains N-terminal longin domain, followed by DENN, and d-DENN domains characteristic of DENN proteins "Differentially Expressed in Normal and Neoplastic cells", known to regulate the GDP/ GTP exchange cycle of RAB/ARF proteins (Levine et al., 2013; Zhang et al., 2012). And in fact, CSW complex has been described to interact, but not limited, with RAB8a and RAB39b (Sellier et al., 2016; Yang et al., 2016), RAB1a (Webster et al., 2016) and/or RAB5 (Farg et al., 2014; Shi et al., 2018), known to regulate autophagy.

This non-exhaustive list enlightens the potential role of CSW in autophagy and demonstrated the complexity of the role of CSW complex in ALS and in autophagy regulation. These results suggest that CSW complex present a crucial role in the regulation of the autophagic machinery and/or at the lysosome. However, it is not clear on how the complex regulate autophagy, at which step and if the interaction with the autophagic regulator are direct or not.

Next part will be devoted to the current ALS treatment and therapies that were approved or that are still under trial.

# 3. ALS and treatments: where is the current state?

To date ALS is an incurable disease. Finding a good treatment to slow down or even stop illness progression is still difficult because the precise underlying causal pathological pathway is uncertain and potentially heterogeneous. Drugs currently approved for ALS treatment differs from country and are currently very limited: the glutamate antagonist Riluzole, the antioxidant Edaravone, and the recently introduced Sodium phenylbutyrate/Taurursodiol. However, they just slowdown the disease progression and allowed to prolong autonomy and increase survival by few months. Recent breakthroughs, especially in the field of targeting genetic disease forms, raise hope for improved care and therapy for ALS patients. We will aim to summarize some of ALS therapies.

## 3.1 Current medical treatment

### 3.1.1 Riluzole

Riluzole (6-(trifluoromethoxy)-2-aminobenzothiazole) was the only medication used to treat ALS patients for a very long time. The main goal of the targeted pathway was to lessen excitotoxicity, particularly glutamate's excitotoxicity (Albo et al., 2004; Fumagalli et al., 2008; He et al., 2002; Kretschmer et al., 1998; Theile and Cummins, 2011). Riluzole was approved by the FDA (Food and Drug Administration) in 1995 and subsequently the EMA (European Medicines Agency) in 1996. In the initial investigation, 155 people took part in a prospective, double-blind, placebo-controlled experiment to examine the use of Riluzole in the treatment of ALS. A considerable delay in the course of the disease was observed after a year of treatment (Bensimon et al., 1994). These findings were validated in 1996 by a second, multicenter, double-blind, placebo-controlled research with 959 patients (Lacomblez et al., 1996). Both studies indicated a survival benefit of two to three months. Real-world assessments, however, point to a bigger survival benefit of up to 19 months (Andrews et al., 2020). Most importantly, the study was able to identify Riluzole as a generally well-tolerated drug and determined the side effects, including asthenia, nausea, gastrointestinal problems, as well as augmentation in hepatic enzymes.

### 3.1.2 Edaravone

No new medication reached the market after Riluzole's approval for several years, until Edaravone (3-methyl-1-phenyl-2-pyrazoline-5-one) was approved in Japan and South Korea in 2015. Following Switzerland's and China's NMPA admissions in 2019 and 2020, Indonesia in 2020, and Malaysia and Thailand in 2021. The FDA approved the product in 2017. Edaravone was created to lessen oxidative stress and the neuroinflammatory response by scavenging free radicals (Ikeda et al., 2015; Watanabe et al., 2001; Yamamoto et al., 1997) and has been utilized in acute-phase stroke management for years in Japan (Watanabe et al., 2018). Its use in ALS treatment is based on a randomized, double-blind, placebo-controlled phase III trial with 137 participants (Writing Group and Edaravone (MCI-186) ALS 19 Study Group, 2017). Inclusion criteria allowed only participants with early stage ALS. Results from this second phase III trial were a 33% reduction of ALSFRS-R (ALS Functional Rating Scale Revised). Prior to that, a previous phase III trial had not shown any significant overall effect of this drug (Abe et al., 2014). Further studies did not yield significant effects, again (Lunetta et al., 2020; Witzel et al., 2022). These results partially explain why Edaravone has not been validated by the EMA yet. Typical side effects of Edaravone treatment were bruising, gait disturbances, headaches, and skin conditions.

### 3.1.3 Sodium Phenylbutyrate and Taurursodiol

Most recently, Sodium Phenylbutyrate and Taurursodiol (also known as PB-TURSO or PB-TUDCA [tauroursodeoxycholic acid] (Sodium 4-pheylbutanoate and 2- [(3α, 7β-dihydroxy-24-oxo-5β-cholan-24-yl) amino] ethane sulfonicacid, dihydrate) have been released in combination.Both drugs were previously licensed for medical use independently and are currently recognized as safe and effective by the FDA and Canada. Taurursodiol has a position in the treatment of chronic cholestatic liver illnesses (Hofmann, 1999), whereas sodium phenylbutyrate can be utilized to treat hyperammonemia brought on by urea-cycle disorders (Peña-Quintana et al., 2017). Both have been identified as inhibitors of neuronal apoptosis and their combined action is proposed to reduce neuronal cell death and oxidative stress by decreasing stress in the endoplasmic reticulum (ER) and mitochondrial dysfunction (Del Signore et al., 2009; Dionísio et al., 2015; Kusaczuk, 2019; Ryu et al., 2005).

FDA approved the product based on the findings of a phase II multicenter, randomized, double-blinded trial (CENTAUR), which evaluated the safety and effectiveness of a fixed-dose combination in 137 people (Paganoni et al., 2022, 2021, 2020). In comparison to the placebo group, the two combine drugs significantly reduced the course of the disease by about 25%. Most frequent side effects were upper respiratory tract infections, diarrhea, and abdominal pain.

Actually, various trials are under investigation to assess their efficacity in ALS treatment. However, the following description is a non-exhaustive list as the field is expanding very quickly. Furthermore, several different techniques and targeted pathway are studied which will not especially be developed here. However, ongoing trials are here divided in three different groups with: (A) development of small molecules, (B) gene-specific therapies and (C) stem-cell therapies.

## 3.2 Development of small molecules

As exposed in part 1.8, ALS could be caused by various genetic causes engendering the disorganization of several pathways. In accordance with it, several small molecules are currently study to directly influence theses dysregulated pathway associated with ALS.

A main mechanism in treatment with Riluzole is targeting excitotoxicity. Other surprising drugs are under investigation for this pathway. For instance, cannabinoids are utilized as a symptomatic treatment for ALS because they could reduce spasticity. MediCabilis CBD Oil (NCT03690791) was tested in a single-center phase III clinical trial in a small sample of participants in Australia to further evaluate a possible disease-modifying effect (Meyer et al., 2019). Oxidative stress, which is the main pathway targeted by Edaravone and Sodium Phenylbutyrate/Taurusodiol shows some other promising results like a phase II/III trial of the medication trazodone, which is licensed for the treatment of depression, is being conducted as a component of the multiarm MND-SMART trial (NCT04302870). Trazodone was also associated with a decreased production of toxic proteins (Westergard et al., 2019). Neuroinflammation is another pathway that had interest in and had two potential new compound that were recently stopped in phase II/III due to their lack of benefit in ALS patients.

Zilucoplan (NCT04436497), stopped in mid of June 2020, and Ravulizumab (NCT04248465), stopped in January 2023.

However, some new insight with Triumeq (NCT05193994) are giving new hopes. Dolutegravir, abacavir, and lamivudine are three HIV therapy drugs that have been repurposed for use in treating ALS. They were chosen for their anti-inflammatory and anti-HERV (human endogenous retroviruses) antiviral properties (Gold et al., 2019). Neuronal cell death has also been investigated to cure ALS. A neurotrophic factor necessary for the growth of the nervous system, insulin-like growth factor-1 (NCT00035815) has been demonstrated in animal models and cell culture systems to protect neuronal cells (Dobrowolny et al., 2005; Dodge et al., 2010; Lepore et al., 2007; Lin et al., 2018). A phase III research that lasted for two years, however, found no effect for ALS patients in terms of survival time or muscular weakness (Sorenson et al., 2008).

Very interestingly boosting autophagy and direct action on protein aggregation are some of the paths pursued in alternative approaches. Autophagy has been described as playing a huge role in ALS notably as playing a double hit mechanisms were dysregulation of autophagy and accumulation of protein aggregates could potentially cause the disease (Boivin, 2020). When targeting autophagy different parameters has to be considered. Indeed, the stage of the disease, which is not easy to establish, can play a huge role. Genetic inhibition of autophagy in mutant Sod1 mice's motor neurons showed that autophagy can be protective early in the course of disease but harmful later in the course of disease (Rudnick et al., 2017). The stage of the disease is likely to reflect variations in the pathogenic substrates accumulating in the affected tissues, such as aggregates, inclusions, protofibrils, fibrils, aggregates, and soluble and insoluble misfolded proteins, oligomers, protofibrils, and fibrils, which may alter the capacity and efficiency of autophagy in cells. Among molecules targeting autophagy, three classes stand out: those mTOR-dependent autophagy activators, such as rapamycin and its derivatives; AMPK-activating acting on AMPK, such as metformin; and those activating autophagy independently of such as trehalose, verapamil, loperamide, clonidine and calpastatin. However, drugs targeting autophagy shows mitigated results.

Rapamycin administration to mice with a mutation in the *Tardp* gene mice gene improved their general condition, with a diminution of neuronal death (R. Wang et al., 2017).

In addition to rapamycin, torkinib, a second mTOR inhibitor, improved the phenotype of primary neuronal cultures and *Drosophila* expressing a mutated version of the FUS protein involved in ALS, suggesting that activation of autophagy could nonetheless be a possible therapeutic target (Marrone et al., 2019, 2018). Also the immunosuppressive effects of rapamycin can offset its positive effects, which could account for why *Sod1* mice without mature lymphocytes have increased survival relative to *Sod1* mice with an intact immune system (Staats et al., 2013). However, to date, no clinical trials are under investigation has targeting mTORC1 in autophagy isn't especially a good idea. Indeed, mTORC1 Is a master regulator of autophagy initiation but also all the linked to numerous pathways like protein synthesis, immunosuppression, cell cycle, and many more.

Concerning AMPK, this kinase responds to the cell's energy level (AMP) and induce autophagy when energy levels are low. Metformin, a stimulator of AMPK stimulator, is used as an antidiabetic and is described as improving the phenotype of FXS and HD mice respectively caused by CGG and CAG repeat expansions (Arnoux et al., 2018; Gantois et al., 2017). The addition of metformin to the water of mice expressing GGGGCC repeat expansions of the *C9orf72* gene results in an expression of DPR proteins and improved locomotor abilities in mice. Parallel to these good results other therapeutic trials that target MTOR-independent autophagy showed interesting results like trehalose (NCT05136885), a disaccharide, is being investigated as one of them in a phase II/III trial in the USA as part of the HEALEY ALS Platform Trial (Castillo et al., 2013; Li et al., 2015). In mice, it can increase autophagy and reduce Sod1 mutant aggregates.

## 3.3 Gene therapies

The genetics fields are a rapid and emerging filed in the last 30 years. In the same time genetic therapies has engender a great interest and some interesting results. Among them Antisense oligonucleotide (ASO), SiRNAs and gene (i.e., either mRNA or cDNA) delivery through viruses (e.g., adeno-associated viral vectors [AAV]) are three of the main options currently for gene therapies to treat ALS (Figure 25).

### 3.3.1 Antisense Oligonucleotides (ASO)

ASO enable precise modulation of gene expression without altering host DNA, a limitation of current gene transfer approaches. ASOs modify protein expression by acting directly on target RNA either prior to or during translation (Schoch and Miller, 2017). The design and the sequence of the ASO play a big role in the mechanism of action of it. Indeed, the most common modifications to the phosphodiester linkages forming the phosphate backbone. Here, the substitution of the non-bridging phosphate oxygen atom for sulfur, creates a phosphorothioate (PS) backbone that confers drug-like properties of many ASOs. This phosphorothioate backbone offers ASO stability and better nuclease resistance, allowing a better chance for RNA targeting. Furthermore, it allows the recruitment of enzyme RNase H to cleave a target transcript, conferring PS-ASOs with degrading capability. Also, the addition of a 2'-O-methyl group on the ribose and a sulfur on the phosphate (phosphorothioate), can increase its stability and affinity for the target RNA, as well as its penetrance into tissues and cells. In a so-called blocking mechanism, the ASO binds to the target RNA and acts by allosteric hindrance. They support non-degrading ASO mechanisms by influencing mRNA processing steps, such as alternative splicing or translational control but do not support RNase H enzymatic activity. There is also a so-called degradative mechanism in which ASOs, called gapmers, are composed of chemically modified RNAs surrounding a DNA sequence, and the pairing between the gapmer DNA and the target RNA induces the recruitment of RNase H1 and thus the degradation of the RNA (For review Boros et al., 2022).

ASOs are now approved for the treatment of > 10 conditions that include spinal muscular atrophy (SMA), a pediatric-onset motor neuron disease (For review (Roberts et al., 2020). In 95% of the general population and in all SMA patients, there is a gene virtually identical to the *SMN1* gene, the *SMN2* gene. However, the *SMN2* gene has a single nucleotide variation in exon 7, which does not alter its coding sequence, but does modify its splicing. The absence of this exon leads to the production of an unstable protein that cannot compensate for the loss of the SMN1 protein (Campbell et al., 1997). An ASO, called Nusinersen, blocks access of the hnRNP protein to an intronic site regulating *SMN2* RNA splicing. The hnRNP protein normally stimulates excision of exon 7, so its absence enables exon 7 to be maintained in the SMN2 protein and a functional protein to be produced.

It was approved in 2016 by the FDA for the treatment of spinal muscular atrophy and caused a massive interest to treat other diseases like ALS (Aartsma-Rus, 2017).

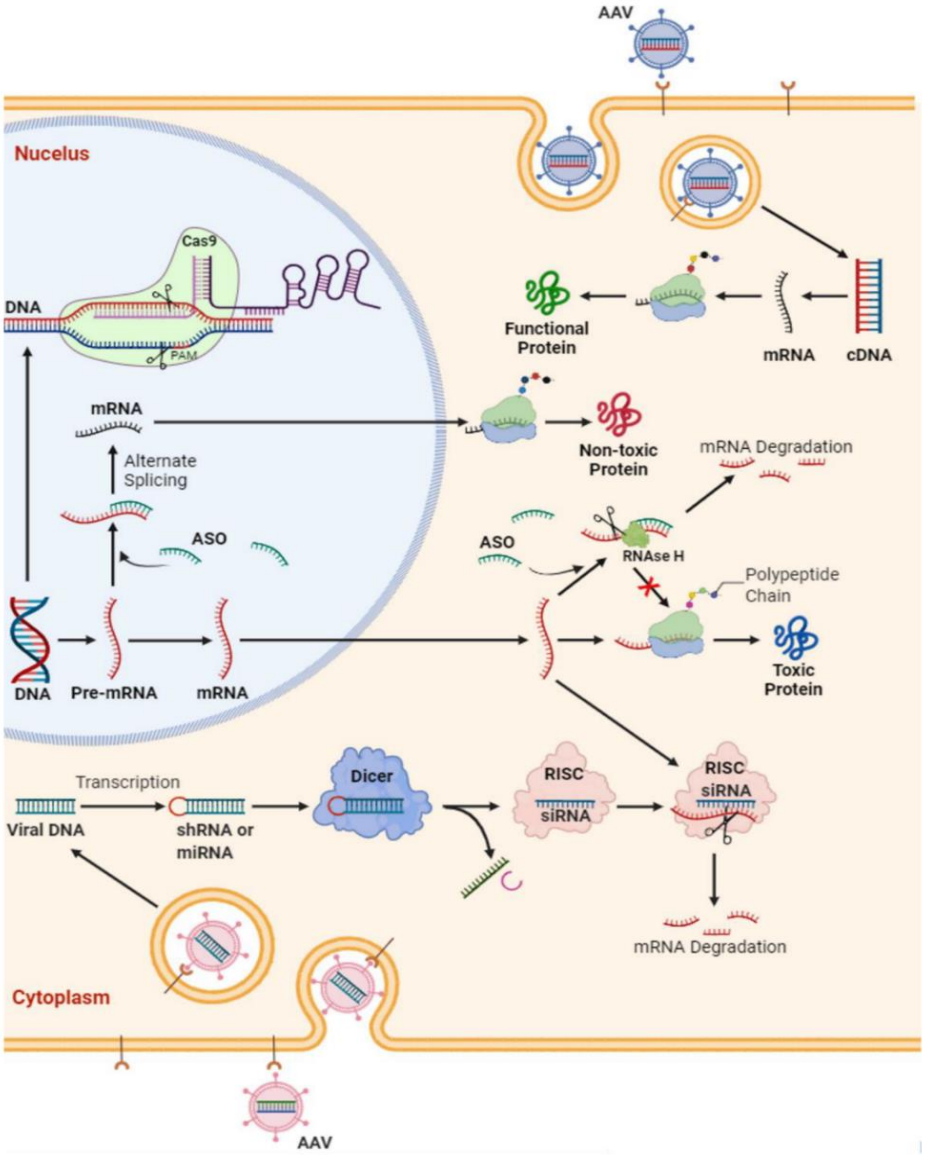


Figure 25 Schematic representation of potential strategies in gene therapy for amyotrophic lateral sclerosis

Antisense oligonucleotide (ASO) are short synthetic oligonucleotides (~20 nucleotides). They bind to the targeted mRNA and either (i) induce the mRNA degradation by endogenous RNase H or (ii) block the mRNA translation. This ultimately decreases the expression of certain proteins. In ALS. SiRNAs are double-stranded RNAs that can bind argonaute proteins as part of the RNA-induced silencing complex (RISC), which ultimately leads to the mRNA cleavage. Gene (i.e., either mRNA or cDNA) delivery through viruses (adeno-associated viral vectors [AAV]) is another option for functional replacement of a missing gene.

The first phase III trial in ALS was with *SOD1* mutation. Tofersen (NCT02623699; BIIB067) shows that the ALSFRS-R levels in ALS patients did not differ from placebo tests but *SOD1*-levels in cerebrospinal fluid (CSF) and neurofilament light chain (NfL) levels in plasma lowered significantly without any adverse events (Miller et al., 2022). Also developed for patients with *fused in sarcoma* (*FUS*) gene mutations, ION363 is currently undergoing a phase III trial as well and shows also interesting outcome like ventilation assistance-free survival with muscle and lung function, survival, and change in CSF FUS protein and neurofilaments (Korobeynikov et al., 2022).

For *C9ORF72* patients' results are mitigated. Indeed, while *SOD1* and *FUS* ALS patients, demonstrate an abnormally high amount of SOD1 and FUS protein, *C9ORF72*-ALS patients, in contrast, demonstrate haploinsufficiency. Furthermore, for *C9ORF72*-ALS patients the RNA production is toxic by the DPR and RNA Foci but not he protein itself (McEachin et al., 2020; Shi et al., 2018). Moreover, C9ORF72 protein has important physiological functions and it is likely not desirable to degrade all *C9ORF72* transcripts (Gendron and Petrucelli, 2018). Interestingly, *C9ORF72* possess multiple transcript variants. Splice variants 1 and 3 contain the intron that harbors the expansion, whereas variant 2 does not. Multiple groups were able to lower variants 1 an 3 containing the repetition while preserving variants 2 and thus not further suppressing C9ORF72 protein levels (Donnelly et al., 2013; Jiang et al., 2016; Lagier-Tourenne et al., 2013; Liu et al., 2021; Sareen et al., 2013). However, *C9ORF72* DNA is transcribed bi-directionally producing both sense and anti-sense RNA. Actually, ASO focused mainly on the sense transcript while the anti-sense transcript is mainly responsible of toxic DPR's and RNA FOCI. This inability to neutralize simultaneously both sense and antisense strands remains an important limitation to current *C9ORF72* ASO therapies (Donnelly et al., 2013).

Clinically, and based on using ASOs in patient-derived cells (Donnelly et al., 2013; Lagier-Tourenne et al., 2013; Sareen et al., 2013) and transgenic mice (Jiang et al., 2016) most promising ASO in *C9ORF72* patient, a phase I clinical trial on IIB078 with an ASO targeting *C9ORF72*, has been stopped due to its lack of efficiency and reported worsening of symptoms in *C9ORF72* ALS patients (NCT03626012B). However, another ongoing phase I/II clinical trial has been initiated on WVE-004.

For this trial, the ASO is targeting transcriptional variants containing hexanucleotide repeat expansion by sparing the protein level of C9ORF72 (NCT04931862). Currently, a single dose of WVE-004 achieved durable reductions in poly(GP) in the CSF, indicating successful target engagement. However, no changes in clinical outcomes has been observed and joined the same conclusion than for the IIB078 trial.

Another counterpart of ASO that is more linked to the strategy. Indeed, ASO cannot cross the blood brain barrier and requires intracerebroventricular (i.c.v.) and intrathecal routes, respectively, into the cerebrospinal fluid (CSF). New delivery approaches such as conjugating ASOs to lipid nanoparticles or cholesterols may soon enable peripheral administration or cell type targeting in the CNS (Kulkarni et al., 2018; Suhr et al., 2015). Furthermore, the details of drug delivery are not entirely clear in humans and off-target toxicity, particularly activation of the immune system is still a problem in ASO trial.

### 3.3.2 RNA interference (RNAi) or CRISPR CAS 9 via Viral Vectors Delivering

In contrast to ASOs, which are single stranded and prepared to immediately bind to their target, RNAs are a double-stranded structure that require stages of enzymatic processing before being active, even though they are more likely to survive delivery. Targeted genes expression is suppressed via the RNAi process, which uses RNAs to damage mRNAs in the cytoplasm through an RNA-induced silencing complex (RISC). Furthermore and in contrast to ASO they can be delivered directly to the central nervous system (CNS) via nonpathogenic adeno-associated viruses (AAVs) and need only one injection to be efficient (Zancanella et al., n.d.). This technique shows promising results in *SOD1* ALS patient. Indeed, once incorporated into nervous cells, APB-102 targets and binds *SOD1* mRNA, subsequently reducing its protein production. Although lower levels of *SOD1* were found on autopsy in the first patient, there was no reduction in CSF *SOD1* in either patient at two weeks (Mueller et al., 2020). These results are promising and could lead to similar outcomes as ASO targeting *SOD1* or *FUS*. UniQure is currently acquiring the rights to develop this technique for phase I/II clinical trials.

In 2022, they also presented AAV-miQURE® results in an ALS *C9orf72* mouse model where they were able to binds the mutant repeat expansion of *C9orf72* mRNA without affecting native *C9orf72* mRNA and protein. However and even these results are promising they didn't start any trial (Zancanella et al., n.d.).

Furthermore, viral vectors can also carry the CRISPR/Cas9 technology. No clinical trials are currently under investigation but first studies trying to aim *C9ORF72* or *SOD1* were recently being published with promising results (Deneault et al., 2022; Deng et al., 2021; Meijboom et al., 2022).

## 3.4 Stem cells

Stem cells could be a promising therapy to cure ALS. Indeed, by having the capacity to develop any specific cells, we could replace damaged or apoptotic neurons by functioning neurons. When injecting mesenchymal stem cells, the immune system could be guided towards an anti-inflammatory, neuroprotective environment by releasing different favorable soluble factors, instead of reacting to oxidative stress. Although preclinical investigations in rodent models, mostly in presymptomatic animals, demonstrated beneficial results, a gap for translation to an effective trial in humans is still a problem. Two studies on bone-marrow-derived mesenchymal stem cells (BM-MSC) are found in advanced trial stages:

NurOwn® (NCT04681118) in an expanded-access protocol for patients who were enrolled in the preceding phase III trial. Significant improvements in cerebrospinal biomarkers of neuroinflammation, neurodegeneration, and neurotrophic factor support were observed (Cudkowicz et al., 2022).

Lenzumestrocel (Neuronata-R® Inj) (NCT04745299), a BM-MSC as well, is currently being tested in a phase III clinical trial (NCT01363401). Repeated intrathecal injections of BM-MSCs demonstrated a possible clinical benefit lasting at least 6 months, with safety, in ALS patients. Group showed decreased proinflammatory and increased anti-inflammatory cytokines but with no significant difference in long-term survival between groups (Oh et al., 2018).

As sated before this list is non-exhaustive and the idea to treat ALS are huge. Indeed other therapies suggest the use of small compounds or genetic modifications targeting repeat RNA secondary structures or repeated RNA to prevent RNA translation or sequestration of RBPs. (Zamiri et al., 2014). Inhibiting DPR production thanks to CRISP CAS 9 technology is also another path studied (Cheng et al., 2019). They are also trying to target downstream pathways directly with the use of GA-antibodies to reduce their aggregation (Zhou et al., 2017).

# 4. Hypothesis and objectives

Amyotrophic lateral sclerosis (ALS) is the third most common neurodegenerative disease worldwide. This disorder is characterized by the degeneration of upper and spinal motor neurons that leads to progressive skeletal muscle paralysis, ultimately resulting in death from respiratory failure generally 3–5 years after age of onset. The main genetic cause of ALS is an expansion of GGGGCC repeats in the *C9ORF72* gene. These repeats are pathogenic by three mechanisms:

- First, transcripts containing expanded repeats accumulate in RNA foci that recruit various RNA-binding proteins (RBP), potentially altering their localization and functions.
- Second, sense G4C2 and antisense C4G2 expanded repeats are repeat-associated non-AUG (RAN) translated into dipeptide repeat (DPR)-containing proteins, which form inclusions throughout the brain of patients with C9-ALS/FTD, as well as in mice expressing expanded G4C2 repeats.
- Third, expanded G4C2 repeats promote DNA epigenetic changes that lead to decreased expression of *C9ORF72* mRNA and protein levels in C9-ALS/FTD individuals.

However, very little is known on the molecular and cellular roles of C9ORF72. During my thesis we mainly focused on this third mechanism of pathogenicity with two different axes.

First we focused on the C9ORF72-SMCR8-WDR41 complex. When I arrived, the team and other found that C9ORF72 form a stable protein complex with two other proteins, SMCR8 and WDR41 (Boivin, 2020; Sellier et al., 2016). To explore the molecular functions of C9ORF72, we decided to solve its 3D structure. Thus, in collaboration with the Patrick Schultz group (IGBMC, Strasbourg), we produced and purified the C9ORF72 complex to obtain a 3D CRYO-EM map.

In parallel, we explored the molecular functions of C9ORF72 and it interactant. Interestingly, both C9ORF72 and SMCR8 present longin domains, characteristic of proteins known to regulate the GDP/ GTP exchange cycle of RAB/ARF proteins. Small GTPases of the ARF-like proteins (ARL), ARF, and RAB families are proteins that can exist in two conformations: an inactive conformation bound to GDP or an active conformation bound to GTP.

This property enables them to regulate all steps of intracellular vesicle trafficking, from their formation, transport, and fusion to their target membranes.

However, the identity of the small GTPase(s) regulated by the C9ORF72 complex is unclear. In that aspect, we and other found that C9ORF72 regulates autophagy, however at an unknown step (Sellier et al., 2016). Thus, we decided to explore the small GTPase regulated by the CSW complex and to elucidate its potential role in autophagy regulation.

# MATERIALS AND METHODS

# 1. Cell culture and molecular biology

## 1.1 Constructs

Optimized cDNAs for human N-terminally or C-terminally HA, FLAG, GFP, STREP-tagged of C9ORF72, SMCR8, WDR41, FIP200, ARL14, ARL4 were cloned into pcDNA purchased form GenScript or PCMV6 from OriGene.

Mutations of C-terminally HA-tagged SMCR8 phosphorylation sites (S400, S402, S492, S562, T666, and T796D) in alanine or aspartate were constructed by inverse PCR.

Mutations of FLAG-tagged ARL14 (T28N and Q68L) or FLAG-tagged ARL4a (T34N and Q79L) mimicking GDP inactive and GTP active forms in Asparginine or Leucine were constructed by inverse PCR.

## 1.1 Cell culture and treatment

HEK-293 cells were cultured and maintained in DMEM 1 g/l glucose with 10% FCS and gentamicin at 37°C in 5% $CO_2$ in T-75 Flask. For transfection, cells were seeds at 1 million cells in 6-well plate 24 hours pre-transfection. For transfection, cells were plated in DMEM and 0.1% fetal bovine serum at 37°C in 5% $CO_2$.

U2OS cells were cultured in DMEM 1 g/l glucose with 10% FCS and gentamicin at 37°C in 5% $CO_2$ in T-25 Flask. For transfection U2OS cells were incubated 24 hours pre-transfection (80 000 cells/well) on 14 mm covers-glasses disposed inside 24 wells plate in DMEM and 0.1% fetal bovine serum at 37°C in 5% $CO_2$.

For autophagy induction cells were washed three time with EBSS (Gibco 24010043) and then 1 ml were added in each well for culture during 8 hours. Dynasore (Abcam120192) was used at 40 mM during 40 min to induce ALR and tubulation.

## 1.2 Immunofluorescence

For immunofluorescence experiment, U2OS cells were incubated 24 hours pre-transfection (80 000 cells/well) on 14 mm covers-glasses disposed inside 24 wells plate. For transfection, 0.5 µg of DNA were mixed in DMEM and 0.1% fetal bovine serum and transfected for 48 h using Lipofectamine 2000 (Fisher Scientific). Coverslips were incubated for 15 min in PBS with 4% paraformaldehyde, washed with PBS, and incubated in PBS plus 0.5% Triton X-100 for 10 min. The cells were washed three times with PBS, and the coverslips were incubated for 1 h with primary antibody against HA (abacam 130275) or HA (abcam 9110), FLAG (cell signaling technology D6W5B) or FLAG (Sigma 3165).After washing with PBS, the coverslips were incubated with goat anti-mouse secondary antibody conjugated with Alexa 488 (Interchim SA) or CY3 (Interchim SA) or CY5 (Interchim SA) for 1 h, washed twice with PBS, and incubated for 2 min in PBS/DAPI (1/10,000 dilution). Coverslips were rinsed twice before mounting in Pro-Long media (Molecular Probes) and were examined using a Leica spinning-disk (https://ici.igbmc.fr/).

## 1.3 Co-immunoprecipitation assay

24 h after transfection of HEK293 cells with 1 µg of plasmid constructs in Lipofectamine 2000 (Invitrogen), cells were lysed in RIPA buffer (50 mM Tris-HCl pH 7.5, 0.15 M NaCl, 0.5% Triton X-100) supplemented with protease inhibitor cocktail (Roche) and clarified by centrifugation at 14000 rpm for 10 min. Immunoprecipitations were performed at 4°C for 1 h using pre-washed Anti-GFP (Abcam ab193983), anti-HA (Pierce 88837), anti-FLAG (Thermofischer A36797) or MagStrep "type3" XT (IBA 2-4090-002) Magnetic Beads, in RIPA buffer, washed three time, then bound proteins were eluted by 3 min denaturation step at 95°C with Laemmli buffer followed by mass spectrometry or western blot.

## 1.4 Western blotting

Proteins were denatured 3 min at 95°C, separated on 4–12% Bis-Tris Gel (NuPAGE),transferred on nitrocellulose membranes (Whatman Protran), blocked with 5% non-fat dry milk in Tris-buffered saline (TBS) buffer, incubated with, anti-FLAG C9ORF72 (Abcam 221137 ), anti-WDR41 (Solarbio K110527P) or anti-WDR41 (Proteintech 26817-1-AP), anti-SCMR8 (GeneTex GTX635798), anti-ARL14 (Thermofischer PA5-113182), anti-FIP200 (Proteintech 17250), anti-HA (Abcam 130275) or anti-HA (Abcam 9110) or anti-HA (Thermofischer 26183), anti-FLAG (Thermofischer PA1-984-b), anti-GFP (Abcam 290) or anti-GFP (Abcam 1218)
in TBS plus 5% non-fat dry milk, washed three times, and incubated with anti-rabbit or mouse peroxidase antibody (1:10,000, Cell Signaling) 1 h in TBS, followed by washing and ECL chemiluminescence revelation (Amersham ECL Prime).

## 1.5 Mass spectrometry analysis

HEK293 cells were transfected with WRD41 GFP-tagged with HA-tagged C9ORF72, SMCR8 and FLAG-tagged ARL14 (Q68L) or HA-tagged GFP plasmid using Lipofectamine 2000 (Fisher Scientific) for 24 hours. Proteins were purified by GFP-immunoprecipitation, trypsin digested and the peptides were extracted twice with acetonitrile/water/formic acid-45/45/10-v/v/v followed by a final extraction with acetonitrile /formic acid (FA)-95/05-v/v. Extracted peptides were then analyzed using an Ultimate 3000 nano-RSLC (Thermo Scientific) coupled in line with an Orbitrap ELITE (Thermo Scientific). Peptides were separated on a C18 nano-column with a linear gradient of acetonitrile and analyzed with in a Top 20 collision-induced dissociation data-dependent mass spectrometry with an inclusion list. Data were processed by database searching using SequestHT (Thermo Fisher Scientific) with Proteome Discoverer 1.4 software (Thermo Fisher Scientific). Precursor and fragment mass tolerance were set at 7 ppm and 0.5 Da respectively. Oxidation (M) and Nterminal Acetylation were set as variable modification, and Carbamidomethylation (C) as fixed modification. Peptides were filtered with the Fixed value node of Proteome Discoverer 1.4.

## 1.6 Coomassie-blue

For Coomassie blue staining, proteins were denatured 3 min at 95°C, separated on 4–12% Bis-Tris Gel (NuPAGE After electrophoresis gel were placed in a clean tray and wash three times for 5 minutes with 50-100 ml of ultrapure water. Fixation as made for 20 min in 40% ethanol and 10% acetic acid under shaking. Then Sufficient volume of stain (Coomassie R-250 Thermofischer 24615) to completely cover gel was added. Typically, 20-25 ml of stain was sufficient for an 8 × 10 cm gel. Tray was placed on a shaker for 1 hours. Staining reagent was then discarded and replaced with 200 ml of ultrapure water to reduce background. Water was replaced frequently during 30 minutes or ON.

# 2. Protein production and CRYO-EM analysis

## 2.1 Recombinant protein production

Concerning C9ORF72 complex, $2 \times 10^6$ of SF9 (*Spodoptera frugiperda*) cells (one T25 flask) were co-transfected with 500 ng of *Bsu36I*-linearized BAC10:KO1629 DNA and 2 µg of pMF-Dual vectors containing either HIS-C9ORF72, STREP-tagged WDR41, HIS- tagged ARL14 (Q68L) untagged FIP200, C9ORF72 and SMCR8 and incubated at 27°C for 6 days. Harvested baculovirus were then tested, amplified and used to infect 2 l of SF9 cell culture for protein production and purification using the HIS purification kit (Novagen) with sonication and washing in 500 mM NaCl, 50 mM Tris–Cl pH 7.5, 50 mM imidazole, elution with 150 mM NaCl, 50 mM Tris–Cl pH 7.5, 1 mM DTT, 5 mM EDTA, 200 mM imidazole, dialysis, and storage in 150 mM NaCl, 20 mM HEPES, 2 mM $MgCl_2$, 20% glycerol.

## 2.2 Protein purification

Buffer A = 100 mM Tris pH 8, 150 mM NaCl, 1 mM EDTA and Buffer B = 100 mM Tris pH 8, 150 mM NaCl, 1 mM EDTA, 50 mM Biotin (M=244, i.e. 12.2 mg/ml,i.e. 610 mg for 50 ml of buffer B) were prepared prior to manipulation. 500 ml of baculovirus production stored at -80°C in 20 ml of bufferA + 1 PIC, 0.5 µl BaseMuncher, 0.2 mM DTT was lysed by sonication on ice for 4 x 30 seconds with large probe (amplitude 40% and cycle 0.5). Ultracentrifugation in Ti 50.2 for 45 min at 30,000 RPM 4°C and recovery of the extract soluble was then performed. The, filtration on a 5 µm filter to eliminate the few remaining pieces of pellet was made.

Column washing with 10 mM NaOH and then equilibration of the 1 ml StrepTactin XT column (0.7 cm x 2.5 cm) with buffer A at 1 ml/min (max pressure = 0.3 MPa) was made prior to sample loading. Soluble fraction of sample was load at 0.5 ml/min (20 ml, i.e. ~40 min). Washing was performed at 15 CV in buffer A and elution at 15 CV in buffer B. 22 mL of Flowthrough was incubated overnight at 4°C with 0.5 ml of buffer-equilibrated StrepTactin resin A (in 50 ml Falcon tube on a roller shaker). Then centrifugation at 500g for 5 minutes was performed and with and FT recovery. Resin was washed with 22 ml of buffer A. New centrifugation was then performed with recovery of washing solution. Re-suspension of the resin in 1 ml of buffer A and transfer to an empty column for elution by gravity was made. Elimination of buffer A and elution in buffer B (3 x 0.75 ml) and final recovery of 3 fractions.

Then an analysis on 12% SDS gel result in several bands visible in the different elution fractions. Concentration of positive fractions on Amicon were made. Finally, injection on gel filtration S200 10/300 balanced at 0.5 ml/min in 20 mM Tris pH 8, 150 mM NaCl, 1 mM EDTA was performed resulting in collection of 0.5 ml fractions with detection at 280, 260 and 230 nm.

## 2.3 Cryo-EM sample preparation and data acquisition

About 3 µl of sample was applied onto a holey carbon grid (Quantifoil R2/2 300 mesh) rendered hydrophilic by a 90-s treatment in a Fischione 1070 plasma cleaner operating at 30% power with a gas mixture of 80% argon:20% oxygen. The grid was blotted for 1 s (blot force 15) and flash-frozen in liquid ethane using a Vitrobot Mark IV (FEI) at 4 °C and 95–100% humidity. mages were acquired on a Cs-corrected Titan Krios (Thermo Fisher) microscope operating at 300 kV in nanoprobe mode using the serialEM software for automated data collection. Movie frames were recorded on a 4k × 4k Gatan K2 summit direct electron detector after a Quantum Ls 967 energy filter using a 20-eV slit width in zero-loss mode. Images were acquired in super-resolution mode at a nominal magnification of 105,000, which yielded a pixel size of 0.55 Å. Forty movie frames were recorded at a dose of 1.32 $e^{-}$ Å$^{-2}$ per frame, corresponding to a total dose of 52.8 $e^{-}$ Å$^{-2}$, but only the last 38 frames were kept for further processing.

## 2.4 Image processing

Movie frames were aligned, dose-weighted, binned by 2 and averaged using Motioncor2 (Zheng et al., 2017) to correct for beam-induced specimen motion and to account for radiation damage by applying an exposure-dependent filter. Non-weighted movie sums were used for contrast transfer function (CTF) estimation with the Gctf (Zhang, 2016) program, while dose-weighted sums were used for all subsequent steps of image processing. After manual screening, images with poor CTF, particle aggregation or ice contamination were discarded. Particles were picked using crYOLO ((Wagner et al., 2019)). These datasets were analysed in RELION 3.0 (Zivanov et al., 2018) cryoSPARC (Punjani et al., 2017) and *cis*TEM (Grant et al., 2018) according to standard protocols. In brief, three rounds of reference-free 2D classification of the individual particle images were performed in RELION to remove images, like ice contaminations or deformed particles, that failed to enter into high-resolution class averages. The selected images were aligned against a low-pass-filtered starting model.

Three rounds of 3D classification with increasing regularization parameter *T* were performed and classes showing high-resolution features were selected for the subsequent steps. These images were imported, and refined in cryoSPARC v.2. Global resolution estimates were determined using the Fourier shell correlation (FSC) = 0.143 criterion after a gold-standard refinement. Local resolutions were estimated with ResMap (Kucukelbir et al., 2014) and cryoSPARC.

# 3. Statistical analysis

All cells experiments are represented as average ± standard error of mean (SEM) with significance determined using Student's *t*-test.

# RESULTS

# 1. C9ORF72-SMCR8-WDR41 complex structure

## 1.1 CRYO-EM overview

In 2016, Sellier and colleagues shows that C9ORF72 forms a trimer with SMCR8 and WDR41. This complex is composed of C9ORF72, WDR41 (or "WD repeat containing protein 41") a 52 kDa protein consisting in six WD40 domains and SMCR8 (or "Smith Magenis syndrome Candidate Chromosome Region 8") a 105 kDa protein that share two similar DENN domains with C9ORF72. However, the function of WDR41 and SMCR8 are unknown (Amick et al., 2016; Sellier et al., 2016; Sullivan et al., 2016; Ugolino et al., 2016; Yang et al., 2016) (Figure 26).

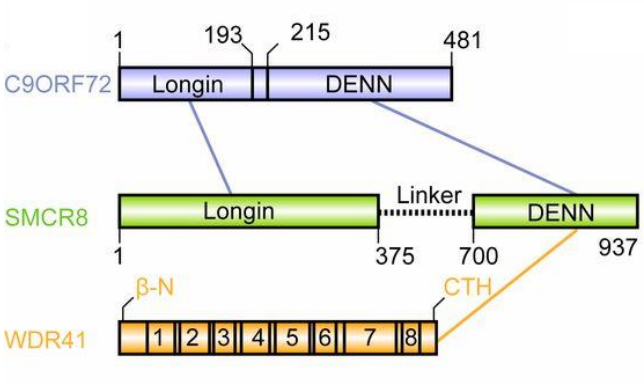


Figure 26 Schematic representation of C9ORF72, SMCR8 and WDR41

Schematic diagram of the domain arrangement of C9ORF72 (light blue), SMCR8 (light green), and WDR41 (orange). The names and boundaries of domains are labeled. CTR, C-terminal helix of WDR41 (Tang et al., 2020).

We decided to explore the molecular functions of the C9ORF72 complex by solving its 3D structure. Harvested baculovirus expressing either HIS-C9ORF72, SMCR8, or WDR41 were tested, cultivated, amplified and used to co-infect 2 liters of SF9 cell culture for protein production and purification (Figure 27-A). Our first attempts to determine the structure was made by using X-ray crystallography, which is by far the most used technique in structure determination. Indeed, in 2020, the crystal structures in the PDB database account for about 89%, the NMR structures account for 8.2%, and the EM structures account for 2.5%. However, the CSW complex was unable to form crystals.

Thus, in collaboration with the Patrick Schultz group (IGBMC, Strasbourg), we decided to use an emerging technique called Cryogenic electron microscopy (CRYO-EM). It presents the benefice of having proteins imaged in vitreous ice in a state virtually identical to their native state in solution, as opposed to tightly packed crystals. In summary, the principle is to scan biological macromolecules frozen and preserved in glassy ice in order to acquire protein molecule projections in all directions. Computing is then utilized to process and calculate a huge number of 2D pictures in order to recreate the biomacromolecule's 3D structure.

However, the sample preparation needs to be optimized and number of different conditions to be screened. The isolation of the complex under the right conditions (protein concentration, right detergent and concentration) is a crucial step. Additionally, the plasma cleaning procedures are crucial for creating homogenous Cryo-EM samples and high-resolution images. Plasma treatment enables aqueous samples to disperse uniformly across the Cryo-EM grid surfaces by making the grids hydrophilic. Optimizing the vitrification process's settings (grid type and blotting duration) is another essential step.

Negative stain electron microscopy (EM) are perform to enables relatively quick and simple observation of macromolecules and macromolecular complexes before adjusting any of these parameters. A range of biological issues can benefit from negative stain electron microscopy, which also offers a quick way to evaluate materials for cryo-electron microscopy (cryo-EM) before optimization. Indeed, it is ideal for assessing sample purity, concentration, heterogeneity, and conformational flexibility (Thompson et al., 2016). Figure 27-B shows the negative coloration of our sample. We can distinguish our complex with a projection of protein molecules in all directions.

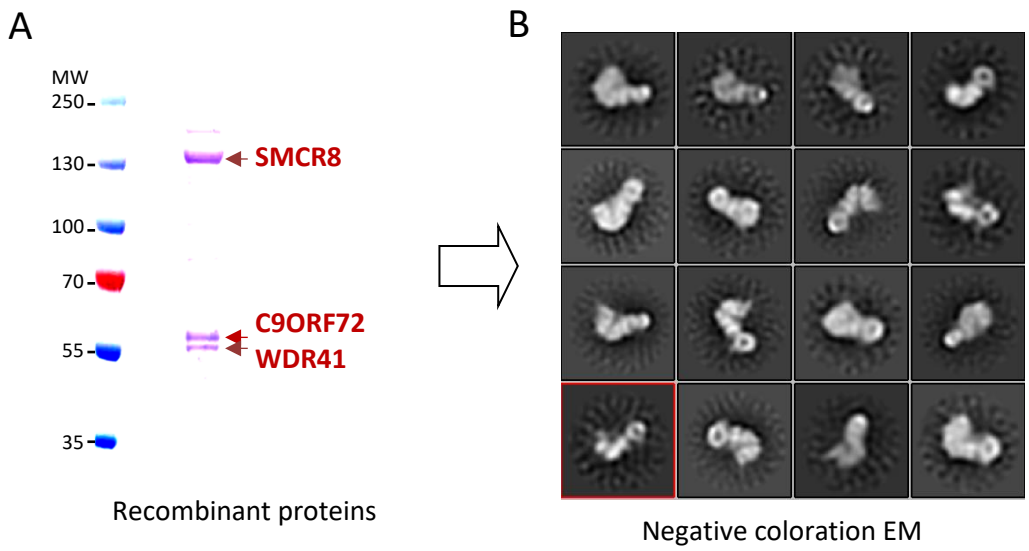


Figure 27 Preliminary results of the recombinant proteins and the Negative coloration EM

(**A**) Coomassie blue staining of Nickel-NTA affinity purification of HIS-C9ORF72, SMCR8, and WDR41 co-expressed in baculovirus-infected insect cells (Sellier et al., 2016). (**B**) Negative coloration EM obtain from the baculovirus SF21 production.

After assessing good quality of samples, we had to achieve grid preparation repeatability. The use of the Thermofisher Vitrobot Mark IV®, a semi-automated device, greatly help to have reproducible vitrification of aqueous suspension. However, various parameters had to be set like the temperature, blotting force, blotting time, orientation of the tweezers and insertion of blotting paper in order to obtain a nice frozen and fixed glassy ice (Figure 28).

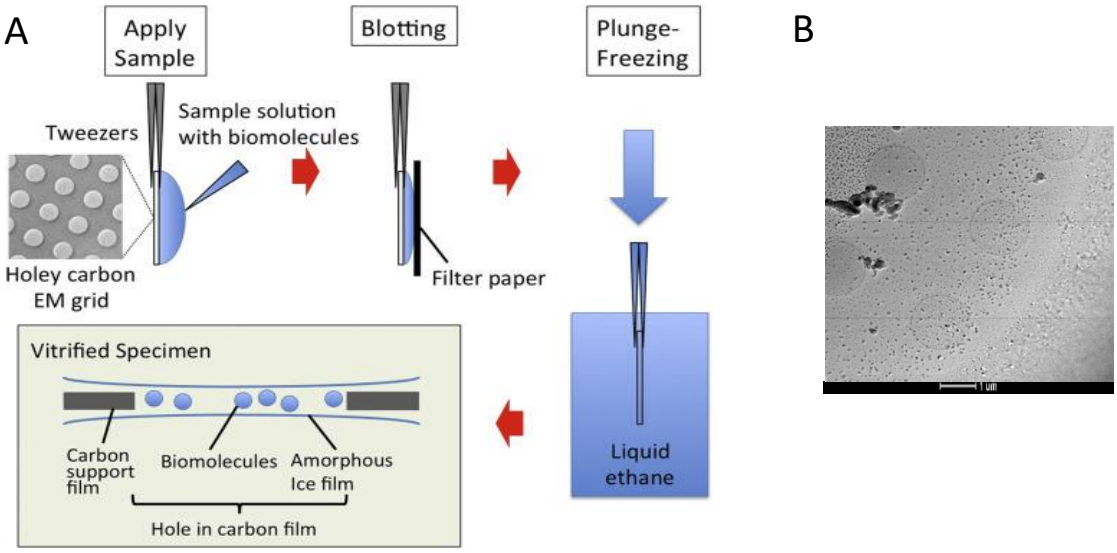


Figure 28 Schematic representation of the grid preparation steps

(**A**) After picking the right grid, the sample has to be applied on the grid. Right after, the tweezer will blot the sample to remove excess of protein with a little piece of paper. It is then instantly plunge into liquid ethane (- 88 °C) to obtain a vitrified specimen with the biomolecules capture inside (Murata and Wolf, 2018). (**B**) Picture of a grid with vitrified ice that wasn't store in the right condition and transformed into "normal" ice.

In fact, without optimization, we frequently run into a number of problems that put the acquisition process on hold. These are the primary problems.

- **Denaturation and disassembly of complex** which is due to the denaturing effects at the air-water interface, the area of which is massively enlarged in relation to the volume during the grid preparation and allows protein particles to interact with it.
- **Detergent artefacts** are due to too high concentrations of detergent. For cryo-EM grids concentration is around 0.2–0.4%. Anything above this results in artefacts: either free visible micelles or long thread.
- **Poor or high particle coverage and protein aggregation** which are mainly dependent on the protein sample and detergent concentration.
- **Ice thickness** which is mostly influenced by the force and blotting time.

## 1.2 Cryo-EM grid optimization

Prior to any acquisition, we had our sample's vitrification technique optimized. Figure 29 show the various challenges that our samples faced. Figure 29-A,B,C represents a unusable grid visualized at different magnification. Indeed, Figure 29-B illustrate a common issue of many preparations, called partial over-blotting, in which the centers of the holes became too thin and excluded the particles from that area. The ''meniscus effect,'' where the ice in the middle of the hole can be much thinner than at the borders, is caused by the presence of too much detergent. Figure 29-C depicts an excessive protein concentration where particles almost overlap with major degradation/disassembling. On the other end, Figure 29-D,E,F represent a proper grid that was used for further experiment. In fact, Figure 29-E,F displays a nicely vitrified sample that allows us to observe our particle with high coverage and no signs of degradation or disassembly.

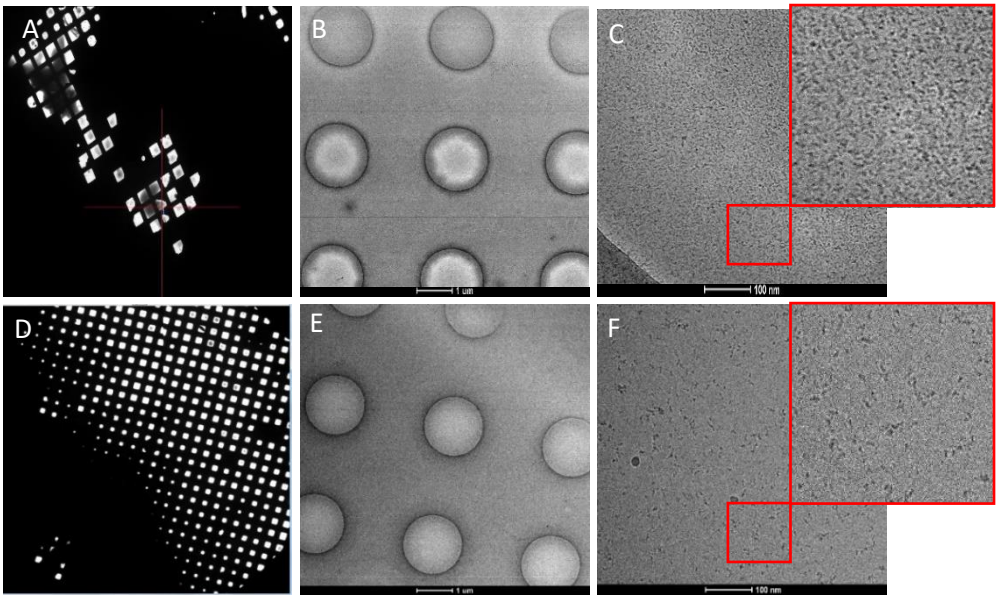


Figure 29 Optimization of the CRYO-EM grids

(**A**),(**B**), and (**C**) represents inappropriate grids samples with too thick vitrified ice and too much protein coverage and/or degradation.

(**D**),(**E**) and (**F**) represents good grids with nice thin vitrification and good protein coverage with few degradation

Images were taken on a FEI Technai T30 Polara.

To find the ideal settings to steer clear of previously encountered problems, several grids were completed. Dodecyl Maltoside (DDM), the most popular detergent for protein crystallization that has already been utilized in the Cryo-EM structures of several proteins, was selected after optimization. We utilized a DDM concentration of 0,01% after diluting our sample five times to ensure good particle coverage. The Vitrobot's blotting force was set to 15 for a duration of 1 second with a temperature of 4°C with 100% humidity.

After optimization proper grids were selected and allows to use the Titan Krios cryo-electron microscope to obtain a final 3D structure (https://frisbi.eu/centers/instruct-center-france-1-igbmc/cryo-electron-microscopy).

## 1.3 CSW structure acquisition

Following acquisition, several images of our grids were computer-processed. Cryolo (Wagner et al., 2019) permits semi-automatic particle picking of around 242 000 particles. Then, using Relion, 2-D classification and selection was carried out (Zivanov et al., 2018). Figure 30 demonstrates the preferred orientation of our structure, with 220,000 protein particles exhibiting the protein's upper side and just 21,000 revealing the protein's side. Finally, an initial structure was obtained after 3-D classification and refinement with a resolution of approximately 5,9 A°. The existence of a preferred orientation, which causes a bias in the calculation, accounts for this relatively low resolution. Increasing the number of grid and acquisition is a solution in order to get rid of it an achieved a CRYO-EM resolution up to 3 A°.

This study, which was initiated at the very beginning of my thesis, was regrettably affected by the COVID pandemic. During this time, two other teams were able to publish the structure with a higher resolution. However, our C9ORF72 structure is identical to the ones very recently reported (Figure 31-C) and will be partially described in part 1.4 (Nörpel et al., 2021; Su et al., 2020; X. Tang et al., 2020).

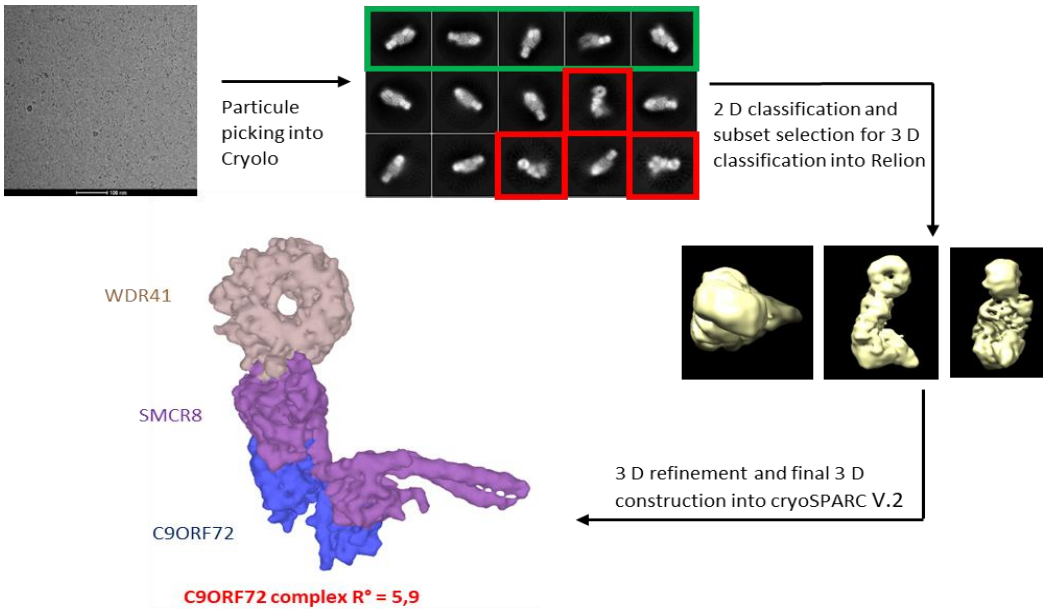


Figure 30 Computer-processed analysis of CSW complex

Schematic representation of the informatic analysis of CSW complex and the final electron density map structure. Green square represents the upper side view of the protein (220 000 particles) and the red square represent the side view (21 000 proteins).

## 1.4 CSW structure analysis

The CSW complex has a width of ~130 Å and a height of 140 Å. The ordered 120 kDa region of the complex, which accounts for about 60% of its overall mass has been resolved. The structure is composed of two longin domains at the tip of the hook, with the bulk corresponding of two DENN domains. While some regions, particularly the longin domains and the section of WDR41 that is most distal to SMCR8, were less resolved, the C9ORF72 and SMCR8 DENN domains were very well resolved. The structure of WDR41 reveals an eight-blade β-propeller with the N-terminal first strand and C-terminal last three strands coming together to form the first propeller (Figure 31-A,B). Without making direct physical contact with C9ORF72, WDR41 binds to the SMCR8 DENN domain through its N-terminal β-strand (βN) and C-terminal helix (CTH). The hook tip portion of the SMCR8 longin domain was assigned to residues I165-A219, which were predicted to comprise a long helical extension unique to SMCR8 longin. SMCR8 longin and SMCR8 DENN are near each other but not in direct contact, and are connected by a helical linker consisting of residues K320-V383. Both domains of C9ORF72 are positioned between SMCR8 longin and SMCR8 DENN. The overall complex has an elongated shape due to the linear arrangement of domains (Figure 31-A,B).

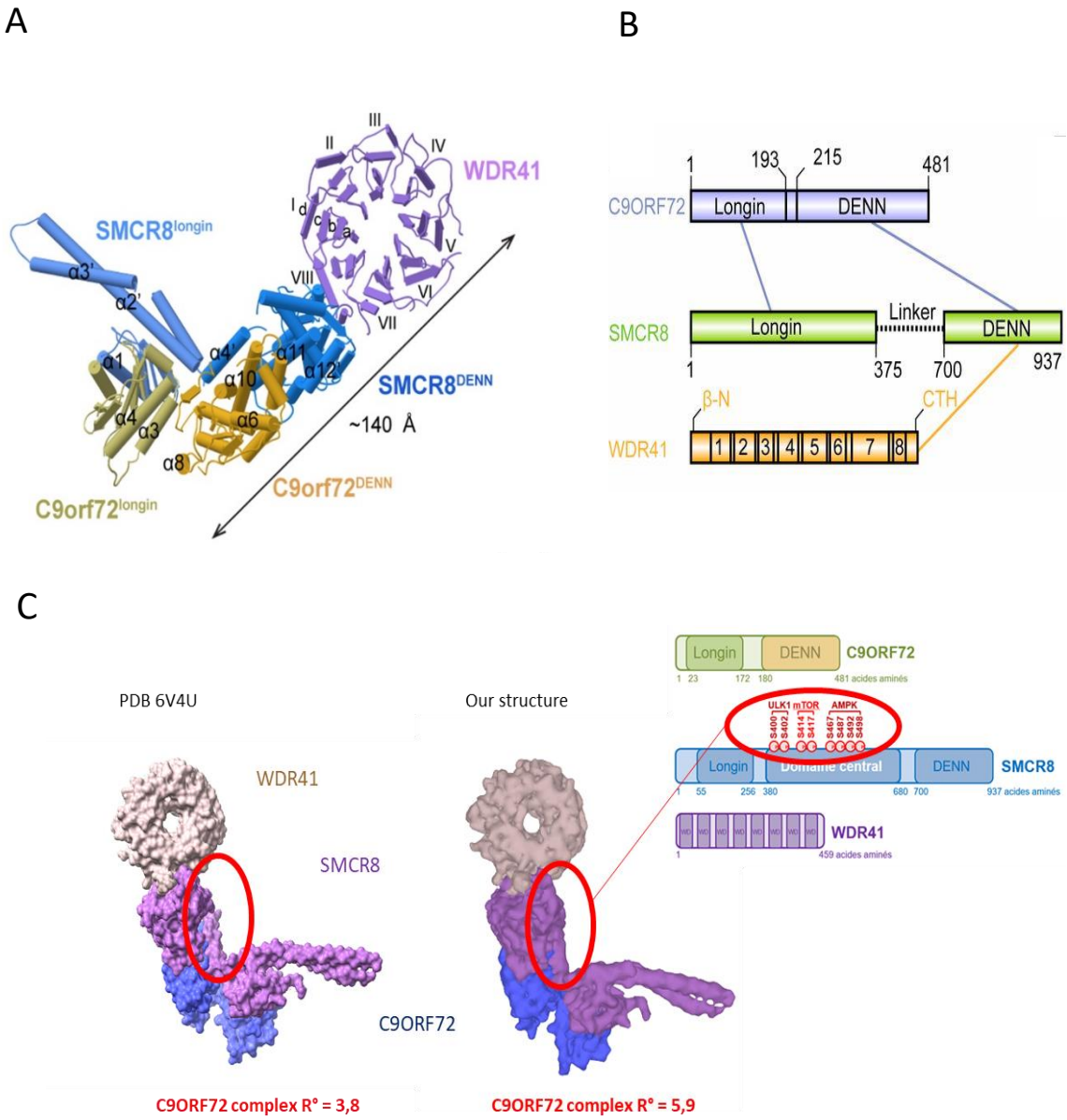


Figure 31 CSW complex structure, organization and domain

(**A**) refined coordinates of the complex shown as pipes and planks for α-helices and β-sheets, respectively. The domains color-coded as follows: SMCR8 longin, cornflower blue; SMCR8 DENN, dodger blue; C9ORF72 longin, olive; C9ORF72 DENN, goldenrod; WDR41, medium purple (Tang et al., 2020). (**B**) Schematic diagram of the domain arrangement of C9ORF72 (light blue), SMCR8 (light green), and WDR41 (orange). The names and boundaries of domains are labeled. CTR, C-terminal helix of WDR41. The interactions between different domains are shown in lines: light-blue line, C9ORF72–SMCR8 interaction; orange line, WDR41–SMCR8 interaction (Su et al., 2020). (**C**) Comparison of our structure (right) and the Tang et al., 2020, PDB 6V4 structure (left). The red circle represents the low-resolution part (between AA 380-700 of SMCR8) rich in phosphorylatable residues.

Despite their structure having better resolution, ours has commonalities. It was remarkable that a sizable part of the complex (between AA 380 and 700 of SMCR8) was unresolved (Figure 31-C). The movement of the protein and the requirement for one or more proteins to maintain the complex, however, can account for it. Interestingly, a number of autophagic regulators, including ULK1 (Behrends et al., 2010; Sellier et al., 2016), TBK1 (Sellier et al., 2016), mTOR (Hsu et al., 2011) and AMPK (Hoffman et al., 2015) are known to modulate the phosphorylatable residues in this central region of SMCR8.

As exposed in chapter 2.4.1, CSW complex is part of the DENN family known to regulate small GTPase. But more interestingly, CSW complex shows great structural similarities with NPRL2–NPRL3 of the GATOR1 complex (Shen et al., 2018) and FLCN–FNIP2 in the lysosomal folliculin complex (Lawrence et al., 2019; Shen et al., 2019). In fact, the longin domain of SMCR8 forms a heterodimer with the longin domain of C9ORF72 in a manner similar to these structures. Furthermore, the NPRL2 and FLCN subunits of these complexes are GAPs for the lysosomal small GTPases RAGA (Bar-Peled et al., 2013) and RAGC (Tsun et al., 2013), respectively. In this way, the major structural similarities with CSW is represented by the RAG GTPase-FLCN-FNIP2 complex where the Arg 164 of FLCN was shown to be the catalytic residue for GAP activity. This arginine finger residues are characteristic of a GAP for small GTPase and would corresponds to the Arg 147 in SMCR8 (Figure 32) (Shen et al., 2019; Su et al., 2020; D. Tang et al., 2020).

Even though the COVID pandemic and significant publications of the structure caused this project to be put on hold, a sizable portion of CSW complex was still left unresolved. Additionally, its interactions with small GTPases and the function of the CSW complex in autophagy remain unclear. To stabilize the complex and clarify its function in autophagy, we focused on identifying the small GTPase that interacts with the CSW complex.

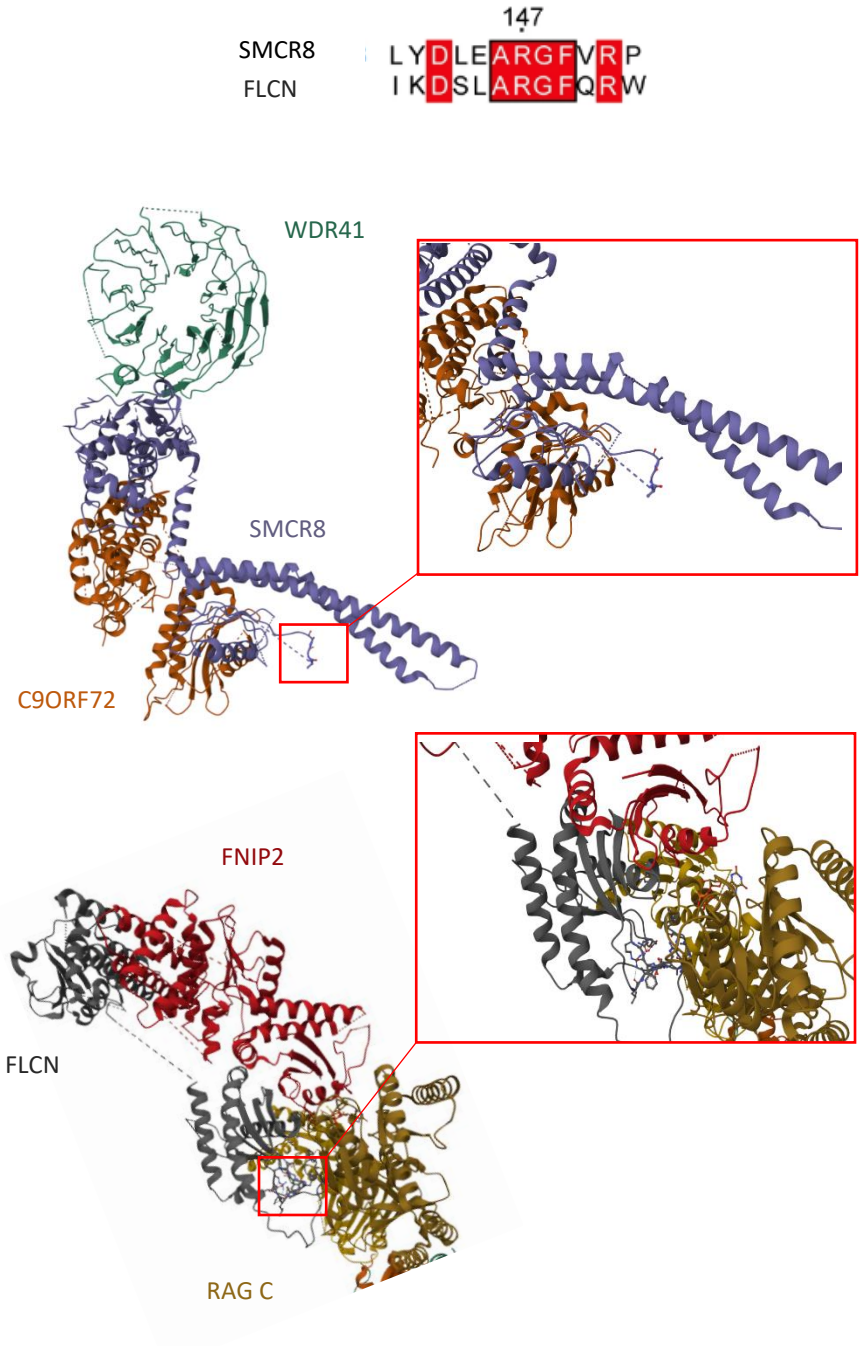


Figure 32 Structural similarities between FLCN-FNIP2 structure and C9ORF72-SMCR8-WDR41

Structure of the CSW complex (Tang et al., 2020) (PDB 6V4U) and the FLCN-FNIP2 (in association with RAGC) (Shen et al., 2019) (PDB 6ULG) and position of the respective characteristic arginine finger, the ARG 147 and the ARG 164.

# 2. Which small GTPase is regulated by CSW complex?

## 2.1 CSW complex and small GTPase screening

Due of structural similarities between CSW and the RAG GTPase regulator, notably FLCN-FNIP2 and NPRL2-NPRL3, we chose to investigate if CSW might regulate RAG GTPase. We showed by HEK-293 (Human Embryonic Kidney-293) cell transfection and co-immunoprecipitation that HA-tagged C9ORF72, SMCR8 and WDR41 didn't interact with any FLAG-tagged RAG A,B,C or D upon starvation or basal conditions (data not shown).

However, with more than 170 small GTPase found in humans, small GTPases constitute a large family potentially regulated by CSW. Several papers shows that CSW could regulate RAB GTPase including RAB8a and RAB39b (Sellier et al., 2016; Yang et al., 2016), RAB1a (Webster et al., 2016) and/or RAB5 (Farg et al., 2014; Shi et al., 2018) in order to regulate autophagy; RAB7 and RAB11 to regulate endocytosis (Farg et al., 2014) or RAB3 to regulate exocytosis (Frick et al., 2018). The majority of these research do, however, demonstrate weak or indirect interactions. In order to select the most pertinent small GTPase, we decided to thoroughly screen the majority of them. The RAB family needs to be the one that has been examined the most in order to determine which is controlled by the CSW complex. However, HEK-293 cell transfection and co-immunoprecipitation experiments revealed that HA-tagged C9ORF72, untagged-SMCR8 and untagged-WDR41 did not strongly interact with FLAG-tagged RAB proteins. We decided to focus on one less studies family, the ARL/ARF family. Surprisingly, some of them, including ARL4, 11, 14 and 15, showed interesting results (Figure 33). Neither of these ARLs proteins has been described to interact with the CSW complex. However, ARL 11 and 15 were glued to the beads and pointed out that the interaction may not be related to CSW (data not shown).

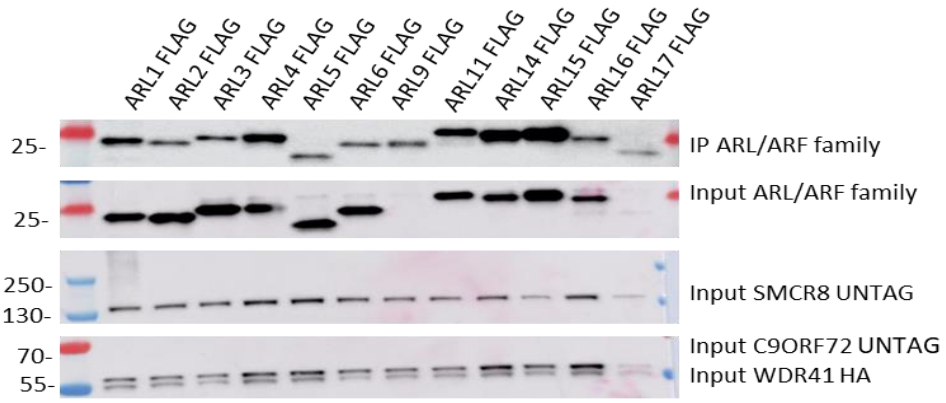


Figure 33 Screening of CSW complex interacting with ARF/ARL protein family

Immunoblot analysis of HA-immunoprecipitated proteins and lysate of HEK293 cells co-expressing HA-tagged WDR41, untagged SMCR8 and untagged C9ORF72 with FLAG-tagged ARL/ARF proteins.

## 2.2 CSW complex interact with ARL4 and ARL14

Structural analysis highlighted that CSW complex should act as a GTPase activating protein (GAP) for small GTPase, promoting the hydrolysis of GTP to leading to inactivation of the GTPase (Figure 34-A). In that aspect, CSW should binds active form of ARL14 to inactivate them. However, HEK-293 cell transfection and co-immunoprecipitation experiments of HA-tagged C9ORF72, SMCR8 and WDR41 interact with both form of either FLAG-tagged ARL14 T28N (mimicking ARL14 GDP inactive state) and ARL14 Q68L (mimicking GTP active state) without any distinction (Figure 34-B). Same conclusion for FLAG-tagged ARL4a T34N and Q79L (mimicking respectively ARL4 GDP inactive and GTP active forms) was observed. ARL4 (Q79L) and ARL14 (Q68L) were used in all subsequent experiments to be consistent with the described GAP activity of CSW. As described in chapter 2.4.2, CSW seems to regulated autophagy at an unknown step (Amick et al., 2020, 2018, 2016; Sullivan et al., 2016; Ugolino et al., 2016). We employed previously identified FLAG-tagged ARL14 (Q68L) and FLAG-tagged ARL4a (Q79L) that were co-immunoprecipitated with HA-tagged C9ORF72, SMCR8, and WDR41 and conducted the same experiment with and without inducing autophagy to see if the complex could have a role in it. Interestingly, prolonged starvation was found to strengthen the interaction between CSW and ARL14 (Q68L). Indeed, after 8 hours of starvation the pull down of ARL14 by the CSW complex is at its peak. However, interaction was less robust and starvation-independent for ARL4 (Q79L) compared to ARL14 (Figure 34-C,D).

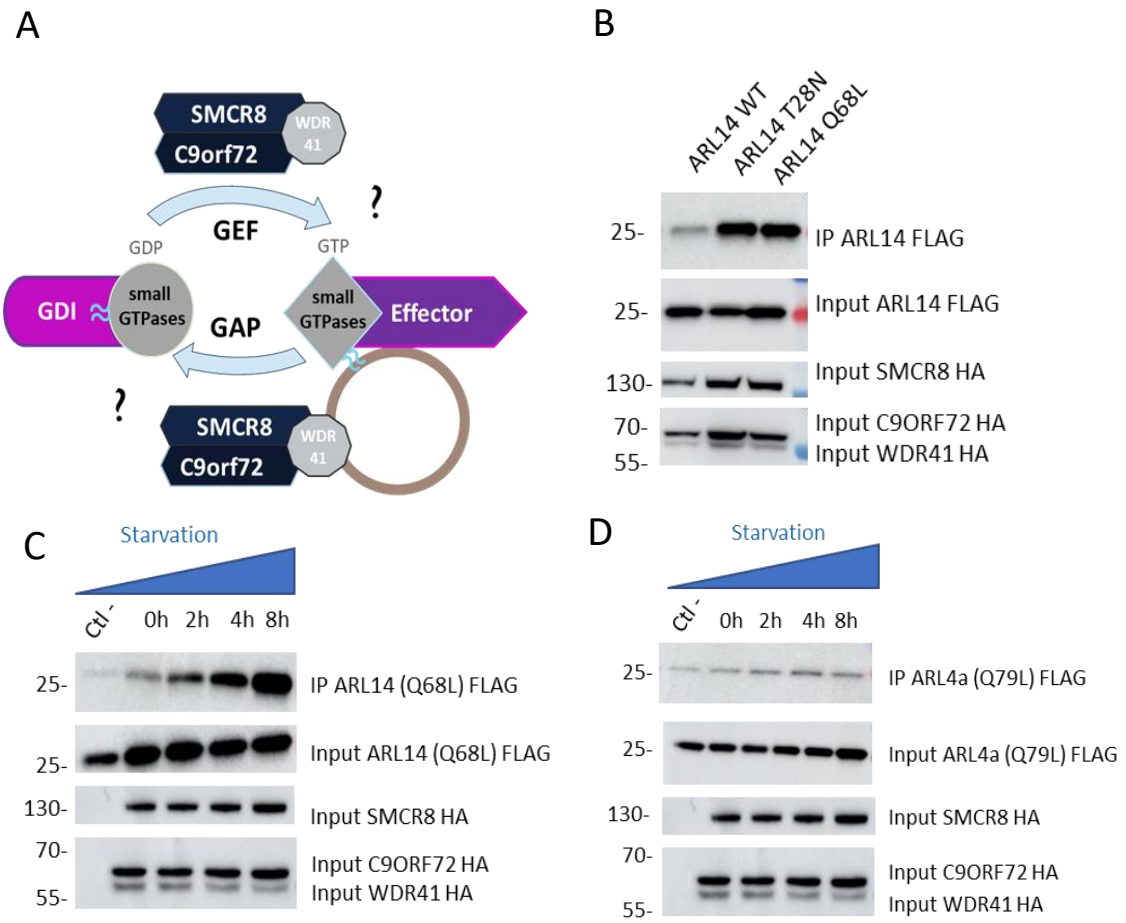


Figure 34 CSW complex interact with ARL4 and ARL14

(**A**) Schematic representation of CSW acting as a GAP or a GEF on smallGTPase. (**B**) Immunoblot analysis of HA-immunoprecipitated proteins and lysate of HEK293 cells co-expressing HA-tagged WDR41, HA-tagged SMCR8 and HA-tagged C9ORF72 with FlAG-tagged ARL14 WT or in GDP or GTP lock state. (**C**) Same experiment with ARL14 locked in GDP state with different starved time as well for (**D**) ARL4a locked in GDP state.

ARL4 and ARL14 are both poorly understood:

- ARL14 interact with MYO1E via the effector protein ARL14EP to controls MHC class II-containing vesicles movement along the actin cytoskeleton (Paul et al., 2011). However, we weren't able to reproduce these interactions or colocalization between ARL14 and ARL14EP or (Myosin IE) MYO1E in U2OS or HEK cells.
- ARL4 interact with (ARF nucleotide-binding site opener) ARNO, which is described as a guanine-nucleotide exchange factor (GEF) for ARF6 (Hofmann et al., 2007), although we didn't replicate these results by co-immunoprecipitation or colocalization.

To further explore CSW-ARL14 role in autophagy, we created U2OS stable cells line expressing LAMP1-cherry, a known marker of lysosomes, along with GFP-tagged ARL14 (Q68L) or GFP-tagged ARL4a (Q79L) and a 2A peptide system (where 2A peptide are inserted between two CDNA encoding different proteins). Briefly, the peptide will be translated into FLAG-tagged C9ORF72 and HA-tagged SMCR8 independently due to ribosome skipping (Liu et al., 2017). In that regard, we first validated of our P2A system by confirming that SCMR8 and C9ORF72 were both completely colocalized and expressed in the cytoplasm (Figure 35-A). Under 8 hours starvation conditions, C9ORF72 and SMCR8 went from a diffuse localization in the cytoplasm to a punctate localization in the cytoplasm (Figure 35-B). ARL4a (Q79L) also exhibits cytoplasmic diffuse localization under prolonged starvation conditions, whereas ARL14 (Q68L) exhibits some colocalization with Lysosomal-Associated Membrane Protein 1 (LAMP-1) positive puncta. (Figure 35-B). Co-expression in U20S cells of C9-S8 P2A and FLAG-tagged ARL4a (Q79L) or FLAG-tagged ARL14 (Q68L) shows a re-colocalization of ARL4a (Q79L) with C9-S8. The same outcome was observed with ARL14 (Q68L) suggesting a recruitment of CSW by ARL4 and/or ARL14 to the lysosome (Figure 35-C).

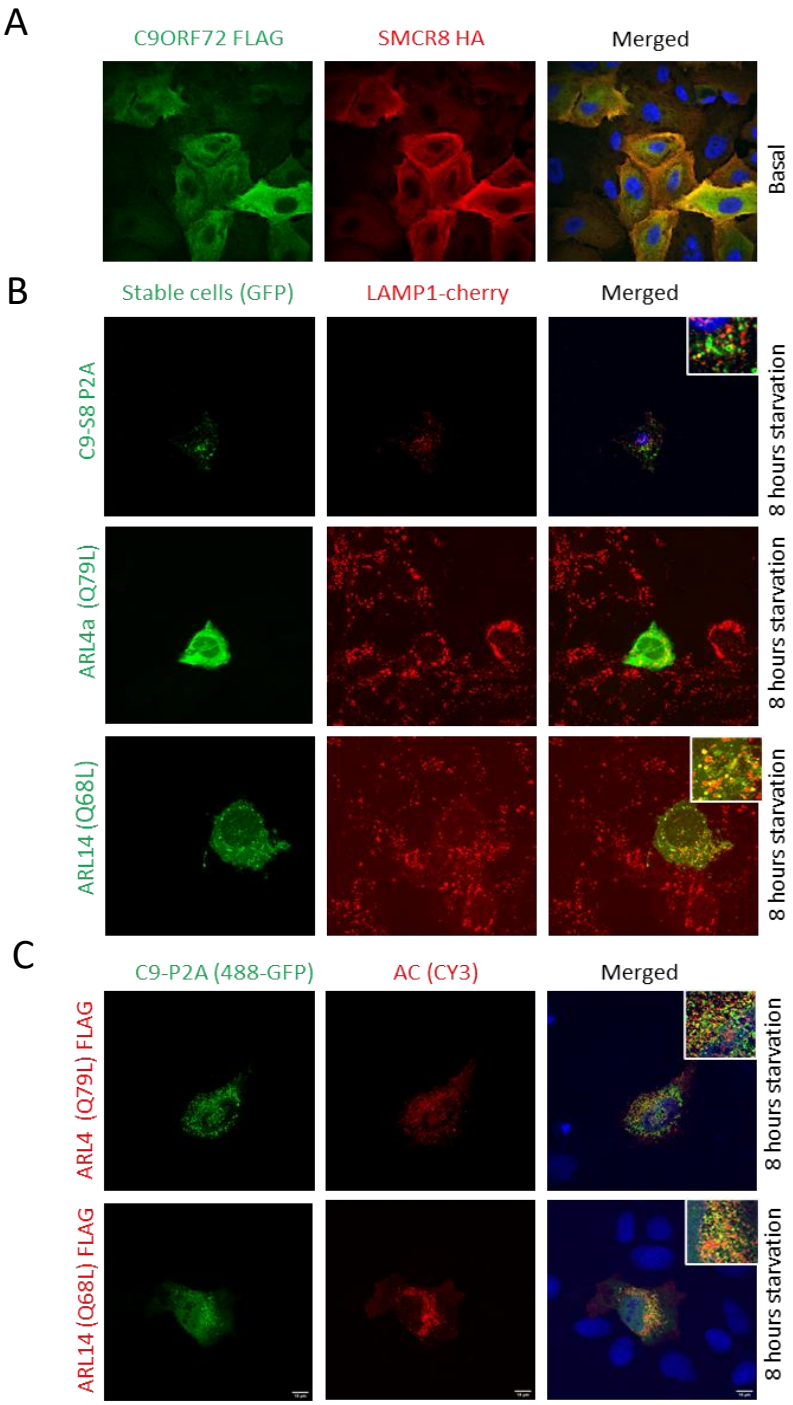


Figure 35 ARL 14 recruit CSW to the lysosome

(**A**) Representative images of immunofluorescence labeling of U2OS stable cells line expressing P2A construct FLAG-tagged C9ORF72 and HA-tagged SMCR8. (**B**) U2OS stable cells line expressing LAMP1-cherry and either C9ORF72-SMCR8 or ARL4a or ARL14 (**C**) U2OS stable cells line expressing C9ORF72-SMCR8 P2A and transfected FLAG-tagged ARL14 or FLAG-tagged ARL4a.

## 2.3 ARL 14 and CSW interaction is dependent on SMCR8 phosphorylation

As previously mentioned (Figure 32), SMCR8 is rich in phosphorylatable serine and threonine residue. We carried out phosphomutations of one to several sites to test whether these sites could have an impact on the interaction between CSW and ARL14. Indeed, mutated serine or threonine residue into alanine mimic an inactive state whereas an aspartate mimic phosphorylation and an active state. Interestingly, we found that S102 D and T140 D mutations in the active state enhance ARL14 interaction with the CSW complex and help stabilize the complex (Figure 36-A,C). Moreover, these phosphorylatables sites are located near the ARG147, the characteristic binding pocket of CSW for small GTPase (Figure 36-C). However, the kinase phosphorylating these sites are unknown. Furthermore, we can also see an increase interaction when the S790D residue is mutated in the active state (Figure 36-A). It's really intriguing that the kinase controlling this phosphorylation, TBK1, has been demonstrated to interact with CSW and have a role in autophagy (Sellier et al., 2016). Moreover, deletion of SMCR8 middle part, were the majority of phosphorylatables autophagic dependent site are located (between AA 380 and 800), increases the interaction between CSW and ARL14 (Q68L), highlighting the importance of autophagy and the regulatory role of SMCR8 phosphorylation in CSW-ALR14 interaction (Figure 36-B,D).

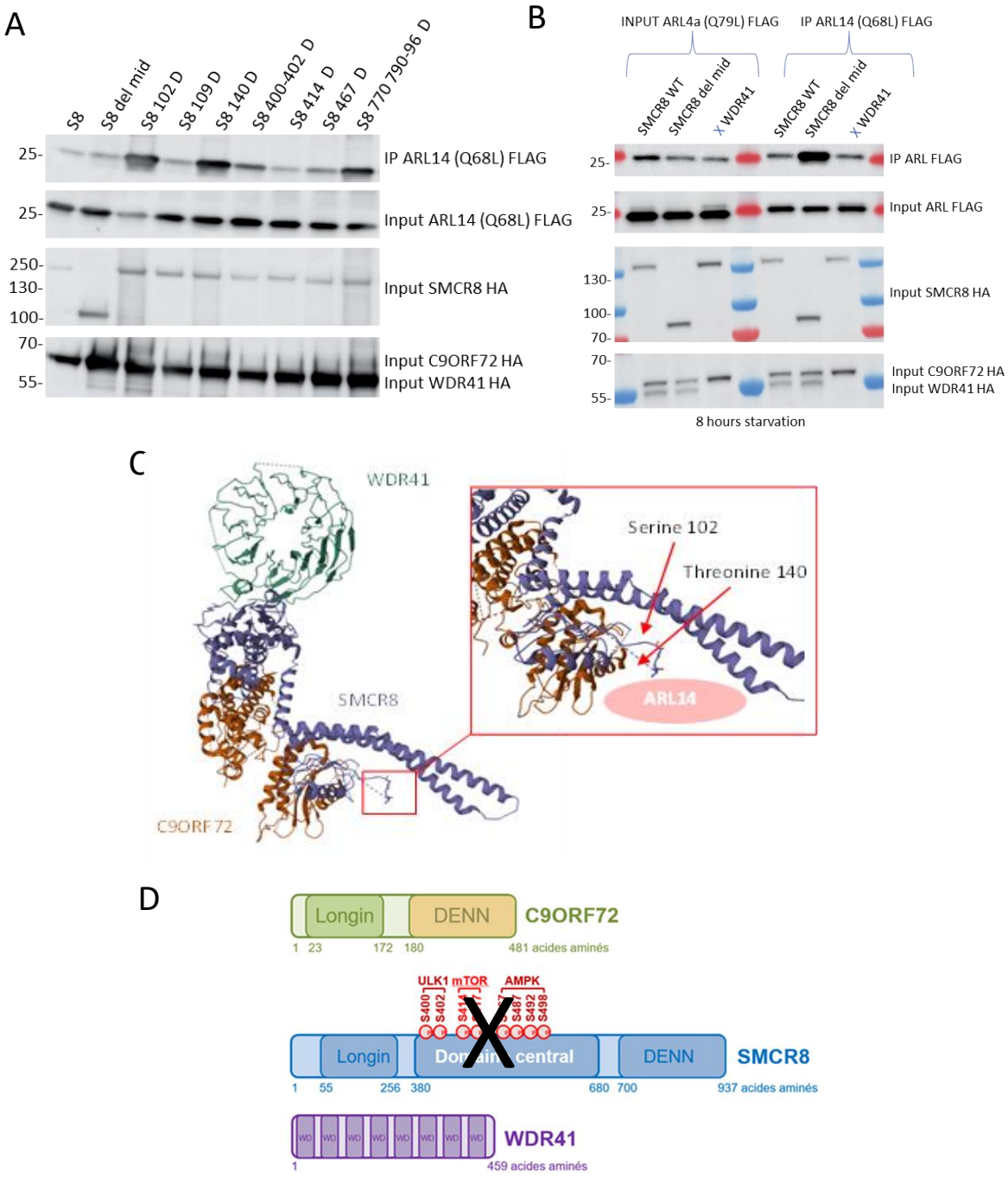


Figure 36 Importance of phosphorylation residues in SMCR8 for ARL14 interaction

(**A**) Immunoblot analysis of HA-immunoprecipitated proteins and lysate of HEK293 cells co-expressing HA-tagged WDR41, HA-tagged C9ORF72 and different phosphorylatables mutated site in HA-tagged SMCR8 with FLAG-tagged ARL14 in basal conditions. (**B**) Immunoblot analysis of HA-immunoprecipitated proteins and lysate of HEK293 cells co-expressing HA-tagged WDR41, HA-tagged C9ORF72, and WT HA-tagged SMCR8 as well as HA-tagged SMCR8 deleted from its middle part with FLAG tagged-ARL4a or ALR14 in starved conditions. (**C**) Structure of the CSW complex and the position of the Serine 102 and threonine 140 nearby the ARG147. The hypothetic binding site of ARL14 is also shown. (**D**) Schematic representation of Longin and Denn domain of CSW complex and the removed central domain (SCMR8 del mid) rich in phosphorylatables residues.

## 2.4 CSW-ARL14 proteomic analysis identified a potential new interaction: FIP200

Co-immunoprecipitation experiments of WRD41 GFP-tagged with HA-tagged C9ORF72, SMCR8 and FLAG-tagged ARL14 (Q68L) followed by nanoscale liquid chromatography coupled to tandem mass spectrometry (nano-LC-MS/MS) analysis identified various proteins including RB1-inducible coiled-coil protein 1 (RB1CC1) also commonly called FIP200 (Table 2). FIP200 is part of the ULK1 kinase complex and is currently one of most upstream regulators of the autophagic pathway. Interestingly, SMCR8 has already been identified as a potential interacting protein of FIP200 (Behrends et al., 2010; Sellier et al., 2016; Sullivan et al., 2016; Webster et al., 2016). HEK-293 cell transfection and co-immunoprecipitation experiments of WDR41 FLAG-tagged C9ORF72 untagged, untagged-SMCR8 and untagged-ARL14 (Q68L) revealed a super-complex CSW-ARL14-FIP200 (Figure 37-A,B). However, whether FIP200 or ARL14 (Q68L) were present or not, had no effect on the intensity of their interactions with CSW.

## 2.5 CSW-FIP200-ARL14 structure

To take advantage of these results, harvested baculovirus containing either STREP-tagged WDR41, HIS-tagged ARL14 (Q68L) and untagged FIP200, C9ORF72 and SMCR8 were then tested, amplified and used to infect 2 liters of SF21 cell culture for protein production and purification. Blue Coomassie staining from co-immunoprecipitated infected SF21 cells reveals FIP200 forming a complex with CSW complex but with very little ARL14 (Q68L) (Figure 37-C). Same experiment was made with ALR14 in isolation with the CSW complex. However, ARL14 expression was still very low. Purification on a strep-tactin XT column followed by a gel filtration S200 results in different fraction analyzed by Western-Blot resulting in a positive purification test with the presence of SMCR8, C9ORF72, WDR41 and FIP200 (Figure 37-D). Unfortunately, first EM negative coloration shows an aggregation of the complex. However, adding low quantity of DDM allows to have less aggregate and results in usable grid. Also, negative coloration EM of CSW-FIP200 complex as a different appearance from the sole CSW complex. These encouraging results are currently under investigation and optimization.

Table 2 Nano-LC MS/MS results of co-immunoprecipitated WRD41 GFP-tagged with HA-tagged C9ORF72, SMCR8 and FLAG-tagged ARL14 (Q68L)

| Description | Ratio SAMPLE/CTL GFP beads | Gene Name | Coverage [%] | # Peptides | # PSMs |
|---|---|---|---|---|---|
| Cytochrome c OS=Homo sapiens OX=9606 | 1926,65 | CYCS | 27 | 2 | 14 |
| SMCR8 HA | 1135,11 | SMCR8 | 65 | 45 | 1373 |
| Guanine nucleotide exchange C9orf72 OS=Homo sapiens OX=9606 | 544,09 | C9orf72 | 24 | 11 | 201 |
| RB1-inducible coiled-coil protein 1 OS=Homo sapiens OX=9606 | 426,20 | RB1CC1 | 12 | 18 | 74 |
| RNA-binding protein 12B OS=Homo sapiens OX=9606 | 125,76 | RBM12B | 10 | 9 | 69 |
| ARL14 CA Flag | 51,34 | ARL14 CA | 14 | 2 | 49 |
| ADP-ribosylation factor-like protein 14 OS=Homo sapiens OX=9606 | 51,34 | ARL14 | 15 | 2 | 49 |
| BAG family molecular chaperone regulator 5 OS=Homo sapiens OX=9606 | 48,58 | BAG5 | 17 | 6 | 35 |
| BAG family molecular chaperone regulator 2 OS=Homo sapiens OX=9606 | 41,30 | BAG2 | 24 | 4 | 32 |
| MMS19 nucleotide excision repair protein homolog OS=Homo sapiens OX=9606 | 35,84 | MMS19 | 2 | 2 | 7 |
| Erlin-2 OS=Homo sapiens OX=9606 | 35,20 | ERLIN2 | 14 | 4 | 12 |
| Probable cytosolic iron-sulfur protein assembly protein CIAO1 OS=Homo sapiens OX=9606 | 28,87 | CIAO1 | 11 | 3 | 8 |
| Cytosolic iron-sulfur assembly component 2B OS=Homo sapiens OX=9606 | 27,16 | CIAO2B | 26 | 2 | 6 |
| Hypoxia-inducible factor 1-alpha inhibitor OS=Homo sapiens OX=9606 | 23,21 | HIF1AN | 17 | 4 | 29 |
| WDR41-GFP | 22,97 | WDR41 | 56 | 32 | 4140 |

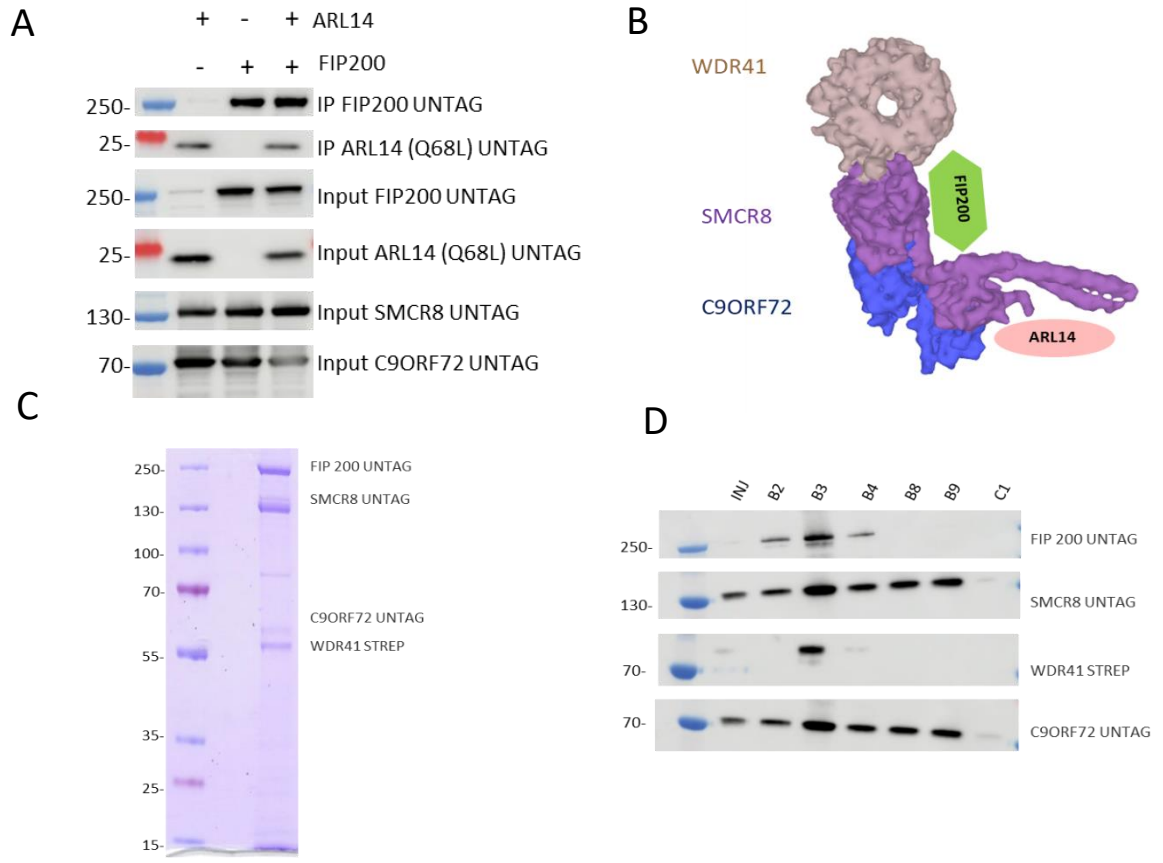


Figure 37 CSW-ARL14 interact with FIP200

(**A**) Immunoblot analysis of HA-immunoprecipitated proteins and lysate of HEK293 cells co-expressing STREP-tagged WDR41, untagged C9ORF72, untagged SMCR8 with FLAG-tagged ARL14 and/or untagged FIP200. (**B**) Schematic representation of CSW-ARL14 and FIP200 supercomplex. (**C**) Comassie blue of STREP- immunoprecipitation of SF21 infected cells revealing FIP-200 forming a complex with CSW complex but with very low quantity of ARL14 (Q68L). (**D**) Immunoblot analysis of SF21 infected cells purified on a strep-tactin XT column followed by a gel filtration S200 resulting in a B3 fraction containing the CSW complex and FIP200.

## 2.6 Mouse models: *C9orf72* $^{-/-}$ and *C9orf72*$^{-/-}$ - *Arl14*$^{-/-}$

*C9orf72* knockout mice shows neither of *c9orf72* hallmarks (TDP-43, P62 or ubiquitin aggregates) nor behavioral or motor phenotypes. Interestingly, mouse *C9orf72* knockout do not present any motor neuron degeneration but an inflammatory phenotype (splenomegaly, enlarged lymph nodes, infiltration of immune cells, increased expression of inflammatory cytokines, presence of autoantibodies and immune-mediated glomerulonephropathy) (Burberry et al., 2016; Jiang et al., 2016; Koppers et al., 2015; O'Rourke et al., 2016; Shi et al., 2018; Sudria-Lopez et al., 2016; Sullivan et al., 2016). Interestingly, increased levels of autophagy and lysosomal proteins and autophagy defects were detected in both the spleen and liver of *C9orf72* deficient mice, supporting an *in-vivo* role of C9ORF72 in regulating the autophagy/lysosome pathway (O'Rourke et al., 2016).

Our recent discovery linking the CSW complex and ARL14 in autophagy and the putative immune system function of ARL14, characterized as a small GTPase recruiting MYO1E to MHC class II-containing vesicles (Paul et al., 2011), led us to construct a double knock-out mouse, *C9orf72 -/- Arl14 -/-*. Our hypothesis suggests a potential rescue of the inflammatory phenotype of *C9orf72* knockout mouse in our double knockout model *c9orf72* $^{-/-}$ *arl14* $^{-/-}$. Unfortunately, both *C9orf72 -/- Arl14 -/-* and *C9orf72 -/-* mice showed the same inflammatory phenotype. However, *Arl14* $^{-/-}$ mice exhibit an intriguing trait in while they does not develop obesity in comparison to WT mice, suggesting a metabolic deficiency (Figure 38).

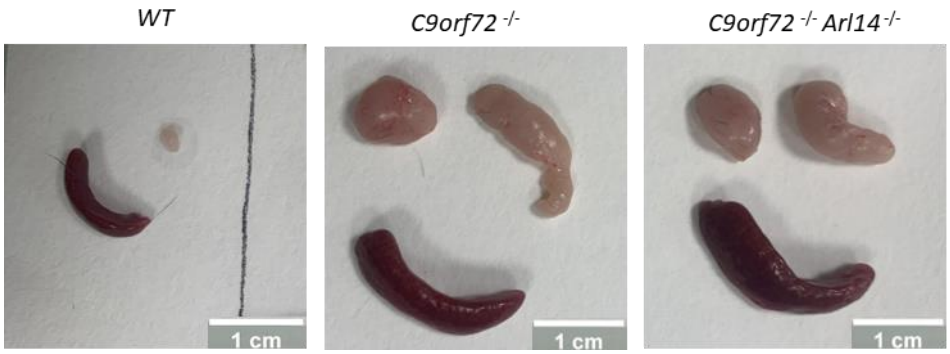


Figure 38 *C9orf72-/- Arl14-/-* double KO mouse do not rescue *C9orf72-/-* inflammatory phenotype

Pictures of splenomegaly and enlarged lymph nodes in *C9orf72* $^{-/-}$ *and C9orf72* $^{-/-}$ *Arl14* $^{-/-}$ mice comparing to WT.

## 2.7 CSW complex has a role in autophagy

The structure determination of CSW with FIP200 or ALR14 is currently still under investigation. However, the increase interaction of CSW with ARL14 during starvation, recruitment of CSW by ARL 14 at the lysosome, the importance of SMCR8 phosphorylatable site by autophagic kinase for CSW-ARL14 complex and its interaction with FIP200, having a key role in autophagy initiation, all point to the possibility that this complex is involved in autophagy. Interestingly, the 8 hours of starvation shift (where CSW-ARL14 interaction is at its spike) corresponds to the timeline when Autophagic Lysosome Regeneration (ALR) start, suggesting a role of the CSW-ARL14 complex in ALR regulation (Rong et al., 2011). Thus, we decided to further explore this hypothesis in part 3.

# 3. C9ORF72 present a role in Autophagic Lysosome Regeneration

## 3.1 CSW complex is localized at the lysosome

To decipher the role of CSW at the lysosome was a primary subject of my thesis. First, we focused on the function of C9ORF72 at lysosome, but observed no difference in PH, number and size of lysosomes upon siRNA-down regulation or CRISPR cas9 deletion of C9ORF72. Second, these cells show no accumulation of P62, a classic autophagic marker. However, a minor reduction in LC3B lipidation correlates with the results reported in previous articles. (Figure 39-A,B,C,D) (Sellier et al., 2016; Sullivan et al., 2016; Ugolino et al., 2016; Webster et al., 2016). Finally, we were also interested in the precise localization of the CSW complex. However, initial cell transfection failed to provide information on the precise localization of C9ORF72 or SMCR8 at the lysosome. Nevertheless, we demonstrated that the WDR41 protein helps recruiting C9ORF72 and SMCR8 to lysosomes after induction of autophagy by amino acid restriction, but also during autophagy induced by molecules that inhibit mTOR such as WYE-354 or torin. Of interest, it was a major breakthrough as we used to tag C9ORF72 and SMCR8 which generated a cytoplasmic localization of the complex (Figure 39-E). These results are consistent with those observed by Amick and colleagues in 2018 (Amick et al., 2018). However, the CSW role at the lysosome and in autophagy is still unclear.

Nevertheless, recent finding on the interaction between CSW and ARL14 during prolonged starvation open a new a new path to study C9ORF72 role in autophagy.

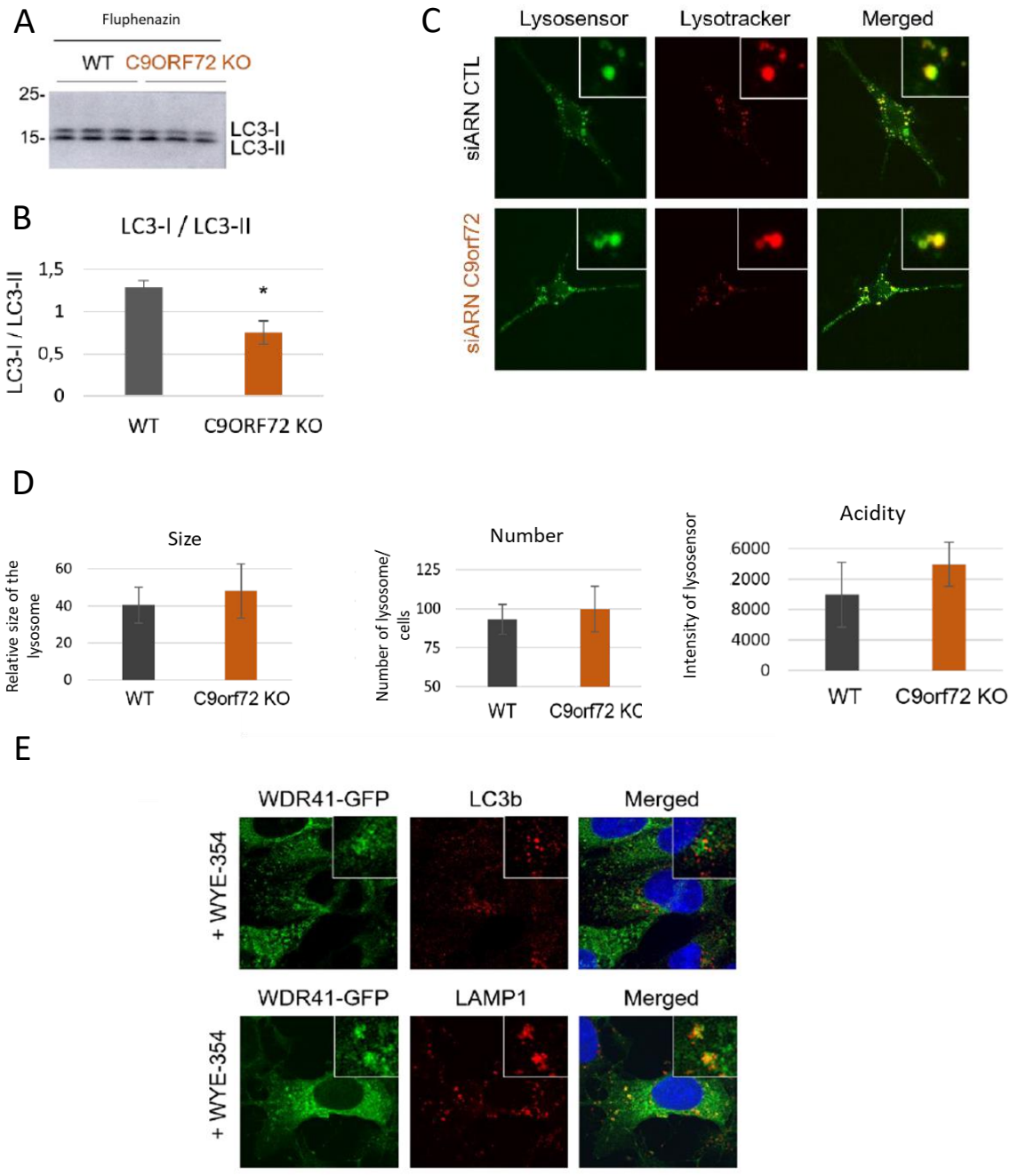


Figure 39 Implication of CSW complex at the lysosome

(**A**) Western blot directed against LC3b after induction of autophagy at fluphenazine for 16 h in U2OS WT or KO cells for the *C9ORF72* gene and, (**B**) its quantization. (**C**) GT1-7 cells depleted or not of *C9ORF72* by siRNA where the lysotrackers and lysosensor were added in order to visualize the lysosomes and quantify their (**D**) acidity, number and size. (**E**) WDR41-GFP is localized to lysosomes after induction of autophagy by WYE-354 for 8 hours (Adaptation from Manon Boivin, 2020).

## 3.2 *C9ORF72* KO cells have a deficit in Autophagic Lysosome regeneration

Considering the interaction between CSW and ARL14 at the lysosome during prolonged starvation, we explored its potential role in Autophagic Lysosome Reformation (ALR). Briefly, short-term cell starvation induces autophagy, a self-cannibalization process that targets non-specific and non-essential cell constituents into the lysosome for their degradation in order to supply nutrients and energy. Autophagy is regulated by inhibition of the mTOR kinase, which senses amino acid at lysosomes. However, after 6 to 8 hours of starvation, mTOR is reactivated and autophagy is stopped to avoid degradation of vital proteins and lysosomes are regenerated, a mechanism unveiled only recently and that was named Autophagic Lysosome Reformation (ALR) (Rong et al., 2012; Yu et al., 2010). This process involves the formation of lysosome membrane patches enriched into PtdIns(4,5)2P that consequently bud into lysosomal tubules, which will be ultimately be scissored by the Dynamin 2 to form novel lysosomes. Thus, to follow ALR by time laps microscopy, we created stable cells lines expressing LAMP1, a known marker of lysosomes, which was tagged by the Cherry fluorescent protein. Furthermore, thanks to CRISPR cas9 we deleted C9ORF72 exons 2 to 4 resulting in creation of a *C9orf72* knockout cell line. Then, cells were starved for 8 hours with Dynasore treatment for 40 minutes (an inhibitor of Dynamin 2 to prevent lysosome tubules excision), resulting in numerous LAMP1-Cherry positive lysosomal tubules. Importantly, the loss of C9ORF72 resulted in a quasi-complete absence of lysosomes tubules, indicating that C9ORF72 is essential for Autophagic Lysosome Reformation (Figure 40-A,B,C,D). Furthermore we also observed an overall decrease number of lysosomes and enlarged lysosome in *C9orf72* KO cells confirming that lysosome were consumed and unable to recover (Figure 40-C,D).

In order to rescue the defective ALR in *C9orf72* KO cells, we overexpressed ARL14 and ARL4 in *C9orf72* KO cells after prolonged starvation. However, we observed no rescue of tubules formation in ALR14 or ARL4 overexpress cells despite a localization of ARL14 at the lysosome (Figure 40-E). Consistent with previous results, ARL14 seems to recruit the CSW complex at the autolysosome/lysosome in order to regulate tubulation. However, its role needs to be clarified (Figure 40-F).

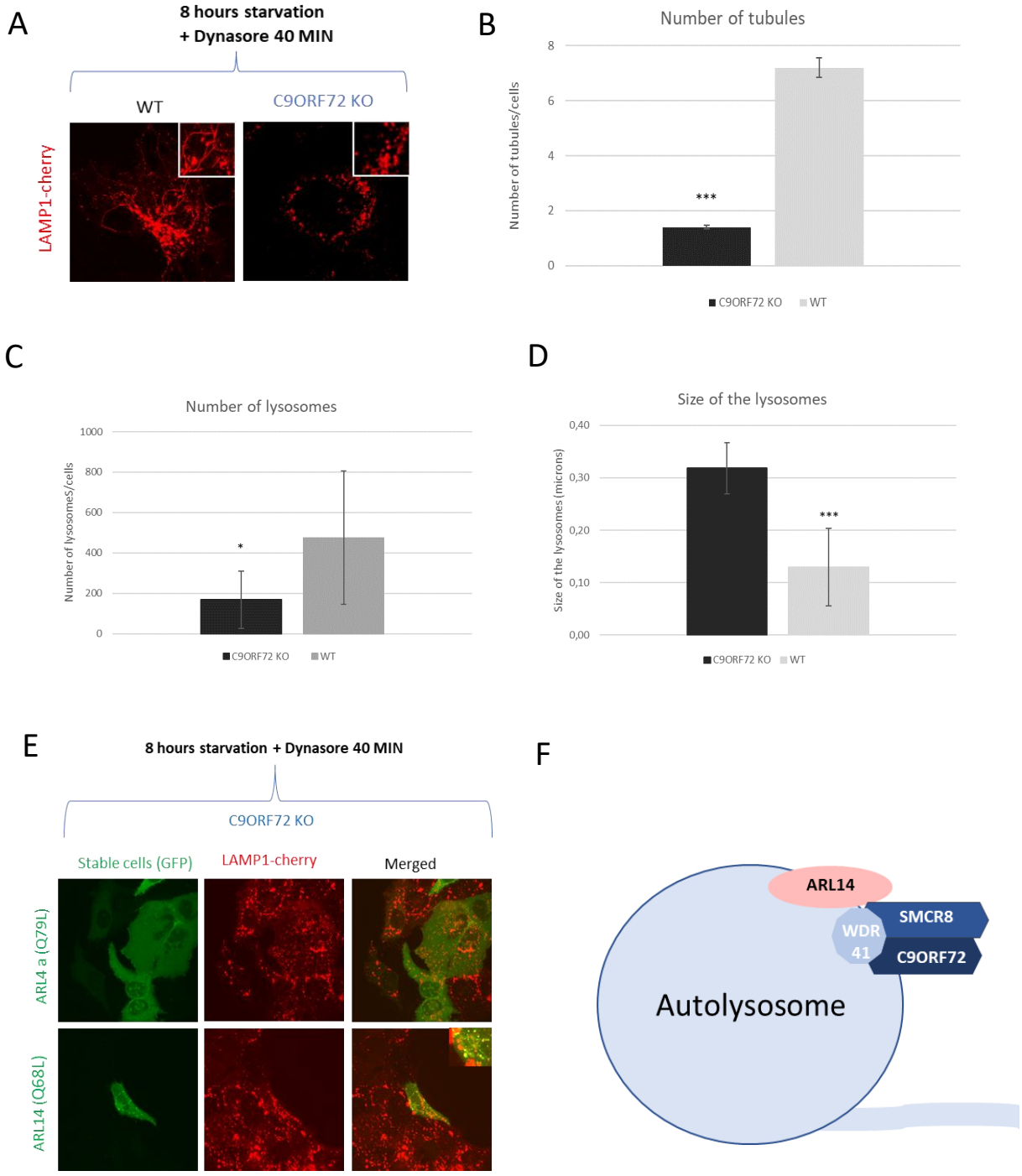


Figure 40 *C9ORF72* KO cells present a deficit in Autophagic Lysosome Reformation (ALR)

(**A**) Representative images of immunofluorescence labeling of U2OS WT or depleted of *C9ORF72* stable cells line expressing LAMP1-cherry after 8 hours of starvation and 40 min of dynasore treatment. (**B**) Quantification of tubules/cells. (**C**) number of lysosomes/cells and (**D**) size of the lysosomes. Mean ± SD are shown. Student-T-TEST, n=15, t-test *pvalue<0,05, ***p-value <0.001. (**E**) Representative images of immunofluorescence labeling of U2OS *C9ORF72* depleted stable cells expressing LAMP1-cherry and GFP-tagged ALR4a or ARL14 after 8 hours of starvation and 40 min of dynasore. (**F**) Schematic representation of the ongoing models of CSW-ARL14 complex regulating ALR.

## 3.3 The CSW complex interact with AP5 complex in order to regulate ALR

*C9ORF72* KO cells show that C9ORF72 is important to induce ALR. However, this new role has never been described and has to be clarified. To take advantage of these results we tried to determine at which steps the CSW complex could regulate ALR. ALR is notably regulated by various AP (adaptor protein) complexes. The AP (adaptor protein) complexes are heterotetrametric protein complexes that mediate intracellular membrane trafficking along endocytic and secretory transport pathways (Park and Guo, 2014). Interestingly, there is 5 different AP-complex : AP-1,2,3,4 and 5 where AP-2 (Du et al., 2016; Höning et al., 2005; Rong et al., 2012) and AP-5-SPG11-15 complex (Chang et al., 2014; Hirst et al., 2021) have already been described to have a role in ALR. HEK-293 cell transfection and co-immunoprecipitation of HA-tagged WDR41, untagged-SMCR8 and untagged-C9ORF72 shows interaction with AP-5 FLAG-tagged subunits (Beta, Zeta, Mu and Sigma) upon starvation (Figure 41-A). However, the lack of SPG11 or SPG15 expression, indicates a low level of expression.

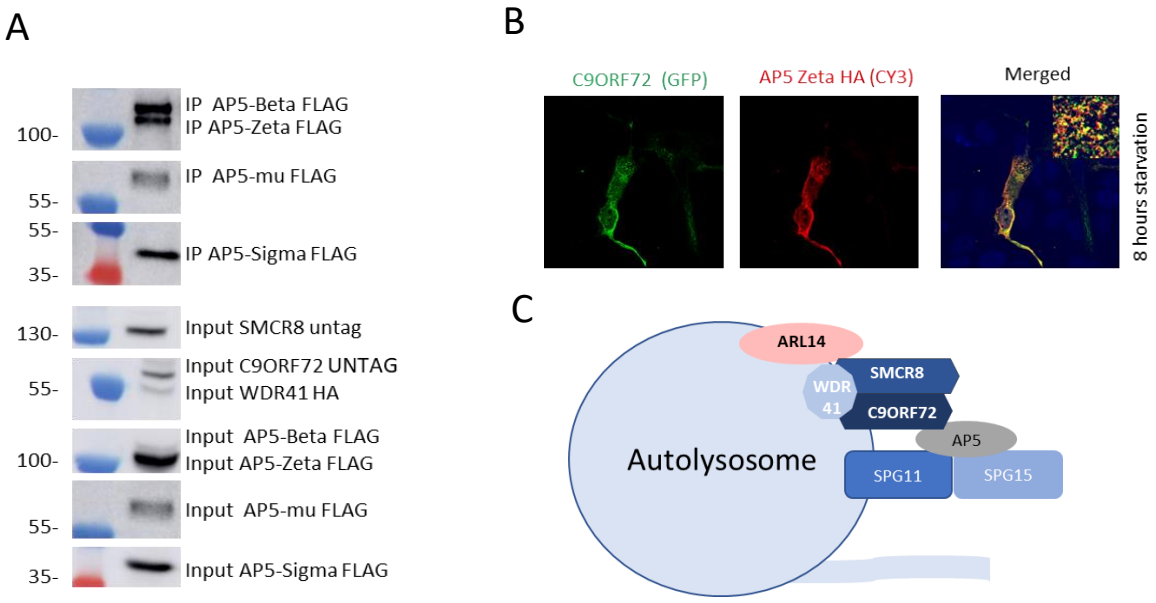


Figure 41 C9ORF72 interact with AP5 complex

(**A**) Immunoblot analysis of HA-immunoprecipitated proteins and lysate of HEK293 cells co-expressing HA-tagged WDR41, untagged C9ORF72, untagged SMCR8 and FLAG-tagged AP5 subunits. (**B**) Representative images of immunofluorescence labeling of U2OS transfected cells expressing GFP-tagged C9ORF72 and HA-tagged AP-Z subunits (red). (**C**) Schematic representation of the ongoing models of CSW-ARL14 complex regulating ALR via AP5-SPG11-15 complex.

Furthermore, GFP-tagged C9ORF72 and FLAG-tagged AP5 Zeta colocalize after 8 hours of starvation in U2OS transfected cells (Figure 41-B). Interestingly, transfected GFP-tagged AP-5-Z shows some discrete puncta distributed fairly and homogenously throughout the cytoplasm (Figure 42). Consistent with recent finding, the FYVE domain of SPG15 has been described to bind phosphoinositide-3 phosphate *in vitro* (PI3P) and have a lysosomal localization (Chang et al., 2014; Sagona et al., 2010). GFP-tagged SPG15 colocalize with LAMP-1 puncta, a known lysosomal marker, suggesting that SPG-11-15 is potentially recruiting and needed for AP5 lysosomal localization. This complex could then interact with CSW-ALR14 to regulate ALR (Figure 41-C), (Figure 42). However, the localization of SPG-15 and AP-5 do not correlate with starvation induction.

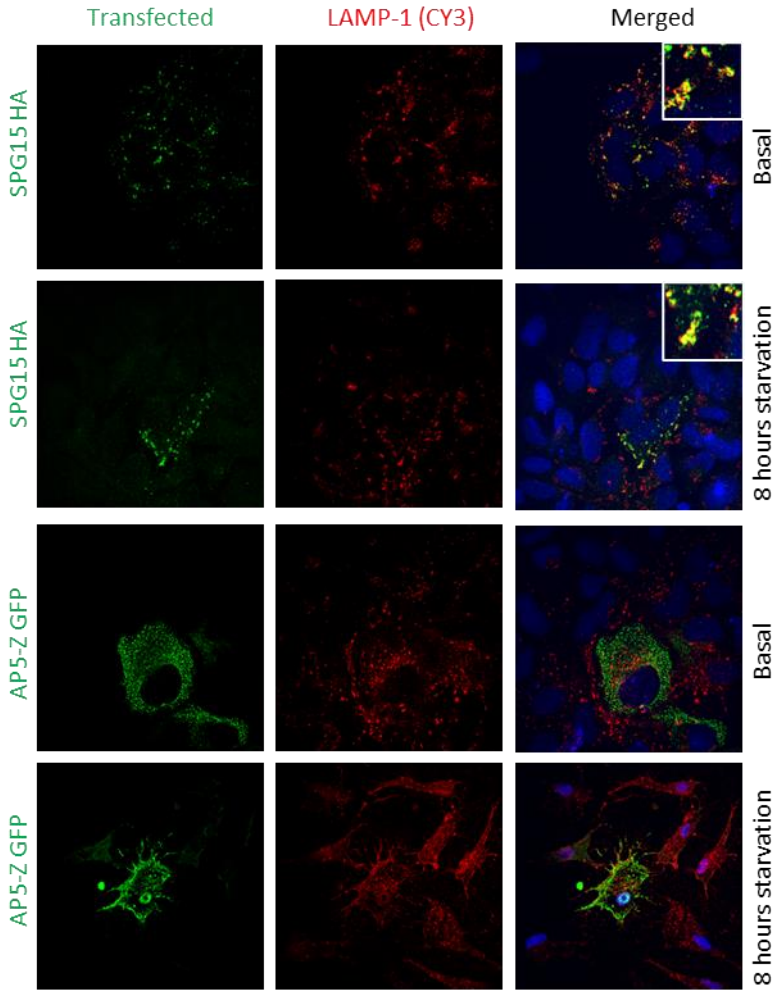


Figure 42 SPG15 recruit AP-5 to the lysosome.

Representative images of immunofluorescence labeling of U2OS transfected cells expressing SPG15 HA (green) or GFP-tagged AP5-Z and LAMP-1 (red) in basal or 8 hours starvation condition.

Interestingly, AP protein localization is frequently dependent on a conformational shift and interaction with a small GTPase, primarily ARF1 for AP-1, 3 and 4, and ARF-6 for AP-2 (Park and Guo, 2014). Surprisingly, the small GTPase of AP-5 has not been yet identified.

## 3.4 ARL4 small GTPase regulate AP-5 complex

Therefore, we searched for the small GTPase that could interact with AP-5 complex. HEK-293 transfected cells and co-immunoprecipitation with HA-tagged AP-5 subunits (Beta, Zeta, Mu and Sigma) and different FLAG-tagged ARL/ARF protein revealed an interaction with ARL4a. Interestingly, this interaction was enhanced when ARL4a was locked in its active state ARL4a (Q79L) and upon prolonged starvation (Figure 43-A). This recall earlier findings, showing a weak interaction between CSW and ARL4a (Q79L), suggesting an indirect interaction of the CSW complex with ARL4a (Figure 34-D). Overall, we propose a model where SPG-11-15 and/or CSW recruit AP5 to the lysosome and thus interact with ARL4 (Figure 43-B).

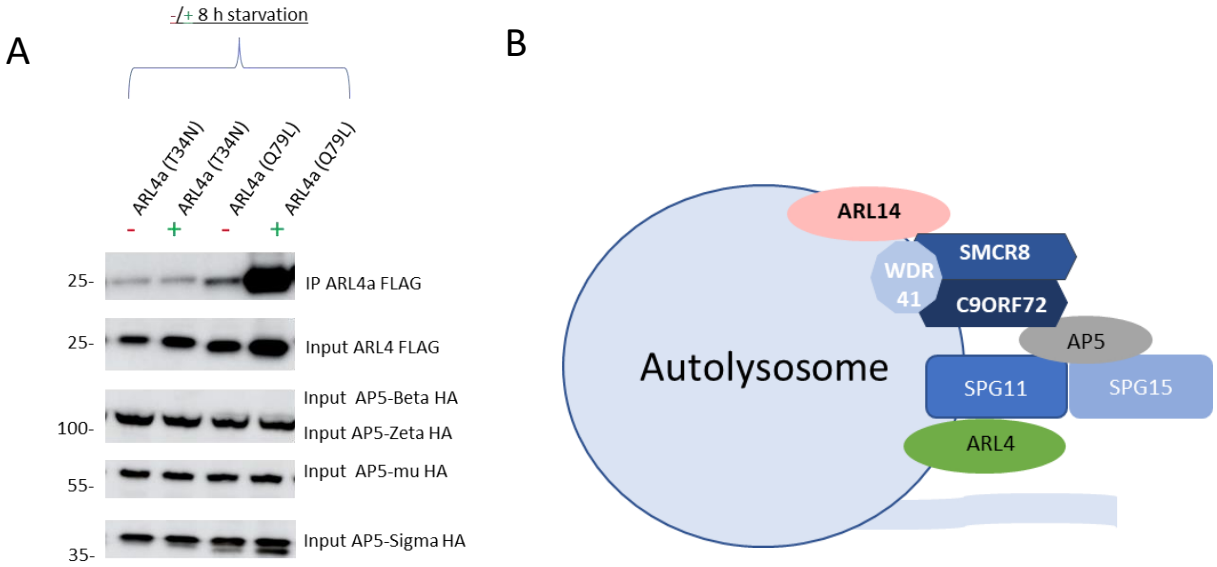


Figure 43 The small GTPase of AP5 complex is ARL4a

(**A**) Immunoblot analysis of HA-immunoprecipitated proteins and lysate of HEK293 cells co-expressing HA-tagged AP-5 subunits and FLAG-tagged ARL4a in GDP or GTP locked state with and without starvation. (**B**) Schematic representation of the ongoing models of CSW-ARL14 complex regulating ALR via AP5-SPG11-15 complex and it's small GTPase ARL4a.

## 3.5 CSW and AP5-ARL4a complex interact with PI4K2B lipid kinase

The absence of tubule in U2OS *C9ORF72* KO cells associating with decrease number of lysosomes and enlarged lysosome suggest that ALR is deficient and more precisely that tubulation of the lysosome reformation is impaired. Phosphoinositide is an important signaling molecule that defines the identity of intracellular membrane systems (Sridhar et al., 2013). Thus, we tested whether if this novel complex AP5-ARL4a may interact with phosphoinositide kinase to control ALR.

HEK-293 transfected cells and co-immunoprecipitation of HA-tagged ARL4a (Q79L) demonstrated interaction with GFP-tagged PI4K2B and weakly with PIP5K1B kinases (Figure 44-A). Phosphatidylinositol 4-Kinase Type 2 Beta (PI4K2B) phosphoinositide kinase is known to phosphorylate PtdIns into PtdIns(4)P and thus regulate vesicular tubulation; while phosphatidylinositol-4-phosphate 5-kinase type 1 beta (PIP5K1B) phosphorylates PtdIns(4)P into PtdIns(4,5)2P which is required for initiation of ALR (Balla et al., 2002; Rong et al., 2012). Interestingly, these interactions are negatively regulated by starvation meaning that they are enhanced in basal conditions. Same results have been observed when co-transfection and co-immunoprecipitation of HA-tagged AP-5 subunits pulling down both FLAG-tagged ARL4a (Q79L) and GFP-tagged PIK42B (Figure 44-B). This demonstrates the existence of a complex including AP5 and ARL4 that regulates PI4K2B. Similar interaction has also been observed between CSW and PI4K2B but was weaker than the AP5-ARL4-PI4K2B interaction, suggesting an indirect interaction (Figure 44-C).

Interestingly, U2OS-LAMP1 transfected cells with GFP-tagged PI4K2B shows some colocalization with LAMP-1 and LC3B, a marker of autophagosome, in either basal or starved conditions. However, as evidenced by earlier studies, the sole expression of PIK2B mostly displays co-localization with early endosomes and recycling endosomes (Balla et al., 2002; Rong et al., 2012) (Figure 44-D).

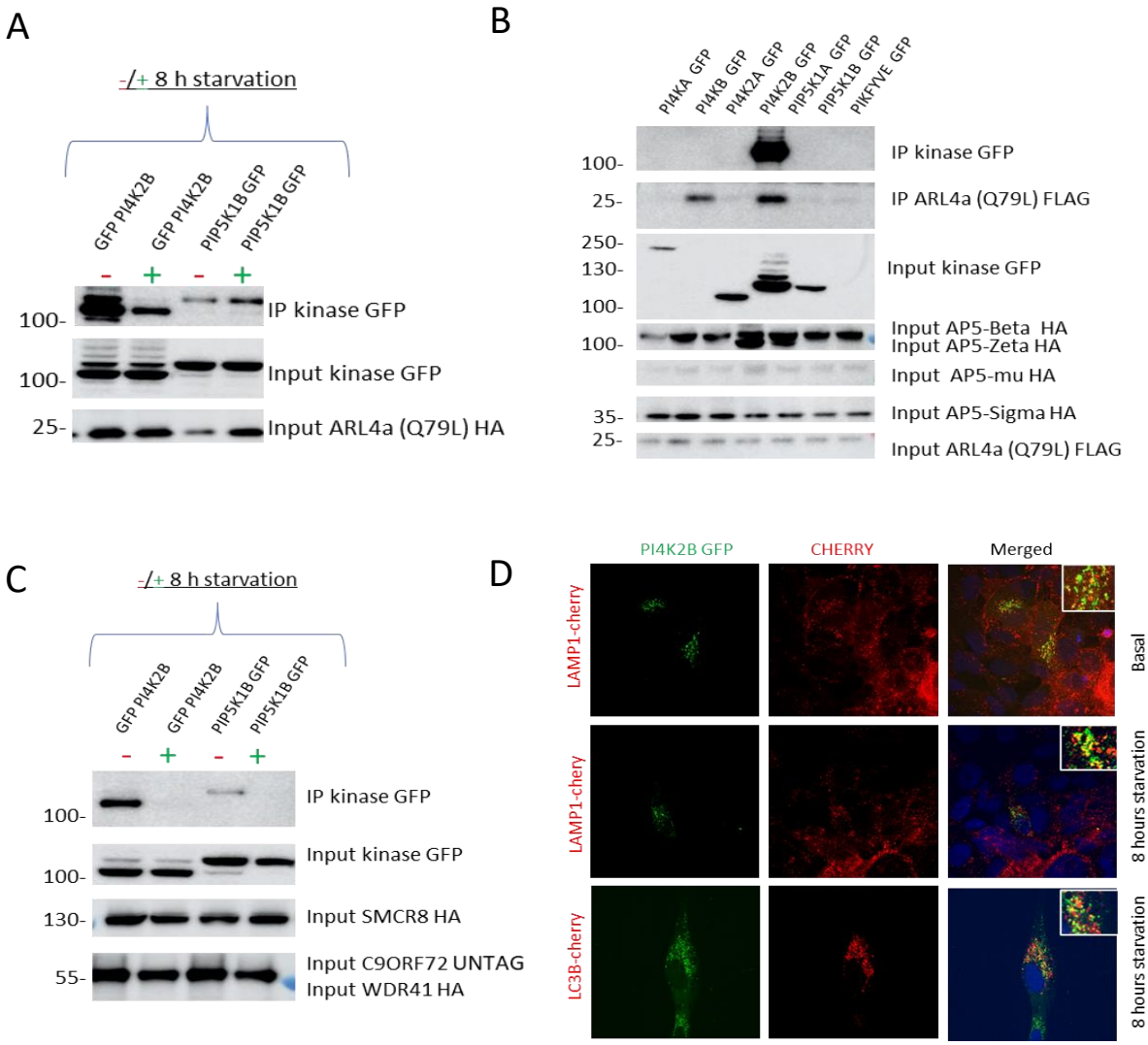


Figure 44 ARL4a interact with AP5-complex and PI4K2B

(**A**) Immunoblot analysis of HA-immunoprecipitated proteins and lysate of HEK293 cells co-expressing HA-tagged ARL4a and GFP-tagged PI4K2B or PIP5K1B with or without starvation. (**B**) Immunoblot analysis of HA-immunoprecipitated proteins and lysate of HEK293 cells co-expressing HA-tagged AP5 subunits and different GFP-tagged Phosphoinositide Kinase and FLAG-tagged ARL4a. (**C**) Immunoblot analysis of HA-immunoprecipitated proteins and lysate of HEK293 cells co-expressing HA-tagged WDR41 and untagged SMCR8 and C9ORF72 and different GFP-tagged phosphoinositide kinase with or without starvation. (**D**) Representative images of immunofluorescence labeling of U2OS LAMP-1 cherry stable cells line and transfected with GFP-tagged PI4K2B with and without starvation.

Nevertheless, U20S transfected cells with GFP-tagged PI4K2B and HA-tagged ARL4a (Q79L) shows perfect colocalization (Figure 45-A). Furthermore, transfection with GFP-tagged PI4K2B and HA-tagged SPG15 results in colocalized puncta (Figure 45-B). These puncta are very similar to lysosome and correlates with the lysosomal localization of SPG11-15 (Figure 42). Finally, transfection with GFP-tagged PIK2B, HA-tagged ARL4a (Q79L) and FLAG-tagged AP5-Z shows a perfect colocalization (Figure 45-C). This is an important result as AP5 is usually localized at the cytoplasm (when expressed alone) (Figure 42) and is here at the lysosome.

## 3.6 CSW-ARL14 play a crucial role in ALR regulation

These results show that CSW-ARL14 and ARL4 complex plays an essential role at the autolysosome to induce Autophagic Lysosome Regeneration. Indeed, knock-out of *C9ORF72* in U2OS cells engender the absence of tubulation during prolonged starvation. Thus, we propose a model where AP5 is recruited by C9ORF72 and/or SPG11-15 at the lysosome and allows tubulation during basal and starved conditions:

- In basal conditions, PI4K2B is recruited by AP5-SPG11-SPG15-ARL4a and play an essential role by phosphorylating PtdIns into PtdIns(4)P and thus regulating basal vesiculation by facilitating lysosome budding managed by clathrin (or other coat proteins) and Dyn2 (Sridhar et al., 2013). Indeed, PI4K2B maintains the amount of lysosomal PtdIns(4)P, which prevent abnormal lysosomal tubulation under feeding conditions. ARL14 localization has not been precisely described in basal conditions but seems to be located at the lysosome, while CSW complex has a diffuse localization in the cytoplasm.

- In prolonged starvation, the recruitment of CSW complex by ARL14 to the lysosome will interact with AP5-SPG11-SPG15-ARL4a complex and promotes Autophagic Lysosome Regeneration by inhibiting recruitment of PI4K2B and thus permits the conversion of PtdIns(4)P to PtdIns(4,5)2P by PIP5K1B at lysosomes which has been suggested to be critical for the initiation of ALR.

The next chapter will be dedicated to the discussion and perspectives of my results.

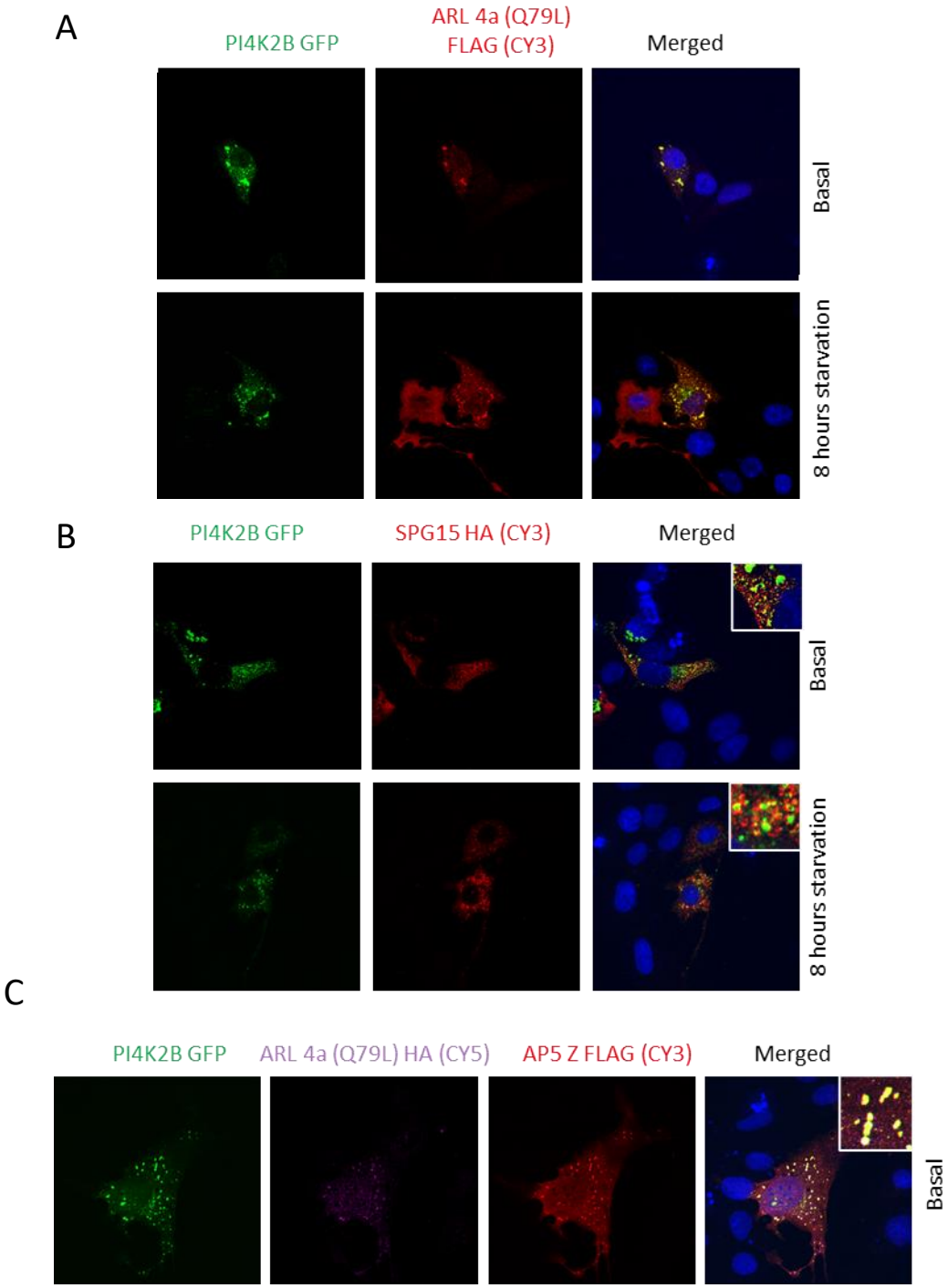


Figure 45 PI4K2B colocalize with AP5-ARL4a complex

(**A**) Representative images of immunofluorescence labeling of U2OS cells transfected with GFP-tagged PI4K2B and FLAG-tagged ARL4a (Red) with and without starvation. (**B**) Representative images of immunofluorescence labeling of U2OS cells transfected with GFP-tagged PI4K2B and HA-tagged SPG15 (Red) with and without starvation. (**C**) Representative images of immunofluorescence labeling of U2OS cells transfected with GFP-tagged PI4K2B, HA-tagged ARL4a (Purple) and AP5Z (Red) without starvation.

# PERSPECTIVES AND DISCUSSIONS

During my thesis I was able to resolved the 3D structure of the C9ORF72-SMCR8-WDR41 complex. Furthermore, I also discovered a new potential interaction with ARL14 and ARL4, two small GTPase of undefined function. All together we identified the small GTPase regulated by the CSW complex but also more interestingly we clarified the long-suspected role of this complex at the lysosome and in autophagy. Indeed, we were able to found that CSW complex has a role in Autophagic Lysosome Regeneration (ALR) and act together with AP-5 to regulate lysosomal tubulation. This last part will focus on the discussion of my project. The structure resolution of the C9ORF72-SMCR8-WDR41 complex will be discussed first, followed by the interaction between the ARL14 and CSW complex and its significance for autophagy. Finally, we will discuss the interaction of the AP5-ARL4-PI4K2B complex, which sheds light on this complex's function in the regeneration of autophagic lysosomes combined with CSW.

## 1. C9ORF72-SMCR8-WDR41 structure

The CSW complex had previously been purified at the start of my thesis. However, only a small number of grids were created, and the ideal vitrification conditions were not found. The Patrick Schultz team helped us to identify the ideal vitrification conditions. As shown in the results section, we were able to obtain our structure with a resolution of 5.9 A° shortly before the COVID epidemic began. Unfortunately, two additional teams simultaneously published the C9ORF72-SMCR8-WDR41 structure. Resolutions of 3.8 A° were attained by the Su et al. team and 3.2 A° by the Tang et al. team (Nörpel et al., 2021; Su et al., 2020; D. Tang et al., 2020). We had a lower resolution due to the preferential orientation of our 2D classification which is a considerable challenge for cryo-electron microscopy (cryo-EM) analysis. The reliability and interpretability of the structural models are impacted by orientation bias, which lowers the quantity of angular data used to produce three-dimensional maps. Nevertheless, expanding the dataset is a simple approach to overcome this problem. We only used 242,000 particles picked by CRYOLO when Tang et al. team and Su et al. team had, respectively, 1,338,452 particles and 4,810,184 auto-picked by Gautomatch. Since our data had a structure that was extremely similar to theirs with the same unresolved middle section of SMCR8, we decided to not expand our dataset (Nörpel et al., 2021; Su et al., 2020; D. Tang et al., 2020).

As most of the middle part of SMCR8 is not resolved, we suggest that the CSW complex is flexible and may need a partner to be stabilize. So, our primary goal was to find a protein that could interact with the CSW complex. According to structural and bioinformatics study, the CSW complex belongs to the DENN family, which is known to regulate small GTPase (See part 2.4.1). Thus, the small GTPase family would be a good candidate to potentially stabilize the complex and resolve the missing part.

# 2. Which small GTPase is regulated by the CSW complex?

## 2.1 CSW complex potentially interacts with various small GTPase

Among literatures there was significant potential small GTPase interacting with the CSW complex. For example RAB1a (Webster et al., 2016) and/or RAB5 (Farg et al., 2014; Shi et al., 2018) in order to regulate autophagy; RAB7 and RAB11 to regulate endocytosis (Farg et al., 2014) or RAB3 to regulate exocytosis (Frick et al., 2018). Table 3 resume most of the small GTPase potentially interacting with C9ORF72 or CSW complex. Most of these studies performed co-immunoprecipitations to found theses potential interaction. However, we were unable to confirm any robust interactions among thus reported in the literature. Indeed, most of these papers studies the interaction of C9ORF72 in isolation and not in complex which can lead to huge discrepancy. Our team previously shows that CSW could regulate RAB GTPase like RAB8a and RAB39b (Sellier et al., 2016), but these interactions were lost when SMCR8 was in complex with C9ORF72, questioning whether if it is relevant to work on the C9ORF72 protein in isolation.

Table 3 Small GTPase interacting with C9ORF72 or CSW complex

Table resuming small GTPase interacting with C9ORF72 (orange) or CSW complex (green) and the pathway involved small GTPase based on recent literatures.

| GTPase | Experiment | GEF | GAP | Pathway involved | References |
|---|---|---|---|---|---|
| Rab1a | Co-IP; in vitro binding assay | √ | | Autophagy | (Farg, 2014; Webster, 2016) |
| Rab3 | Co-IP | √ | | Synapses | (Frick, 2018) |
| Rab5 | Co-IP | √ | | Vesicle trafficking/ Autophagy | (Farg, 2014) |
| Rab7 | Co-IP | √ | | Vesicle trafficking | (Farg, 2014) |
| Rab8a | Co-IP | √ | | Autophagy | (Sellier, 2016) |
| Rab11a | Co-IP | √ | | Autophagy/synapses | (Farg, 2014) |
| Rab39b | Co-IP | √ | | Autophagy | (Sellier, 2016) |
| Arf1 | Co-IP | | √ | mTORC1/autophagy | (Sivadasan, 2016) |
| Arf6 | Co-IP | | √ | Autophagy/TLR | (Sivadasan, 2016) |
| Rag | Co-IP | √ | | mTORC1/autophagy | (Wang 2020; Ji 2020) |
| Rag | Co-IP | | | mTORC1/autophagy | (Sellier 2016; Amick 2016; Amick 2020) |
| Rab8a, Rab11a | Bioluminescence-based GTPase activity | | √ | Autophagy | (Su 2020) |
| Arf1 | Trp fluorescence and HPLC-based assays | | √ | mTORC1 | (X.Tang 2020) |

C9ORF72
CSW complex

Indeed, prior to the discovery of the CSW complex, the majority of teams focused solely on C9ORF72 and discovered numerous interactions and/or roles for this protein in various biological pathways. Even while it seems unlikely, it should not be ruled out that C9ORF72 might play a role as a single protein. Finally, we used 300 mM NaCl to wash our beads and remove any weak interactions during the co-immunoprecipitation that we carried out. However, in various reports, the amount of NaCl used to wash the beads ranged from 50 to 100 mM, which may be insufficient to completely rule out any weak interactions.

The majority of articles focusing on C9ORF72 alone demonstrate that C9ORF72 may serve as a GEF for most of the identified small GTPase (Farg et al., 2014; Frick et al., 2018; Sellier et al., 2016; Webster et al., 2016). However, recent papers which worked on the CSW complex or at least C9ORF72-SMCR8 complex shows that the complex is a GAP for RAB8a, RAB11a and ARF1 (Su et al., 2021, 2020; D. Tang et al., 2020). Though, it makes sense that when C9ORF72 is used alone, the GAP activity is missing as SMCR8 is carrying the GAP arginine finger. Indeed, CSW complex share great structural similarities with NPRL2–NPRL3 of the GATOR1 complex (Shen et al., 2018) and FLCN–FNIP2 in the lysosomal folliculin complex (Lawrence et al., 2019; Shen et al., 2019). As a result, the RAG GTPase-FLCN-FNIP2 complex illustrates the major structural similarities with CSW. It was discovered that FLCN's Arg 164 is the catalytic residue for GAP activity and that this arginine finger residues are characteristic of a GAP for small GTPase which would corresponds to the Arg 147 in SMCR8. In that aspect, we decided to test whether CSW could regulated RAG GTPase. Indeed, other teams (Ji et al., 2020; Wang et al., 2020) found a potential interaction of C9ORF72 with RAG GTPase. However, we didn’t found any interaction with either active or inactive form of RAG GTPase consistent with the results found by Sellier and Amick (Amick et al., 2016; Sellier et al., 2016).

Of interest, recent publication, identified potential new interacting small GTPase, namely RAB8a, RAB11a and ARF1 (Su et al., 2021, 2020; Tang et al., 2020). We tested co-immunoprecipitation with the CSW complex co-expressed with either RAB8a, RAB11a and ARF1 but didn’t find any strong interaction in HEK cells. However, the fact that deleting the ARG147 of SMCR8 greatly reduce the stimulatory effect on RAB8a, RAB11a and ARF1 suggest a close linked between CSW complex and these small GTPase (Su et al., 2021, 2020; D. Tang et al., 2020).

Discrepancy can be explained by the fact that they used different techniques than co-immunoprecipitation to asses of the interaction. Indeed, Tang and colleagues carried a bioluminescence-based GTPase activity assay to asses if the CSW complex could stimulates these RABs. In this type of assay, unhydrolyzed GTP can be transformed into a bioluminescence signal (Mondal et al., 2015). They showed that stimulation by either the CSW complex or the C9ORF72–SMCR8 complex but not C9ORF72 alone, the amount of GTP consumed by RAB8a and RAB11 increased by ∼100% and 50%, respectively (D. Tang et al., 2020). On the other end, Su and colleagues, used HPLC-based assay to analyze the activation status of small GTPases by directly quantifying the amounts of guanine nucleotides bound to them (Araki et al., 2021) and Trp fluorescence assays based on the fact that GEF and GAP activity can be conveniently monitored using protein fluorescence (Goody, 2016). They found that C9orf72-SMCR8-WDR41 was an efficient GAP for ARF1 and has also activity against other ARF family members, ARF5 and ARF6. Furthermore, they showed that the activity toward RAB8 was 10 times less effective than ARF1 (Su et al., 2021, 2020).

Unlike them, we used co-immunoprecipitation with magnetic beads which is one of the most widely used methods for identification of proteins-proteins interaction. Indeed, it allows the detection of protein binding, the screening of interactor proteins and purification of protein complex in minimal time with great reproducibility without extensive manipulation. Additionally, it primarily evaluates the direct interaction of proteins and/or complexes. Co-immunoprecipitation confirms interactions using a whole cell extract with proteins present in their native form in a complex mixture of cellular components. In addition, use of eukaryotic cells enables posttranslational modification (Rao et al., 2014). Techniques such as bioluminescence-based GTPase activity assay, the HPLC-based assay, and the Trp fluorescence-based assay primarily measure an activity toward a protein without any obvious indication of a direct interaction between CSW and either of these RAB/ARF. It can be inappropriate when identifying an interacting protein to resolve a structure. All together, these results suggest than the interaction between ARF1 and other RAB is either weak or indirect, as our co-immunoprecipitation assay with CSW weren't able to confirm interaction with any of these small GTPase.

Fortunately, we were able to identified two other strong proteins interactions, ARL14 and FIP200 that could potentially stabilize the complex and thus resolve the total structure by Cryo-EM.

## 2.2 Importance of tagging in CRYO-EM optimization

Among all the small GTPase tested, one interaction was strong enough to potentially be purified with CSW in complex. With ARL14 identified as a small GTPase interacting with C9ORF72-SMCR8-WDR41 complex, we decided to produce and purified the CSW complex with ARL14. However, some parameters had to be improved. Indeed, most of our co-immunoprecipitation were performed using a HA, FLAG or GFP tags as commercially available magnetics beads and antibodies are the most efficient. However, the use of large tag like the GFP (28 kDa) is often avoid in protein purification and CRYO-EM experiments are they can significantly impact on the structure and biological activity of the fusion partner protein and often need an extra step of removal before acquisition (Kimple et al., 2013; Zhao et al., 2013). Since removal is not required upon acquisition, it is preferable to employ smaller tags such as the HA tag (1.1 kDa), FLAG tag (1,01 kDa), Strep tag (1,06 kDa), or Hexahistidine (6x His) tag (0,84 kDa). However, even small tag can significant changes the patterns of preferred orientation of the protein in cryo-em grid preparation (Bromberg et al., 2022). Nevertheless, His-tagged protein purification generally has the highest capacity, but can yield lower purity compared to other tags. The strep-tag allows a very high purity, but its binding capacity is lower. On the other hand, some tags like FLAG-tag or HA-tag often involves a low or high pH elution which can irreversibly affect the properties of the fusion protein, and employs resin which has limited reusability. FLAG and HA tags are therefore not the first choice when the main goals are high-level expression and fusion protein purification. In our case, the use of the STREP-tag was a primary choice for our recombinant protein purification. Indeed, Strep-tag®II binds specifically to the engineered streptavidins, Strep-Tactin® by occupying the binding pocket of the natural ligand biotin. The interaction is based on biotin and streptavidin which is among the strongest non-covalent interactions seen in nature. Ultimately, by competing with the biotin and the STREP-tag, which had a lesser affinity to streptavidin, the addition of a buffer containing biotin allowed for the purification of our combination in its native state.

Furthermore, we decided to use dual affinity tags for recombinant protein expression and purification which is becoming increasingly common since it simplifies purification and gives homogeneous preparations of the proteins of interest. The use of two sequential phases of affinity chromatography enables for the effective removal of contaminating proteins, including proteolytic breakdown products of the fusion protein that lack either N- or C-terminal tags (Yeliseev et al., 2007).

Moreover, tags are commonly added to either the N- or C-terminus of the target protein depending on the properties of the protein (e.g., the presence of subcellular localization sequences, downstream cleavage sites, or post-translational modification sites). For instance, RAB small GTPases are usually N-terminal tagged as they generally undergo C-terminal isoprenylation. However, ARF GTPases are C-terminally HA-tagged because they are post-translationally modified by N-terminal myristoylation (Prakash and Gorfe, 2013). Figure 46-A demonstrates the impact of various WDR41, SMCR8 and C9ORF72 tags on the interaction with ARL14. Conclusion tend to show that tagging C9ORF72 or SMCR8 can drastically diminish ARL14 interaction. In addition, we discovered that tagging FIP200 impairs its expression.

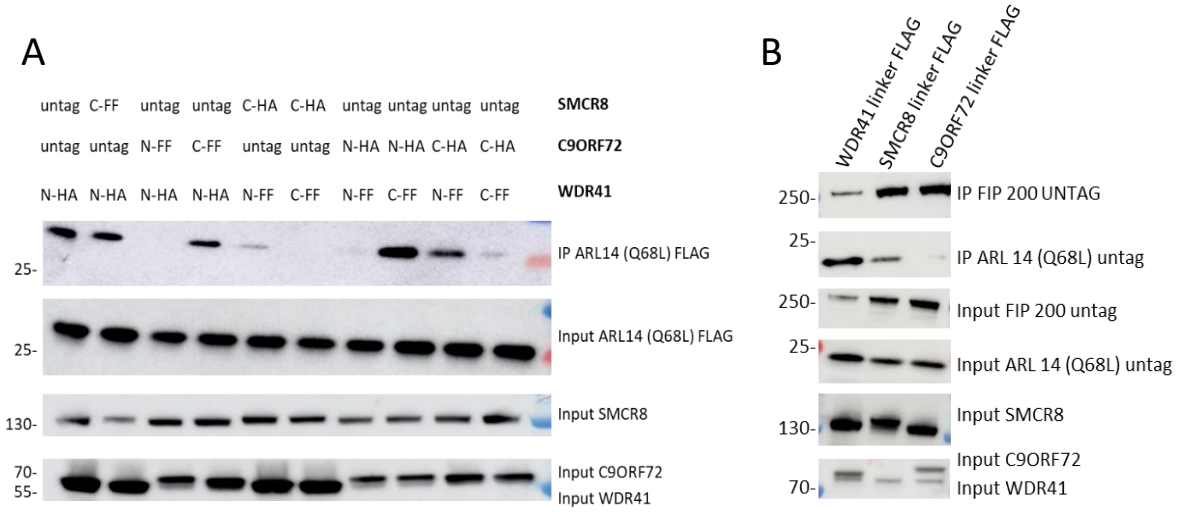


Figure 46 Importance of linker and tag in CSW and ARL14 interaction

(**A**) Immunoblot analysis of C- or N- terminal HA or FLAG immunoprecipitated proteins and lysate of HEK293 cells co-expressing C9ORF72, SMCR8, WDR41 and ARL14. (**B**) Immunoblot analysis of FLAG-immunoprecipitated proteins and lysate of HEK293 cells using a linker or not on WDR41, SMCR8 or C9ORF72.

Additionally, it is possible to use linkers to fuse distal part of proteins, which have been shown to increase expression yield, improve biological activity, or avoid steric hindrance (For review Chen et al., 2013). We discovered that using a linker on WDR41 improved the interaction with ARL14 but not FIP200 (Figure 46-B). Overall, it seems better to tag WDR41 as it has no direct role on ARL14 interaction. In conclusion, the impact of the tag on the target protein's is often underestimated and need optimization, as even small changes can lead to dramatic down effect.

## 2.3 CSW interacts with ARL14

In that aspect we used baculovirus containing either STREP-tagged WDR41, HIS-tagged ARL14 (Q68L) and untagged FIP200, C9ORF72 and SMCR8 were then tested, amplified and used to infect 2 l of SF21 cell culture for protein production and purification. However, we encountered significant challenges while attempting to purify the CSW-ARL14 complex. We shared a similar problem with Su and colleagues on ARF1, where the CSW complex dissociate from ARL14. Indeed, Su and colleagues tried to purify the C9ORF72:SMCR8:WDR41 in complex with ARF1. However, gel-filtration chromatography and cryo-EM revealed that ARF1 was dissociated from the CSW complex. Thus, they fused the C-terminus of ARF1 to the flexible N-terminus of SMCR8, and co-expressed the fusion with C9ORF72 and WDR41. Unfortunately, they weren't able to resolved the missing part of SMCR8 suggesting a lack of biological relevance due to the only chemical bond between ARF1 and SMCR8 unable to stabilize the complex (Su et al., 2021). Small GTPase interaction with their regulator is by all means complicated due to excessive conformational flexibility or structural heterogeneity resulting from weak or transient protein–protein association. In fact, interaction only takes place when the small GTPase is in its GDP or GTP form, and then quickly dissociates. Studies demonstrate the utility of chemical crosslinking to stabilize transient protein–protein complexes for cryo-EM structural analysis as Su and colleagues did (Faylo and Christianson, 2021; Su et al., 2021).

Currently, we were able to produce baculovirus SF21 infected cells which expressed C-terminus of ARL14 fused to N-terminus of C9ORF72 and SMCR8. Next step would be to fuse ARL14 to SMCR8 in complex with C9ORF72 and WDR41 by hopping it will stabilize the complex.

## 2.4 CSW-FIP200 is stabilizing the complex

As we lost the ARL14 interaction during the purification processes, we focus on FIP200, another putative CSW interacting protein. We were able to purify FIP200 in complex with CSW on a strep-tactin XT column followed by a gel filtration S200 resulting in different fraction analyzed by Western-Blot test with the presence of SMCR8, C9ORF72, WDR41 and FIP200. Our most recent findings on CSW's interactions with FIP200 supports earlier findings that identified SMCR8 as a candidate FIP200 interacting protein. Interestingly, FIP200 is part of the ULK1 kinase complex and is one of most upstream regulators of the autophagic pathway (Behrends et al., 2010; Sellier et al., 2016; Sullivan et al., 2016; Webster et al., 2016).

According to structural analysis, a coiled-coil region within the uDenn domain of SMCR8 could act as an interaction platform for other coiled-coil proteins. Interestingly, FIP200 harbors a coiled-coil region and suggest that SMCR8 coiled coil region could interact with a FIP200 coiled-coil dimer. Furthermore, this interaction will place it close to the catalytic Arg 147 of SMCR8 (Figure 47-A,B). Interestingly, Nörpel and colleagues found that a SCMR8 mutant lacking its coiled-coil region ($SMCR8_{\Delta CC}$, missing residues 181 to 250), reduce the levels of FIP200 in interaction by approximately 50% between the fed and starved condition by using $SMCR8_{\Delta CC}$. Interestingly, while the interaction of WDR41 with SMCR8 WT was not affected by starvation, binding of WDR41 to $SMCR8_{\Delta CC}$ was increased by approximately 4.5-fold (fed) and approximately 5.5-fold (starved) (Nörpel et al., 2021) suggesting that FIP200 and WDR41 could act independently.

Altogether these results suggest that SMCR8 coiled coil region is important for its interaction with FIP200. It's proximity with the Arg 147, necessary for the catalytic activity as a GAP, suggest that FIP200 could directly influence the activity of the CSW complex. This proximity could explain why we observed very low quantity of ARL14 when trying to purify the complex with FIP200. Indeed, any interaction with this site would clash with the potential GTPase binding site (Figure 47-A,B). It is not surprising that the interaction with WDR41 increased when the coiled coil region of SMCR8 was removed. Indeed, we were able to show that removing WDR41 had only minor influence on the interaction of C9ORF72-SMCR8 with ARL14 but also on the stability of the minimal complex C9ORF72-SMCR8 (Figure 47-C).

Therefore, depending on its binding state, the coiled-coil region of SMCR8 may affect the GAP activity of this complex and may also control its localization by increasing its interaction with WDR41. Currently, negative coloration EM of CSW-FIP200 complex as a different appearance from the sole CSW complex. We anticipate that this interaction will help to stabilize the complex and enable the resolution of the SMCR8 missing part, which appears to play a significant role in the regulation and interaction of small GTPases. These encouraging results on CSW complex structure are currently under investigation and optimization.

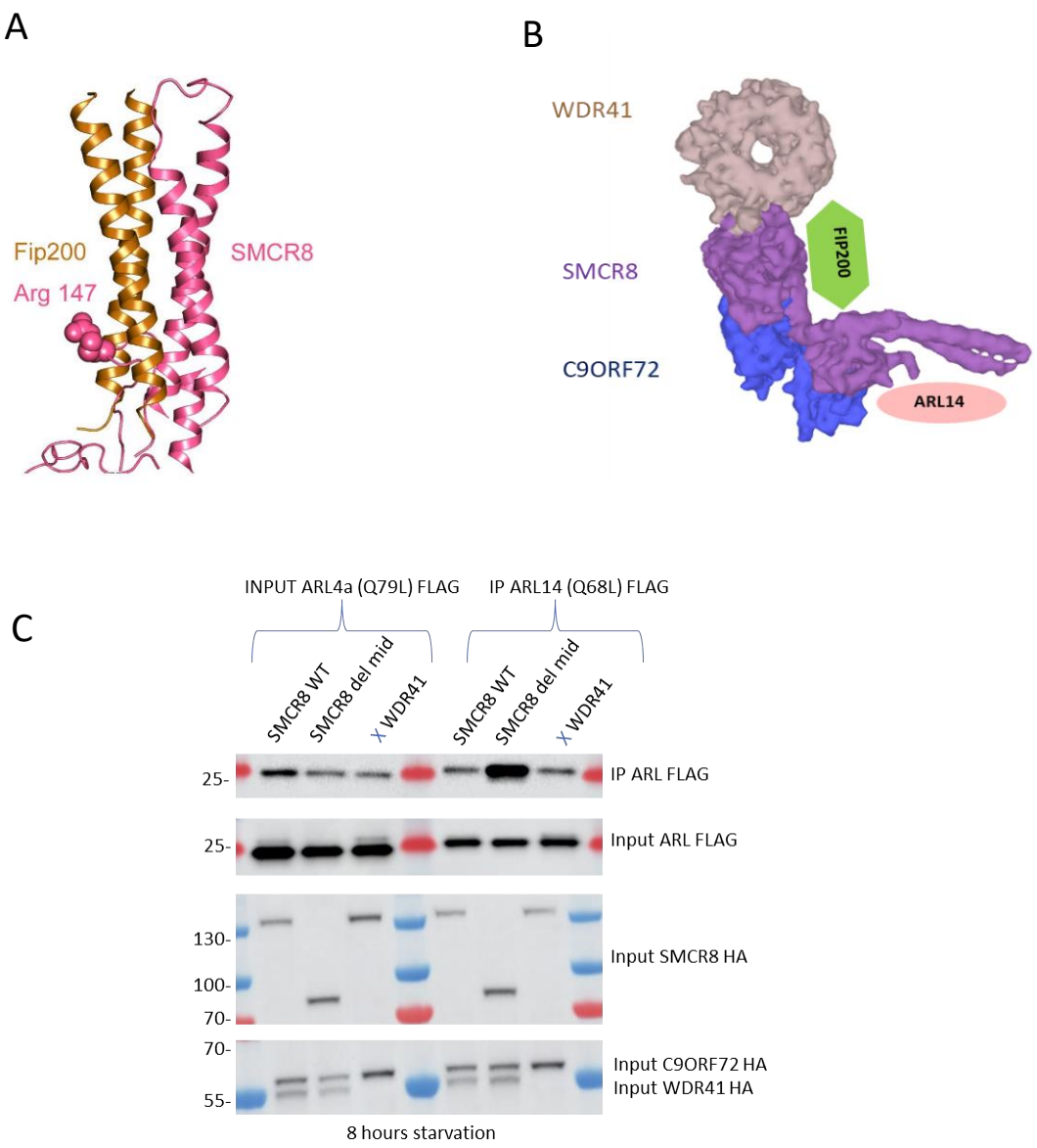


Figure 47 CSW, ARL14 and FIP200 structure organization

(**A**) Model of a 4-helix bundle formed by SMCR8N-C coiled coil (pink) and FIP200 coiled-coil dimer (gold, PDB: 6GMA) (Turco et al., 2019) based on the artificial 4 helix bundle (PDB: 6DLC) (Chen et al., 2019). Arg 147 of SMCR8 is shown in sphere representation. (**B**) Schematic representation of CSW-ARL14 and FIP200 supercomplex. (**C**) Immunoblot analysis of HA-immunoprecipitated proteins and lysate of HEK293 cells co-expressing HA-tagged WDR41, HA-tagged C9ORF72 and WT HA-tagged SMCR8 as well as HA-tagged SMCR8 deleted from its middle part with FLAG tagged-ARL4a or ALR14 in starved conditions. Last point is using C9ORF72-SMCR8 minimal complex (without WDR41).

# 3. What is the cellular role of C9ORF72?

## 3.1 Role of CSW and ARL14 in the immune system

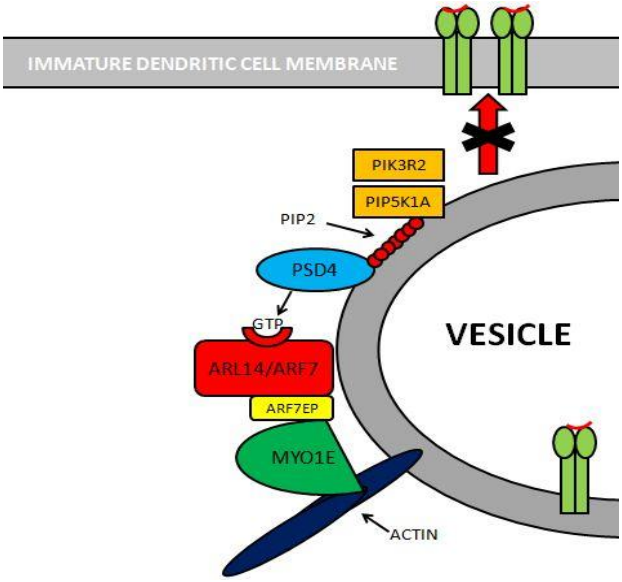


Figure 48 Predictive model of Paul and colleagues'

Two kinases, PIK3R2 and PIP5K1A, phosphorylate Phosphatidylinositol (PIP), giving PSD4 substrates for its capacity to load GTP. Guanine exchange factor PSD4 supplies GTP to ARL14/ARF7. ARF7EP then interacts with MYO1E, which has bound actin myofibers. Together, these factors help to keep MHC-II-loaded vesicles inside the developing dendritic cell, preventing it from moving to the cell membrane (Adaptation from Paul et al., 2011).

We observed a substantial interaction with two small GTPases, ARL14 and to a lesser extent, ARL4, out of 18 small GTPases tested. Very little is known about ARL14, beside its interaction with MYO1E via the effector protein ARL14EP to controls MHC class II-containing vesicles movement along the actin cytoskeleton (Figure 48) (Paul et al., 2011). However, we didn't find any interaction or colocalization between ARL14 and ARL14EP or (Myosin IE) MYO1E in U2OS or HEK cells. Nevertheless, Paul and colleagues shows colocalization between ARL14 and MHC-II in immature human monocyte-derived DCs. This is a drawback of our approach since we mostly use the non-immune cells U2OS and HEK 293 in our investigations. Compared to their work, our cell models may produce some inconsistency.

Interestingly, *C9orf72* knockout mice shows no ALS hallmarks (TDP-43, P62 or ubiquitin aggregates) as no behavioral, motor phenotypes and motor neuron degeneration but present an inflammatory phenotype (splenomegaly, enlarged lymph nodes, infiltration of immune cells, increased expression of inflammatory cytokines, presence of autoantibodies and immune-mediated glomerulonephropathy) (Burberry et al., 2016; Jiang et al., 2016; Koppers et al., 2015; O'Rourke et al., 2016; Shi et al., 2018; Sudria-Lopez et al., 2016; Sullivan et al., 2016).

Effects of *C9orf72* deletion are perhaps not surprising since *C9orf72* is highly expressed in myeloid cells, which are critically important for antigen presentation and development of autoimmunity. Loss of *C9ORF72* in myeloid cells led to lysosomal accumulation and hyperactive immune responses in bone marrow macrophages (Heng et al., 2008; Nataf and Pays, 2015; O'Rourke et al., 2016; Rizzu et al., 2016). All together these results encouraged us to develop a double knock-out mouse *C9orf72* -/- *Arl14* -/- with the hypothesis that *arl14* knockout could rescue the inflammatory phenotype of *C9orf72* knock-out mouse. However, we didn't observe a rescue of the inflammatory phenotype but rather observe a metabolism defect. Indeed, *Arl14* -/- mouse does not develop obesity in comparison to WT mice, which is consistent with *ARL14* mainly expressed in the gut. Interestingly, immunometabolism, the term for the relationship between inflammation and metabolic problems, is emerging along with new molecular connections to neurological disorders. Specifically, it suggests a global shift in resources during inflammation, in which glucose is redirected from peripheral tissues to immune cells (and specifically microglia) to support their inflammatory actions leading to neurodegeneration progression (for review (Lo and Lee, 2020; Wang et al., 2022). The potential role of ARL14 and C9ORF72 in the inflammatory and metabolic phenotype is path to explore. Indeed, the use of immune cells could give a broader idea of the CSW-ARL14 complex role in ALS and the inflammatory-metabolic phenotype.

Also, CSW interaction with FIP200 could also be interesting to study in mice. Indeed, it has been shown that apart from its crucial role in the regulation of selective autophagy, FIP200 could also have a role in inflammatory processes. Indeed, depletion of *Fip200* also induced pro-inflammatory responses. In fact, an earlier observation was made when residual MMTV-Cre (mouse mammary tumor virus promoter driven Cre recombinase) activity in the skin led to FIP200 deletion and inflammatory skin disorder that was associated with increased leukocyte infiltration and NF-κB (nuclear factor kappa B) activation (Wei et al., 2009). In the context of NSC differentiation, ablation of *FIP200* increased CCL5 (C–C motif chemokine ligand 5) and CCL10 (C–C motif chemokine ligand 10) expression. This led to non-cell autonomous effects, namely, the infiltration of microglia into the NSC niche which perturbs NSC differentiation (C. Wang et al., 2017).

## 3.2 Role of CSW-ARL14 complex at the lysosome

We concentrated on the CSW complex and ARL14's function in addition to trying to study the CSW-ARL14 structure. We mainly focused on the potential role of C9ORF72 in Autophagic Lysosome Regeneration. In fact, the interaction between ARL14 and C9ORF72 peaks at eight hours after starvation, which corresponds to the timeframe at which ALR begins. According to chapter 2.4.2, CSW seems to regulated autophagy at an unknown step (Amick et al., 2020, 2018, 2016; Sullivan et al., 2016; Ugolino et al., 2016). This new discovery could be a major breakthrough to highlight its role in autophagy.

We tried to determine the localization of ARL14 and the CSW complex. When C9ORF72-SMCR8 is expressed in a minimum complex, it largely localizes as diffuse under basal conditions and as cytolytic punctate with some LAMP-1 positive punctate after 8 hours of starvation. However, subcellular localization of C9ORF72 is a long-time debate among the scientific community. Indeed, further studies using tagged C9ORF72, transfected or CRISPR modified, or immunocytochemical detection of endogenous C9ORF72 in cell lines or human iPSC-derived neurons have revealed the co-localization of C9ORF72 with various organelles: the Golgi apparatus (Aoki et al., 2017), stress granules (Chitiprolu et al., 2018; Maharjan et al., 2017), mitochondria (Wang et al., 2021), and, most of all, compartments of the endolysosomal pathway (Amick et al., 2016; Farg et al., 2014; Frick et al., 2018; Sellier et al., 2016; Shi et al., 2018; Wang et al., 2020). The poor specificity of the commercial antibodies, explained the vast confusing results on protein expression and subcellular localization. Indeed, a recent publication compare different commercial antibodies, found that only 15% of C9ORF72 was localized to the lysosomes, 25% being membrane associated and 75% remaining in the soluble/cytosolic fraction. Furthermore cells line and different tag used can drastically change the subcellular localization of the proteins and could also explained these confusing results (Laflamme et al., 2019). Our results are however consistent with the results found by Amick and colleagues. Indeed, in one study they revealed a diffuse cytoplasmic localization for tagged C9ORF72 under basal cell culture conditions, with the observation that the protein became concentrated on lysosomes after starvation (Amick et al., 2016).

Furthermore, we found that WDR41 is needed to recruit C9ORF72 and SMCR8 to the lysosome. These results are consistent with those observed by Amick and colleagues in 2018 (Amick et al., 2018). However, after starvation, the minimum complex C9ORF72-SMCR8 does not entirely relocate to the lysosome. Interestingly we showed that ARL14 colocalizes with LAMP1 and is able to recruit C9ORF72 and SMCR8 to the lysosome. This suggest that ARL14 in sufficient to recruit C9-S8 minimal complex to the lysosome. This is consistent with previous results were WDR41 doesn't influence the stability of the C9ORF72-SMCR8 complex and its interaction with ARL14 (Figure 47-C).

ARL14 study is challenging as its expression is toxic in U2OS cells which makes research on ARL14 subcellular location difficult. Thus, we developed ARL14 stable cell line using a doxycycline inducible system and found that ARL14 is located at the endolysosme.

## 3.3 CSW-ARL14 and ARL4 complex play a role in ALR

We investigated the potential function of CSW in autophagic lysosome reformation (ALR), considering the interaction between CSW and ARL14 at the lysosome during prolonged starvation. Absence of tubules in *C9ORF72* KO cells cells highlights the significance of C9ORF72 ALR regulation. After extended starvation, ALR enables lysosome renewal. However, *C9ORF72* KO cells lack tubules, have fewer and larger lysosomes, suggesting that C9ORF72 plays a role in the initiation of the tubulation. These results are consistent with other studies showing enlarged LAMP-1 positive organelles in ALR deficient cells (Chang et al., 2014; Yu et al., 2010). We attempted to clarify the role of C9ORF72 and ARL14 in the start of ALR but ran across some obstacles. Lysosome tubulation is a dynamic and erratic state that is complex to monitor, since tubules are damaged during the fixation process, preventing possibility to fix cells. In this way, the use of live imaging is necessary but limit the number of fluorescent channels used for protein visualization. Furthermore, the co-localization of the autophagosome and lysosome to form the autolysosome is an important step in the autophagic process. In fact, the tubules are beginning to emerge within the autolysosome after this particular stage. However, the measuring of LC3/LAMP1 puncta alone is not always sufficient to quantify autophagy and the autolysosome state.

The use or new methods like multispectral imaging flow cytometry can distinguish between autophagosomes and autolysosomes accumulation could be a solution (Pugsley, 2017). Furthermore, we weren't able to observe any rescue by ARL14 in *C9ORF72* KO cells, still lacking tubulation. It is currently necessary to clarify the role of the CSW complex in ALR tubulation. However, it appears that in order to trigger tubulation following extended starvation, ARL14 is required for CSW and thus AP5 complex recruitment at the lysosome/autolysosome.

## 3.4 AP-5 and CSW are interacting to initiate tubulation during ALR

Autophagic lysosome regeneration is a relatively new phenomenon. However, a number of researches were able to partially define the pathways involved. Among the protein regulating ALR, AP (adaptor protein) complexes are playing an important role in intracellular membrane trafficking along endocytic and secretory transport pathways (Park and Guo, 2014). Interestingly, we found that AP-5 is interacting with CSW complex and that this interaction is dependent on starvation. However, we faced some difficulties to express all the subunits of AP5 with SPG-11, SPG-15 and CSW complex as cells typically can only handle 30–50 µg of plasmid DNA. However, we were able to immunoprecipitated AP5 with SPG11-SPG15 confirming that here are forming a complex. These findings concur with those of Hirst and colleagues (Chang et al., 2014; Hirst et al., 2013). The colocalization of SPG11 and 15 with LAMP-1 positive organelles as well as the recruitment of AP5 from the cytoplasm to the lysosome was confirmed. Interestingly, the localization at the lysosome doesn't seems to depend on starvation, suggesting that the complex could play a dual role at the lysosome/autolysosome under basal and starvation conditions. The subcellular localization of SPG11 has been however controversial, with different studies reporting its localization to ER, mitochondria, early/late endosomes, and lysosomes and along microtubules (Chang et al., 2014; Hirst et al., 2013; Khundadze et al., 2021; Oakes et al., 2017). AP-5 is the most recently identified AP complex, and comparatively little is known about its function. The lack of AP-5 in a number of model organisms, in addition to the relatively low level of sequence conservation and low abundance of the complex, probably explain why AP-5 escaped identification for so long. However, a recent publication show that AP-5-SPG11-15 complex play role in ALR which is consistent with our results (Chang et al., 2014; Hirst et al., 2021).

## 3.5 ARL4a and PI4K2B are major regulator of lysosome regeneration

AP protein localization is frequently dependent on a conformational shift and interaction with a small GTPase, primarily ARF1 for AP-1, 3 and 4, and ARF-6 for AP-2 (Park and Guo, 2014). We tested if AP-5 could interact with ARL14 but didn't find any interaction. However, ARL4a (Q79L) shows strong interaction with AP5-SPG11-15 upon starvation. This explains the weak interaction between ARL4a and the CSW complex, which may be linked to their proximity with AP5. Very little is known about ARL4a beside its interaction with ARNO (ARF nucleotide-binding site opener), which is a guanine-nucleotide exchange factor (GEF) for ARF6 (Hofmann et al., 2007). However, we didn't replicate these results by co-immunoprecipitation or colocalization. We discovered that ARL4 is toxic in U2OS cells, just like ARL14, which makes research on ARL4a subcellular location challenging. Thus, we recently developed an ARL4a stable cell line under a doxycycline inducible system, which will hopefully enable a deeper comprehension of this protein.

In addition, we found that this novel complex AP5-ARL4a may interact with phosphoinositide kinase to control ALR especially PI4K2B and PIP5K1B. Interestingly, the PI4K2B-AP5-ARL4a supercomplex localizes to some LAMP-1 puncta and this colocalization is enhanced in basal condition. These results are consistent with observation of Chang and colleagues who reported that SPG11 and SPG15 colocalize with PI4KB, a orthologue of PI4K2B from the PI4Ks family (Chang et al., 2014). Our results showed that, under basal conditions, PI4K2B is recruited by AP5-SPG11-SPG15-ARL4a and plays an essential role by phosphorylating PtdIns into PtdIns(4)P and thus regulating vesicular tubulation by facilitating lysosome budding managed by clathrin (or other coat proteins) and Dyn2 (Sridhar et al., 2013). Indeed, PI4K2B maintains the amount of lysosomal PtdIns(4)P, which facilitates vesiculation by preventing abnormal lysosomal tubulation under feeding conditions. Absence or loss of kinase activity of PI4K2B reduces the level of lysosomal PtdIns(4)P, which prevents its inhibiting role and results in lysosomal hypertubulation (Sridhar et al., 2013). Interestingly, Chang and colleagues show that double knockdown of *Spg11* and *Pi4k2b* did not induce hypertubulation, indicating that SPG11-15-AP5 are essential for ALR initiation (Chang et al., 2014).

PIP5K1B interaction was overall 10 times weaker than ARL4a/PI4K2B interaction and has not been studied further. However, it would be interesting to enlighten its role in ALR regulation. In that aspect, PIP5K1B has already been described to phosphorylates PtdIns(4)P into PtdIns(4,5)2P which is required for initiation of ALR (Rong et al., 2012).

## 3.6 *SPG11* and *SPG15* are mutated in hereditary spastic paraplegia (HSP)

Interestingly, mutations in the *SPG11* and *SPG15* genes (also known as spatacsin and spastizin/ZFYVE26/FYVE-CENT) are the main causes of Hereditary Spastic Paraplegia (HSP), which is characterized by a thin corpus callosum, mental impairment and progressive stiffness in the lower limbs (Boukhris et al., 2008). Additionally, *spg11* and *spg15* knockdowns in *zebrafish* result in similar defects impacting the growth of motor neurons (Martin et al., 2012). An important insight into the function of AP-5 came from the discovery by Słabicki et al. that AP-5 subunits could be co-immunoprecipitated with SPG11 and SPG15 and that mutations in *AP5Z1* also cause HSP. However, in this instance the patients' condition manifested later in life (Słabicki et al., 2010).

# 4. Conclusion

We searched to resolve and find an interactant of C9ORF72-SMCR8-WDR41, notably by using different tags and linkers to improve purity and quality of our complex. Despite having some challenges using ARL14 to stabilize the complex, FIP200 produces encouraging results. The structure determination of CSW with FIP200 or ALR14 is still under investigation. However, the increase interaction of CSW with ARL14 during starvation, recruitment of CSW by ARL 14 at the lysosome, the importance of SMCR8 phosphorylatable site by autophagic kinase for CSW-ARL14 complex and its interaction with FIP200 all point to the fact that this complex is involved in autophagy. Interestingly, the 8 hours of starvation shift (where CSW-ARL14 interaction is at its spike) corresponds to the timeline when Autophagic Lysosome Regeneration (ALR) begins, suggesting a role of the CSW-ARL14 complex in ALR regulation.

Here, I propose a model were lysosome are reformed by two complementary pathways in basal or starved conditions (Figure 49):

In basal conditions, lysosomes are reformed at a normal rate under AP5-SPG11-SPG15-ARL4a and PI4K2B regulation. Indeed, PI4K2B is recruited by AP5-SPG11-SPG15-ARL4a and play an essential role by phosphorylating PtdIns into PtdIns(4)P and thus regulating basal vesiculation by facilitating lysosome budding managed by clathrin (or other coat proteins) and Dyn2 (Sridhar et al., 2013). Indeed, PI4K2B maintains the amount of lysosomal PtdIns(4)P, which prevent abnormal lysosomal tubulation under feeding conditions. ARL14 localization has not been precisely described in basal conditions but seems to be located at the lysosome while CSW complex has a diffuse localization in the cytoplasm.

In prolonged starvation, to rapidly generate energy sources, cells used an enhanced pathway, which reforms lysosomes more efficiently, called ALR. Recruitment of CSW complex by ARL14 to the lysosome will interact with AP5-SPG11-SPG15-ARL4a complex and promotes Autophagic Lysosome Regeneration by inhibiting recruitment of PI4K2B. As a results, it will lower the production of PtdIns(4)P and permit the conversion of PtdIns(4)P to PtdIns(4,5)2P by PIP5K1B at lysosomes which has been suggested to be critical for the initiation of ALR (Balla et al., 2002; Rong et al., 2012). Absence of tubulation in *C9ORF72* KO cells, enlighten the importance of CSW-ARL14 complex in tubulation regulation during prolonged starvation which act downstream of AP5-ARL4a complex to inhibit recruitment of PI4K2B. CSW-AR14 could also interact with PIP5K1B to induce ALR.

However, some questions remain, notably how AP5 and ARL4a are recruited to the lysosome. One hypothesis is that under starved conditions ARL14 recruits CSW complex that will in turn recruit AP5 to the lysosome. A Second hypothesis is that CSW complex is not useful to recruit AP5, which is mainly driven by SPG11-15. Finally, this newly formed complex will recruit ARL4a to regulate PI4K2B at the lysosome. Under basal conditions, SPG11 and SPG15 are recruiting AP5 to the lysosome which will in turn recruit ARL4a and PI4K2B. However, expression of ARL4a and ARL14 are toxic in U2OS cells, preventing the study of their subcellular localization. Thus, we recently developed ARL4a and ARL14 stable cells lines under a doxycycline inducible system, which will enable a deeper comprehension of these proteins.

Furthermore, we conclude that changes in the PtdIns(4)P levels at the lysosomal membrane modulate conversion from basal vesiculation to enhanced tubulation in ALR, either by diminution of recruitment of PI4K2B by AP5 complex or/and active conversion into PtdIns(4,5)2P by PIP5K1B. However, it is not clear on how PtdIns(4) levels are maintained during prolonged starvation. It is possible that PI4K2B has always a basal activity regulated by AP5-ARL4 complex to generate PtdIns(4)P from PtdIns, allowing constant conversion into PtdIns(4,5)2P by PIP5K1B. Furthermore, PIP5K1B is known to have a role downstream of adaptor protein 2 (AP-2). In that aspect, ARL4a and CSW show weak interaction with PIP5K1B but not with AP2 suggesting that this part of the tubulation may not be linked to CSW or AP5-ARL4a pathways.

Overall, we demonstrate two interconnected systems for controlling the steady state of the lysosome under basal and deprived settings, with CSW-ARL14 complex as its core. Lysosomal steady state has to be maintained during high consumption of lysosome (during starvation) but also in basal conditions which is necessary to balance the incessant flow of cargo into lysosomes and maintain steady-state number, size, and function of lysosomes. Various questions related to ALR emerged, including how cells shift between vesiculation versus tubulation, and whether there are distinct forms of ALR (Saffi and Botelho, 2019). Thus, C9ORF72 plays a role in ALR regulation but further research will be needed to deeply comprehend its role and regulation.

Hopefully, this PhD will help to better understand C9ORF72-SCMR8-WDR41 structure and long suspected function in autophagy while giving hope to ALS/FTD patients.

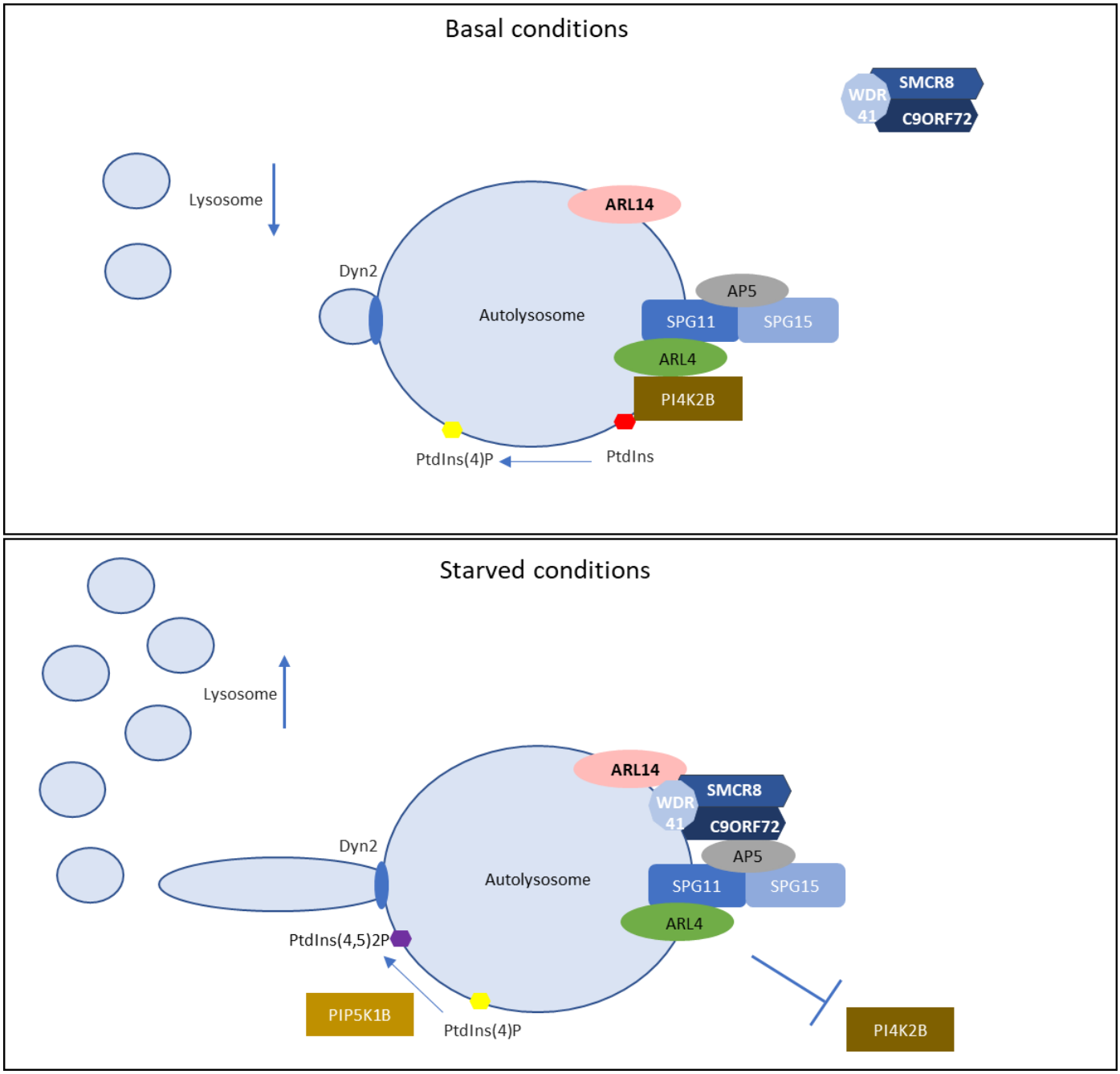


Figure 49 Schematic representation of the regulation of Lysosome Reformation and Tubulation

# ANNEX SCA36

# 1. Background

Amyotrophic lateral sclerosis (ALS) is the third most common neurodegenerative disease worldwide. This disorder is characterized by the degeneration of upper and spinal motor neurons that leads to progressive skeletal muscle paralysis, ultimately resulting in death from respiratory failure generally 3–5 years after age of onset. The main genetic cause of ALS is an expansion of GGGGCC repeats in the *C9ORF72* gene. These repeats are pathogenic by three mechanisms:

- First, transcripts containing expanded repeats accumulate in RNA foci that recruit various RNA-binding proteins (RBP), potentially altering their localization and functions.
- Second, expanded G4C2 repeats promote DNA epigenetic changes that lead to decreased expression of *C9ORF72* mRNA and protein levels in C9-ALS/FTD individuals.
- Third, sense G4C2 and antisense C4G2 expanded repeats are repeat-associated non-AUG (RAN) translated into dipeptide repeat (DPR)-containing proteins, which form inclusions throughout the brain of patients with C9-ALS/FTD, as well as in mice expressing expanded G4C2 repeats (Ash et al., 2013; Mori et al., 2013b; Zhang et al., 2014; Zu et al., 2013).

In this aspect, DPRs translated from C9 GGGGCC sense repeats are poly-(Gly-Ala) (GA) and poly-(Gly-Arg) (GR) while C9 CCCCGG anti-sense repeats are translated in poly-(Pro-Arg) (PR) and poly-(Pro-Ala) (PA). Poly-(Gly-Pro) (GP) are translated from both the sense and antisense transcripts (Ash et al., 2013; Mori et al., 2013b; Zhang et al., 2014; Zu et al., 2013). Of interest, the poly(GA) and poly(GP) DPR are the most readily visible in p62/ubiquitin positive inclusions in the brain and spinal cord of patients with ALS/FTD (May et al., 2014; Zhang et al., 2014). However, *in-vitro* and *in-vivo* studies showed that poly(GR) and poly(PR) are the most toxic, as they induced developmental, locomotor and survival deficit in mice, *Drosophila* and *zebrafish* (Boeynaems et al., 2016; Cook et al., 2020; Freibaum et al., 2015; Lee et al., 2016; Li et al., 2020; Maor-Nof et al., 2021; Mizielinska et al., 2014; Riemslagh et al., 2021; Tao et al., 2015; Wen et al., 2014).

In contrast, Poly(GA) overexpression induce lesser toxicity in various models like mice, *zebrafish*, primary neurons and cultured cells (Schludi et al., 2017; Zhang et al., 2016).

Spinocerebellar Ataxia 36 (SCA36) is a progressive cerebellar ataxia that has been primarily identified in Japan (Ikeda et al., 2012; Kobayashi et al., 2011) and Spain (García-Murias et al., 2012). This disease is characterized by the loss of cerebellar Purkinje cells and associated brainstem neurons, resulting in pronounced ataxic symptoms (García-Murias et al., 2012; Ikeda et al., 2012; Kobayashi et al., 2011). This disease is caused by an expansion of GGGCCT repeats located in the first intron of the NOP56 gene (García-Murias et al., 2012; Ikeda et al., 2012; Kobayashi et al., 2011). The nucleotide sequence of this expansion, as well as its location, recall the intronic GGGGCC expansion of C9ORF72 gene. Alike C9ORF72 repeats expansions, SCA36 repeats expansions also forms RNA foci detected in the brain of patients (Liu et al., 2014), and both repeat expansions are believed to form similar RNA secondary structures (Yuan Zhang et al., 2018). Moreover, GGGCCT expansion in SCA36 can also putatively encode 5 DPR proteins: poly(WA), poly(GL), poly(PR), poly(AQ) and poly(GP). Interestingly, the development of a mouse model expressing the GGGCCT repeat expansion presents sense and antisense RNA foci and the DPR proteins poly(WA), poly(GL), poly(PR) and poly(GP) are detected (Todd et al., 2020), alike what is observed in mouse models of ALS expressing repeats GGGGCC (Jiang et al., 2016; Liu et al., 2016; O'Rourke et al., 2015). **These data question what are the mechanisms of toxicity of the GGGCCT repeats in SCA36?**

As we found that the C9 G4C2 sense repeats are primarily translated into poly(glycine–alanine) (polyGA) and, to a lesser extent, into poly(glycine–proline) (polyGP) and poly(glycine–arginine) (polyGR)-containing proteins through initiation to near-cognate start codons that are located upstream of the G4C2 repeats (Boivin, 2020), we used similar approach to study SCA36 GGGCCT repeats in *NOP56.*

## 2. Results and discussions

To assess translation of the sense GGGCCT repeats, we cloned 80 G3C2T repeats embedded within the natural human *NOP56* sequence and fused these repeats to the GFP sequence in all three possible frames. These frames were named according to the DPR protein potentially encoded by the expanded G3C2T repeats, namely glycine–leucine (GL), glycine–proline (GP), and alanine–tryptophan (AW) (Figure 50-A). Cell transfection and immunoblotting against the GFP indicated that expanded G3C2T repeats embedded in the natural *NOP56* sequence are predominantly translated into the GP frame. In contrast, we found no or very limited translation of the G3C2T repeats into the poly(GL) and poly(AW) frame (Figure 50-B,C). Direct observation of the GFP fluorescence and flow-cytometry analysis confirmed that expanded G3C2T repeats embedded in the natural *NOP56* sequence are predominantly translated into the GP frame, excluding a potential bias of aggregation and insolubility that would impair detection of poly(GL) and poly(AW) protein by immunoblotting. As a further control, evaluation of the cherry protein, expressed independently of the repeats, confirmed that all of the three constructs are expressed (Figure 50-B,C,D,E).

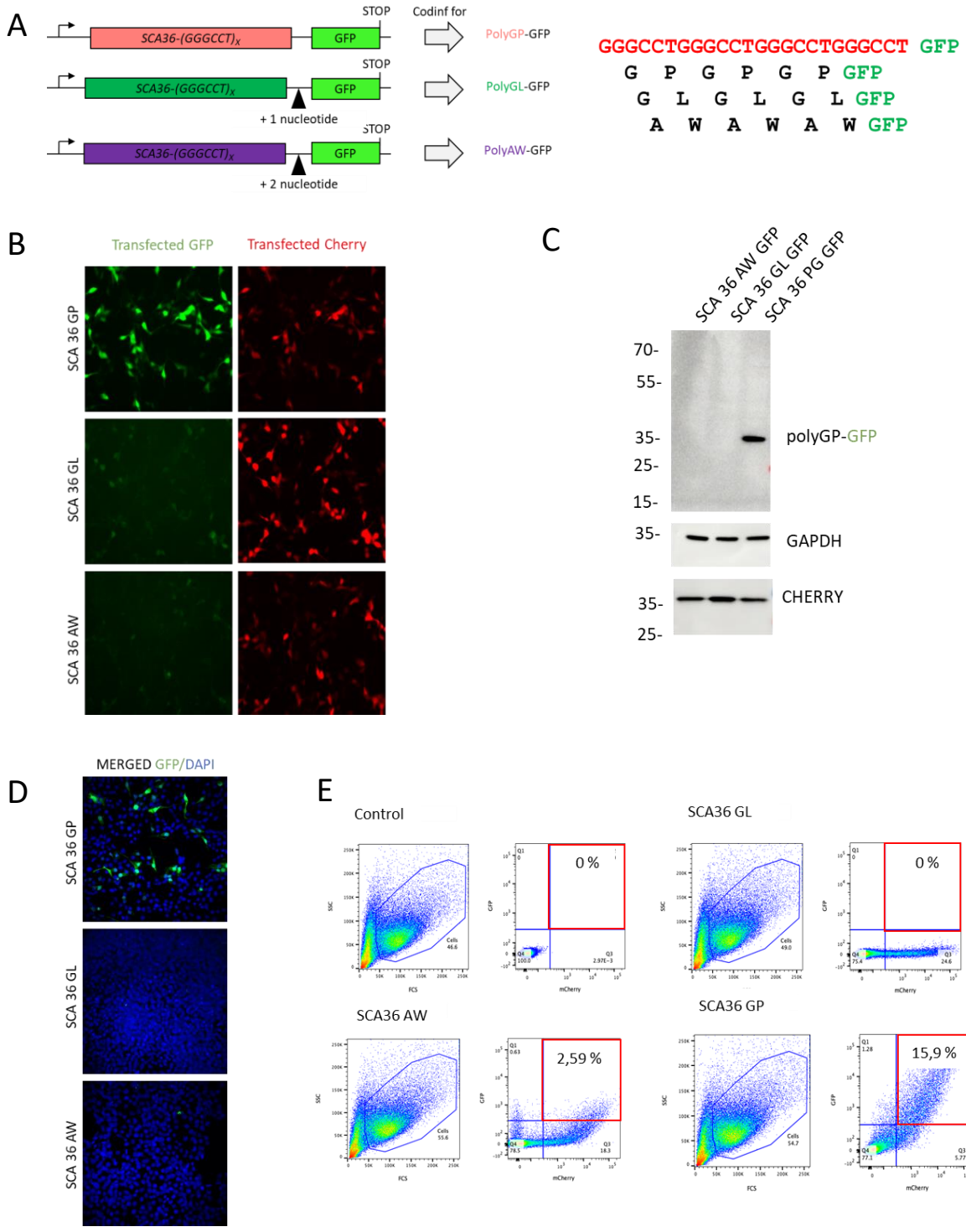


Figure 50 Expanded G4C2 repeats are translated into poly(GP) proteins

(**A**) Scheme and sequence of the human *NOP56* sense transcript with 80 G3C2T repeats fused to the eGFP in the three possible frames and cloned into the pcDNA3.1 plasmid. (**B**) Fluorescence and (**C**) immunoblotting of GFP and CHERRY from HEK293 cells transfected for 24 h with 80 G3C2T repeats embedded in the human sense *NOP56* sequence and fused in all three possible frames. (**D**) Immunoblotting and (**E**) flux cytometry of GFP and CHERRY from HEK293 cells transfected for 24 h with 80 G3C2T repeats embedded in the human sense *NOP56* sequence and fused in all three possible frames.

Next, we characterized the translation initiation sites of this poly(GP) proteins. Expanded G3C2T repeats embedded in their natural *NOP56* sequence were modified so that a lysine, target of the LysC enzyme, is present downstream of three G3C2T repeats in the GP frame. Immunoprecipitation of the poly(GP)-GFP tagged DPR protein followed by LysC digestion and LC-MS/MS analysis revealed a translation initiation of an ATG codon embedded in a correct Kozak consensus sequence and located 72 nucleotides upstream of the G3C2T repeats. Mutation of this ATG codon abolished poly(GP) DPR protein expression, confirming the importance of this start codon for translation of the G3C2T repeats in the GP frame (Figure 51- A,B,C,D).

Overall, our work confirmed that 80 G3C2T repeats embedded within the natural human *NOP56* sequence express the poly-(GP) DPR like protein. Our results differ from those found by Todd and collaborators, where they were able to detect poly(GP), poly(GL) and poly(AW) proteins in cultured cells. However, in their SCA36 mice, they only detected poly(GP) protein corelating with our findings (Todd et al., 2020).

To confirm presence of poly(GP) proteins, we will develop antibodies toward *NOP56*-poly(GP) protein to confirm their presence in patients samples. Furthermore, we will inject AAV PHP.eB in mice with either G3C2T repeats embedded within the natural human *NOP56* sequence or removed Nter-*NOP56* sequence to express only the poly(GP) DPR protein under an artificial ATG. Indeed, we recently showed that G4C2 repeats are extremely toxic only when they are embedded in their natural *C9ORF72* sequence. Removing the Nter-*C9ORF72* sequence and expressing the poly(PG) DPR protein under an artificial ATG, results in an absence of locomotor phenotype and a normal lifespan. Fortunately, this will permit to understand the importance of flanking region of *C9ORF72* and *NOP56* in their corresponding diseases.

To conclude, our work confirmed that 80 G3C2T repeats embedded within the natural human *NOP56* sequence expressed a poly(GP) DPR, alike the G4C2 repeats in *C9ORF72* gene. Future studies focusing on whether SCA36 present a similar toxic DPR-like protein mechanisms as C9-ALS has to be completed. Also, similarly to *C9ORF72* we should not rule out the possibility of a double-hit mechanism. For example reduced expression of *C9ORF72* synergizes the accumulation and toxicity of DPR proteins (Boivin, 2020). Thus, disruption on *NOP56* expression and associated pathways could synergize with poly(GP) DPR accumulation and toxicity. However, further studies have to be conducted on *NOP56* expression and pathway involvement.

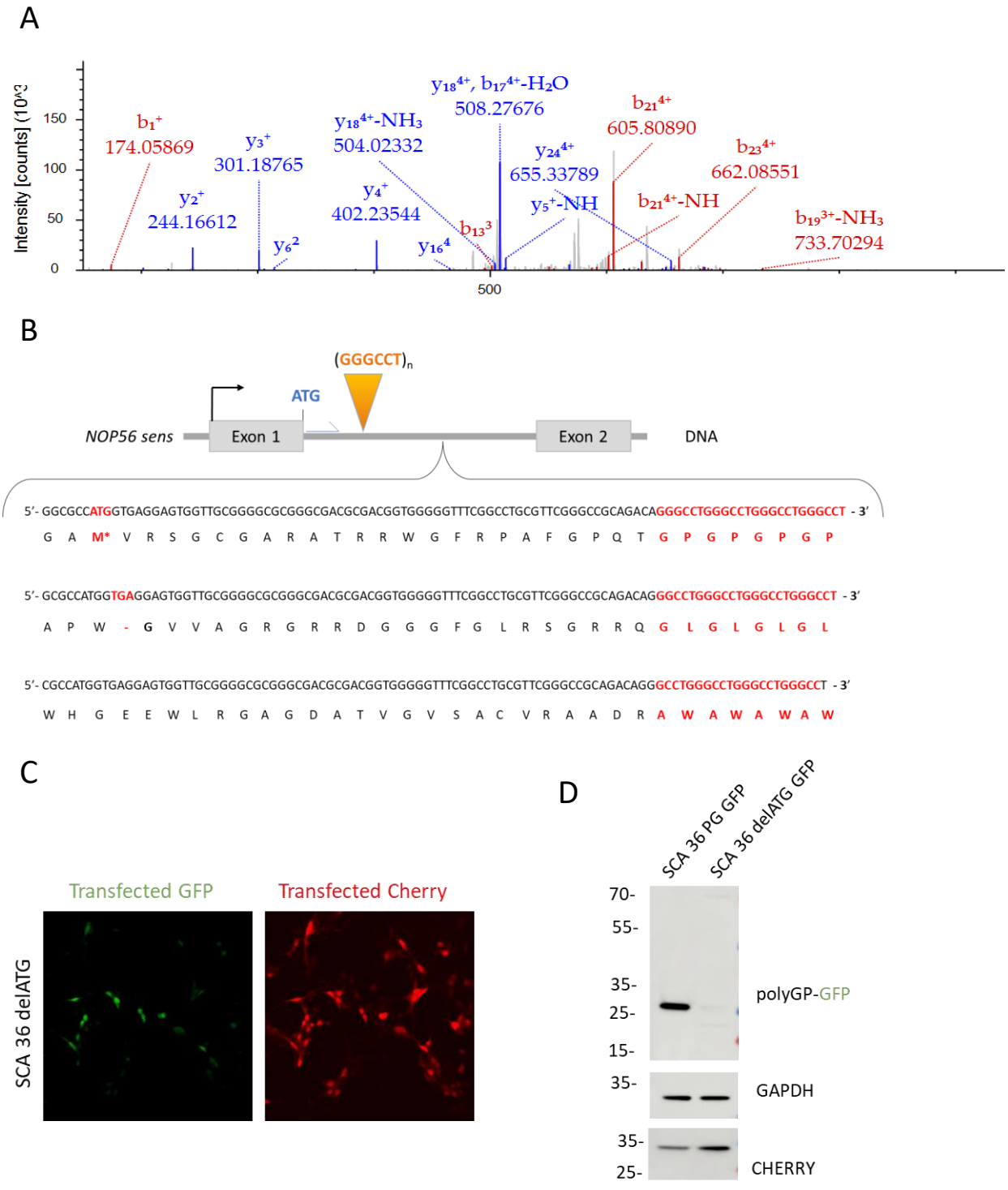


Figure 51 Expanded *NOP56* repeats are translated into poly(GP) through an ATG start codon

(**A**) LC-MS/MS spectra of the N-terminal part of the GFP-immunoprecipitated and LysC-digested poly(GP) protein.(**B**) Scheme of human *NOP56* sense transcript in all three possible frame. Start codon, stop codon and G3C2T repeats are indicated in red. (**C**) Fluorescence and (**D**) immunoblotting of GFP and CHERRY from HEK293 cells transfected for 24 h with 80 G3C2T repeats embedded in the human sense *NOP56* sequence or deleted form its ATG start codon.

# RESUMÉ EN FRANÇAIS

# 1. Introduction

## 1.1 La Sclérose Latérale Amyotrophique (SLA) et la démence frontotemporale (DFT)

**La Sclérose Latérale Amyotrophique (SLA)**, également connue sous le nom de maladie de Charcot, est une maladie neurodégénérative dévastatrice caractérisée par la perte progressive des neurones moteurs supérieurs et inférieurs, entraînant une atrophie musculaire et une paralysie. Bien qu'elle ait été initialement considérée comme bien comprise, la SLA reste complexe et diverse dans sa présentation clinique. Il existe deux formes principales : la forme spinale et la forme bulbaire.

- La forme spinale représente 2/3 des cas et débute par une faiblesse asymétrique et indolore d'un membre supérieur ou inférieur. La forme spinale se caractérise par une dégénérescence des motoneurones inférieurs, ce qui se traduit par un examen clinique révélant une atrophie et une faiblesse musculaire, des fasciculations et une hyperréflexie.

- La forme bulbaire touche 1/3 des patients et débute dans le muscle bulbaire en raison de la dégénérescence des motoneurones supérieurs entraînant une dysarthrie, une dysphagie et des fasciculations de la langue.

**La démence frontotemporale (DFT)** est la troisième démence la plus fréquente, avec trois variantes cliniques basées sur des altérations du comportement ou du langage. La DFT et la sclérose latérale amyotrophique (SLA) partagent un lien clinique et génétique, coexistant souvent au sein de familles ou d'individus. Les chevauchements génétiques incluent *TARDBP, SQSTM1, VCP, TBK1, CHCHD10 et C9ORF72*, avec des implications pour l'autophagie, le traitement de l'ARN et la formation de vésicules dans la neurodégénérescence. Les études épidémiologiques sur la SLA et la DFT sont difficiles à réaliser en raison de la variabilité de leur apparition, de leur faible incidence et de la diversité de leurs symptômes. Les registres européens fournissent des données montrant une prévalence de la SLA de 6,22 et une incidence de 2,31 pour 100 000 personnes-années, avec une prédominance masculine. La SLA survient généralement entre 54 et 69 ans. Les données relatives à la prévalence et à l'incidence de la DFT sont limitées, mais les études suggèrent une répartition égale entre les sexes, une apparition entre 55 et 70 ans et une implication génétique dans 30 à 50 % des cas.

Les examens post-mortem des patients atteints de SLA révèlent une perte de neurones moteurs, une neuro-inflammation et une dénervation musculaire. Les patients atteints de DFT présentent une atrophie des lobes frontaux et temporaux à l'IRM. L'agrégation de TDP-43 est une caractéristique commune de la SLA, observée dans 97 % des cas de SLA et 50 % des cas de DFT, bien que la mutation du gène TARDBP ne soit présente que dans 4 % des cas de SLA. Certains sous-types de SLA présentent d'autres agrégats protéiques, tels que SOD1 et FUS. Les mutations du gène *C9ORF72* entraînent différentes inclusions impliquant des protéines à répétition di-peptidique appelés DPR. Ces agrégats de protéines contribuent à diverses voies perturbées dans la SLA et la FTD. La sclérose latérale amyotrophique (SLA) et la démence frontotemporale (DFT) sont des maladies neurodégénératives complexes à composante génétique.

## 1.2 Les mutations génétiques misent en causes dans la SLA

Plusieurs gènes ont été associés à ces maladies et les patients présentent souvent diverses mutations génétiques. Ces mutations perturbent plusieurs voies cellulaires résumés ci-dessous :

**Altération de l'homéostasie protéique** : Plusieurs gènes liés à la SLA codent pour des protéines impliquées dans les voies de dégradation des protéines, comme le système Ubiquitin-Proteasome (UPS), l'autophagie et le stress du réticulum endoplasmique (RE). Les mutations de ces gènes perturbent la capacité cellulaire à maintenir l'équilibre protéique, entraînant l'accumulation de protéines mal repliées et une altération de la protéostase.

**Métabolisme aberrant de l'ARN** : Les mutations de gènes tels que *FUS* et *TDP-43* affectent le métabolisme de l'ARN, notamment la traduction, le traitement des ARNm et le transport de l'ARN. La dérégulation de ces protéines de liaison à l'ARN entraîne des défauts d'épissage et des événements d'épissage alternatif, affectant les transcrits de l'ARNm.

**Déficit du transport axonal** : Les patients atteints de SLA présentent une altération du transport axonal, ce qui entraîne des problèmes de trafic d'organelles, un dysfonctionnement mitochondrial et une dégénérescence des motoneurones. Des mutations dans des gènes tels que *PFN1*, *TUBA4A* et *DCTN1* affectent la dynamique de l'actine, les microtubules et le transport de marchandises le long du cytosquelette des microtubules.

**Stress oxydatif** : Les patients atteints de SLA subissent un stress oxydatif accru, caractérisé par un déséquilibre entre la production d'espèces réactives de l'oxygène (ROS) et leur détoxification. Les mutations du gène *SOD1* et d'autres gènes entraînent des dommages liés aux ROS, affectant diverses voies cellulaires.

**Dysfonctionnement des mitochondries** : Les mitochondries sont essentielles à la production d'énergie cellulaire, et les mutations de gènes tels que *SOD1* et *CHCHD10* entraînent des anomalies mitochondriales. Les mitochondries dysfonctionnelles affectent l'homéostasie ionique, les voies métaboliques et contribuent aux dommages oxydatifs.

**Excitotoxicité** : La surstimulation des récepteurs du glutamate provoque une excitotoxicité qui entraîne des lésions des motoneurones. Les mutations des récepteurs AMPA et du transporteur d'acides aminés excitateurs 2 (EAAT2) chez les patients atteints de SLA augmentent la susceptibilité à l'excitotoxicité.

**Voie endosomale et sécrétion de vésicules** : L'endocytose et la formation de vésicules extracellulaires sont altérées dans la SLA. Des gènes comme *ALS2* et *CHMP2B* sont liés à des perturbations du transport endosomal et vésiculaire. La mutation *C9ORF72*, une cause majeure de la SLA, influence la formation et le trafic des vésicules.

L'interaction complexe entre ces voies peut créer une cascade de dysfonctionnements, conduisant finalement à la mort des motoneurones. La SLA présente souvent une hérédité oligogénique, où plusieurs gènes contribuent à la maladie, et certains gènes ont des effets pléiotropes, provoquant diverses manifestations phénotypiques. Il est essentiel de comprendre ces mécanismes à multiples facettes pour mettre au point des traitements efficaces de la SLA et de la DFT. L'un des principaux gènes associés à la SLA, *C9ORF*72, et son rôle dans l'autophagie sont particulièrement intéressants et feront l'objet d'une étude plus approfondie.

## 1.3 Implication de C9ORF72 dans l'ALS et la FTD

La découverte en 2011 de l'expansion hexa-nucléotidique GGGGCC dans le gène *C9ORF72* a marqué une avancée significative dans la compréhension de la SLA et de la DFT, qui constituent la cause génétique la plus fréquente, en particulier en Europe et en Amérique du Nord, avec 80 à 90 % des cas familiaux mais plus rare en Asie et au Moyen-Orient. Alors que les individus normaux présentent de 2 à 24 répétitions, les expansions pathologiques dépassent souvent 30, atteignant parfois des centaines de milliers. La variabilité clinique peut être due à l'instabilité somatique du nombre de répétitions dans différents tissus, même chez un seul individu. Le gène *C9ORF72* présente trois variantes de transcription et code pour deux isoformes, *C9ORF72*-S et *C9ORF7*2-L, cette dernière étant plus abondante. Les mécanismes pathogènes sous-jacents à la sclérose latérale amyotrophique (SLA) et à la démence frontotemporale (DFT) sont décrits en trois mécanismes principaux :

**Foci d'ARN**

Premièrement, l'expansion des répétitions GGCCCC dans *C9ORF72* conduit à la formation de foyers d'ARN qui s'accumulent dans le noyau cellulaire. Ces foyers d'ARN séquestrent diverses protéines de liaison à l'ARN (RBP), affectant leur localisation et leurs fonctions. Plusieurs études ont confirmé la présence de foyers d'ARN sens et antisens chez les patients C9-ALS et dans divers types de cellules dérivées de ces patients. Ces foyers d'ARN peuvent former des structures secondaires complexes, telles que des G-quadruplexes et des boucles R, qui séquestrent les RBP jouant un rôle dans l'épissage, la régulation de la traduction, le transport et la dégradation de l'ARN.

**Toxicité par les DPR**

Deuxièmement, les répétitions sens et antisens étendues subissent une traduction RAN (Repeat Associated Non-ATG), produisant des protéines contenant des répétitions di-peptidiques (DPR). Ces DPR forment des inclusions cytoplasmiques dans les neurones des patients atteints de C9-ALS/FTD. Certaines études suggèrent que certaines DPR, telles que les poly(GR) et les poly(PR), sont plus toxiques que d'autres, affectant le transport nucléocytoplasmique et les mécanismes de dégradation des protéines. Cependant, le rôle exact des DPR dans la neurodégénérescence reste un sujet de débat.

La toxicité a été observée à la fois en présence et en l'absence de DPR dans divers modèles animaux et cellulaires, ce qui indique l'implication potentielle d'autres facteurs.

**Perte de fonction de C9ORF72**

Troisièmement, l'expansion de la répétition GGGGCC dans le gène *C9ORF72* conduit à des modifications épigénétiques, telles que l'hyperméthylation du promoteur du gène C9ORF72 et la tri-méthylation des histones qui provoquent une diminution de la transcription du gène *C9ORF72*. La protéine C9ORF72 est principalement exprimée dans le cerveau, la moelle épinière et le système immunitaire, avec des niveaux plus faibles dans d'autres tissus. Des études récentes utilisant la spectrométrie de masse ont confirmé une réduction significative des niveaux de protéine *C9ORF72* dans le cortex frontal des patients atteints de C9-FTD. L'haploinsuffisance potentielle de *C9ORF72* a été débattue, car les preuves génétiques ne soutiennent pas systématiquement cette idée. En outre, les modèles *in vitro* et *in vivo* ont produit des résultats variables concernant l'impact de la perte de *c9orf72*. Si certains modèles suggèrent l'importance de *C9ORF72* dans la neurodégénérescence, la pertinence de ces résultats pour la maladie humaine reste incertaine. Des modèles *in vivo* ont montré que la déficience en *C9ORF72* chez la souris peut conduire à un phénotype inflammatoire, ce qui suggère un rôle dans la régulation de la voie autophagie/lysosome. Cependant, ces résultats ne correspondent pas aux phénotypes moteurs observés dans les organismes d'ordre inférieur.

Il est suggéré que la perte de cellules neuronales dans la maladie de C9-ALS/FTD pourrait résulter d'une combinaison de ces mécanismes, y compris une autophagie suboptimale due à une expression réduite de *C9ORF72*. L'accent est mis sur l'interaction complexe des foyers d'ARN, des DPR et d'autres facteurs potentiels dans la pathogenèse de la SLA et de la DFT associées à *C9ORF72*. Des recherches supplémentaires sont nécessaires pour comprendre pleinement les contributions relatives de ces mécanismes à ces maladies.

Dans l'ensemble, le rôle de C9ORF72 dans la pathogenèse de la SLA et de la FTD reste un domaine de recherche complexe et en constante évolution. Cependant, une question subsiste : quel est le rôle de C9ORF72 ?

## 1.4 C9ORF72 forme un complexe avec SMCR8 et WDR41

La protéine C9ORF72 forme un complexe avec les protéines SMCR8 et WDR41, formant le complexe CSW, qui partage des caractéristiques structurelles avec les protéines DENN connues pour réguler le cycle d'échange Guanosine Diphosphate/Guanosine Triphosphate (GDP/GTP) des protéines RAB/ARF, impliquées dans le trafic des vésicules et les processus cellulaires. Il a été démontré que le complexe CSW régule diverses GTPases RAB, telles que RAB8a, RAB39b, RAB1a, RAB5, RAB7, RAB11 et RAB3, ayant un rôle dans l'autophagie, l'endocytose et l'exocytose. En outre, le complexe CSW interagit avec le complexe Unc-51-like kinase 1 (ULK1) pour influencer l'autophagie. La compréhension de la structure du complexe CSW et de son rôle dans la régulation des petites GTPases et de l'autophagie est l'un des principaux objectifs de cette thèse.

## 1.5 Le rôle de CSW dans l'autophagie

L'autophagie est un processus cellulaire essentiel pour la dégradation des composants cellulaires non essentiels ou endommagés. Elle comprend trois types d'autophagie : l'autophagie médiée par les chaperons, la microautophagie et la macroautophagie. La macroautophagie reste la plus étudié et comprend des étapes d'initiation, de nucléation, d'élongation, de maturation et de fusion, aboutissant finalement à la formation d'autolysosomes où les composants cellulaires sont dégradés. La découverte de Christian de Duve en 1963 et les travaux révolutionnaires de Yoshinori Ohsumi en 1993, identifiant les protéines liées à l'autophagie (ATG), ont considérablement élargi nos connaissances. Aujourd'hui, plus de 40 ATG ont été identifiées, faisant de l'autophagie un domaine d'étude en pleine expansion. L'autophagie est un processus cellulaire hautement régulé.

**Dans la phase d'initiation et de nucléation**, le complexe ULK, composé de protéines telles que ULK1, ATG13, FIP200 et ATG101, forme le complexe d'initiation de l'autophagie. Il est modulé par mTORC1, un complexe de kinases comprenant mTOR, RAPTOR, mLST8, DEPTOR et PRAS40. Dans des conditions riches en nutriments, mTORC1 phosphoryle et inhibe le complexe ULK, empêchant ainsi l'autophagie. Toutefois, en cas de privation de nutriments, mTORC1 se dissocie, ce qui permet le déclenchement de l'autophagie.

Les GTPases RAG détectent également les niveaux d'acides aminés pour réguler l'activation de mTORC1. L'AMPK, un capteur d'énergie, peut activer ULK1 dans des conditions telles que la privation de glucose, ce qui favorise l'autophagie. Après l'initiation, le complexe de nucléation PI3KC3, qui comprend VPS15, VPS34, BECN1, ATG14 et AMBRA1, est recruté et génère les PtdIns3P nécessaire à la formation de la membrane d'isolation.

**Dans la phase d'élongation et de maturation**, des protéines comme WIPIs, DFCP1, et les systèmes Atg12-Atg5-Atg16L1 et Atg8/LC3 contribuent à l'expansion du phagophore. L'achèvement et la fusion des autophagosomes impliquent le complexe HOPS, les microtubules et les GTPases RAB, conduisant à la formation de l'autolysosome, où les enzymes lysosomales dégradent le contenu autophagosomal en vue d'un recyclage métabolique.

Des recherches récentes menées par Yu et al ont mis en évidence un phénomène connu sous le nom de régénération autophagique des lysosomes (ALR). Ils ont constaté qu'au cours d'une privation de nutriments prolongée, le nombre de lysosomes diminuait dans un premier temps, puis se rétablissait grâce à la régénération autophagique des lysosomes. Ce processus implique un remodelage de la membrane par les phosphoinositides et l'action de protéines telles que AP-2, KIF5B et DNM2. Il est intéressant de noter que des perturbations de l'ALR sont associées à certaines maladies. Par exemple, dans la maladie de Parkinson, les variations du gène GAK altèrent l'autophagie et l'ALR, tandis que les paraplégies spastiques héréditaires (HSP) impliquent des mutations dans *SPG11* et *SPG15*, qui ont un impact sur le déclenchement de l'ALR et d'autres fonctions cellulaires, entraînant des déficiences motrices.

L’implication de C9ORF72 et d’un dérèglement de l'autophagie dans les maladies neurodégénératives telles que la sclérose latérale amyotrophique (SLA) ont été largement étudié. Un dysfonctionnement de la voie autophagie-lysosome peut contribuer à l'agrégation des protéines, une caractéristique de diverses maladies neurodégénératives avec C9ORF72 et son complexe, C9ORF72-SMCR8-WDR41 étant décrit comme impliqués dans la régulation de l'autophagie et interagissant avec des protéines autophagiques clés. Une dysrégulation des lysosomes est observée dans les cellules dépourvues de C9ORF72 suggérant que C9ORF72 est un régulateur négatif de l'autophagie et joue un rôle critique dans le processus autophagique, ce qui permet de mieux comprendre son implication potentielle dans la SLA et d'autres troubles neurodégénératifs.

La SLA, caractérisée par la dégénérescence des motoneurones, a une cause génétique majeure dans les mutations du gène *C9ORF72*. Cette thèse se concentrera sur le complexe C9ORF72-SMCR8-WDR41, sa structure 3D et son rôle dans la régulation de l'autophagie et le trafic des vésicules intracellulaires, dans le but de découvrir les mécanismes de la pathogenèse de la SLA.

## 1.6 L'ALS et les traitements : Où en sommes-nous ?

A ce jour la sclérose latérale amyotrophique (SLA) reste une maladie incurable et dévastatrice dont les options thérapeutiques sont limitées. Les médicaments actuellement autorisés, notamment le Riluzole, l'Edaravone et le Phénylbutyrate de sodium/Taurursodiol, n'offrent que des avantages modestes, ralentissant la progression de la maladie mais ne l'arrêtant pas. Des progrès récents, en particulier dans le domaine des thérapies génétiques, permettent d'espérer une amélioration des traitements de la SLA. Le riluzole, approuvé par la FDA et l'EMA, vise à réduire l'excitotoxicité, principalement causée par le glutamate. Il a montré un bénéfice en termes de survie pouvant aller jusqu'à trois mois. L'edaravone, approuvé au Japon et dans d'autres pays, cible le stress oxydatif et la neuro-inflammation, bien que son efficacité soit quelque peu discutée. Le phénylbutyrate de sodium et le taurursodiol, administrés en association, ont récemment été approuvés pour le traitement de la SLA. Ils agissent sur la mort des cellules neuronales et le stress oxydatif en réduisant le stress du réticulum endoplasmique et le dysfonctionnement des mitochondries. Lors d'essais cliniques, ces composés ont permis de réduire de 25 % l'évolution de la maladie.

Plusieurs approches sont explorées dans le traitement de la SLA. De petites molécules sont à l'étude, telles que les cannabinoïdes, la trazodone et la metformine, ciblant diverses voies comme l'excitotoxicité, le stress oxydatif et la neuro-inflammation. La modulation de l'autophagie et le contrôle de l'agrégation des protéines sont également des voies prometteuses. Les thérapies géniques émergent quand a-t-elle rapidement, les oligonucléotides antisens (ASO) étant des candidats prometteurs. Les ASO modulent précisément l'expression des gènes et des essais ont montré des résultats positifs dans les cas de SOD1 et de FUS. Cependant, les ASO ont du mal à cibler efficacement les cas de *C9ORF72*. L'interférence ARN (ARNi) et la technologie CRISPR/Cas9 délivrée par des vecteurs viraux retiennent aussi l'attention.

L'APB-102 et l'AAV-miQURE® présentent un potentiel dans les cas de SOD1 et de SLA C9ORF72. La thérapie par cellules souches mésenchymateuses (BM-MSC) comme NurOwn® et Lenzumestrocel (Neuronata-R® Inj) démontre un potentiel dans la SLA, en déplaçant le système immunitaire vers un environnement neuroprotecteur. Bien que la SLA reste une maladie complexe et difficile à traiter, les diverses approches thérapeutiques permettent d'espérer des traitements plus efficaces et, en fin de compte, un avenir plus radieux pour les patients atteints de SLA.

# 2. Résultats

## 2.1 Structure du complexe C9ORF72-SMCR8-WDR41

Nous avons tenté d'élucider les fonctions moléculaires de C9ORF72 en déterminant sa structure 3D. Les premières tentatives de cristallographie ont échoué en raison de la difficulté à former des cristaux. Nous nous sommes donc tournés vers la microscopie électronique cryogénique (Cryo-EM), une technique plus récente. La Cryo-microscopie électronique permet d'obtenir des images de macromolécules biologiques dans un état similaire à leur forme native, ce qui permet d'éviter les problèmes liés à la formation de cristaux. L'optimisation de l'échantillon, le nettoyage par plasma et les paramètres de vitrification ont été des étapes cruciales. Nous avons optimisé la préparation des grilles à l'aide du Thermofisher Vitrobot Mark IV, en surmontant des défis tels que la dénaturation, les artefacts dus aux détergents, la couverture des particules, l'agrégation des protéines et l'épaisseur de la glace.

En utilisant un détergent spécifique (DDM) et des paramètres contrôlés, nous avons réussi à préparer correctement les grilles et avons ensuite utilisé le Cryo-microscope électronique Titan Krios pour obtenir les structures 3D finales. Ensuite, nous avons utilisé Cryolo et Relion pour la sélection des particules, la classification 2-D et la classification 3-D, ce qui a permis d'obtenir une structure 3D d'une résolution de 5,9 A°. La COVID-19 ont affecté l'étude, mais notre structure de C9ORF72 s'aligne sur les publications précédentes. Le complexe CSW a une structure 3D d'une largeur d'environ 130 Å et d'une hauteur de 140 Å, composée des domaines longin et DENN. Bien que notre structure présente des points communs avec d'autres, une partie importante n'a pas été résolue.

Le complexe CSW, qui fait partie de la famille DENN régulant des petites GTPases, présente des similitudes structurelles avec d'autres complexes tels que NPRL2-NPRL3 et FLCN-FNIP2 (Figure 1-A,B).

Nous avons donc cherché à identifier la petite GTPase à identifier la petite GTPase qui interagit avec le complexe CSW afin de mieux le comprendre. Nous avons cherché à savoir si le complexe CSW régulait les GTPases RAG, mais n'avons pas trouvé d'interaction. Pour identifier la petite GTPase concernée, un criblage approfondi a été réalisé, en se concentrant sur la famille ARL/ARF, avec les ARL4, 11, 14 et 15 présentant des interactions prometteuses (Figure 2-A,B).

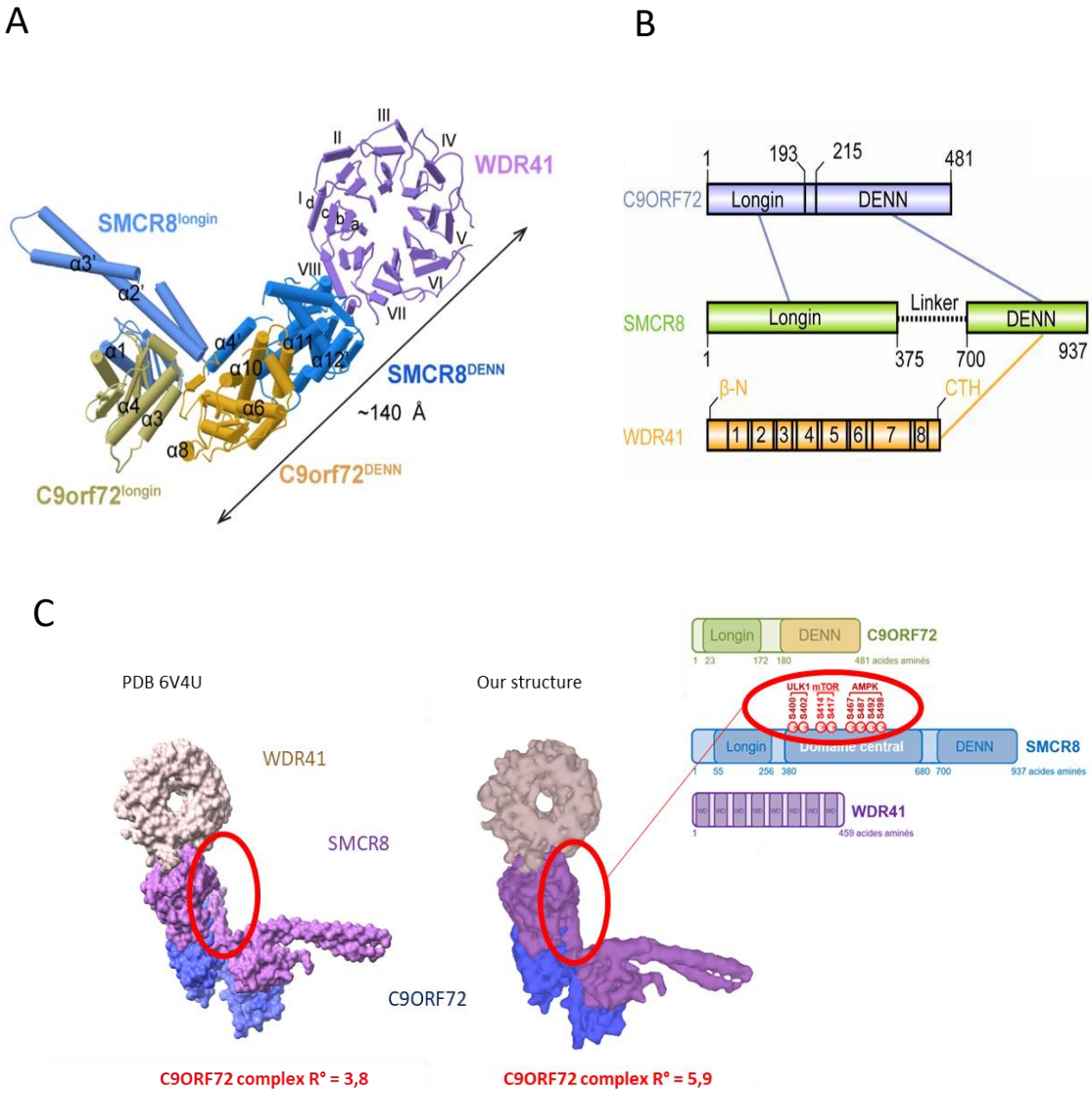


Figure 1 : Structure, organisation et domaine du complexe CSW

(**A**) Coordonnées affinées du complexe représenté par des tuyaux et des planches pour les α-tranches et les β-feuillets, respectivement. Les domaines sont codés en couleur comme suit : SMCR8longin, bleu bleuet ; SMCR8DENN, bleu cagnard ; C9orf72longin, olive ; C9orf72DENN, verge d'or ; WDR41, violet moyen (Tang et al., 2020). (**B**) Schéma de l'agencement des domaines de C9ORF72 (bleu clair), SMCR8 (vert clair) et WDR41 (orange). Les noms et les limites des domaines sont indiqués. CTR, hélice C-terminale de la WDR41. Les interactions entre les différents domaines sont représentées par des lignes : ligne bleu clair, interaction C9ORF72-SMCR8 ; ligne orange, interaction WDR41-SMCR8 (Su et al., 2020). (**C**) Comparaison de notre structure (à droite) et de la structure PDB 6V4 de Tang et al. Le cercle rouge représente la partie basse résolution (entre AA 380-700 de SMCR8) riche en résidus phosphorylables.

## 2.2 Quelle petite GTPase est régulée par le complexe CSW ?

Le complexe CSW a donc ensuite été étudié pour son rôle de protéine activatrice de GTPase (GAP) pour les petites GTPases. Nous avons démontré qu'il interagit avec les formes inactives et actives d'ARL14 et d'ARL4a. La privation de nutriments renforce l'interaction avec ARL14 (Q68L), ce qui suggère un rôle dans la régulation de l'autophagie (Figure 2-A,B). De plus, ARL14 (Q68L) présente une colocalisation partielle avec les lysosomes. Des expériences menées sur des cellules U2OS ont montré que ARL4a (Q79L) et ARL14 (Q68L) se relocalisaient avec CSW en cas de famine prolongée, ce qui implique le recrutement de CSW dans les lysosomes. Ces résultats mettent en lumière les rôles potentiels de l'interaction CSW-ARL14 dans l'autophagie. Des mutations imitant des états actifs de phosphorylation (S102D, T140D et S790D) dans SMCR8 renforcent son interaction avec ARL14. Ces sites phosphorylables sont proches de la poche de liaison ARL14 de CSW. La suppression de la partie centrale de SMCR8 renforce également l'interaction CSW-ARL14 (Figure 1-C). Des expériences de co-immunoprécipitation ont notamment permis d'identifier l'interaction du complexe CSW avec RB1CC1 (FIP200), un régulateur clé de la voie autophagique. Des interactions CSW-ARL14-FIP200 ont notamment été observées dans des cellules HEK-293. Les protéines produites par baculovirus et l'analyse EM suggèrent la formation d'un complexe entre CSW et FIP200, bien qu'avec une quantité limitée d'ARL14.

Les recherches structurelles en cours laissent entrevoir l'implication du complexe CSW-ARL14 dans l'autophagie. En particulier, leurs interactions, la phosphorylation de SMCR8 et l'association avec FIP200 suggèrent un rôle, potentiellement dans la régénération des lysosomes autophagiques (ALR). Le rôle du complexe CSW dans les processus lysosomaux et autophagiques ont notamment été largement étudié dans cette thèse (Figure 2-A,B,C,D,E). Dans un premier temps, les tentatives pour déterminer la fonction précise de C9ORF72 au niveau du lysosome n'ont pas révélé de changements significatifs dans les paramètres lysosomaux, à l'exception d'une réduction mineure de la lipidation LC3B. Il a ensuite été établi que le recrutement du complexe CSW au lysosome dépend du WDR41 et est facilité lors de l'induction de l'autophagie. Ce développement a été crucial car l'ajout d'étiquette sur C9ORF72 et SMCR8 altère la localisation de ce complexe.

Une étude plus approfondie de l'interaction entre CSW et ARL14 pendant la privation de nutriments a suggéré un rôle dans la régénération du lysosome autophagique (ALR). L'ALR implique la régénération des lysosomes après une période d'autophagie et est vital pour la fonction cellulaire. L'absence de tubules dans les cellules *C9ORF72* KO a été liée à un déficit en ALR. Les tentatives de sauvetage de la formation de tubules avec la surexpression de ARL14 et ARL4 n'ont pas apporté d'améliorations significatives, indiquant un mécanisme de régulation plus complexe (Figure 2-E).

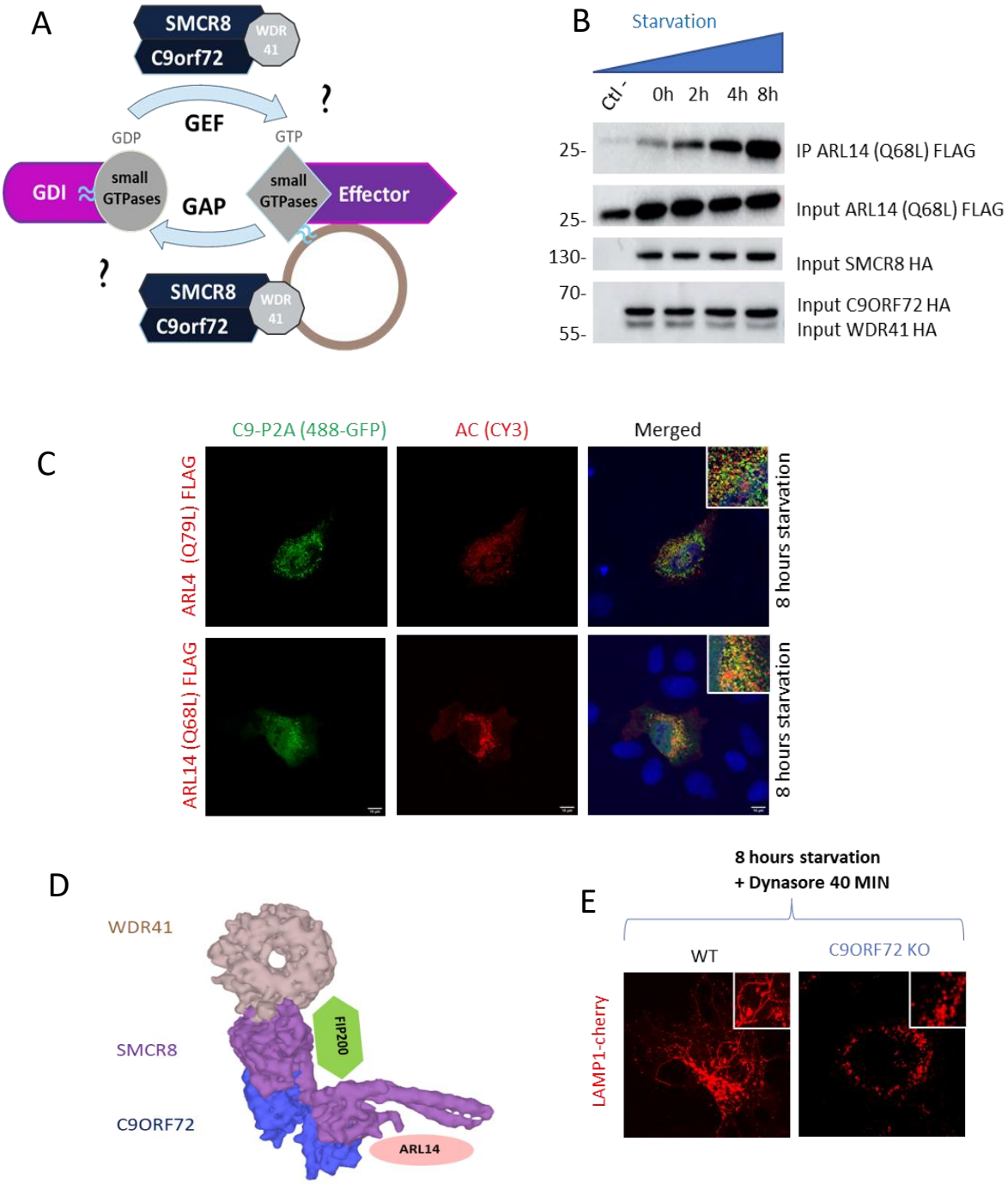


Figure 2 : Le complexe CSW interagit avec ARL14 et joue un rôle dans l'ALR.
(**A**) Représentation schématique de CSW agissant comme GAP ou GEF sur la petite GTPase. (**B**) Analyse par immunoblot des protéines immunoprécipitées par HA et du lysat de cellules HEK293 co-exprimant WDR41 HA-marqué, SMCR8 HA-marqué et C9ORF72 HA-marqué avec ARL14 Flag-marqué dans l'état de verrouillage du GDP. (**C**) Lignée de cellules stables U2OS exprimant C9ORF72-SMCR8 P2A et transfectées avec ARL14 ou ARL4a marqués FLAG. (**D**) Représentation schématique du supercomplexe CSW-ARL14 et FIP200. (**E**) Images représentatives du marquage par immunofluorescence de la lignée de cellules stables U2OS WT ou dépourvues de C9orf72 exprimant LAMP1-cherry après 8 heures de privation de nutriments et 40 minutes de traitement au dynasore.

## 2.3 C9ORF72 joue un rôle dans la régénération des lysosomes autophagiques (ALR)

Nous avons donc ensuite exploré l'interaction du complexe CSW avec le complexe AP-5 et ARL4a. Le complexe semble jouer un rôle dans ALR, avec AP-5 et ARL4a régulant potentiellement la localisation lysosomale. De plus, l'étude des phosphoinositides kinases a révélé des interactions entre ARL4a et PI4K2B, qui est connu pour réguler la tubulation du lysosome. Les cellules transfectées par U2OS-LAMP1 présentaient une colocalisation entre PI4K2B, ARL4a et AP5 (Figure 3-A,B,C,D,E).

En résumé, cette thèse met en lumière l'implication du complexe CSW dans les processus lysosomaux et autophagiques, soulignant son rôle potentiel dans la reformation des lysosomes autophagiques (ALR) et ses interactions avec d'autres protéines clés impliquées dans ces processus. Il introduit une nouvelle voie qui relie le complexe CSW à la régulation ALR, fournissant de nouvelles informations sur les mécanismes complexes régissant l'autophagie et la fonction lysosome. CSW-ARL14 jouant un rôle crucial dans la régénération du lysosome autophagique et un super complexe avec AP5 et ARL4 régulant la tubulation de lysosome.

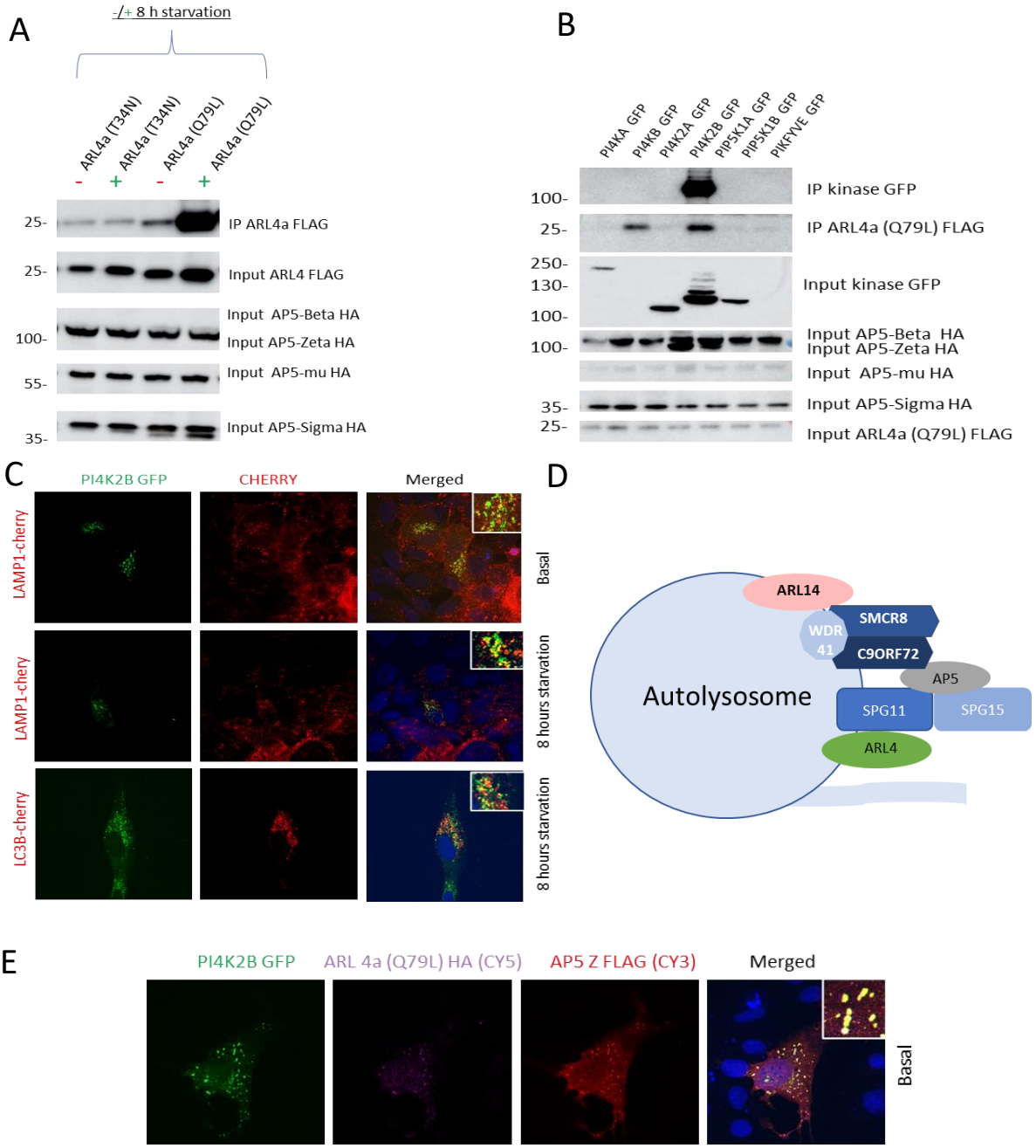


Figure 3 : AP5 interagit avec ARL4 et PI4K2B pour réguler l'ALR.

(**A**) Analyse par immunoblot des protéines HA-immunoprécipitées et du lysat de cellules HEK293 coexprimant les sous-unités AP-5 marquées HA et ARL4a marquée FLAG à l'état bloqué par le GDP ou le GTP avec et sans famine. (**B**) Analyse immunoblot des protéines immunoprécipitées par HA et du lysat des cellules HEK293 coexprimant les sous-unités AP5 marquées par HA et différentes phosphoinositide kinase marquées par GFP et ARL4a marquée par FLAG. (**C**) Images représentatives du marquage par immunofluorescence de la lignée de cellules U2OS LAMP-1 cherry stable et transfectée avec la GFP. (**D**) Représentation schématique des modèles en cours du complexe CSW-ARL14 régulant l'ALR via le complexe AP5-SPG11-15 et sa petite GTPase ARL4a. (**E**) Images représentatives du marquage par immunofluorescence de cellules U2OS transfectées avec PI4K2B marqué GFP, ARL4a marqué HA (violet) et AP5Z (rouge) sans famine.

# 3. Discussions et perspectives

Cette thèse révèle la structure 3D du complexe C9ORF72-SMCR8-WDR41, identifie une interaction avec ARL14 et découvre le rôle de CSW dans l'autophagie et la régénération des lysosomes.

## 3.1 Structure de C9ORF72-SMCR8-WDR41

Cette thèse traite de l'analyse structurelle du complexe C9ORF72-SMCR8-WDR41 et de ses interactions potentielles avec des petites GTPases (ARL4 et ARL14) et FIP200, mettant en lumière le rôle du complexe dans l'autophagie. Les premières tentatives de résolution de la structure du complexe se sont heurtées à des difficultés dues à l'orientation préférentielle du complexe, ce qui s'est traduit par une résolution inférieure à celle d'études ultérieures. La complexité des interactions entre les petites GTPases et l'impact des étiquettes sur les interactions protéine-protéine ont été étudiés. Alors que les co-immunoprécipitation n'ont révélé aucune interaction robuste avec des petites GTPases précédemment publiés, nous avons identifié des interactions potentielles avec ARL4a et ARL14 en utilisant des méthodes alternatives. Cette thèse souligne l'importance des étiquettes pour stabiliser les complexes protéine-protéine transitoires où ARL4 et ARL14 ont été identifiées comme un partenaire d'interaction potentiel avec le complexe C9ORF72-SMCR8-WDR41. L'utilisation de petits marqueurs, tels que le STREP-tag, a été mise en avant pour la purification effective des protéines et les expériences de Cryo-EM.

## 3.2 Quelle petite GTPase est régulée par le complexe CSW ?

En outre, cette thèse explore les interactions du complexe CSW avec FIP200, un régulateur clé de la voie autophagique. L'analyse structurelle suggère que la région à enroulement de SMCR8 joue un rôle crucial dans les interactions, en particulier avec FIP200. Cette thèse indique que FIP200 pourrait influencer l'activité GAP du complexe CSW, en affectant ses interactions avec les petites GTPases. Les résultats suggèrent que l'interaction CSW-FIP200 pourrait aider à stabiliser le complexe et potentiellement faciliter la résolution de la partie manquante de SMCR8, qui est vitale pour la régulation et l'interaction avec les petites GTPases. Dans l'ensemble, cette thèse donne un aperçu de l'interaction complexe des protéines impliquées dans la régulation de l'autophagie.

Nous examinons notamment les résultats liés au rôle du complexe CSW, en particulier C9ORF72, ARL14 et ARL4a, dans la régénération des lysosomes autophagiques et leurs interactions avec d'autres protéines impliquées dans ce processus. Nous révélons des informations importantes sur l'interaction complexe de diverses protéines et voies dans la régulation de la régénération des lysosomes autophagiques.

## 3.3 Quel est le rôle de C9ORF72 ?

L'interaction entre le complexe CSW et les petites GTPases ARL14 et ARL4a jouis d'une place importante dans cette thèse. On se penche notamment sur la localisation subcellulaire de C9ORF72, dont les résultats montrent qu'il se localise principalement dans les lysosomes lors d'une privation en acide aminées prolongée. L'implication du complexe CSW dans la régulation de l'autophagie est mise en évidence. En outre, la thèse suggère que ARL14 joue un rôle dans le recrutement du complexe CSW dans les lysosomes/autolysosomes, ce qui est essentiel pour la tubulation de l'ALR. Nous abordons aussi l'interaction du complexe CSW avec le complexe AP-5 et ARL4a, révélant leur rôle dans l'ALR. Elle met notamment en avant que le complexe AP-5-ARL4a est aussi associé à des phosphoinositides kinases, en particulier PI4K2B, impliquées dans l'ALR et souligne l'importance de ces interactions dans la régulation de l'ALR.

En résumé, une exploration complète de l'interaction complexe des protéines impliquées dans l'ALR avec C9ORF72 est mise en avant, mettant en lumière les rôles de C9ORF72, ARL14, ARL4a et leurs interactions dans ce processus cellulaire critique. Nous révélons l'importance du complexe CSW-ARL14 dans la régénération des lysosomes autophagiques dans des conditions basales et autophagique. Cette recherche donne un aperçu des processus dynamiques impliqués dans le maintien de l'homéostasie lysosomale et de leurs implications potentielles pour la fonction cellulaire et les maladies tels que l'ALS.

# BIBLIOGRAPHY

Aartsma-Rus, A., 2017. FDA Approval of Nusinersen for Spinal Muscular Atrophy Makes 2016 the Year of Splice Modulating Oligonucleotides. Nucleic Acid Ther 27, 67–69. https://doi.org/10.1089/nat.2017.0665

Abe, K., Aoki, M., Tsuji, S., Itoyama, Y., Sobue, G., Togo, M., Hamada, C., Tanaka, M., Akimoto, M., Nakamura, K., Takahashi, F., Kondo, K., Yoshino, H., Abe, K., Aoki, M., Tsuji, S., Itoyama, Y., Sobue, G., Togo, M., Hamada, C., Sasaki, H., Yabe, I., Doi, S., Warita, H., Imai, T., Ito, H., Fukuchi, M., Osumi, E., Wada, M., Nakano, I., Morita, M., Ogata, K., Maruki, Y., Ito, K., Kano, O., Yamazaki, M., Takahashi, Y., Ishiura, H., Ogino, M., Koike, R., Ishida, C., Uchiyama, T., Mizoguchi, K., Obi, T., Watanabe, H., Atsuta, N., Aiba, I., Taniguchi, A., Sawada, H., Hazama, T., Fujimura, H., Kusaka, H., Kunieda, T., Kikuchi, H., Matsuo, H., Ueyama, H., Uekawa, K., Tanaka, M., Akimoto, M., Ueda, M., Murakami, A., Sumii, R., Kudou, T., Nakamura, K., Morimoto, K., Yoneoka, T., Hirai, M., Sasaki, K., Terai, H., Natori, T., Matsui, H., Kotani, K., Yoshida, K., Iwasaki, T., Takahashi, F., Kondo, K., Yoshino, H., 2017. Safety and efficacy of edaravone in well defined patients with amyotrophic lateral sclerosis: a randomised, double-blind, placebo-controlled trial. The Lancet Neurology 16, 505–512. https://doi.org/10.1016/S1474-4422(17)30115-1

Abe, K., Itoyama, Y., Sobue, G., Tsuji, S., Aoki, M., Doyu, M., Hamada, C., Kondo, K., Yoneoka, T., Akimoto, M., Yoshino, H., 2014. Confirmatory double-blind, parallel-group, placebo-controlled study of efficacy and safety of edaravone (MCI-186) in amyotrophic lateral sclerosis patients. Amyotroph Lateral Scler Frontotemporal Degener 15, 610–617. https://doi.org/10.3109/21678421.2014.959024

Abramzon, Y.A., Fratta, P., Traynor, B.J., Chia, R., 2020. The Overlapping Genetics of Amyotrophic Lateral Sclerosis and Frontotemporal Dementia. Front Neurosci 14, 42. https://doi.org/10.3389/fnins.2020.00042

Albo, F., Pieri, M., Zona, C., 2004. Modulation of AMPA receptors in spinal motor neurons by the neuroprotective agent riluzole. J Neurosci Res 78, 200–207. https://doi.org/10.1002/jnr.20244

Almeida, S., Gascon, E., Tran, H., Chou, H.J., Gendron, T.F., DeGroot, S., Tapper, A.R., Sellier, C., Charlet-Berguerand, N., Karydas, A., Seeley, W.W., Boxer, A.L., Petrucelli, L., Miller, B.L., Gao, F.-B., 2013. Modeling key pathological features of frontotemporal dementia with C9ORF72 repeat expansion in iPSC-derived human neurons. Acta Neuropathol 126, 385–399. https://doi.org/10.1007/s00401-013-1149-y

Al-Sarraj, S., King, A., Troakes, C., Smith, B., Maekawa, S., Bodi, I., Rogelj, B., Al-Chalabi, A., Hortobágyi, T., Shaw, C.E., 2011. p62 positive, TDP-43 negative, neuronal cytoplasmic and intranuclear inclusions in the cerebellum and hippocampus define the pathology of C9orf72-linked FTLD and MND/ALS. Acta Neuropathol 122, 691–702. https://doi.org/10.1007/s00401-011-0911-2

Alsultan, A.A., Waller, R., Heath, P.R., Kirby, J., 2016. The genetics of amyotrophic lateral sclerosis: current insights. Degener Neurol Neuromuscul Dis 6, 49–64. https://doi.org/10.2147/DNND.S84956

Amador-Ortiz, C., Lin, W.-L., Ahmed, Z., Personett, D., Davies, P., Duara, R., Graff-Radford, N.R., Hutton, M.L., Dickson, D.W., 2007. TDP-43 immunoreactivity in hippocampal sclerosis and Alzheimer's disease. Annals of Neurology 61, 435–445. https://doi.org/10.1002/ana.21154

Amick, J., Roczniak-Ferguson, A., Ferguson, S.M., 2016. C9orf72 binds SMCR8, localizes to lysosomes, and regulates mTORC1 signaling. Mol Biol Cell 27, 3040–3051. https://doi.org/10.1091/mbc.E16-01-0003

Amick, J., Tharkeshwar, A.K., Amaya, C., Ferguson, S.M., 2018. WDR41 supports lysosomal response to changes in amino acid availability. Mol Biol Cell 29, 2213–2227. https://doi.org/10.1091/mbc.E17-12-0703

Amick, J., Tharkeshwar, A.K., Talaia, G., Ferguson, S.M., 2020. PQLC2 recruits the C9orf72 complex to lysosomes in response to cationic amino acid starvation. J Cell Biol 219, e201906076. https://doi.org/10.1083/jcb.201906076

Amlie-Wolf, A., Ryvkin, P., Tong, R., Dragomir, I., Suh, E., Xu, Y., Deerlin, V.M.V., Gregory, B.D., Kwong, L.K., Trojanowski, J.Q., Lee, V.M.-Y., Wang, L.-S., Lee, E.B., 2015. Transcriptomic Changes Due to Cytoplasmic TDP-43 Expression Reveal Dysregulation of Histone Transcripts and Nuclear Chromatin. PLOS ONE 10, e0141836. https://doi.org/10.1371/journal.pone.0141836

Andrews, J.A., Jackson, C.E., Heiman-Patterson, T.D., Bettica, P., Brooks, B.R., Pioro, E.P., 2020. Real-world evidence of riluzole effectiveness in treating amyotrophic lateral sclerosis. Amyotroph Lateral Scler Frontotemporal Degener 21, 509–518. https://doi.org/10.1080/21678421.2020.1771734

Aoki, Y., Manzano, R., Lee, Y., Dafinca, R., Aoki, M., Douglas, A.G.L., Varela, M.A., Sathyaprakash, C., Scaber, J., Barbagallo, P., Vader, P., Mäger, I., Ezzat, K., Turner, M.R., Ito, N., Gasco, S., Ohbayashi, N., El Andaloussi, S., Takeda, S., Fukuda, M., Talbot, K., Wood, M.J.A., 2017. C9orf72 and RAB7L1 regulate vesicle trafficking in amyotrophic lateral sclerosis and frontotemporal dementia. Brain 140, 887–897. https://doi.org/10.1093/brain/awx024

Arai, T., Hasegawa, M., Akiyama, H., Ikeda, K., Nonaka, T., Mori, H., Mann, D., Tsuchiya, K., Yoshida, M., Hashizume, Y., Oda, T., 2006. TDP-43 is a component of ubiquitin-positive tau-negative inclusions in frontotemporal lobar degeneration and amyotrophic lateral sclerosis. Biochemical and Biophysical Research Communications 351, 602–611. https://doi.org/10.1016/j.bbrc.2006.10.093

Arai, T., Mackenzie, I.R.A., Hasegawa, M., Nonoka, T., Niizato, K., Tsuchiya, K., Iritani, S., Onaya, M., Akiyama, H., 2009. Phosphorylated TDP-43 in Alzheimer's disease and dementia with Lewy bodies. Acta Neuropathol 117, 125–136. https://doi.org/10.1007/s00401-008-0480-1

Arai, T., Nonaka, T., Hasegawa, M., Akiyama, H., Yoshida, M., Hashizume, Y., Tsuchiya, K., Oda, T., Ikeda, K., 2003. Neuronal and glial inclusions in frontotemporal dementia with or without motor neuron disease are immunopositive for p62. Neurosci Lett 342, 41–44. https://doi.org/10.1016/s0304-3940(03)00216-7

Araki, M., Yoshimoto, K., Ohta, M., Katada, T., Kontani, K., 2021. Development of a versatile HPLC-based method to evaluate the activation status of small GTPases. J Biol Chem 297, 101428. https://doi.org/10.1016/j.jbc.2021.101428

Armstrong, R.A., 2017. Neuronal cytoplasmic inclusions in tau, TDP-43, and FUS molecular subtypes of frontotemporal lobar degeneration share similar spatial patterns. Folia Neuropathol 55, 185–192. https://doi.org/10.5114/fn.2017.70482

Arnoux, I., Willam, M., Griesche, N., Krummeich, J., Watari, H., Offermann, N., Weber, S., Narayan Dey, P., Chen, C., Monteiro, O., Buettner, S., Meyer, K., Bano, D., Radyushkin, K., Langston, R., Lambert, J.J., Wanker, E., Methner, A., Krauss, S., Schweiger, S., Stroh,

A., 2018. Metformin reverses early cortical network dysfunction and behavior changes in Huntington's disease. Elife 7, e38744. https://doi.org/10.7554/eLife.38744

Ash, P.E.A., Bieniek, K.F., Gendron, T.F., Caulfield, T., Lin, W.-L., DeJesus-Hernandez, M., van Blitterswijk, M.M., Jansen-West, K., Paul, J.W., Rademakers, R., Boylan, K.B., Dickson, D.W., Petrucelli, L., 2013. Unconventional translation of C9ORF72 GGGGCC expansion generates insoluble polypeptides specific to c9FTD/ALS. Neuron 77, 639–646. https://doi.org/10.1016/j.neuron.2013.02.004

Balchin, D., Hayer-Hartl, M., Hartl, F.U., 2016. In vivo aspects of protein folding and quality control. Science 353, aac4354. https://doi.org/10.1126/science.aac4354

Balla, A., Tuymetova, G., Barshishat, M., Geiszt, M., Balla, T., 2002. Characterization of type II phosphatidylinositol 4-kinase isoforms reveals association of the enzymes with endosomal vesicular compartments. J Biol Chem 277, 20041–20050. https://doi.org/10.1074/jbc.M111807200

Bañez-Coronel, M., Ayhan, F., Tarabochia, A.D., Zu, T., Perez, B.A., Tusi, S.K., Pletnikova, O., Borchelt, D.R., Ross, C.A., Margolis, R.L., Yachnis, A.T., Troncoso, J.C., Ranum, L.P.W., 2015. RAN Translation in Huntington Disease. Neuron 88, 667–677. https://doi.org/10.1016/j.neuron.2015.10.038

Bar-Peled, L., Chantranupong, L., Cherniack, A.D., Chen, W.W., Ottina, K.A., Grabiner, B.C., Spear, E.D., Carter, S.L., Meyerson, M., Sabatini, D.M., 2013. A Tumor suppressor complex with GAP activity for the Rag GTPases that signal amino acid sufficiency to mTORC1. Science 340, 1100–1106. https://doi.org/10.1126/science.1232044

Batool, S., Raza, H., Zaidi, J., Riaz, S., Hasan, S., Syed, N.I., 2019. Synapse formation: from cellular and molecular mechanisms to neurodevelopmental and neurodegenerative disorders. J Neurophysiol 121, 1381–1397. https://doi.org/10.1152/jn.00833.2018

Beck, J., Poulter, M., Hensman, D., Rohrer, J.D., Mahoney, C.J., Adamson, G., Campbell, T., Uphill, J., Borg, A., Fratta, P., Orrell, R.W., Malaspina, A., Rowe, J., Brown, J., Hodges, J., Sidle, K., Polke, J.M., Houlden, H., Schott, J.M., Fox, N.C., Rossor, M.N., Tabrizi, S.J., Isaacs, A.M., Hardy, J., Warren, J.D., Collinge, J., Mead, S., 2013. Large C9orf72 Hexanucleotide Repeat Expansions Are Seen in Multiple Neurodegenerative Syndromes and Are More Frequent Than Expected in the UK Population. The American Journal of Human Genetics 92, 345–353. https://doi.org/10.1016/j.ajhg.2013.01.011

Behrends, C., Sowa, M.E., Gygi, S.P., Harper, J.W., 2010. Network organization of the human autophagy system. Nature 466, 68–76. https://doi.org/10.1038/nature09204

Belzil, V.V., Bauer, P.O., Gendron, T.F., Murray, M.E., Dickson, D., Petrucelli, L., 2014. Characterization of DNA hypermethylation in the cerebellum of c9FTD/ALS patients. Brain Res 1584, 15–21. https://doi.org/10.1016/j.brainres.2014.02.015

Belzil, V.V., Bauer, P.O., Prudencio, M., Gendron, T.F., Stetler, C.T., Yan, I.K., Pregent, L., Daughrity, L., Baker, M.C., Rademakers, R., Boylan, K., Patel, T.C., Dickson, D.W., Petrucelli, L., 2013. Reduced C9orf72 gene expression in c9FTD/ALS is caused by histone trimethylation, an epigenetic event detectable in blood. Acta Neuropathol 126, 895–905. https://doi.org/10.1007/s00401-013-1199-1

Bensimon, G., Lacomblez, L., Meininger, V., 1994. A controlled trial of riluzole in amyotrophic lateral sclerosis. ALS/Riluzole Study Group. N Engl J Med 330, 585–591. https://doi.org/10.1056/NEJM199403033300901

Boeynaems, S., Bogaert, E., Michiels, E., Gijselinck, I., Sieben, A., Jovičić, A., De Baets, G., Scheveneels, W., Steyaert, J., Cuijt, I., Verstrepen, K.J., Callaerts, P., Rousseau, F.,

Schymkowitz, J., Cruts, M., Van Broeckhoven, C., Van Damme, P., Gitler, A.D., Robberecht, W., Van Den Bosch, L., 2016. Drosophila screen connects nuclear transport genes to DPR pathology in c9ALS/FTD. Sci Rep 6, 20877. https://doi.org/10.1038/srep20877

Boivin, M., 2020. Reduced autophagy upon C9ORF72 loss synergizes with dipeptide repeat protein toxicity in G4C2 repeat expansion disorders. The EMBO Journal 39, e100574. https://doi.org/10.15252/embj.2018100574

Boros, B.D., Schoch, K.M., Kreple, C.J., Miller, T.M., 2022. Antisense Oligonucleotides for the Study and Treatment of ALS. Neurotherapeutics 19, 1145–1158. https://doi.org/10.1007/s13311-022-01247-2

Boukhris, A., Stevanin, G., Feki, I., Denis, E., Elleuch, N., Miladi, M.I., Truchetto, J., Denora, P., Belal, S., Mhiri, C., Brice, A., 2008. Hereditary spastic paraplegia with mental impairment and thin corpus callosum in Tunisia: SPG11, SPG15, and further genetic heterogeneity. Arch Neurol 65, 393–402. https://doi.org/10.1001/archneur.65.3.393

Brand, M.D., Orr, A.L., Perevoshchikova, I.V., Quinlan, C.L., 2013. The role of mitochondrial function and cellular bioenergetics in ageing and disease. Br J Dermatol 169, 1–8. https://doi.org/10.1111/bjd.12208

Breuer, A.C., Lynn, M.P., Atkinson, M.B., Chou, S.M., Wilbourn, A.J., Marks, K.E., Culver, J.E., Fleegler, E.J., 1987. Fast axonal transport in amyotrophic lateral sclerosis: An intra-axonal organelle traffic analysis. Neurology 37, 738–738. https://doi.org/10.1212/WNL.37.5.738

Bromberg, R., Cai, K., Guo, Y., Plymire, D., Emde, T., Puzio, M., Borek, D., Otwinowski, Z., 2022. The His-tag as a decoy modulating preferred orientation in cryoEM. Front Mol Biosci 9, 912072. https://doi.org/10.3389/fmolb.2022.912072

Brooks, B.R., 1994. El escorial World Federation of Neurology criteria for the diagnosis of amyotrophic lateral sclerosis. Journal of the Neurological Sciences 124, 96–107. https://doi.org/10.1016/0022-510X(94)90191-0

Brooks, B.R., Miller, R.G., Swash, M., Munsat, T.L., World Federation of Neurology Research Group on Motor Neuron Diseases, 2000. El Escorial revisited: revised criteria for the diagnosis of amyotrophic lateral sclerosis. Amyotroph Lateral Scler Other Motor Neuron Disord 1, 293–299. https://doi.org/10.1080/146608200300079536

Brown, C.A., Lally, C., Kupelian, V., Flanders, W.D., 2021. Estimated Prevalence and Incidence of Amyotrophic Lateral Sclerosis and SOD1 and C9orf72 Genetic Variants. NED 55, 342–353. https://doi.org/10.1159/000516752

Bug, M., Meyer, H., 2012. Expanding into new markets – VCP/p97 in endocytosis and autophagy. Journal of Structural Biology, AAA + Proteins 179, 78–82. https://doi.org/10.1016/j.jsb.2012.03.003

Buratti, E., Baralle, F.E., 2001. Characterization and Functional Implications of the RNA Binding Properties of Nuclear Factor TDP-43, a Novel Splicing Regulator ofCFTR Exon 9 *. Journal of Biological Chemistry 276, 36337–36343. https://doi.org/10.1074/jbc.M104236200

Buratti, E., Brindisi, A., Giombi, M., Tisminetzky, S., Ayala, Y.M., Baralle, F.E., 2005. TDP-43 Binds Heterogeneous Nuclear Ribonucleoprotein A/B through Its C-terminal Tail: AN IMPORTANT REGION FOR THE INHIBITION OF CYSTIC FIBROSIS TRANSMEMBRANE CONDUCTANCE REGULATOR EXON 9 SPLICING*. Journal of Biological Chemistry 280, 37572–37584. https://doi.org/10.1074/jbc.M505557200

Burberry, A., Suzuki, N., Wang, J.-Y., Moccia, R., Mordes, D.A., Stewart, M., Suzuki-Uematsu, S., Ghosh, S., Singh, A., Merkle, F.T., Koszka, K., Li, Q.-Z., Zon, L., Rossi, D.J., Trowbridge, J.J., Notarangelo, L.D., Eggan, K., 2016. Loss-of-function mutations in the C9ORF72 mouse ortholog cause fatal autoimmune disease. Sci Transl Med 8, 347ra93. https://doi.org/10.1126/scitranslmed.aaf6038

Bussi, C., Peralta Ramos, J.M., Arroyo, D.S., Gallea, J.I., Ronchi, P., Kolovou, A., Wang, J.M., Florey, O., Celej, M.S., Schwab, Y., Ktistakis, N.T., Iribarren, P., 2018. Alpha-synuclein fibrils recruit TBK1 and OPTN to lysosomal damage sites and induce autophagy in microglial cells. J Cell Sci 131, jcs226241. https://doi.org/10.1242/jcs.226241

Byrne, S., Walsh, C., Lynch, C., Bede, P., Elamin, M., Kenna, K., McLaughlin, R., Hardiman, O., 2011. Rate of familial amyotrophic lateral sclerosis: a systematic review and meta-analysis. Journal of Neurology, Neurosurgery & Psychiatry 82, 623–627. https://doi.org/10.1136/jnnp.2010.224501

Campbell, L., Potter, A., Ignatius, J., Dubowitz, V., Davies, K., 1997. Genomic variation and gene conversion in spinal muscular atrophy: implications for disease process and clinical phenotype. Am J Hum Genet 61, 40–50. https://doi.org/10.1086/513886

Castillo, K., Nassif, M., Valenzuela, V., Rojas, F., Matus, S., Mercado, G., Court, F.A., van Zundert, B., Hetz, C., 2013. Trehalose delays the progression of amyotrophic lateral sclerosis by enhancing autophagy in motoneurons. Autophagy 9, 1308–1320. https://doi.org/10.4161/auto.25188

Chang, J., Lee, S., Blackstone, C., 2014. Spastic paraplegia proteins spastizin and spatacsin mediate autophagic lysosome reformation. J Clin Invest 124, 5249–5262. https://doi.org/10.1172/JCI77598

Chang, Y., Kong, Q., Shan, X., Tian, G., Ilieva, H., Cleveland, D.W., Rothstein, J.D., Borchelt, D.R., Wong, P.C., Lin, C.G., 2008. Messenger RNA Oxidation Occurs Early in Disease Pathogenesis and Promotes Motor Neuron Degeneration in ALS. PLOS ONE 3, e2849. https://doi.org/10.1371/journal.pone.0002849

Chang, Y.-J., Jeng, U.-S., Chiang, Y.-L., Hwang, I.-S., Chen, Y.-R., 2016. The Glycine-Alanine Dipeptide Repeat from C9orf72 Hexanucleotide Expansions Forms Toxic Amyloids Possessing Cell-to-Cell Transmission Properties. J Biol Chem 291, 4903–4911. https://doi.org/10.1074/jbc.M115.694273

Chen, H.-J., Anagnostou, G., Chai, A., Withers, J., Morris, A., Adhikaree, J., Pennetta, G., de Belleroche, J.S., 2010. Characterization of the Properties of a Novel Mutation in VAPB in Familial Amyotrophic Lateral Sclerosis*. Journal of Biological Chemistry 285, 40266–40281. https://doi.org/10.1074/jbc.M110.161398

Chen, X., Zaro, J., Shen, W.-C., 2013. Fusion Protein Linkers: Property, Design and Functionality. Adv Drug Deliv Rev 65, 1357–1369. https://doi.org/10.1016/j.addr.2012.09.039

Cheng, W., Wang, S., Zhang, Z., Morgens, D.W., Hayes, L.R., Lee, S., Portz, B., Xie, Y., Nguyen, B.V., Haney, M.S., Yan, S., Dong, D., Coyne, A.N., Yang, J., Xian, F., Cleveland, D.W., Qiu, Z., Rothstein, J.D., Shorter, J., Gao, F.-B., Bassik, M.C., Sun, S., 2019. CRISPR-Cas9 Screens Identify the RNA Helicase DDX3X as a Repressor of C9ORF72 (GGGGCC)n Repeat-Associated Non-AUG Translation. Neuron 104, 885-898.e8. https://doi.org/10.1016/j.neuron.2019.09.003

Chitiprolu, M., Jagow, C., Tremblay, V., Bondy-Chorney, E., Paris, G., Savard, A., Palidwor, G., Barry, F.A., Zinman, L., Keith, J., Rogaeva, E., Robertson, J., Lavallée-Adam, M., Woulfe,

J., Couture, J.-F., Côté, J., Gibbings, D., 2018. A complex of C9ORF72 and p62 uses arginine methylation to eliminate stress granules by autophagy. Nat Commun 9, 2794. https://doi.org/10.1038/s41467-018-05273-7

Chowdhury, S., Otomo, C., Leitner, A., Ohashi, K., Aebersold, R., Lander, G.C., Otomo, T., 2018. Insights into autophagosome biogenesis from structural and biochemical analyses of the ATG2A-WIPI4 complex. Proceedings of the National Academy of Sciences 115, E9792–E9801. https://doi.org/10.1073/pnas.1811874115

Cirulli, E.T., Lasseigne, B.N., Petrovski, S., Sapp, P.C., Dion, P.A., Leblond, C.S., Couthouis, J., Lu, Y.-F., Wang, Q., Krueger, B.J., Ren, Z., Keebler, J., Han, Y., Levy, S.E., Boone, B.E., Wimbish, J.R., Waite, L.L., Jones, A.L., Carulli, J.P., Day-Williams, A.G., Staropoli, J.F., Xin, W.W., Chesi, A., Raphael, A.R., McKenna-Yasek, D., Cady, J., Vianney de Jong, J.M.B., Kenna, K.P., Smith, B.N., Topp, S., Miller, J., Gkazi, A., FALS Sequencing Consortium, Al-Chalabi, A., van den Berg, L.H., Veldink, J., Silani, V., Ticozzi, N., Shaw, C.E., Baloh, R.H., Appel, S., Simpson, E., Lagier-Tourenne, C., Pulst, S.M., Gibson, S., Trojanowski, J.Q., Elman, L., McCluskey, L., Grossman, M., Shneider, N.A., Chung, W.K., Ravits, J.M., Glass, J.D., Sims, K.B., Van Deerlin, V.M., Maniatis, T., Hayes, S.D., Ordureau, A., Swarup, S., Landers, J., Baas, F., Allen, A.S., Bedlack, R.S., Harper, J.W., Gitler, A.D., Rouleau, G.A., Brown, R., Harms, M.B., Cooper, G.M., Harris, T., Myers, R.M., Goldstein, D.B., 2015. Exome sequencing in amyotrophic lateral sclerosis identifies risk genes and pathways. Science 347, 1436–1441. https://doi.org/10.1126/science.aaa3650

Ciura, S., Lattante, S., Le Ber, I., Latouche, M., Tostivint, H., Brice, A., Kabashi, E., 2013. Loss of function of C9orf72 causes motor deficits in a zebrafish model of amyotrophic lateral sclerosis. Ann Neurol 74, 180–187. https://doi.org/10.1002/ana.23946

Cleary, J.D., Ranum, L.P.W., 2013. Repeat-associated non-ATG (RAN) translation in neurological disease. Hum Mol Genet 22, R45–R51. https://doi.org/10.1093/hmg/ddt371

Conlon, E.G., Lu, L., Sharma, A., Yamazaki, T., Tang, T., Shneider, N.A., Manley, J.L., 2016. The C9ORF72 GGGGCC expansion forms RNA G-quadruplex inclusions and sequesters hnRNP H to disrupt splicing in ALS brains. eLife 5, e17820. https://doi.org/10.7554/eLife.17820

Cook, C.N., Wu, Y., Odeh, H.M., Gendron, T.F., Jansen-West, K., Del Rosso, G., Yue, M., Jiang, P., Gomes, E., Tong, J., Daughrity, L.M., Avendano, N.M., Castanedes-Casey, M., Shao, W., Oskarsson, B., Tomassy, G.S., McCampbell, A., Rigo, F., Dickson, D.W., Shorter, J., Zhang, Y.-J., Petrucelli, L., 2020. C9orf72 poly(GR) aggregation induces TDP-43 proteinopathy. Sci Transl Med 12, eabb3774. https://doi.org/10.1126/scitranslmed.abb3774

Cooper-Knock, J., Walsh, M.J., Higginbottom, A., Robin Highley, J., Dickman, M.J., Edbauer, D., Ince, P.G., Wharton, S.B., Wilson, S.A., Kirby, J., Hautbergue, G.M., Shaw, P.J., 2014. Sequestration of multiple RNA recognition motif-containing proteins by C9orf72 repeat expansions. Brain 137, 2040–2051. https://doi.org/10.1093/brain/awu120

Costa, J., Swash, M., de Carvalho, M., 2012. Awaji Criteria for the Diagnosis of Amyotrophic Lateral Sclerosis: A Systematic Review. Archives of Neurology 69, 1410–1416. https://doi.org/10.1001/archneurol.2012.254

Coyle-Gilchrist, I.T.S., Dick, K.M., Patterson, K., Vázquez Rodríquez, P., Wehmann, E., Wilcox, A., Lansdall, C.J., Dawson, K.E., Wiggins, J., Mead, S., Brayne, C., Rowe, J.B., 2016.

Prevalence, characteristics, and survival of frontotemporal lobar degeneration syndromes. Neurology 86, 1736–1743. https://doi.org/10.1212/WNL.0000000000002638

Cudkowicz, M.E., Lindborg, S.R., Goyal, N.A., Miller, R.G., Burford, M.J., Berry, J.D., Nicholson, K.A., Mozaffar, T., Katz, J.S., Jenkins, L.J., Baloh, R.H., Lewis, R.A., Staff, N.P., Owegi, M.A., Berry, D.A., Gothelf, Y., Levy, Y.S., Aricha, R., Kern, R.Z., Windebank, A.J., Brown, R.H., 2022. A randomized placebo-controlled phase 3 study of mesenchymal stem cells induced to secrete high levels of neurotrophic factors in amyotrophic lateral sclerosis. Muscle Nerve 65, 291–302. https://doi.org/10.1002/mus.27472

Davidson, Y.S., Flood, L., Robinson, A.C., Nihei, Y., Mori, K., Rollinson, S., Richardson, A., Benson, B.C., Jones, M., Snowden, J.S., Pickering-Brown, S., Haass, C., Lashley, T., Mann, D.M.A., 2017. Heterogeneous ribonuclear protein A3 (hnRNP A3) is present in dipeptide repeat protein containing inclusions in Frontotemporal Lobar Degeneration and Motor Neurone disease associated with expansions in C9orf72 gene. Acta Neuropathol Commun 5, 31. https://doi.org/10.1186/s40478-017-0437-5

De Duve, C., 1963. The lysosome. Sci Am 208, 64–72. https://doi.org/10.1038/scientificamerican0563-64

DeJesus-Hernandez, M., Mackenzie, I.R., Boeve, B.F., Boxer, A.L., Baker, M., Rutherford, N.J., Nicholson, A.M., Finch, N.A., Flynn, H., Adamson, J., Kouri, N., Wojtas, A., Sengdy, P., Hsiung, G.-Y.R., Karydas, A., Seeley, W.W., Josephs, K.A., Coppola, G., Geschwind, D.H., Wszolek, Z.K., Feldman, H., Knopman, D.S., Petersen, R.C., Miller, B.L., Dickson, D.W., Boylan, K.B., Graff-Radford, N.R., Rademakers, R., 2011. Expanded GGGGCC Hexanucleotide Repeat in Noncoding Region of C9ORF72 Causes Chromosome 9p-Linked FTD and ALS. Neuron 72, 245–256. https://doi.org/10.1016/j.neuron.2011.09.011

Del Signore, S.J., Amante, D.J., Kim, J., Stack, E.C., Goodrich, S., Cormier, K., Smith, K., Cudkowicz, M.E., Ferrante, R.J., 2009. Combined riluzole and sodium phenylbutyrate therapy in transgenic amyotrophic lateral sclerosis mice. Amyotroph Lateral Scler 10, 85–94. https://doi.org/10.1080/17482960802226148

Deneault, E., Chaineau, M., Nicouleau, M., Castellanos Montiel, M.J., Franco Flores, A.K., Haghi, G., Chen, C.X.-Q., Abdian, N., Shlaifer, I., Beitel, L.K., Durcan, T.M., 2022. A streamlined CRISPR workflow to introduce mutations and generate isogenic iPSCs for modeling amyotrophic lateral sclerosis. Methods 203, 297–310. https://doi.org/10.1016/j.ymeth.2021.09.002

Deng, H.-X., Chen, W., Hong, S.-T., Boycott, K.M., Gorrie, G.H., Siddique, N., Yang, Y., Fecto, F., Shi, Y., Zhai, H., Jiang, H., Hirano, M., Rampersaud, E., Jansen, G.H., Donkervoort, S., Bigio, E.H., Brooks, B.R., Ajroud, K., Sufit, R.L., Haines, J.L., Mugnaini, E., Pericak-Vance, M.A., Siddique, T., 2011. Mutations in UBQLN2 cause dominant X-linked juvenile and adult-onset ALS and ALS/dementia. Nature 477, 211–215. https://doi.org/10.1038/nature10353

Deng, H.-X., Zhai, H., Bigio, E.H., Yan, J., Fecto, F., Ajroud, K., Mishra, M., Ajroud-Driss, S., Heller, S., Sufit, R., Siddique, N., Mugnaini, E., Siddique, T., 2010. FUS-immunoreactive inclusions are a common feature in sporadic and non-SOD1 familial amyotrophic lateral sclerosis. Ann Neurol 67, 739–748. https://doi.org/10.1002/ana.22051

Deng, H.-X., Zhai, H., Shi, Y., Liu, G., Lowry, J., Liu, B., Ryan, É.B., Yan, J., Yang, Y., Zhang, N., Yang, Z., Liu, E., Ma, Y.C., Siddique, T., 2021. Efficacy and long-term safety of

CRISPR/Cas9 genome editing in the SOD1-linked mouse models of ALS. Commun Biol 4, 396. https://doi.org/10.1038/s42003-021-01942-4

Deng, J., Wang, P., Chen, X., Cheng, H., Liu, J., Fushimi, K., Zhu, L., Wu, J.Y., 2018. FUS interacts with ATP synthase beta subunit and induces mitochondrial unfolded protein response in cellular and animal models. Proc Natl Acad Sci U S A 115, E9678–E9686. https://doi.org/10.1073/pnas.1806655115

Deng, Z., Purtell, K., Lachance, V., Wold, M.S., Chen, S., Yue, Z., 2017. Autophagy Receptors and Neurodegenerative Diseases. Trends in Cell Biology 27, 491–504. https://doi.org/10.1016/j.tcb.2017.01.001

Devon, R.S., Orban, P.C., Gerrow, K., Barbieri, M.A., Schwab, C., Cao, L.P., Helm, J.R., Bissada, N., Cruz-Aguado, R., Davidson, T.-L., Witmer, J., Metzler, M., Lam, C.K., Tetzlaff, W., Simpson, E.M., McCaffery, J.M., El-Husseini, A.E., Leavitt, B.R., Hayden, M.R., 2006. Als2-deficient mice exhibit disturbances in endosome trafficking associated with motor behavioral abnormalities. Proceedings of the National Academy of Sciences 103, 9595–9600. https://doi.org/10.1073/pnas.0510197103

Di Bartolomeo, S., Corazzari, M., Nazio, F., Oliverio, S., Lisi, G., Antonioli, M., Pagliarini, V., Matteoni, S., Fuoco, C., Giunta, L., D'Amelio, M., Nardacci, R., Romagnoli, A., Piacentini, M., Cecconi, F., Fimia, G.M., 2010. The dynamic interaction of AMBRA1 with the dynein motor complex regulates mammalian autophagy. J Cell Biol 191, 155–168. https://doi.org/10.1083/jcb.201002100

Dionísio, P.A., Amaral, J.D., Ribeiro, M.F., Lo, A.C., D'Hooge, R., Rodrigues, C.M.P., 2015. Amyloid-β pathology is attenuated by tauroursodeoxycholic acid treatment in APP/PS1 mice after disease onset. Neurobiol Aging 36, 228–240. https://doi.org/10.1016/j.neurobiolaging.2014.08.034

Dobrowolny, G., Giacinti, C., Pelosi, L., Nicoletti, C., Winn, N., Barberi, L., Molinaro, M., Rosenthal, N., Musarò, A., 2005. Muscle expression of a local Igf-1 isoform protects motor neurons in an ALS mouse model. J Cell Biol 168, 193–199. https://doi.org/10.1083/jcb.200407021

Dodge, J.C., Treleaven, C.M., Fidler, J.A., Hester, M., Haidet, A., Handy, C., Rao, M., Eagle, A., Matthews, J.C., Taksir, T.V., Cheng, S.H., Shihabuddin, L.S., Kaspar, B.K., 2010. AAV4-mediated Expression of IGF-1 and VEGF Within Cellular Components of the Ventricular System Improves Survival Outcome in Familial ALS Mice. Mol Ther 18, 2075–2084. https://doi.org/10.1038/mt.2010.206

Donnelly, C.J., Zhang, P.-W., Pham, J.T., Haeusler, A.R., Mistry, N.A., Vidensky, S., Daley, E.L., Poth, E.M., Hoover, B., Fines, D.M., Maragakis, N., Tienari, P.J., Petrucelli, L., Traynor, B.J., Wang, J., Rigo, F., Bennett, C.F., Blackshaw, S., Sattler, R., Rothstein, J.D., 2013. RNA Toxicity from the ALS/FTD C9ORF72 Expansion Is Mitigated by Antisense Intervention. Neuron 80, 415–428. https://doi.org/10.1016/j.neuron.2013.10.015

Du, W., Su, Q.P., Chen, Y., Zhu, Y., Jiang, D., Rong, Y., Zhang, S., Zhang, Y., Ren, H., Zhang, C., Wang, X., Gao, N., Wang, Y., Sun, L., Sun, Y., Yu, L., 2016. Kinesin 1 Drives Autolysosome Tubulation. Developmental Cell 37, 326–336. https://doi.org/10.1016/j.devcel.2016.04.014

Dugger, B.N., Dickson, D.W., 2017. Pathology of Neurodegenerative Diseases. Cold Spring Harb Perspect Biol 9, a028035. https://doi.org/10.1101/cshperspect.a028035

Edbauer, D., Haass, C., 2016. An amyloid-like cascade hypothesis for C9orf72 ALS/FTD. Curr Opin Neurobiol 36, 99–106. https://doi.org/10.1016/j.conb.2015.10.009

Elden, A.C., Kim, H.-J., Hart, M.P., Chen-Plotkin, A.S., Johnson, B.S., Fang, X., Armakola, M., Geser, F., Greene, R., Lu, M.M., Padmanabhan, A., Clay, D., McCluskey, L., Elman, L., Juhr, D., Gruber, P.J., Rüb, U., Auburger, G., Trojanowski, J.Q., Lee, V.M.-Y., Van Deerlin, V.M., Bonini, N.M., Gitler, A.D., 2010. Ataxin-2 intermediate-length polyglutamine expansions are associated with increased risk for ALS. Nature 466, 1069–1075. https://doi.org/10.1038/nature09320

Elkin, S.R., Lakoduk, A.M., Schmid, S.L., 2016. Endocytic Pathways and Endosomal Trafficking: A Primer. Wien Med Wochenschr 166, 196–204. https://doi.org/10.1007/s10354-016-0432-7

Eramo, M.J., Gurung, R., Mitchell, C.A., McGrath, M.J., 2021. Bidirectional interconversion between PtdIns4P and PtdIns(4,5)P2 is required for autophagic lysosome reformation and protection from skeletal muscle disease. Autophagy 17, 1287–1289. https://doi.org/10.1080/15548627.2021.1916195

Fader, C.M., Sánchez, D.G., Mestre, M.B., Colombo, M.I., 2009. TI-VAMP/VAMP7 and VAMP3/cellubrevin: two v-SNARE proteins involved in specific steps of the autophagy/multivesicular body pathways. Biochim Biophys Acta 1793, 1901–1916. https://doi.org/10.1016/j.bbamcr.2009.09.011

Farg, M.A., Sundaramoorthy, V., Sultana, J.M., Yang, S., Atkinson, R.A.K., Levina, V., Halloran, M.A., Gleeson, P.A., Blair, I.P., Soo, K.Y., King, A.E., Atkin, J.D., 2014. C9ORF72, implicated in amytrophic lateral sclerosis and frontotemporal dementia, regulates endosomal trafficking. Hum Mol Genet 23, 3579–3595. https://doi.org/10.1093/hmg/ddu068

Faylo, J.L., Christianson, D.W., 2021. Visualizing transiently associated catalytic domains in assembly-line biosynthesis using cryo-electron microscopy. Journal of Structural Biology 213, 107802. https://doi.org/10.1016/j.jsb.2021.107802

Fecto, F., Yan, J., Vemula, S.P., Liu, E., Yang, Y., Chen, W., Zheng, J.G., Shi, Y., Siddique, N., Arrat, H., Donkervoort, S., Ajroud-Driss, S., Sufit, R.L., Heller, S.L., Deng, H.-X., Siddique, T., 2011. SQSTM1 mutations in familial and sporadic amyotrophic lateral sclerosis. Arch Neurol 68, 1440–1446. https://doi.org/10.1001/archneurol.2011.250

Fil, D., DeLoach, A., Yadav, S., Alkam, D., MacNicol, M., Singh, A., Compadre, C.M., Goellner, J.J., O'Brien, C.A., Fahmi, T., Basnakian, A.G., Calingasan, N.Y., Klessner, J.L., Beal, F.M., Peters, O.M., Metterville, J., Brown, R.H., Jr, Ling, K.K.Y., Rigo, F., Ozdinler, P.H., Kiaei, M., 2017. Mutant Profilin1 transgenic mice recapitulate cardinal features of motor neuron disease. Human Molecular Genetics 26, ddw429. https://doi.org/10.1093/hmg/ddw429

Fischer, L.R., Li, Y., Asress, S.A., Jones, D.P., Glass, J.D., 2012. Absence of SOD1 leads to oxidative stress in peripheral nerve and causes a progressive distal motor axonopathy. Experimental Neurology, Special Issue: Stress and neurological disease 233, 163–171. https://doi.org/10.1016/j.expneurol.2011.09.020

Flood, D.G., Reaume, A.G., Gruner, J.A., Hoffman, E.K., Hirsch, J.D., Lin, Y.-G., Dorfman, K.S., Scott, R.W., 1999. Hindlimb Motor Neurons Require Cu/Zn Superoxide Dismutase for Maintenance of Neuromuscular Junctions. The American Journal of Pathology 155, 663–672. https://doi.org/10.1016/S0002-9440(10)65162-0

Fomin, V., Richard, P., Hoque, M., Li, C., Gu, Z., Fissore-O'Leary, M., Tian, B., Prives, C., Manley, J.L., 2018. The C9ORF72 Gene, Implicated in Amyotrophic Lateral Sclerosis and Frontotemporal Dementia, Encodes a Protein That Functions in Control of Endothelin

and Glutamate Signaling. Mol Cell Biol 38, e00155-18. https://doi.org/10.1128/MCB.00155-18

Forsberg, K., Jonsson, P.A., Andersen, P.M., Bergemalm, D., Graffmo, K.S., Hultdin, M., Jacobsson, J., Rosquist, R., Marklund, S.L., Brännström, T., 2010. Novel antibodies reveal inclusions containing non-native SOD1 in sporadic ALS patients. PLoS One 5, e11552. https://doi.org/10.1371/journal.pone.0011552

Fournier, C., Barbier, M., Camuzat, A., Anquetil, V., Lattante, S., Clot, F., Cazeneuve, C., Rinaldi, D., Couratier, P., Deramecourt, V., Sabatelli, M., Belliard, S., Vercelletto, M., Forlani, S., Jornea, L., Brice, A., Auriacombe, S., Belliard, S., Blanc, F., Bouteleau-Bretonnière, C., Ceccaldi, M., Couratier, P., Didic, M., Dubois, B., Duyckaerts, C., Etcharry-Bouix, F., Golfier, V., Hannequin, D., Lacomblez, L., Le Ber, I., Levy, R., Michel, B.-F., Pasquier, F., Thomas-Anterion, C., Pariente, J., Sellal, F., Vercelletto, M., Benchetrit, E., Bertin, H., Bertrand, A., Bissery, A., Bombois, S., Boncoeur, M.-P., Cassagnaud, P., Chastan, M., Chen, Y., Chupin, M., Colliot, O., Couratier, P., Delbeucq, X., Deramecourt, V., Delmaire, C., Gerardin, E., Hossein-Foucher, C., Dubois, B., Habert, M.-O., Hannequin, D., Lautrette, G., Lebouvier, T., Le Ber, I., Lehéricy, S., Le Toullec, B., Levy, R., Martineau, K., Mackowiak, M.-A., Monteil, J., Pasquier, F., Petyt, G., Pradat, P.-F., Oya, A.-H., Rinaldi, D., Rollin-Sillaire, A., Salachas, F., Sayah, S., Wallon, D., Leguern, E., Brice, A., Le Ber, I., 2019. Relations between C9orf72 expansion size in blood, age at onset, age at collection and transmission across generations in patients and presymptomatic carriers. Neurobiology of Aging 74, 234.e1-234.e8. https://doi.org/10.1016/j.neurobiolaging.2018.09.010

Fratta, P., Poulter, M., Lashley, T., Rohrer, J.D., Polke, J.M., Beck, J., Ryan, N., Hensman, D., Mizielinska, S., Waite, A.J., Lai, M.-C., Gendron, T.F., Petrucelli, L., Fisher, E.M.C., Revesz, T., Warren, J.D., Collinge, J., Isaacs, A.M., Mead, S., 2013. Homozygosity for the C9orf72 GGGGCC repeat expansion in frontotemporal dementia. Acta Neuropathol 126, 401–409. https://doi.org/10.1007/s00401-013-1147-0

Freibaum, B.D., Lu, Y., Lopez-Gonzalez, R., Kim, N.C., Almeida, S., Lee, K.-H., Badders, N., Valentine, M., Miller, B.L., Wong, P.C., Petrucelli, L., Kim, H.J., Gao, F.-B., Taylor, J.P., 2015. GGGGCC repeat expansion in C9orf72 compromises nucleocytoplasmic transport. Nature 525, 129–133. https://doi.org/10.1038/nature14974

Freischmidt, A., Wieland, T., Richter, B., Ruf, W., Schaeffer, V., Müller, K., Marroquin, N., Nordin, F., Hübers, A., Weydt, P., Pinto, S., Press, R., Millecamps, S., Molko, N., Bernard, E., Desnuelle, C., Soriani, M.-H., Dorst, J., Graf, E., Nordström, U., Feiler, M.S., Putz, S., Boeckers, T.M., Meyer, T., Winkler, A.S., Winkelman, J., de Carvalho, M., Thal, D.R., Otto, M., Brännström, T., Volk, A.E., Kursula, P., Danzer, K.M., Lichtner, P., Dikic, I., Meitinger, T., Ludolph, A.C., Strom, T.M., Andersen, P.M., Weishaupt, J.H., 2015. Haploinsufficiency of TBK1 causes familial ALS and fronto-temporal dementia. Nat Neurosci 18, 631–636. https://doi.org/10.1038/nn.4000

Frick, P., Sellier, C., Mackenzie, I.R.A., Cheng, C.-Y., Tahraoui-Bories, J., Martinat, C., Pasterkamp, R.J., Prudlo, J., Edbauer, D., Oulad-Abdelghani, M., Feederle, R., Charlet-Berguerand, N., Neumann, M., 2018. Novel antibodies reveal presynaptic localization of C9orf72 protein and reduced protein levels in C9orf72 mutation carriers. Acta Neuropathol Commun 6, 72. https://doi.org/10.1186/s40478-018-0579-0

Fumagalli, E., Funicello, M., Rauen, T., Gobbi, M., Mennini, T., 2008. Riluzole enhances the activity of glutamate transporters GLAST, GLT1 and EAAC1. Eur J Pharmacol 578, 171–176. https://doi.org/10.1016/j.ejphar.2007.10.023

Fumagalli, L., Young, F.L., Boeynaems, S., De Decker, M., Mehta, A.R., Swijsen, A., Fazal, R., Guo, W., Moisse, M., Beckers, J., Dedeene, L., Selvaraj, B.T., Vandoorne, T., Madan, V., van Blitterswijk, M., Raitcheva, D., McCampbell, A., Poesen, K., Gitler, A.D., Koch, P., Berghe, P.V., Thal, D.R., Verfaillie, C., Chandran, S., Van Den Bosch, L., Bullock, S.L., Van Damme, P., 2021. C9orf72-derived arginine-containing dipeptide repeats associate with axonal transport machinery and impede microtubule-based motility. Science Advances 7, eabg3013. https://doi.org/10.1126/sciadv.abg3013

Ganley, I.G., Lam, D.H., Wang, J., Ding, X., Chen, S., Jiang, X., 2009. ULK1·ATG13·FIP200 Complex Mediates mTOR Signaling and Is Essential for Autophagy. J Biol Chem 284, 12297–12305. https://doi.org/10.1074/jbc.M900573200

Gantois, I., Khoutorsky, A., Popic, J., Aguilar-Valles, A., Freemantle, E., Cao, R., Sharma, V., Pooters, T., Nagpal, A., Skalecka, A., Truong, V.T., Wiebe, S., Groves, I.A., Jafarnejad, S.M., Chapat, C., McCullagh, E.A., Gamache, K., Nader, K., Lacaille, J.-C., Gkogkas, C.G., Sonenberg, N., 2017. Metformin ameliorates core deficits in a mouse model of fragile X syndrome. Nat Med 23, 674–677. https://doi.org/10.1038/nm.4335

García-Murias, M., Quintáns, B., Arias, M., Seixas, A.I., Cacheiro, P., Tarrío, R., Pardo, J., Millán, M.J., Arias-Rivas, S., Blanco-Arias, P., Dapena, D., Moreira, R., Rodríguez-Trelles, F., Sequeiros, J., Carracedo, Á., Silveira, I., Sobrido, M.J., 2012. 'Costa da Morte' ataxia is spinocerebellar ataxia 36: clinical and genetic characterization. Brain 135, 1423–1435. https://doi.org/10.1093/brain/aws069

Gendron, T.F., Bieniek, K.F., Zhang, Y.-J., Jansen-West, K., Ash, P.E.A., Caulfield, T., Daughrity, L., Dunmore, J.H., Castanedes-Casey, M., Chew, J., Cosio, D.M., van Blitterswijk, M., Lee, W.C., Rademakers, R., Boylan, K.B., Dickson, D.W., Petrucelli, L., 2013. Antisense transcripts of the expanded C9ORF72 hexanucleotide repeat form nuclear RNA foci and undergo repeat-associated non-ATG translation in c9FTD/ALS. Acta Neuropathol 126, 829–844. https://doi.org/10.1007/s00401-013-1192-8

Gendron, T.F., Chew, J., Stankowski, J.N., Hayes, L.R., Zhang, Y.-J., Prudencio, M., Carlomagno, Y., Daughrity, L.M., Jansen-West, K., Perkerson, E.A., O'Raw, A., Cook, C., Pregent, L., Belzil, V., van Blitterswijk, M., Tabassian, L.J., Lee, C.W., Yue, M., Tong, J., Song, Y., Castanedes-Casey, M., Rousseau, L., Phillips, V., Dickson, D.W., Rademakers, R., Fryer, J.D., Rush, B.K., Pedraza, O., Caputo, A.M., Desaro, P., Palmucci, C., Robertson, A., Heckman, M.G., Diehl, N.N., Wiggs, E., Tierney, M., Braun, L., Farren, J., Lacomis, D., Ladha, S., Fournier, C.N., McCluskey, L.F., Elman, L.B., Toledo, J.B., McBride, J.D., Tiloca, C., Morelli, C., Poletti, B., Solca, F., Prelle, A., Wuu, J., Jockel-Balsarotti, J., Rigo, F., Ambrose, C., Datta, A., Yang, W., Raitcheva, D., Antognetti, G., McCampbell, A., Van Swieten, J.C., Miller, B.L., Boxer, A.L., Brown, R.H., Bowser, R., Miller, T.M., Trojanowski, J.Q., Grossman, M., Berry, J.D., Hu, W.T., Ratti, A., Traynor, B.J., Disney, M.D., Benatar, M., Silani, V., Glass, J.D., Floeter, M.K., Rothstein, J.D., Boylan, K.B., Petrucelli, L., 2017. Poly(GP) proteins are a useful pharmacodynamic marker for C9ORF72-associated amyotrophic lateral sclerosis. Sci Transl Med 9, eaai7866. https://doi.org/10.1126/scitranslmed.aai7866

Gendron, T.F., Petrucelli, L., 2018. Disease Mechanisms of C9ORF72 Repeat Expansions. Cold Spring Harb Perspect Med 8, a024224. https://doi.org/10.1101/cshperspect.a024224

Genin, E.C., Plutino, M., Bannwarth, S., Villa, E., Cisneros-Barroso, E., Roy, M., Ortega-Vila, B., Fragaki, K., Lespinasse, F., Pinero-Martos, E., Augé, G., Moore, D., Burté, F., Lacas-Gervais, S., Kageyama, Y., Itoh, K., Yu-Wai-Man, P., Sesaki, H., Ricci, J.-E., Vives-Bauza, C., Paquis-Flucklinger, V., 2016. CHCHD10 mutations promote loss of mitochondrial cristae junctions with impaired mitochondrial genome maintenance and inhibition of apoptosis. EMBO Molecular Medicine 8, 58–72. https://doi.org/10.15252/emmm.201505496

Gijselinck, I., Van Mossevelde, S., van der Zee, J., Sieben, A., Engelborghs, S., De Bleecker, J., Ivanoiu, A., Deryck, O., Edbauer, D., Zhang, M., Heeman, B., Bäumer, V., Van den Broeck, M., Mattheijssens, M., Peeters, K., Rogaeva, E., De Jonghe, P., Cras, P., Martin, J.-J., de Deyn, P.P., Cruts, M., Van Broeckhoven, C., 2016. The C9orf72 repeat size correlates with onset age of disease, DNA methylation and transcriptional downregulation of the promoter. Mol Psychiatry 21, 1112–1124. https://doi.org/10.1038/mp.2015.159

Glick, D., Barth, S., Macleod, K.F., 2010. Autophagy: cellular and molecular mechanisms. J Pathol 221, 3–12. https://doi.org/10.1002/path.2697

Gold, J., Rowe, D.B., Kiernan, M.C., Vucic, S., Mathers, S., van Eijk, R.P.A., Nath, A., Garcia Montojo, M., Norato, G., Santamaria, U.A., Rogers, M.-L., Malaspina, A., Lombardi, V., Mehta, P.R., Westeneng, H.-J., van den Berg, L.H., Al-Chalabi, A., 2019. Safety and tolerability of Triumeq in amyotrophic lateral sclerosis: the Lighthouse trial. Amyotroph Lateral Scler Frontotemporal Degener 20, 595–604. https://doi.org/10.1080/21678421.2019.1632899

Gomez-Deza, J., Lee, Y., Troakes, C., Nolan, M., Al-Sarraj, S., Gallo, J.-M., Shaw, C.E., 2015. Dipeptide repeat protein inclusions are rare in the spinal cord and almost absent from motor neurons in C9ORF72 mutant amyotrophic lateral sclerosis and are unlikely to cause their degeneration. Acta Neuropathol Commun 3, 38. https://doi.org/10.1186/s40478-015-0218-y

Goody, P.R., 2016. Intrinsic protein fluorescence assays for GEF, GAP and post-translational modifications of small GTPases. Analytical Biochemistry 515, 22–25. https://doi.org/10.1016/j.ab.2016.09.019

Grant, T., Rohou, A., Grigorieff, N., 2018. cisTEM, user-friendly software for single-particle image processing. Elife 7, e35383. https://doi.org/10.7554/eLife.35383

Greco, C.M., Hagerman, R.J., Tassone, F., Chudley, A.E., Del Bigio, M.R., Jacquemont, S., Leehey, M., Hagerman, P.J., 2002. Neuronal intranuclear inclusions in a new cerebellar tremor/ataxia syndrome among fragile X carriers. Brain 125, 1760–1771. https://doi.org/10.1093/brain/awf184

Groenewoud, M.J., Zwartkruis, F.J.T., 2013. Rheb and Rags come together at the lysosome to activate mTORC1. Biochem Soc Trans 41, 951–955. https://doi.org/10.1042/BST20130037

Guo, C., Sun, L., Chen, X., Zhang, D., 2013. Oxidative stress, mitochondrial damage and neurodegenerative diseases. Neural Regen Res 8, 2003–2014. https://doi.org/10.3969/j.issn.1673-5374.2013.21.009

Guo, Q., Lehmer, C., Martínez-Sánchez, A., Rudack, T., Beck, F., Hartmann, H., Pérez-Berlanga, M., Frottin, F., Hipp, M.S., Hartl, F.U., Edbauer, D., Baumeister, W., Fernández-Busnadiego, R., 2018. In Situ Structure of Neuronal C9orf72 Poly-GA Aggregates

Reveals Proteasome Recruitment. Cell 172, 696-705.e12. https://doi.org/10.1016/j.cell.2017.12.030

Gutierrez, M.G., Munafó, D.B., Berón, W., Colombo, M.I., 2004. Rab7 is required for the normal progression of the autophagic pathway in mammalian cells. J Cell Sci 117, 2687–2697. https://doi.org/10.1242/jcs.01114

Haeusler, A.R., Donnelly, C.J., Periz, G., Simko, E.A.J., Shaw, P.G., Kim, M.-S., Maragakis, N.J., Troncoso, J.C., Pandey, A., Sattler, R., Rothstein, J.D., Wang, J., 2014. C9orf72 Nucleotide Repeat Structures Initiate Molecular Cascades of Disease. Nature 507, 195–200. https://doi.org/10.1038/nature13124

Haidet-Phillips, A.M., Hester, M.E., Miranda, C.J., Meyer, K., Braun, L., Frakes, A., Song, S., Likhite, S., Murtha, M.J., Foust, K.D., Rao, M., Eagle, A., Kammesheidt, A., Christensen, A., Mendell, J.R., Burghes, A.H.M., Kaspar, B.K., 2011. Astrocytes from Familial and Sporadic ALS Patients are Toxic to Motor Neurons. Nat Biotechnol 29, 824–828. https://doi.org/10.1038/nbt.1957

Hamasaki, M., Furuta, N., Matsuda, A., Nezu, A., Yamamoto, A., Fujita, N., Oomori, H., Noda, T., Haraguchi, T., Hiraoka, Y., Amano, A., Yoshimori, T., 2013. Autophagosomes form at ER-mitochondria contact sites. Nature 495, 389–393. https://doi.org/10.1038/nature11910

Hara, T., Takamura, A., Kishi, C., Iemura, S., Natsume, T., Guan, J.-L., Mizushima, N., 2008. FIP200, a ULK-interacting protein, is required for autophagosome formation in mammalian cells. J Cell Biol 181, 497–510. https://doi.org/10.1083/jcb.200712064

He, Y., Benz, A., Fu, T., Wang, M., Covey, D.F., Zorumski, C.F., Mennerick, S., 2002. Neuroprotective agent riluzole potentiates postsynaptic GABA(A) receptor function. Neuropharmacology 42, 199–209. https://doi.org/10.1016/s0028-3908(01)00175-7

Heng, T.S.P., Painter, M.W., Elpek, K., Lukacs-Kornek, V., Mauermann, N., Turley, S.J., Koller, D., Kim, F.S., Wagers, A.J., Asinovski, N., Davis, S., Fassett, M., Feuerer, M., Gray, D.H.D., Haxhinasto, S., Hill, J.A., Hyatt, G., Laplace, C., Leatherbee, K., Mathis, D., Benoist, C., Jianu, R., Laidlaw, D.H., Best, J.A., Knell, J., Goldrath, A.W., Jarjoura, J., Sun, J.C., Zhu, Y., Lanier, L.L., Ergun, A., Li, Z., Collins, J.J., Shinton, S.A., Hardy, R.R., Friedline, R., Sylvia, K., Kang, J., 2008. The Immunological Genome Project: networks of gene expression in immune cells. Nat Immunol 9, 1091–1094. https://doi.org/10.1038/ni1008-1091

Hershko, A., Ciechanover, A., 1998. The Ubiquitin System. Annual Review of Biochemistry 67, 425–479. https://doi.org/10.1146/annurev.biochem.67.1.425

Higgins, C.M.J., Jung, C., Xu, Z., 2003. ALS-associated mutant SOD1G93A causes mitochondrial vacuolation by expansion of the intermembrane space and by involvement of SOD1 aggregation and peroxisomes. BMC Neurosci 4, 16. https://doi.org/10.1186/1471-2202-4-16

Hiji, M., Takahashi, T., Fukuba, H., Yamashita, H., Kohriyama, T., Matsumoto, M., 2008. White matter lesions in the brain with frontotemporal lobar degeneration with motor neuron disease: TDP-43-immunopositive inclusions co-localize with p62, but not ubiquitin. Acta Neuropathol 116, 183–191. https://doi.org/10.1007/s00401-008-0402-2

Hirst, J., Borner, G.H.H., Edgar, J., Hein, M.Y., Mann, M., Buchholz, F., Antrobus, R., Robinson, M.S., 2013. Interaction between AP-5 and the hereditary spastic paraplegia proteins SPG11 and SPG15. Mol Biol Cell 24, 2558–2569. https://doi.org/10.1091/mbc.E13-03-0170

Hirst, J., Hesketh, G.G., Gingras, A.-C., Robinson, M.S., 2021. Rag GTPases and phosphatidylinositol 3-phosphate mediate recruitment of the AP-5/SPG11/SPG15 complex. J Cell Biol 220, e202002075. https://doi.org/10.1083/jcb.202002075

Hoffman, N.J., Parker, B.L., Chaudhuri, R., Fisher-Wellman, K.H., Kleinert, M., Humphrey, S.J., Yang, P., Holliday, M., Trefely, S., Fazakerley, D.J., Stöckli, J., Burchfield, J.G., Jensen, T.E., Jothi, R., Kiens, B., Wojtaszewski, J.F.P., Richter, E.A., James, D.E., 2015. Global Phosphoproteomic Analysis of Human Skeletal Muscle Reveals a Network of Exercise-Regulated Kinases and AMPK Substrates. Cell Metab 22, 922–935. https://doi.org/10.1016/j.cmet.2015.09.001

Hofmann, A.F., 1999. The continuing importance of bile acids in liver and intestinal disease. Arch Intern Med 159, 2647–2658. https://doi.org/10.1001/archinte.159.22.2647

Hofmann, I., Thompson, A., Sanderson, C.M., Munro, S., 2007. The Arl4 Family of Small G Proteins Can Recruit the Cytohesin Arf6 Exchange Factors to the Plasma Membrane. Current Biology 17, 711–716. https://doi.org/10.1016/j.cub.2007.03.007

Höning, S., Ricotta, D., Krauss, M., Späte, K., Spolaore, B., Motley, A., Robinson, M., Robinson, C., Haucke, V., Owen, D.J., 2005. Phosphatidylinositol-(4,5)-bisphosphate regulates sorting signal recognition by the clathrin-associated adaptor complex AP2. Mol Cell 18, 519–531. https://doi.org/10.1016/j.molcel.2005.04.019

Hosokawa, N., Hara, T., Kaizuka, T., Kishi, C., Takamura, A., Miura, Y., Iemura, S., Natsume, T., Takehana, K., Yamada, N., Guan, J.-L., Oshiro, N., Mizushima, N., 2009. Nutrient-dependent mTORC1 Association with the ULK1–Atg13–FIP200 Complex Required for Autophagy. Mol Biol Cell 20, 1981–1991. https://doi.org/10.1091/mbc.E08-12-1248

Hsu, P.P., Kang, S.A., Rameseder, J., Zhang, Y., Ottina, K.A., Lim, D., Peterson, T.R., Choi, Y., Gray, N.S., Yaffe, M.B., Marto, J.A., Sabatini, D.M., 2011. The mTOR-regulated phosphoproteome reveals a mechanism of mTORC1-mediated inhibition of growth factor signaling. Science 332, 1317–1322. https://doi.org/10.1126/science.1199498

Ikeda, K., Iwasaki, Y., Kaji, R., 2015. Neuroprotective effect of ultra-high dose methylcobalamin in wobbler mouse model of amyotrophic lateral sclerosis. J Neurol Sci 354, 70–74. https://doi.org/10.1016/j.jns.2015.04.052

Ikeda, Y., Ohta, Y., Kobayashi, H., Okamoto, M., Takamatsu, K., Ota, T., Manabe, Y., Okamoto, K., Koizumi, A., Abe, K., 2012. Clinical features of SCA36: a novel spinocerebellar ataxia with motor neuron involvement (Asidan). Neurology 79, 333–341. https://doi.org/10.1212/WNL.0b013e318260436f

Ingre, C., Roos, P.M., Piehl, F., Kamel, F., Fang, F., 2015. Risk factors for amyotrophic lateral sclerosis. Clin Epidemiol 7, 181–193. https://doi.org/10.2147/CLEP.S37505

Ishiguro, T., Sato, N., Ueyama, M., Fujikake, N., Sellier, C., Kanegami, A., Tokuda, E., Zamiri, B., Gall-Duncan, T., Mirceta, M., Furukawa, Y., Yokota, T., Wada, K., Taylor, J.P., Pearson, C.E., Charlet-Berguerand, N., Mizusawa, H., Nagai, Y., Ishikawa, K., 2017. Regulatory Role of RNA Chaperone TDP-43 for RNA Misfolding and Repeat-Associated Translation in SCA31. Neuron 94, 108-124.e7. https://doi.org/10.1016/j.neuron.2017.02.046

Itakura, E., Kishi, C., Inoue, K., Mizushima, N., 2008. Beclin 1 Forms Two Distinct Phosphatidylinositol 3-Kinase Complexes with Mammalian Atg14 and UVRAG. Mol Biol Cell 19, 5360–5372. https://doi.org/10.1091/mbc.E08-01-0080

Ito, Hidefumi, Wate, R., Zhang, J., Ohnishi, S., Kaneko, S., Ito, Hisashi, Nakano, S., Kusaka, H., 2008. Treatment with edaravone, initiated at symptom onset, slows motor decline and

decreases SOD1 deposition in ALS mice. Experimental Neurology 213, 448–455. https://doi.org/10.1016/j.expneurol.2008.07.017

Jahn, R., Scheller, R.H., 2006. SNAREs--engines for membrane fusion. Nat Rev Mol Cell Biol 7, 631–643. https://doi.org/10.1038/nrm2002

Ji, Y.J., Ugolino, J., Zhang, T., Lu, J., Kim, D., Wang, J., 2020. C9orf72/ALFA-1 controls TFEB/HLH-30-dependent metabolism through dynamic regulation of Rag GTPases. PLOS Genetics 16, e1008738. https://doi.org/10.1371/journal.pgen.1008738

Jiang, J., Zhu, Q., Gendron, T.F., Saberi, S., McAlonis-Downes, M., Seelman, A., Stauffer, J.E., Jafar-nejad, P., Drenner, K., Schulte, D., Chun, S., Sun, S., Ling, S.-C., Myers, B., Engelhardt, J., Katz, M., Baughn, M., Platoshyn, O., Marsala, M., Watt, A., Heyser, C.J., Ard, M.C., De Muynck, L., Daughrity, L.M., Swing, D.A., Tessarollo, L., Jung, C.J., Delpoux, A., Utzschneider, D.T., Hedrick, S.M., de Jong, P.J., Edbauer, D., Van Damme, P., Petrucelli, L., Shaw, C.E., Bennett, C.F., Da Cruz, S., Ravits, J., Rigo, F., Cleveland, D.W., Lagier-Tourenne, C., 2016. Gain of Toxicity from ALS/FTD-Linked Repeat Expansions in C9ORF72 Is Alleviated by Antisense Oligonucleotides Targeting GGGGCC-Containing RNAs. Neuron 90, 535–550. https://doi.org/10.1016/j.neuron.2016.04.006

Jiang, P., Nishimura, T., Sakamaki, Y., Itakura, E., Hatta, T., Natsume, T., Mizushima, N., 2014. The HOPS complex mediates autophagosome–lysosome fusion through interaction with syntaxin 17. Mol Biol Cell 25, 1327–1337. https://doi.org/10.1091/mbc.E13-08-0447

Jin, M., Liu, X., Klionsky, D.J., 2013. SnapShot: Selective Autophagy. Cell 152, 368-368.e2. https://doi.org/10.1016/j.cell.2013.01.004

Johnson, J.O., Mandrioli, J., Benatar, M., Abramzon, Y., Van Deerlin, V.M., Trojanowski, J.Q., Gibbs, J.R., Brunetti, M., Gronka, S., Wuu, J., Ding, J., McCluskey, L., Martinez-Lage, M., Falcone, D., Hernandez, D.G., Arepalli, S., Chong, S., Schymick, J.C., Rothstein, J., Landi, F., Wang, Y.-D., Calvo, A., Mora, G., Sabatelli, M., Monsurrò, M.R., Battistini, S., Salvi, F., Spataro, R., Sola, P., Borghero, G., Galassi, G., Scholz, S.W., Taylor, J.P., Restagno, G., Chiò, A., Traynor, B.J., 2010. Exome Sequencing Reveals VCP Mutations as a Cause of Familial ALS. Neuron 68, 857–864. https://doi.org/10.1016/j.neuron.2010.11.036

Johnson, J.O., Pioro, E.P., Boehringer, A., Chia, R., Feit, H., Renton, A.E., Pliner, H.A., Abramzon, Y., Marangi, G., Winborn, B.J., Gibbs, J.R., Nalls, M.A., Morgan, S., Shoai, M., Hardy, J., Pittman, A., Orrell, R.W., Malaspina, A., Sidle, K.C., Fratta, P., Harms, M.B., Baloh, R.H., Pestronk, A., Weihl, C.C., Rogaeva, E., Zinman, L., Drory, V.E., Borghero, G., Mora, G., Calvo, A., Rothstein, J.D., Drepper, C., Sendtner, M., Singleton, A.B., Taylor, J.P., Cookson, M.R., Restagno, G., Sabatelli, M., Bowser, R., Chiò, A., Traynor, B.J., 2014. Mutations in the Matrin 3 gene cause familial amyotrophic lateral sclerosis. Nat Neurosci 17, 664–666. https://doi.org/10.1038/nn.3688

Jung, C.H., Jun, C.B., Ro, S.-H., Kim, Y.-M., Otto, N.M., Cao, J., Kundu, M., Kim, D.-H., 2009. ULK-Atg13-FIP200 Complexes Mediate mTOR Signaling to the Autophagy Machinery. Mol Biol Cell 20, 1992–2003. https://doi.org/10.1091/mbc.E08-12-1249

Kabashi, E., Valdmanis, P.N., Dion, P., Spiegelman, D., McConkey, B.J., Velde, C.V., Bouchard, J.-P., Lacomblez, L., Pochigaeva, K., Salachas, F., Pradat, P.-F., Camu, W., Meininger, V., Dupre, N., Rouleau, G.A., 2008. TARDBP mutations in individuals with sporadic and familial amyotrophic lateral sclerosis. Nat Genet 40, 572–574. https://doi.org/10.1038/ng.132

Kalluri, R., LeBleu, V.S., 2020. The biology, function, and biomedical applications of exosomes. Science 367, eaau6977. https://doi.org/10.1126/science.aau6977

Kapeli, K., Pratt, G.A., Vu, A.Q., Hutt, K.R., Martinez, F.J., Sundararaman, B., Batra, R., Freese, P., Lambert, N.J., Huelga, S.C., Chun, S.J., Liang, T.Y., Chang, J., Donohue, J.P., Shiue, L., Zhang, J., Zhu, H., Cambi, F., Kasarskis, E., Hoon, S., Ares Jr., M., Burge, C.B., Ravits, J., Rigo, F., Yeo, G.W., 2016. Distinct and shared functions of ALS-associated proteins TDP-43, FUS and TAF15 revealed by multisystem analyses. Nat Commun 7, 12143. https://doi.org/10.1038/ncomms12143

Kassubek, J., Pagani, M., 2019. Imaging in amyotrophic lateral sclerosis: MRI and PET. Current Opinion in Neurology 32, 740–746. https://doi.org/10.1097/WCO.0000000000000728

Kato, S., Horiuchi, S., Nakashima, K., Hirano, A., Shibata, N., Nakano, I., Saito, M., Kato, M., Asayama, K., Ohama, E., 1999. Astrocytic hyaline inclusions contain advanced glycation endproducts in familial amyotrophic lateral sclerosis with superoxide dismutase 1 gene mutation: immunohistochemical and immunoelectron microscopical analyses. Acta Neuropathol 97, 260–266. https://doi.org/10.1007/s004010050983

Katsuragi, Y., Ichimura, Y., Komatsu, M., 2015. p62/SQSTM1 functions as a signaling hub and an autophagy adaptor. The FEBS Journal 282, 4672–4678. https://doi.org/10.1111/febs.13540

Kaushik, S., Cuervo, A.M., 2012. Chaperone-mediated autophagy: a unique way to enter the lysosome world. Trends Cell Biol 22, 407–417. https://doi.org/10.1016/j.tcb.2012.05.006

Khundadze, M., Ribaudo, F., Hussain, A., Stahlberg, H., Brocke-Ahmadinejad, N., Franzka, P., Varga, R.-E., Zarkovic, M., Pungsrinont, T., Kokal, M., Ganley, I.G., Beetz, C., Sylvester, M., Hübner, C.A., 2021. Mouse models for hereditary spastic paraplegia uncover a role of PI4K2A in autophagic lysosome reformation. Autophagy 17, 3690–3706. https://doi.org/10.1080/15548627.2021.1891848

Kikuchi, S., Shinpo, K., Ogata, A., Tsuji, S., Takeuchi, M., Makita, Z., Tashiro, K., 2002. Detection of N epsilon-(carboxymethyl)lysine (CML) and non-CML advanced glycation end-products in the anterior horn of amyotrophic lateral sclerosis spinal cord. Amyotroph Lateral Scler Other Motor Neuron Disord 3, 63–68. https://doi.org/10.1080/146608202760196020

Kim, E., Goraksha-Hicks, P., Li, L., Neufeld, T.P., Guan, K.-L., 2008. Regulation of TORC1 by Rag GTPases in nutrient response. Nat Cell Biol 10, 935–945. https://doi.org/10.1038/ncb1753

Kim, J., Dalton, V.M., Eggerton, K.P., Scott, S.V., Klionsky, D.J., 1999. Apg7p/Cvt2p Is Required for the Cytoplasm-to-Vacuole Targeting, Macroautophagy, and Peroxisome Degradation Pathways. Mol Biol Cell 10, 1337–1351.

Kim, J., Kundu, M., Viollet, B., Guan, K.-L., 2011. AMPK and mTOR regulate autophagy through direct phosphorylation of Ulk1. Nat Cell Biol 13, 132–141. https://doi.org/10.1038/ncb2152

Kimple, M.E., Brill, A.L., Pasker, R.L., 2013. Overview of Affinity Tags for Protein Purification. Curr Protoc Protein Sci 73, Unit-9.9. https://doi.org/10.1002/0471140864.ps0909s73

Kobayashi, H., Abe, K., Matsuura, T., Ikeda, Y., Hitomi, T., Akechi, Y., Habu, T., Liu, W., Okuda, H., Koizumi, A., 2011. Expansion of intronic GGCCTG hexanucleotide repeat in NOP56 causes SCA36, a type of spinocerebellar ataxia accompanied by motor neuron

involvement. Am J Hum Genet 89, 121–130. https://doi.org/10.1016/j.ajhg.2011.05.015

Kocaturk, N.M., Gozuacik, D., 2018. Crosstalk Between Mammalian Autophagy and the Ubiquitin-Proteasome System. Front Cell Dev Biol 6, 128. https://doi.org/10.3389/fcell.2018.00128

Koerver, L., Papadopoulos, C., Liu, B., Kravic, B., Rota, G., Brecht, L., Veenendaal, T., Polajnar, M., Bluemke, A., Ehrmann, M., Klumperman, J., Jäättelä, M., Behrends, C., Meyer, H., 2019. The ubiquitin-conjugating enzyme UBE2QL1 coordinates lysophagy in response to endolysosomal damage. EMBO Rep 20, e48014. https://doi.org/10.15252/embr.201948014

Koppers, M., Blokhuis, A.M., Westeneng, H., Terpstra, M.L., Zundel, C.A.C., Vieira de Sá, R., Schellevis, R.D., Waite, A.J., Blake, D.J., Veldink, J.H., van den Berg, L.H., Pasterkamp, R.J., 2015. C9orf72 ablation in mice does not cause motor neuron degeneration or motor deficits. Ann Neurol 78, 426–438. https://doi.org/10.1002/ana.24453

Korobeynikov, V.A., Lyashchenko, A.K., Blanco-Redondo, B., Jafar-Nejad, P., Shneider, N.A., 2022. Antisense oligonucleotide silencing of FUS expression as a therapeutic approach in amyotrophic lateral sclerosis. Nat Med 28, 104–116. https://doi.org/10.1038/s41591-021-01615-z

Kotani, T., Kirisako, H., Koizumi, M., Ohsumi, Y., Nakatogawa, H., 2018. The Atg2-Atg18 complex tethers pre-autophagosomal membranes to the endoplasmic reticulum for autophagosome formation. Proceedings of the National Academy of Sciences 115, 10363–10368. https://doi.org/10.1073/pnas.1806727115

Kretschmer, B.D., Kratzer, U., Schmidt, W.J., 1998. Riluzole, a glutamate release inhibitor, and motor behavior. Naunyn Schmiedebergs Arch Pharmacol 358, 181–190. https://doi.org/10.1007/pl00005241

Kucukelbir, A., Sigworth, F.J., Tagare, H.D., 2014. Quantifying the local resolution of cryo-EM density maps. Nat Methods 11, 63–65. https://doi.org/10.1038/nmeth.2727

Kulkarni, J.A., Cullis, P.R., van der Meel, R., 2018. Lipid Nanoparticles Enabling Gene Therapies: From Concepts to Clinical Utility. Nucleic Acid Therapeutics 28, 146–157. https://doi.org/10.1089/nat.2018.0721

Kumar, D.R., Aslinia, F., Yale, S.H., Mazza, J.J., 2011. Jean-Martin Charcot: The Father of Neurology. Clin Med Res 9, 46–49. https://doi.org/10.3121/cmr.2009.883

Kusaczuk, M., 2019. Tauroursodeoxycholate—Bile Acid with Chaperoning Activity: Molecular and Cellular Effects and Therapeutic Perspectives. Cells 8, 1471. https://doi.org/10.3390/cells8121471

Kwiatkowski, T.J., Bosco, D.A., Leclerc, A.L., Tamrazian, E., Vanderburg, C.R., Russ, C., Davis, A., Gilchrist, J., Kasarskis, E.J., Munsat, T., Valdmanis, P., Rouleau, G.A., Hosler, B.A., Cortelli, P., de Jong, P.J., Yoshinaga, Y., Haines, J.L., Pericak-Vance, M.A., Yan, J., Ticozzi, N., Siddique, T., McKenna-Yasek, D., Sapp, P.C., Horvitz, H.R., Landers, J.E., Brown, R.H., 2009. Mutations in the FUS/TLS gene on chromosome 16 cause familial amyotrophic lateral sclerosis. Science 323, 1205–1208. https://doi.org/10.1126/science.1166066

Kwon, I., Xiang, S., Kato, M., Wu, L., Theodoropoulos, P., Wang, T., Kim, J., Yun, J., Xie, Y., McKnight, S.L., 2014. Poly-dipeptides encoded by the C9ORF72 repeats bind nucleoli, impede RNA biogenesis, and kill cells. Science 345, 1139–1145. https://doi.org/10.1126/science.1254917

La Spada, A.R., Taylor, J.P., 2010. Repeat expansion disease: Progress and puzzles in disease pathogenesis. Nat Rev Genet 11, 247–258. https://doi.org/10.1038/nrg2748

Lacomblez, L., Bensimon, G., Leigh, P.N., Guillet, P., Powe, L., Durrleman, S., Delumeau, J.C., Meininger, V., 1996. A confirmatory dose-ranging study of riluzole in ALS. ALS/Riluzole Study Group-II. Neurology 47, S242-250. https://doi.org/10.1212/wnl.47.6_suppl_4.242s

Laflamme, C., McKeever, P.M., Kumar, R., Schwartz, J., Kolahdouzan, M., Chen, C.X., You, Z., Benaliouad, F., Gileadi, O., McBride, H.M., Durcan, T.M., Edwards, A.M., Healy, L.M., Robertson, J., McPherson, P.S., 2019. Implementation of an antibody characterization procedure and application to the major ALS/FTD disease gene C9ORF72. Elife 8, e48363. https://doi.org/10.7554/eLife.48363

Lagier-Tourenne, C., Baughn, M., Rigo, F., Sun, S., Liu, P., Li, H.-R., Jiang, J., Watt, A.T., Chun, S., Katz, M., Qiu, J., Sun, Y., Ling, S.-C., Zhu, Q., Polymenidou, M., Drenner, K., Artates, J.W., McAlonis-Downes, M., Markmiller, S., Hutt, K.R., Pizzo, D.P., Cady, J., Harms, M.B., Baloh, R.H., Vandenberg, S.R., Yeo, G.W., Fu, X.-D., Bennett, C.F., Cleveland, D.W., Ravits, J., 2013. Targeted degradation of sense and antisense C9orf72 RNA foci as therapy for ALS and frontotemporal degeneration. Proceedings of the National Academy of Sciences 110, E4530–E4539. https://doi.org/10.1073/pnas.1318835110

Lagier-Tourenne, C., Polymenidou, M., Hutt, K.R., Vu, A.Q., Baughn, M., Huelga, S.C., Clutario, K.M., Ling, S.-C., Liang, T.Y., Mazur, C., Wancewicz, E., Kim, A.S., Watt, A., Freier, S., Hicks, G.G., Donohue, J.P., Shiue, L., Bennett, C.F., Ravits, J., Cleveland, D.W., Yeo, G.W., 2012. Divergent roles of ALS-linked proteins FUS/TLS and TDP-43 intersect in processing long pre-mRNAs. Nat Neurosci 15, 1488–1497. https://doi.org/10.1038/nn.3230

Larkin, L.M., Davis, C.S., Sims-Robinson, C., Kostrominova, T.Y., Remmen, H.V., Richardson, A., Feldman, E.L., Brooks, S.V., 2011. Skeletal muscle weakness due to deficiency of CuZn-superoxide dismutase is associated with loss of functional innervation. American Journal of Physiology-Regulatory, Integrative and Comparative Physiology 301, R1400–R1407. https://doi.org/10.1152/ajpregu.00093.2011

Laslo, P., Lipski, J., Nicholson, L.F., Miles, G.B., Funk, G.D., 2001. GluR2 AMPA receptor subunit expression in motoneurons at low and high risk for degeneration in amyotrophic lateral sclerosis. Exp Neurol 169, 461–471. https://doi.org/10.1006/exnr.2001.7653

Lawrence, R.E., Fromm, S.A., Fu, Y., Yokom, A.L., Kim, D.J., Thelen, A.M., Young, L.N., Lim, C.-Y., Samelson, A.J., Hurley, J.H., Zoncu, R., 2019. Structural mechanism of a Rag GTPase activation checkpoint by the lysosomal folliculin complex. Science 366, 971–977. https://doi.org/10.1126/science.aax0364

Lee, K.-H., Zhang, P., Kim, H.J., Mitrea, D.M., Sarkar, M., Freibaum, B.D., Cika, J., Coughlin, M., Messing, J., Molliex, A., Maxwell, B.A., Kim, N.C., Temirov, J., Moore, J., Kolaitis, R.-M., Shaw, T.I., Bai, B., Peng, J., Kriwacki, R.W., Taylor, J.P., 2016. C9orf72 Dipeptide Repeats Impair the Assembly, Dynamics, and Function of Membrane-Less Organelles. Cell 167, 774-788.e17. https://doi.org/10.1016/j.cell.2016.10.002

Lee, Y.-B., Chen, H.-J., Peres, J.N., Gomez-Deza, J., Attig, J., Stalekar, M., Troakes, C., Nishimura, A.L., Scotter, E.L., Vance, C., Adachi, Y., Sardone, V., Miller, J.W., Smith, B.N., Gallo, J.-M., Ule, J., Hirth, F., Rogelj, B., Houart, C., Shaw, C.E., 2013. Hexanucleotide repeats in ALS/FTD form length-dependent RNA foci, sequester RNA binding proteins, and are neurotoxic. Cell Rep 5, 1178–1186. https://doi.org/10.1016/j.celrep.2013.10.049

Lee, Y.-K., Lee, J.-A., 2016. Role of the mammalian ATG8/LC3 family in autophagy: differential and compensatory roles in the spatiotemporal regulation of autophagy. BMB Rep 49, 424–430. https://doi.org/10.5483/BMBRep.2016.49.8.081

Lehmer, C., Oeckl, P., Weishaupt, J.H., Volk, A.E., Diehl-Schmid, J., Schroeter, M.L., Lauer, M., Kornhuber, J., Levin, J., Fassbender, K., Landwehrmeyer, B., Schludi, M.H., Arzberger, T., Kremmer, E., Flatley, A., Feederle, R., Steinacker, P., Weydt, P., Ludolph, A.C., Edbauer, D., Otto, M., Danek, A., Feneberg, E., Anderl-Straub, S., von Arnim, C., Jahn, H., Schneider, A., Maler, M., Polyakova, M., Riedl, L., Wiltfang, J., Ziegler, G., 2017. Poly-GP in cerebrospinal fluid links C9orf72-associated dipeptide repeat expression to the asymptomatic phase of ALS/FTD. EMBO Mol Med 9, 859–868. https://doi.org/10.15252/emmm.201607486

LEIGH, P.N., WHITWELL, H., GAROFALO, O., BULLER, J., SWASH, M., MARTIN, J.E., GALLO, J.-M., WELLER, R.O., ANDERTON, B.H., 1991. UBIQUITIN-IMMUNOREACTIVE INTRANEURONAL INCLUSIONS IN AMYOTROPHIC LATERAL SCLEROSIS: MORPHOLOGY, DISTRIBUTION, AND SPECIFICITY. Brain 114, 775–788. https://doi.org/10.1093/brain/114.2.775

Lepore, A.C., Haenggeli, C., Gasmi, M., Bishop, K.M., Bartus, R.T., Maragakis, N.J., Rothstein, J.D., 2007. Intraparenchymal spinal cord delivery of adeno-associated virus IGF-1 is protective in the SOD1G93A model of ALS. Brain Res 1185, 256–265. https://doi.org/10.1016/j.brainres.2007.09.034

Levine, B., Kroemer, G., 2008. Autophagy in the Pathogenesis of Disease. Cell 132, 27–42. https://doi.org/10.1016/j.cell.2007.12.018

Levine, T.P., Daniels, R.D., Gatta, A.T., Wong, L.H., Hayes, M.J., 2013. The product of C9orf72, a gene strongly implicated in neurodegeneration, is structurally related to DENN Rab-GEFs. Bioinformatics 29, 499–503. https://doi.org/10.1093/bioinformatics/bts725

Li, S., Wu, Z., Li, Y., Tantray, I., De Stefani, D., Mattarei, A., Krishnan, G., Gao, F.-B., Vogel, H., Lu, B., 2020. Altered MICOS Morphology and Mitochondrial Ion Homeostasis Contribute to Poly(GR) Toxicity Associated with C9-ALS/FTD. Cell Rep 32, 107989. https://doi.org/10.1016/j.celrep.2020.107989

Li, W., Li, J., Bao, J., 2012. Microautophagy: lesser-known self-eating. Cell. Mol. Life Sci. 69, 1125–1136. https://doi.org/10.1007/s00018-011-0865-5

Li, Y., Guo, Y., Wang, X., Yu, X., Duan, W., Hong, K., Wang, J., Han, H., Li, C., 2015. Trehalose decreases mutant SOD1 expression and alleviates motor deficiency in early but not end-stage amyotrophic lateral sclerosis in a SOD1-G93A mouse model. Neuroscience 298, 12–25. https://doi.org/10.1016/j.neuroscience.2015.03.061

Liang, C., Lee, J., Inn, K., Gack, M.U., Li, Q., Roberts, E.A., Vergne, I., Deretic, V., Feng, P., Akazawa, C., Jung, J.U., 2008. Beclin1-binding UVRAG targets the class C Vps complex to coordinate autophagosome maturation and endocytic trafficking. Nat Cell Biol 10, 776–787. https://doi.org/10.1038/ncb1740

Liang, X.H., Jackson, S., Seaman, M., Brown, K., Kempkes, B., Hibshoosh, H., Levine, B., 1999. Induction of autophagy and inhibition of tumorigenesis by beclin 1. Nature 402, 672–676. https://doi.org/10.1038/45257

Lin, H., Hu, H., Duan, W., Liu, YaLing, Tan, G., Li, Z., Liu, YaKun, Deng, B., Song, X., Wang, W., Wen, D., Wang, Y., Li, C., 2018. Intramuscular Delivery of scAAV9-hIGF1 Prolongs Survival in the hSOD1G93A ALS Mouse Model via Upregulation of D-Amino Acid Oxidase. Mol Neurobiol 55, 682–695. https://doi.org/10.1007/s12035-016-0335-z

Lin, Y., Mori, E., Kato, M., Xiang, S., Wu, L., Kwon, I., McKnight, S.L., 2016. Toxic PR Poly-Dipeptides Encoded by the C9orf72 Repeat Expansion Target LC Domain Polymers. Cell 167, 789-802.e12. https://doi.org/10.1016/j.cell.2016.10.003

Ling, S.-C., Polymenidou, M., Cleveland, D.W., 2013. Converging mechanisms in ALS and FTD: disrupted RNA and protein homeostasis. Neuron 79, 416–438. https://doi.org/10.1016/j.neuron.2013.07.033

Liu, F., Liu, Q., Lu, C.X., Cui, B., Guo, X.N., Wang, R.R., Liu, M.S., Li, X.G., Cui, L., Zhang, X., 2016. Identification of a novel loss-of-function C9orf72 splice site mutation in a patient with amyotrophic lateral sclerosis. Neurobiology of Aging 47, 219.e1-219.e5. https://doi.org/10.1016/j.neurobiolaging.2016.07.027

Liu, W., Ikeda, Y., Hishikawa, N., Yamashita, T., Deguchi, K., Abe, K., 2014. Characteristic RNA foci of the abnormal hexanucleotide GGCCUG repeat expansion in spinocerebellar ataxia type 36 (Asidan). Eur J Neurol 21, 1377–1386. https://doi.org/10.1111/ene.12491

Liu, Y., Dodart, J.-C., Tran, H., Berkovitch, S., Braun, M., Byrne, M., Durbin, A.F., Hu, X.S., Iwamoto, N., Jang, H.G., Kandasamy, P., Liu, F., Longo, K., Ruschel, J., Shelke, J., Yang, H., Yin, Y., Donner, A., Zhong, Z., Vargeese, C., Brown, R.H., 2021. Variant-selective stereopure oligonucleotides protect against pathologies associated with C9orf72-repeat expansion in preclinical models. Nat Commun 12, 847. https://doi.org/10.1038/s41467-021-21112-8

Liu, Z., Chen, O., Wall, J.B.J., Zheng, M., Zhou, Y., Wang, L., Ruth Vaseghi, H., Qian, L., Liu, J., 2017. Systematic comparison of 2A peptides for cloning multi-genes in a polycistronic vector. Sci Rep 7, 2193. https://doi.org/10.1038/s41598-017-02460-2

Lo, M.W., Lee, J.D., 2020. Complement: a global immunometabolic regulator in amyotrophic lateral sclerosis. Neural Regen Res 16, 1210–1211. https://doi.org/10.4103/1673-5374.300441

Logroscino, G., Traynor, B.J., Hardiman, O., Chiò, A., Mitchell, D., Swingler, R.J., Millul, A., Benn, E., Beghi, E., 2010. Incidence of Amyotrophic Lateral Sclerosis in Europe. J Neurol Neurosurg Psychiatry 81, 385–390. https://doi.org/10.1136/jnnp.2009.183525

Long, X., Lin, Y., Ortiz-Vega, S., Yonezawa, K., Avruch, J., 2005. Rheb binds and regulates the mTOR kinase. Curr Biol 15, 702–713. https://doi.org/10.1016/j.cub.2005.02.053

Longinetti, E., Fang, F., 2019. Epidemiology of amyotrophic lateral sclerosis: an update of recent literature. Curr Opin Neurol 32, 771–776. https://doi.org/10.1097/WCO.0000000000000730

Lunetta, C., Moglia, C., Lizio, A., Caponnetto, C., Dubbioso, R., Giannini, F., Matà, S., Mazzini, L., Sabatelli, M., Siciliano, G., Simone, I.L., Sorarù, G., Toriello, A., Trojsi, F., Vedovello, M., D'Ovidio, F., Filippi, M., Calvo, A., and EDARAVALS Study Group, 2020. The Italian multicenter experience with edaravone in amyotrophic lateral sclerosis. J Neurol 267, 3258–3267. https://doi.org/10.1007/s00415-020-09993-z

Lystad, A.H., Carlsson, S.R., de la Ballina, L.R., Kauffman, K.J., Nag, S., Yoshimori, T., Melia, T.J., Simonsen, A., 2019. Distinct functions of ATG16L1 isoforms in membrane binding and LC3B lipidation in autophagy-related processes. Nat Cell Biol 21, 372–383. https://doi.org/10.1038/s41556-019-0274-9

Mackenzie, I.R., Arzberger, T., Kremmer, E., Troost, D., Lorenzl, S., Mori, K., Weng, S.-M., Haass, C., Kretzschmar, H.A., Edbauer, D., Neumann, M., 2013. Dipeptide repeat

protein pathology in C9ORF72 mutation cases: clinico-pathological correlations. Acta Neuropathol 126, 859–879. https://doi.org/10.1007/s00401-013-1181-y

Mackenzie, I.R.A., Frick, P., Grässer, F.A., Gendron, T.F., Petrucelli, L., Cashman, N.R., Edbauer, D., Kremmer, E., Prudlo, J., Troost, D., Neumann, M., 2015. Quantitative analysis and clinico-pathological correlations of different dipeptide repeat protein pathologies in C9ORF72 mutation carriers. Acta Neuropathol 130, 845–861. https://doi.org/10.1007/s00401-015-1476-2

Magrané, J., Cortez, C., Gan, W.-B., Manfredi, G., 2014. Abnormal mitochondrial transport and morphology are common pathological denominators in SOD1 and TDP43 ALS mouse models. Hum Mol Genet 23, 1413–1424. https://doi.org/10.1093/hmg/ddt528

Maharjan, N., Künzli, C., Buthey, K., Saxena, S., 2017. C9ORF72 Regulates Stress Granule Formation and Its Deficiency Impairs Stress Granule Assembly, Hypersensitizing Cells to Stress. Mol Neurobiol 54, 3062–3077. https://doi.org/10.1007/s12035-016-9850-1

Majounie, E., Renton, A.E., Mok, K., Dopper, E.G., Waite, A., Rollinson, S., Chiò, A., Restagno, G., Nicolaou, N., Simon-Sanchez, J., van Swieten, J.C., Abramzon, Y., Johnson, J.O., Sendtner, M., Pamphlett, R., Orrell, R.W., Mead, S., Sidle, K.C., Houlden, H., Rohrer, J.D., Morrison, K.E., Pall, H., Talbot, K., Ansorge, O., Hernandez, D.G., Arepalli, S., Sabatelli, M., Mora, G., Corbo, M., Giannini, F., Calvo, A., Englund, E., Borghero, G., Floris, G.L., Remes, A.M., Laaksovirta, H., McCluskey, L., Trojanowski, J.Q., Van Deerlin, V.M., Schellenberg, G.D., Nalls, M.A., Drory, V.E., Lu, C.-S., Yeh, T.-H., Ishiura, H., Takahashi, Y., Tsuji, S., Le Ber, I., Brice, A., Drepper, C., Williams, N., Kirby, J., Shaw, P., Hardy, J., Tienari, P.J., Heutink, P., Morris, H.R., Pickering-Brown, S., Traynor, B.J., 2012. Frequency of the C9orf72 hexanucleotide repeat expansion in patients with amyotrophic lateral sclerosis and frontotemporal dementia: a cross-sectional study. The Lancet Neurology 11, 323–330. https://doi.org/10.1016/S1474-4422(12)70043-1

Maor-Nof, M., Shipony, Z., Lopez-Gonzalez, R., Nakayama, L., Zhang, Y.-J., Couthouis, J., Blum, J.A., Castruita, P.A., Linares, G.R., Ruan, K., Ramaswami, G., Simon, D.J., Nof, A., Santana, M., Han, K., Sinnott-Armstrong, N., Bassik, M.C., Geschwind, D.H., Tessier-Lavigne, M., Attardi, L.D., Lloyd, T.E., Ichida, J.K., Gao, F.-B., Greenleaf, W.J., Yokoyama, J.S., Petrucelli, L., Gitler, A.D., 2021. p53 is a central regulator driving neurodegeneration caused by C9orf72 poly(PR). Cell 184, 689-708.e20. https://doi.org/10.1016/j.cell.2020.12.025

Marrone, L., Drexler, H.C.A., Wang, J., Tripathi, P., Distler, T., Heisterkamp, P., Anderson, E.N., Kour, S., Moraiti, A., Maharana, S., Bhatnagar, R., Belgard, T.G., Tripathy, V., Kalmbach, N., Hosseinzadeh, Z., Crippa, V., Abo-Rady, M., Wegner, F., Poletti, A., Troost, D., Aronica, E., Busskamp, V., Weis, J., Pandey, U.B., Hyman, A.A., Alberti, S., Goswami, A., Sterneckert, J., 2019. FUS pathology in ALS is linked to alterations in multiple ALS-associated proteins and rescued by drugs stimulating autophagy. Acta Neuropathol 138, 67–84. https://doi.org/10.1007/s00401-019-01998-x

Marrone, L., Poser, I., Casci, I., Japtok, J., Reinhardt, P., Janosch, A., Andree, C., Lee, H.O., Moebius, C., Koerner, E., Reinhardt, L., Cicardi, M.E., Hackmann, K., Klink, B., Poletti, A., Alberti, S., Bickle, M., Hermann, A., Pandey, U.B., Hyman, A.A., Sterneckert, J.L., 2018. Isogenic FUS-eGFP iPSC Reporter Lines Enable Quantification of FUS Stress Granule Pathology that Is Rescued by Drugs Inducing Autophagy. Stem Cell Reports 10, 375–389. https://doi.org/10.1016/j.stemcr.2017.12.018

Martin, E., Yanicostas, C., Rastetter, A., Alavi Naini, S.M., Maouedj, A., Kabashi, E., Rivaud-Péchoux, S., Brice, A., Stevanin, G., Soussi-Yanicostas, N., 2012. Spatacsin and spastizin act in the same pathway required for proper spinal motor neuron axon outgrowth in zebrafish. Neurobiol Dis 48, 299–308. https://doi.org/10.1016/j.nbd.2012.07.003

Maruyama, H., Morino, H., Ito, H., Izumi, Y., Kato, H., Watanabe, Y., Kinoshita, Y., Kamada, M., Nodera, H., Suzuki, H., Komure, O., Matsuura, S., Kobatake, K., Morimoto, N., Abe, K., Suzuki, N., Aoki, M., Kawata, A., Hirai, T., Kato, T., Ogasawara, K., Hirano, A., Takumi, T., Kusaka, H., Hagiwara, K., Kaji, R., Kawakami, H., 2010. Mutations of optineurin in amyotrophic lateral sclerosis. Nature 465, 223–226. https://doi.org/10.1038/nature08971

Matoba, K., Kotani, T., Tsutsumi, A., Tsuji, T., Mori, T., Noshiro, D., Sugita, Y., Nomura, N., Iwata, S., Ohsumi, Y., Fujimoto, T., Nakatogawa, H., Kikkawa, M., Noda, N.N., 2020. Atg9 is a lipid scramblase that mediates autophagosomal membrane expansion. Nat Struct Mol Biol 27, 1185–1193. https://doi.org/10.1038/s41594-020-00518-w

May, S., Hornburg, D., Schludi, M.H., Arzberger, T., Rentzsch, K., Schwenk, B.M., Grässer, F.A., Mori, K., Kremmer, E., Banzhaf-Strathmann, J., Mann, M., Meissner, F., Edbauer, D., 2014. C9orf72 FTLD/ALS-associated Gly-Ala dipeptide repeat proteins cause neuronal toxicity and Unc119 sequestration. Acta Neuropathol 128, 485–503. https://doi.org/10.1007/s00401-014-1329-4

McEachin, Z.T., Parameswaren, J., Raj, N., Bassell, G.J., Jiang, J., 2020. RNA-mediated toxicity in C9orf72 ALS and FTD. Neurobiol Dis 145, 105055. https://doi.org/10.1016/j.nbd.2020.105055

Medina, L., Figueredo-Cardenas, G., Rothstein, J., Reiner, A., 1997. Differential Abundance of Glutamate Transporter Subtypes in Amyotrophic Lateral Sclerosis (ALS)-Vulnerable versus ALS-Resistant Brain Stem Motor Cell Groups. Experimental neurology 142, 287–95. https://doi.org/10.1006/exnr.1996.0198

Meeter, L.H.H., Gendron, T.F., Sias, A.C., Jiskoot, L.C., Russo, S.P., Donker Kaat, L., Papma, J.M., Panman, J.L., van der Ende, E.L., Dopper, E.G., Franzen, S., Graff, C., Boxer, A.L., Rosen, H.J., Sanchez-Valle, R., Galimberti, D., Pijnenburg, Y.A.L., Benussi, L., Ghidoni, R., Borroni, B., Laforce, R., Del Campo, M., Teunissen, C.E., van Minkelen, R., Rojas, J.C., Coppola, G., Geschwind, D.H., Rademakers, R., Karydas, A.M., Öijerstedt, L., Scarpini, E., Binetti, G., Padovani, A., Cash, D.M., Dick, K.M., Bocchetta, M., Miller, B.L., Rohrer, J.D., Petrucelli, L., van Swieten, J.C., Lee, S.E., 2018. Poly(GP), neurofilament and grey matter deficits in *C9orf72* expansion carriers. Ann Clin Transl Neurol 5, 583–597. https://doi.org/10.1002/acn3.559

Meijboom, K.E., Abdallah, A., Fordham, N.P., Nagase, H., Rodriguez, T., Kraus, C., Gendron, T.F., Krishnan, G., Esanov, R., Andrade, N.S., Rybin, M.J., Ramic, M., Stephens, Z.D., Edraki, A., Blackwood, M.T., Kahriman, A., Henninger, N., Kocher, J.-P.A., Benatar, M., Brodsky, M.H., Petrucelli, L., Gao, F.-B., Sontheimer, E.J., Brown, R.H., Zeier, Z., Mueller, C., 2022. CRISPR/Cas9-mediated excision of ALS/FTD-causing hexanucleotide repeat expansion in C9ORF72 rescues major disease mechanisms in vivo and in vitro. Nat Commun 13, 6286. https://doi.org/10.1038/s41467-022-33332-7

Menzies, F.M., Fleming, A., Caricasole, A., Bento, C.F., Andrews, S.P., Ashkenazi, A., Füllgrabe, J., Jackson, A., Sanchez, M.J., Karabiyik, C., Licitra, F., Ramirez, A.L., Pavel, M., Puri, C., Renna, M., Ricketts, T., Schlotawa, L., Vicinanza, M., Won, H., Zhu, Y., Skidmore, J., Rubinsztein, D.C., 2017. Autophagy and Neurodegeneration: Pathogenic Mechanisms

and Therapeutic Opportunities. Neuron 93, 1015–1034. https://doi.org/10.1016/j.neuron.2017.01.022

Mercer, C.A., Kaliappan, A., Dennis, P.B., 2009. A novel, human Atg13 binding protein, Atg101, interacts with ULK1 and is essential for macroautophagy. Autophagy 5, 649–662. https://doi.org/10.4161/auto.5.5.8249

Mercer, T.J., Ohashi, Y., Boeing, S., Jefferies, H.B.J., De Tito, S., Flynn, H., Tremel, S., Zhang, W., Wirth, M., Frith, D., Snijders, A.P., Williams, R.L., Tooze, S.A., 2021. Phosphoproteomic identification of ULK substrates reveals VPS15-dependent ULK/VPS34 interplay in the regulation of autophagy. EMBO J 40, e105985. https://doi.org/10.15252/embj.2020105985

Mercy, L., Hodges, J.R., Dawson, K., Barker, R.A., Brayne, C., 2008. Incidence of early-onset dementias in Cambridgeshire, United Kingdom. Neurology 71, 1496–1499. https://doi.org/10.1212/01.wnl.0000334277.16896.fa

Meyer, T., Funke, A., Münch, C., Kettemann, D., Maier, A., Walter, B., Thomas, A., Spittel, S., 2019. Real world experience of patients with amyotrophic lateral sclerosis (ALS) in the treatment of spasticity using tetrahydrocannabinol:cannabidiol (THC:CBD). BMC Neurol 19, 222. https://doi.org/10.1186/s12883-019-1443-y

Miller, T.M., Cudkowicz, M.E., Genge, A., Shaw, P.J., Sobue, G., Bucelli, R.C., Chiò, A., Van Damme, P., Ludolph, A.C., Glass, J.D., Andrews, J.A., Babu, S., Benatar, M., McDermott, C.J., Cochrane, T., Chary, S., Chew, S., Zhu, H., Wu, F., Nestorov, I., Graham, D., Sun, P., McNeill, M., Fanning, L., Ferguson, T.A., Fradette, S., VALOR and OLE Working Group, 2022. Trial of Antisense Oligonucleotide Tofersen for SOD1 ALS. N Engl J Med 387, 1099–1110. https://doi.org/10.1056/NEJMoa2204705

Miyazaki, M., Hiramoto, M., Takano, N., Kokuba, H., Takemura, J., Tokuhisa, M., Hino, H., Kazama, H., Miyazawa, K., 2021. Targeted disruption of GAK stagnates autophagic flux by disturbing lysosomal dynamics. International Journal of Molecular Medicine 48, 1–18. https://doi.org/10.3892/ijmm.2021.5028

Mizielinska, S., Grönke, S., Niccoli, T., Ridler, C.E., Clayton, E.L., Devoy, A., Moens, T., Norona, F.E., Woollacott, I.O.C., Pietrzyk, J., Cleverley, K., Nicoll, A.J., Pickering-Brown, S., Dols, J., Cabecinha, M., Hendrich, O., Fratta, P., Fisher, E.M.C., Partridge, L., Isaacs, A.M., 2014. C9orf72 repeat expansions cause neurodegeneration in Drosophila through arginine-rich proteins. Science 345, 1192–1194. https://doi.org/10.1126/science.1256800

Mizuno, Y., Amari, M., Takatama, M., Aizawa, H., Mihara, B., Okamoto, K., 2006. Immunoreactivities of p62, an ubiqutin-binding protein, in the spinal anterior horn cells of patients with amyotrophic lateral sclerosis. J Neurol Sci 249, 13–18. https://doi.org/10.1016/j.jns.2006.05.060

Mizushima, N., Kuma, A., Kobayashi, Y., Yamamoto, A., Matsubae, M., Takao, T., Natsume, T., Ohsumi, Y., Yoshimori, T., 2003. Mouse Apg16L, a novel WD-repeat protein, targets to the autophagic isolation membrane with the Apg12-Apg5 conjugate. J Cell Sci 116, 1679–1688. https://doi.org/10.1242/jcs.00381

Mizushima, N., White, E., Rubinsztein, D.C., 2021. Breakthroughs and bottlenecks in autophagy research. Trends Mol Med 27, 835–838. https://doi.org/10.1016/j.molmed.2021.06.012

Moens, T.G., Mizielinska, S., Niccoli, T., Mitchell, J.S., Thoeng, A., Ridler, C.E., Grönke, S., Esser, J., Heslegrave, A., Zetterberg, H., Partridge, L., Isaacs, A.M., 2018. Sense and antisense

RNA are not toxic in Drosophila models of C9orf72-associated ALS/FTD. Acta Neuropathol 135, 445–457. https://doi.org/10.1007/s00401-017-1798-3

Monastyrska, I., Rieter, E., Klionsky, D.J., Reggiori, F., 2009. Multiple roles of the cytoskeleton in autophagy. Biol Rev Camb Philos Soc 84, 431–448. https://doi.org/10.1111/j.1469-185X.2009.00082.x

Mondal, S., Hsiao, K., Goueli, S.A., 2015. A Homogenous Bioluminescent System for Measuring GTPase, GTPase Activating Protein, and Guanine Nucleotide Exchange Factor Activities. Assay Drug Dev Technol 13, 444–455. https://doi.org/10.1089/adt.2015.643

Mori, K., Arzberger, T., Grässer, F.A., Gijselinck, I., May, S., Rentzsch, K., Weng, S.-M., Schludi, M.H., van der Zee, J., Cruts, M., Van Broeckhoven, C., Kremmer, E., Kretzschmar, H.A., Haass, C., Edbauer, D., 2013a. Bidirectional transcripts of the expanded C9orf72 hexanucleotide repeat are translated into aggregating dipeptide repeat proteins. Acta Neuropathol 126, 881–893. https://doi.org/10.1007/s00401-013-1189-3

Mori, K., Weng, S.-M., Arzberger, T., May, S., Rentzsch, K., Kremmer, E., Schmid, B., Kretzschmar, H.A., Cruts, M., Van Broeckhoven, C., Haass, C., Edbauer, D., 2013b. The C9orf72 GGGGCC repeat is translated into aggregating dipeptide-repeat proteins in FTLD/ALS. Science 339, 1335–1338. https://doi.org/10.1126/science.1232927

Moss, D.J.H., Poulter, M., Beck, J., Hehir, J., Polke, J.M., Campbell, T., Adamson, G., Mudanohwo, E., McColgan, P., Haworth, A., Wild, E.J., Sweeney, M.G., Houlden, H., Mead, S., Tabrizi, S.J., 2014. C9orf72 expansions are the most common genetic cause of Huntington disease phenocopies. Neurology 82, 292. https://doi.org/10.1212/WNL.0000000000000061

Mueller, C., Berry, J.D., McKenna-Yasek, D.M., Gernoux, G., Owegi, M.A., Pothier, L.M., Douthwright, C.L., Gelevski, D., Luppino, S.D., Blackwood, M., Wightman, N.S., Oakley, D.H., Frosch, M.P., Flotte, T.R., Cudkowicz, M.E., Brown, R.H., 2020. SOD1 Suppression with Adeno-Associated Virus and MicroRNA in Familial ALS. N Engl J Med 383, 151–158. https://doi.org/10.1056/NEJMoa2005056

Munson, M.J., Allen, G.F., Toth, R., Campbell, D.G., Lucocq, J.M., Ganley, I.G., 2015. mTOR activates the VPS34-UVRAG complex to regulate autolysosomal tubulation and cell survival. EMBO J 34, 2272–2290. https://doi.org/10.15252/embj.201590992

Murphy, N.A., Arthur, K.C., Tienari, P.J., Houlden, H., Chiò, A., Traynor, B.J., 2017. Age-related penetrance of the C9orf72 repeat expansion. Sci Rep 7, 2116. https://doi.org/10.1038/s41598-017-02364-1

Nakatogawa, H., Suzuki, K., Kamada, Y., Ohsumi, Y., 2009. Dynamics and diversity in autophagy mechanisms: lessons from yeast. Nat Rev Mol Cell Biol 10, 458–467. https://doi.org/10.1038/nrm2708

Nalbandian, A., Donkervoort, S., Dec, E., Badadani, M., Katheria, V., Rana, P., Nguyen, C., Mukherjee, J., Caiozzo, V., Martin, B., Watts, G.D., Vesa, J., Smith, C., Kimonis, V.E., 2011. The Multiple Faces of Valosin-Containing Protein-Associated Diseases: Inclusion Body Myopathy with Paget's Disease of Bone, Frontotemporal Dementia, and Amyotrophic Lateral Sclerosis. J Mol Neurosci 45, 522. https://doi.org/10.1007/s12031-011-9627-y

Nataf, S., Pays, L., 2015. Gene co-expression analysis unravels a link between C9orf72 and RNA metabolism in myeloid cells. Acta Neuropathol Commun 3, 64. https://doi.org/10.1186/s40478-015-0242-y

Neumann, M., Sampathu, D.M., Kwong, L.K., Truax, A.C., Micsenyi, M.C., Chou, T.T., Bruce, J., Schuck, T., Grossman, M., Clark, C.M., McCluskey, L.F., Miller, B.L., Masliah, E., Mackenzie, I.R., Feldman, H., Feiden, W., Kretzschmar, H.A., Trojanowski, J.Q., Lee, V.M.-Y., 2006. Ubiquitinated TDP-43 in Frontotemporal Lobar Degeneration and Amyotrophic Lateral Sclerosis. Science 314, 130–133. https://doi.org/10.1126/science.1134108

Niedzielska, E., Smaga, I., Gawlik, M., Moniczewski, A., Stankowicz, P., Pera, J., Filip, M., 2016. Oxidative Stress in Neurodegenerative Diseases. Mol Neurobiol 53, 4094–4125. https://doi.org/10.1007/s12035-015-9337-5

Nishitoh, H., Kadowaki, H., Nagai, A., Maruyama, T., Yokota, T., Fukutomi, H., Noguchi, T., Matsuzawa, A., Takeda, K., Ichijo, H., 2008. ALS-linked mutant SOD1 induces ER stress- and ASK1-dependent motor neuron death by targeting Derlin-1. Genes Dev. 22, 1451–1464. https://doi.org/10.1101/gad.1640108

Nordin, A., Akimoto, C., Wuolikainen, A., Alstermark, H., Jonsson, P., Birve, A., Marklund, S.L., Graffmo, K.S., Forsberg, K., Brännström, T., Andersen, P.M., 2015. Extensive size variability of the GGGGCC expansion in C9orf72 in both neuronal and non-neuronal tissues in 18 patients with ALS or FTD. Human Molecular Genetics 24, 3133–3142. https://doi.org/10.1093/hmg/ddv064

Nörpel, J., Cavadini, S., Schenk, A.D., Graff-Meyer, A., Hess, D., Seebacher, J., Chao, J.A., Bhaskar, V., 2021. Structure of the human C9orf72-SMCR8 complex reveals a multivalent protein interaction architecture. PLoS Biol 19, e3001344. https://doi.org/10.1371/journal.pbio.3001344

Oakes, J.A., Davies, M.C., Collins, M.O., 2017. TBK1: a new player in ALS linking autophagy and neuroinflammation. Mol Brain 10, 5. https://doi.org/10.1186/s13041-017-0287-x

Oh, K., Noh, M., Kwon, M., Kim, H.Y., Oh, S., Park, J., Kim, H., Ki, C., Kim, S.H., 2018. Repeated Intrathecal Mesenchymal Stem Cells for Amyotrophic Lateral Sclerosis. Ann Neurol 84, 361–373. https://doi.org/10.1002/ana.25302

O'Rourke, J.G., Bogdanik, L., Muhammad, A.K.M.G., Gendron, T.F., Kim, K.J., Austin, A., Cady, J., Liu, E.Y., Zarrow, J., Grant, S., Ho, R., Bell, S., Carmona, S., Simpkinson, M., Lall, D., Wu, K., Daughrity, L., Dickson, D.W., Harms, M.B., Petrucelli, L., Lee, E.B., Lutz, C.M., Baloh, R.H., 2015. C9orf72 BAC Transgenic Mice Display Typical Pathologic Features of ALS/FTD. Neuron 88, 892–901. https://doi.org/10.1016/j.neuron.2015.10.027

O'Rourke, J.G., Bogdanik, L., Yáñez, A., Lall, D., Wolf, A.J., Muhammad, A.K.M.G., Ho, R., Carmona, S., Vit, J.P., Zarrow, J., Kim, K.J., Bell, S., Harms, M.B., Miller, T.M., Dangler, C.A., Underhill, D.M., Goodridge, H.S., Lutz, C.M., Baloh, R.H., 2016. C9orf72 is required for proper macrophage and microglial function in mice. Science 351, 1324–1329. https://doi.org/10.1126/science.aaf1064

Paganoni, S., Hendrix, S., Dickson, S.P., Knowlton, N., Berry, J.D., Elliott, M.A., Maiser, S., Karam, C., Caress, J.B., Owegi, M.A., Quick, A., Wymer, J., Goutman, S.A., Heitzman, D., Heiman-Patterson, T.D., Jackson, C., Quinn, C., Rothstein, J.D., Kasarskis, E.J., Katz, J., Jenkins, L., Ladha, S.S., Miller, T.M., Scelsa, S.N., Vu, T.H., Fournier, C., Johnson, K.M., Swenson, A., Goyal, N., Pattee, G.L., Babu, S., Chase, M., Dagostino, D., Hall, M., Kittle, G., Eydinov, M., Ostrow, J., Pothier, L., Randall, R., Shefner, J.M., Sherman, A.V., Tustison, E., Vigneswaran, P., Yu, H., Cohen, J., Klee, J., Tanzi, R., Gilbert, W., Yeramian, P., Cudkowicz, M., 2022. Effect of sodium phenylbutyrate/taurursodiol on tracheostomy/ventilation-free survival and hospitalisation in amyotrophic lateral

sclerosis: long-term results from the CENTAUR trial. J Neurol Neurosurg Psychiatry 93, 871–875. https://doi.org/10.1136/jnnp-2022-329024

Paganoni, S., Hendrix, S., Dickson, S.P., Knowlton, N., Macklin, E.A., Berry, J.D., Elliott, M.A., Maiser, S., Karam, C., Caress, J.B., Owegi, M.A., Quick, A., Wymer, J., Goutman, S.A., Heitzman, D., Heiman-Patterson, T.D., Jackson, C.E., Quinn, C., Rothstein, J.D., Kasarskis, E.J., Katz, J., Jenkins, L., Ladha, S., Miller, T.M., Scelsa, S.N., Vu, T.H., Fournier, C.N., Glass, J.D., Johnson, K.M., Swenson, A., Goyal, N.A., Pattee, G.L., Andres, P.L., Babu, S., Chase, M., Dagostino, D., Hall, M., Kittle, G., Eydinov, M., McGovern, M., Ostrow, J., Pothier, L., Randall, R., Shefner, J.M., Sherman, A.V., St Pierre, M.E., Tustison, E., Vigneswaran, P., Walker, J., Yu, H., Chan, J., Wittes, J., Yu, Z.-F., Cohen, J., Klee, J., Leslie, K., Tanzi, R.E., Gilbert, W., Yeramian, P.D., Schoenfeld, D., Cudkowicz, M.E., 2021. Long-term survival of participants in the CENTAUR trial of sodium phenylbutyrate-taurursodiol in amyotrophic lateral sclerosis. Muscle Nerve 63, 31–39. https://doi.org/10.1002/mus.27091

Paganoni, S., Macklin, E.A., Hendrix, S., Berry, J.D., Elliott, M.A., Maiser, S., Karam, C., Caress, J.B., Owegi, M.A., Quick, A., Wymer, J., Goutman, S.A., Heitzman, D., Heiman-Patterson, T., Jackson, C.E., Quinn, C., Rothstein, J.D., Kasarskis, E.J., Katz, J., Jenkins, L., Ladha, S., Miller, T.M., Scelsa, S.N., Vu, T.H., Fournier, C.N., Glass, J.D., Johnson, K.M., Swenson, A., Goyal, N.A., Pattee, G.L., Andres, P.L., Babu, S., Chase, M., Dagostino, D., Dickson, S.P., Ellison, N., Hall, M., Hendrix, K., Kittle, G., McGovern, M., Ostrow, J., Pothier, L., Randall, R., Shefner, J.M., Sherman, A.V., Tustison, E., Vigneswaran, P., Walker, J., Yu, H., Chan, J., Wittes, J., Cohen, J., Klee, J., Leslie, K., Tanzi, R.E., Gilbert, W., Yeramian, P.D., Schoenfeld, D., Cudkowicz, M.E., 2020. Trial of Sodium Phenylbutyrate–Taurursodiol for Amyotrophic Lateral Sclerosis. N Engl J Med 383, 919–930. https://doi.org/10.1056/NEJMoa1916945

Pang, S.Y.-Y., Hsu, J.S., Teo, K.-C., Li, Y., Kung, M.H.W., Cheah, K.S.E., Chan, D., Cheung, K.M.C., Li, M., Sham, P.-C., Ho, S.-L., 2017. Burden of rare variants in ALS genes influences survival in familial and sporadic ALS. Neurobiol Aging 58, 238.e9-238.e15. https://doi.org/10.1016/j.neurobiolaging.2017.06.007

Papadopoulos, C., Kirchner, P., Bug, M., Grum, D., Koerver, L., Schulze, N., Poehler, R., Dressler, A., Fengler, S., Arhzaouy, K., Lux, V., Ehrmann, M., Weihl, C.C., Meyer, H., 2017. VCP/p97 cooperates with YOD1, UBXD1 and PLAA to drive clearance of ruptured lysosomes by autophagy. EMBO J 36, 135–150. https://doi.org/10.15252/embj.201695148

Paré, B., Lehmann, M., Beaudin, M., Nordström, U., Saikali, S., Julien, J.-P., Gilthorpe, J.D., Marklund, S.L., Cashman, N.R., Andersen, P.M., Forsberg, K., Dupré, N., Gould, P., Brännström, T., Gros-Louis, F., 2018. Misfolded SOD1 pathology in sporadic Amyotrophic Lateral Sclerosis. Sci Rep 8, 14223. https://doi.org/10.1038/s41598-018-31773-z

Park, S.Y., Guo, X., 2014. Adaptor protein complexes and intracellular transport. Biosci Rep 34, e00123. https://doi.org/10.1042/BSR20140069

Parkinson, N., Ince, P.G., Smith, M.O., Highley, R., Skibinski, G., Andersen, P.M., Morrison, K.E., Pall, H.S., Hardiman, O., Collinge, J., Shaw, P.J., Fisher, E.C., 2006. ALS phenotypes with mutations in CHMP2B (charged multivesicular body protein 2B). Neurology 67, 1074–1077. https://doi.org/10.1212/01.wnl.0000231510.89311.8b

Parone, P.A., Da Cruz, S., Han, J.S., McAlonis-Downes, M., Vetto, A.P., Lee, S.K., Tseng, E., Cleveland, D.W., 2013. Enhancing mitochondrial calcium buffering capacity reduces aggregation of misfolded SOD1 and motor neuron cell death without extending survival in mouse models of inherited amyotrophic lateral sclerosis. J Neurosci 33, 4657–4671. https://doi.org/10.1523/JNEUROSCI.1119-12.2013

Paul, P., van den Hoorn, T., Jongsma, M.L.M., Bakker, M.J., Hengeveld, R., Janssen, L., Cresswell, P., Egan, D.A., van Ham, M., ten Brinke, A., Ovaa, H., Beijersbergen, R.L., Kuijl, C., Neefjes, J., 2011. A Genome-wide Multidimensional RNAi Screen Reveals Pathways Controlling MHC Class II Antigen Presentation. Cell 145, 268–283. https://doi.org/10.1016/j.cell.2011.03.023

Peña-Quintana, L., Llarena, M., Reyes-Suárez, D., Aldámiz-Echevarria, L., 2017. Profile of sodium phenylbutyrate granules for the treatment of urea-cycle disorders: patient perspectives. Patient Prefer Adherence 11, 1489–1496. https://doi.org/10.2147/PPA.S136754

Pensato, V., Castellotti, B., Gellera, C., Pareyson, D., Ciano, C., Nanetti, L., Salsano, E., Piscosquito, G., Sarto, E., Eoli, M., Moroni, I., Soliveri, P., Lamperti, E., Chiapparini, L., Di Bella, D., Taroni, F., Mariotti, C., 2014. Overlapping phenotypes in complex spastic paraplegias SPG11, SPG15, SPG35 and SPG48. Brain 137, 1907–1920. https://doi.org/10.1093/brain/awu121

Perlson, E., Maday, S., Fu, M., Moughamian, A.J., Holzbaur, E.L.F., 2010. Retrograde axonal transport: pathways to cell death? Trends in Neurosciences 33, 335–344. https://doi.org/10.1016/j.tins.2010.03.006

Pitt, D., Werner, P., Raine, C.S., 2000. Glutamate excitotoxicity in a model of multiple sclerosis. Nat Med 6, 67–70. https://doi.org/10.1038/71555

Pizzino, G., Irrera, N., Cucinotta, M., Pallio, G., Mannino, F., Arcoraci, V., Squadrito, F., Altavilla, D., Bitto, A., 2017. Oxidative Stress: Harms and Benefits for Human Health. Oxid Med Cell Longev 2017, 8416763. https://doi.org/10.1155/2017/8416763

Pizzo, E., Sarcinelli, C., Sheng, J., Fusco, S., Formiggini, F., Netti, P., Yu, W., D'Alessio, G., Hu, G., 2013. Ribonuclease/angiogenin inhibitor 1 regulates stress-induced subcellular localization of angiogenin to control growth and survival. J Cell Sci 126, 4308–4319. https://doi.org/10.1242/jcs.134551

Polymenidou, M., Lagier-Tourenne, C., Hutt, K.R., Huelga, S.C., Moran, J., Liang, T.Y., Ling, S.-C., Sun, E., Wancewicz, E., Mazur, C., Kordasiewicz, H., Sedaghat, Y., Donohue, J.P., Shiue, L., Bennett, C.F., Yeo, G.W., Cleveland, D.W., 2011. Long pre-mRNA depletion and RNA missplicing contribute to neuronal vulnerability from loss of TDP-43. Nat Neurosci 14, 459–468. https://doi.org/10.1038/nn.2779

Prakash, P., Gorfe, A.A., 2013. Lessons from computer simulations of Ras proteins in solution and in membrane. Biochim Biophys Acta 1830, 5211–5218. https://doi.org/10.1016/j.bbagen.2013.07.024

Punjani, A., Rubinstein, J.L., Fleet, D.J., Brubaker, M.A., 2017. cryoSPARC: algorithms for rapid unsupervised cryo-EM structure determination. Nat Methods 14, 290–296. https://doi.org/10.1038/nmeth.4169

Qu, L., Pan, C., He, S.-M., Lang, B., Gao, G.-D., Wang, X.-L., Wang, Y., 2019. The Ras Superfamily of Small GTPases in Non-neoplastic Cerebral Diseases. Frontiers in Molecular Neuroscience 12.

Quaegebeur, A., Glaria, I., Lashley, T., Isaacs, A.M., 2020. Soluble and insoluble dipeptide repeat protein measurements in C9orf72-frontotemporal dementia brains show regional differential solubility and correlation of poly-GR with clinical severity. Acta Neuropathologica Communications 8, 184. https://doi.org/10.1186/s40478-020-01036-y

Rao, V.S., Srinivas, K., Sujini, G.N., Kumar, G.N.S., 2014. Protein-Protein Interaction Detection: Methods and Analysis. Int J Proteomics 2014, 147648. https://doi.org/10.1155/2014/147648

Ratovitski, T., Corson, L.B., Strain, J., Wong, P., Cleveland, D.W., Culotta, V.C., Borchelt, D.R., 1999. Variation in the Biochemical/Biophysical Properties of Mutant Superoxide Dismutase 1 Enzymes and the Rate of Disease Progression in Familial Amyotrophic Lateral Sclerosis Kindreds. Human Molecular Genetics 8, 1451–1460. https://doi.org/10.1093/hmg/8.8.1451

Rayner, S.L., Cheng, F., Hogan, A.L., Grima, N., Yang, S., Ke, Y.D., Au, C.G., Morsch, M., De Luca, A., Davidson, J.M., Molloy, M.P., Shi, B., Ittner, L.M., Blair, I., Chung, R.S., Lee, A., 2021. ALS/FTD-causing mutation in cyclin F causes the dysregulation of SFPQ. Hum Mol Genet 30, 971–984. https://doi.org/10.1093/hmg/ddab073

Reaume, A.G., Elliott, J.L., Hoffman, E.K., Kowall, N.W., Ferrante, R.J., Siwek, D.F., Wilcox, H.M., Flood, D.G., Beal, M.F., Brown, R.H., Scott, R.W., Snider, W.D., 1996. Motor neurons in Cu/Zn superoxide dismutase-deficient mice develop normally but exhibit enhanced cell death after axonal injury. Nat Genet 13, 43–47. https://doi.org/10.1038/ng0596-43

Reddy, K., Zamiri, B., Stanley, S.Y.R., Macgregor, R.B., Pearson, C.E., 2013. The disease-associated r(GGGGCC)n repeat from the C9orf72 gene forms tract length-dependent uni- and multimolecular RNA G-quadruplex structures. J Biol Chem 288, 9860–9866. https://doi.org/10.1074/jbc.C113.452532

Renton, A.E., Chiò, A., Traynor, B.J., 2014. State of play in amyotrophic lateral sclerosis genetics. Nat Neurosci 17, 17–23. https://doi.org/10.1038/nn.3584

Renton, A.E., Majounie, E., Waite, A., Simón-Sánchez, J., Rollinson, S., Gibbs, J.R., Schymick, J.C., Laaksovirta, H., van Swieten, J.C., Myllykangas, L., Kalimo, H., Paetau, A., Abramzon, Y., Remes, A.M., Kaganovich, A., Scholz, S.W., Duckworth, J., Ding, J., Harmer, D.W., Hernandez, D.G., Johnson, J.O., Mok, K., Ryten, M., Trabzuni, D., Guerreiro, R.J., Orrell, R.W., Neal, J., Murray, A., Pearson, J., Jansen, I.E., Sondervan, D., Seelaar, H., Blake, D., Young, K., Halliwell, N., Callister, J.B., Toulson, G., Richardson, A., Gerhard, A., Snowden, J., Mann, D., Neary, D., Nalls, M.A., Peuralinna, T., Jansson, L., Isoviita, V.-M., Kaivorinne, A.-L., Hölttä-Vuori, M., Ikonen, E., Sulkava, R., Benatar, M., Wuu, J., Chiò, A., Restagno, G., Borghero, G., Sabatelli, M., Heckerman, D., Rogaeva, E., Zinman, L., Rothstein, J.D., Sendtner, M., Drepper, C., Eichler, E.E., Alkan, C., Abdullaev, Z., Pack, S.D., Dutra, A., Pak, E., Hardy, J., Singleton, A., Williams, N.M., Heutink, P., Pickering-Brown, S., Morris, H.R., Tienari, P.J., Traynor, B.J., 2011. A Hexanucleotide Repeat Expansion in C9ORF72 Is the Cause of Chromosome 9p21-Linked ALS-FTD. Neuron 72, 257–268. https://doi.org/10.1016/j.neuron.2011.09.010

Riemslagh, F.W., Verhagen, R.F.M., van der Toorn, E.C., Smits, D.J., Quint, W.H., van der Linde, H.C., van Ham, T.J., Willemsen, R., 2021. Reduction of oxidative stress suppresses poly-GR-mediated toxicity in zebrafish embryos. Dis Model Mech 14, dmm049092. https://doi.org/10.1242/dmm.049092

Ringholz, G.M., Appel, S.H., Bradshaw, M., Cooke, N.A., Mosnik, D.M., Schulz, P.E., 2005. Prevalence and patterns of cognitive impairment in sporadic ALS. Neurology 65, 586–590. https://doi.org/10.1212/01.wnl.0000172911.39167.b6

Rizzu, P., Blauwendraat, C., Heetveld, S., Lynes, E.M., Castillo-Lizardo, M., Dhingra, A., Pyz, E., Hobert, M., Synofzik, M., Simón-Sánchez, J., Francescatto, M., Heutink, P., 2016. C9orf72 is differentially expressed in the central nervous system and myeloid cells and consistently reduced in C9orf72, MAPT and GRN mutation carriers. Acta Neuropathol Commun 4, 37. https://doi.org/10.1186/s40478-016-0306-7

Roberts, R., Ktistakis, N.T., 2013. Omegasomes: PI3P platforms that manufacture autophagosomes. Essays Biochem 55, 17–27. https://doi.org/10.1042/bse0550017

Roberts, T.C., Langer, R., Wood, M.J.A., 2020. Advances in oligonucleotide drug delivery. Nat Rev Drug Discov 19, 673–694. https://doi.org/10.1038/s41573-020-0075-7

Roggenbuck, J., Quick, A., Kolb, S.J., 2017. Genetic testing and genetic counseling for amyotrophic lateral sclerosis: an update for clinicians. Genetics in Medicine 19, 267–274. https://doi.org/10.1038/gim.2016.107

Rohrer, J.D., Guerreiro, R., Vandrovcova, J., Uphill, J., Reiman, D., Beck, J., Isaacs, A.M., Authier, A., Ferrari, R., Fox, N.C., Mackenzie, I.R.A., Warren, J.D., de Silva, R., Holton, J., Revesz, T., Hardy, J., Mead, S., Rossor, M.N., 2009. The heritability and genetics of frontotemporal lobar degeneration. Neurology 73, 1451–1456. https://doi.org/10.1212/WNL.0b013e3181bf997a

Rong, Y., Liu, M., Ma, L., Du, W., Zhang, H., Tian, Y., Cao, Z., Li, Y., Ren, H., Zhang, C., Li, L., Chen, S., Xi, J., Yu, L., 2012. Clathrin and phosphatidylinositol-4,5-bisphosphate regulate autophagic lysosome reformation. Nat Cell Biol 14, 924–934. https://doi.org/10.1038/ncb2557

Rong, Y., McPhee, C.K., Deng, S., Huang, L., Chen, L., Liu, M., Tracy, K., Baehrecke, E.H., Yu, L., Lenardo, M.J., 2011. Spinster is required for autophagic lysosome reformation and mTOR reactivation following starvation. Proceedings of the National Academy of Sciences 108, 7826–7831. https://doi.org/10.1073/pnas.1013800108

Rosen, D.R., Siddique, T., Patterson, D., Figlewicz, D.A., Sapp, P., Hentati, A., Donaldson, D., Goto, J., O'Regan, J.P., Deng, H.X., 1993. Mutations in Cu/Zn superoxide dismutase gene are associated with familial amyotrophic lateral sclerosis. Nature 362, 59–62. https://doi.org/10.1038/362059a0

Rothstein, J.D., Dykes-Hoberg, M., Pardo, C.A., Bristol, L.A., Jin, L., Kuncl, R.W., Kanai, Y., Hediger, M.A., Wang, Y., Schielke, J.P., Welty, D.F., 1996. Knockout of Glutamate Transporters Reveals a Major Role for Astroglial Transport in Excitotoxicity and Clearance of Glutamate. Neuron 16, 675–686. https://doi.org/10.1016/S0896-6273(00)80086-0

Rudnick, N.D., Griffey, C.J., Guarnieri, P., Gerbino, V., Wang, X., Piersaint, J.A., Tapia, J.C., Rich, M.M., Maniatis, T., 2017. Distinct roles for motor neuron autophagy early and late in the SOD1G93A mouse model of ALS. Proc Natl Acad Sci U S A 114, E8294–E8303. https://doi.org/10.1073/pnas.1704294114

Ruegsegger, C., Saxena, S., 2016. Proteostasis impairment in ALS. Brain Res 1648, 571–579. https://doi.org/10.1016/j.brainres.2016.03.032

Russell, R.C., Tian, Y., Yuan, H., Park, H.W., Chang, Y.-Y., Kim, J., Kim, H., Neufeld, T.P., Dillin, A., Guan, K.-L., 2013. ULK1 induces autophagy by phosphorylating Beclin-1 and

activating Vps34 lipid kinase. Nat Cell Biol 15, 741–750. https://doi.org/10.1038/ncb2757

Rutter-Locher, Z., Turner, M.R., Leigh, P.N., Al-Chalabi, A., 2016. Analysis of terms used for the diagnosis and classification of amyotrophic lateral sclerosis and motor neuron disease. Amyotrophic Lateral Sclerosis and Frontotemporal Degeneration 17, 600–604. https://doi.org/10.1080/21678421.2016.1181766

Ryan, T.A., Tumbarello, D.A., 2018. Optineurin: A Coordinator of Membrane-Associated Cargo Trafficking and Autophagy. Frontiers in Immunology 9.

Ryu, H., Smith, K., Camelo, S.I., Carreras, I., Lee, J., Iglesias, A.H., Dangond, F., Cormier, K.A., Cudkowicz, M.E., Brown, R.H., Ferrante, R.J., 2005. Sodium phenylbutyrate prolongs survival and regulates expression of anti-apoptotic genes in transgenic amyotrophic lateral sclerosis mice. J Neurochem 93, 1087–1098. https://doi.org/10.1111/j.1471-4159.2005.03077.x

Saberi, S., Stauffer, J.E., Jiang, J., Garcia, S.D., Taylor, A.E., Schulte, D., Ohkubo, T., Schloffman, C.L., Maldonado, M., Baughn, M., Rodriguez, M.J., Pizzo, D., Cleveland, D., Ravits, J., 2018. Sense-encoded poly-GR dipeptide repeat proteins correlate to neurodegeneration and uniquely co-localize with TDP-43 in dendrites of repeat-expanded C9orf72 amyotrophic lateral sclerosis. Acta Neuropathol 135, 459–474. https://doi.org/10.1007/s00401-017-1793-8

Saffi, G.T., Botelho, R.J., 2019. Lysosome Fission: Planning for an Exit. Trends in Cell Biology 29, 635–646. https://doi.org/10.1016/j.tcb.2019.05.003

Sagona, A.P., Nezis, I.P., Pedersen, N.M., Liestøl, K., Poulton, J., Rusten, T.E., Skotheim, R.I., Raiborg, C., Stenmark, H., 2010. PtdIns(3)P controls cytokinesis through KIF13A-mediated recruitment of FYVE-CENT to the midbody. Nat Cell Biol 12, 362–371. https://doi.org/10.1038/ncb2036

Sancak, Y., Peterson, T.R., Shaul, Y.D., Lindquist, R.A., Thoreen, C.C., Bar-Peled, L., Sabatini, D.M., 2008. The Rag GTPases Bind Raptor and Mediate Amino Acid Signaling to mTORC1. Science 320, 1496–1501. https://doi.org/10.1126/science.1157535

Sareen, D., O'Rourke, J.G., Meera, P., Muhammad, A.K.M.G., Grant, S., Simpkinson, M., Bell, S., Carmona, S., Ornelas, L., Sahabian, A., Gendron, T., Petrucelli, L., Baughn, M., Ravits, J., Harms, M.B., Rigo, F., Bennett, C.F., Otis, T.S., Svendsen, C.N., Baloh, R.H., 2013. Targeting RNA foci in iPSC-derived motor neurons from ALS patients with C9ORF72 repeat expansion. Sci Transl Med 5, 208ra149. https://doi.org/10.1126/scitranslmed.3007529

Sasaki, S., Iwata, M., 1996. Impairment of fast axonal transport in the proximal axons of anterior horn neurons in amyotrophic lateral sclerosis. Neurology 47, 535–540. https://doi.org/10.1212/WNL.47.2.535

Sawa-Makarska, J., Baumann, V., Coudevylle, N., von Bülow, S., Nogellova, V., Abert, C., Schuschnig, M., Graef, M., Hummer, G., Martens, S., 2020. Reconstitution of autophagosome nucleation defines Atg9 vesicles as seeds for membrane formation. Science 369, eaaz7714. https://doi.org/10.1126/science.aaz7714

Saxton, R.A., Sabatini, D.M., 2017. mTOR Signaling in Growth, Metabolism, and Disease. Cell 168, 960–976. https://doi.org/10.1016/j.cell.2017.02.004

Schipper, L.J., Raaphorst, J., Aronica, E., Baas, F., de Haan, R., de Visser, M., Troost, D., 2016. Prevalence of brain and spinal cord inclusions, including dipeptide repeat proteins, in patients with the C9ORF72 hexanucleotide repeat expansion: a systematic

neuropathological review. Neuropathol Appl Neurobiol 42, 547–560. https://doi.org/10.1111/nan.12284

Schludi, M.H., Becker, L., Garrett, L., Gendron, T.F., Zhou, Q., Schreiber, F., Popper, B., Dimou, L., Strom, T.M., Winkelmann, J., von Thaden, A., Rentzsch, K., May, S., Michaelsen, M., Schwenk, B.M., Tan, J., Schoser, B., Dieterich, M., Petrucelli, L., Hölter, S.M., Wurst, W., Fuchs, H., Gailus-Durner, V., de Angelis, M.H., Klopstock, T., Arzberger, T., Edbauer, D., 2017. Spinal poly-GA inclusions in a C9orf72 mouse model trigger motor deficits and inflammation without neuron loss. Acta Neuropathol 134, 241–254. https://doi.org/10.1007/s00401-017-1711-0

Schulze, R.J., Weller, S.G., Schroeder, B., Krueger, E.W., Chi, S., Casey, C.A., McNiven, M.A., 2013. Lipid droplet breakdown requires dynamin 2 for vesiculation of autolysosomal tubules in hepatocytes. J Cell Biol 203, 315–326. https://doi.org/10.1083/jcb.201306140

Schwartz, J.C., Ebmeier, C.C., Podell, E.R., Heimiller, J., Taatjes, D.J., Cech, T.R., 2012. FUS binds the CTD of RNA polymerase II and regulates its phosphorylation at Ser2. Genes Dev. 26, 2690–2695. https://doi.org/10.1101/gad.204602.112

Sellier, C., Campanari, M., Julie Corbier, C., Gaucherot, A., Kolb-Cheynel, I., Oulad-Abdelghani, M., Ruffenach, F., Page, A., Ciura, S., Kabashi, E., Charlet-Berguerand, N., 2016. Loss of C9ORF72 impairs autophagy and synergizes with polyQ Ataxin-2 to induce motor neuron dysfunction and cell death. EMBO J 35, 1276–1297. https://doi.org/10.15252/embj.201593350

Shaid, S., Brandts, C.H., Serve, H., Dikic, I., 2013. Ubiquitination and selective autophagy. Cell Death Differ 20, 21–30. https://doi.org/10.1038/cdd.2012.72

Shao, Q., Yang, M., Liang, Chen, Ma, L., Zhang, W., Jiang, Z., Luo, J., Lee, J.-K., Liang, Chengyu, Chen, J.-F., 2020. C9orf72 and smcr8 mutant mice reveal MTORC1 activation due to impaired lysosomal degradation and exocytosis. Autophagy 16, 1635–1650. https://doi.org/10.1080/15548627.2019.1703353

Shaw, P.J., Forrest, V., Ince, P.G., Richardson, J.P., Wastell, H.J., 1995. CSF and Plasma Amino Acid Levels in Motor Neuron Disease: Elevation of CSF Glutamate in a Subset of Patients. Neurodegeneration 4, 209–216. https://doi.org/10.1006/neur.1995.0026

Shefner, J.M., Al-Chalabi, A., Baker, M.R., Cui, L.-Y., de Carvalho, M., Eisen, A., Grosskreutz, J., Hardiman, O., Henderson, R., Matamala, J.M., Mitsumoto, H., Paulus, W., Simon, N., Swash, M., Talbot, K., Turner, M.R., Ugawa, Y., van den Berg, L.H., Verdugo, R., Vucic, S., Kaji, R., Burke, D., Kiernan, M.C., 2020. A proposal for new diagnostic criteria for ALS. Clin Neurophysiol 131, 1975–1978. https://doi.org/10.1016/j.clinph.2020.04.005

Shen, K., Huang, R.K., Brignole, E.J., Condon, K.J., Valenstein, M.L., Chantranupong, L., Bomaliyamu, A., Choe, A., Hong, C., Yu, Z., Sabatini, D.M., 2018. Architecture of the human GATOR1 and GATOR1-Rag GTPases complexes. Nature 556, 64–69. https://doi.org/10.1038/nature26158

Shen, K., Rogala, K.B., Chou, H.-T., Huang, R.K., Yu, Z., Sabatini, D.M., 2019. Cryo-EM Structure of the Human FLCN-FNIP2-Rag-Ragulator Complex. Cell 179, 1319-1329.e8. https://doi.org/10.1016/j.cell.2019.10.036

Shi, Y., Lin, S., Staats, K.A., Li, Y., Chang, W.-H., Hung, S.-T., Hendricks, E., Linares, G.R., Wang, Y., Son, E.Y., Wen, X., Kisler, K., Wilkinson, B., Menendez, L., Sugawara, T., Woolwine, P., Huang, M., Cowan, M.J., Ge, B., Koutsodendris, N., Sandor, K.P., Komberg, J., Vangoor, V.R., Senthilkumar, K., Hennes, V., Seah, C., Nelson, A.R., Cheng, T.-Y., Lee,

S.-J.J., August, P.R., Chen, J.A., Wisniewski, N., Hanson-Smith, V., Belgard, T.G., Zhang, A., Coba, M., Grunseich, C., Ward, M.E., van den Berg, L.H., Pasterkamp, R.J., Trotti, D., Zlokovic, B.V., Ichida, J.K., 2018. Haploinsufficiency leads to neurodegeneration in C9ORF72 ALS/FTD human induced motor neurons. Nat Med 24, 313–325. https://doi.org/10.1038/nm.4490

Shu, L., Sun, Q., Zhang, Y., Xu, Q., Guo, J., Yan, X., Tang, B., 2016. The Association between C9orf72 Repeats and Risk of Alzheimer's Disease and Amyotrophic Lateral Sclerosis: A Meta-Analysis. Parkinsons Dis 2016, 5731734. https://doi.org/10.1155/2016/5731734

Silverman, J.M., Christy, D., Shyu, C.C., Moon, K.-M., Fernando, S., Gidden, Z., Cowan, C.M., Ban, Y., Stacey, R.G., Grad, L.I., McAlary, L., Mackenzie, I.R., Foster, L.J., Cashman, N.R., 2019. CNS-derived extracellular vesicles from superoxide dismutase 1 (SOD1)G93A ALS mice originate from astrocytes and neurons and carry misfolded SOD1. Journal of Biological Chemistry 294, 3744–3759. https://doi.org/10.1074/jbc.RA118.004825

Simpson, C.L., Lemmens, R., Miskiewicz, K., Broom, W.J., Hansen, V.K., van Vught, P.W.J., Landers, J.E., Sapp, P., Van Den Bosch, L., Knight, J., Neale, B.M., Turner, M.R., Veldink, J.H., Ophoff, R.A., Tripathi, V.B., Beleza, A., Shah, M.N., Proitsi, P., Van Hoecke, A., Carmeliet, P., Horvitz, H.R., Leigh, P.N., Shaw, C.E., van den Berg, L.H., Sham, P.C., Powell, J.F., Verstreken, P., Brown, R.H., Robberecht, W., Al-Chalabi, A., 2009. Variants of the elongator protein 3 (ELP3) gene are associated with motor neuron degeneration. Hum Mol Genet 18, 472–481. https://doi.org/10.1093/hmg/ddn375

Skourti-Stathaki, K., Proudfoot, N.J., Gromak, N., 2011. Human senataxin resolves RNA/DNA hybrids formed at transcriptional pause sites to promote Xrn2-dependent termination. Mol Cell 42, 794–805. https://doi.org/10.1016/j.molcel.2011.04.026

Słabicki, M., Theis, M., Krastev, D.B., Samsonov, S., Mundwiller, E., Junqueira, M., Paszkowski-Rogacz, M., Teyra, J., Heninger, A.-K., Poser, I., Prieur, F., Truchetto, J., Confavreux, C., Marelli, C., Durr, A., Camdessanche, J.P., Brice, A., Shevchenko, A., Pisabarro, M.T., Stevanin, G., Buchholz, F., 2010. A Genome-Scale DNA Repair RNAi Screen Identifies SPG48 as a Novel Gene Associated with Hereditary Spastic Paraplegia. PLoS Biol 8, e1000408. https://doi.org/10.1371/journal.pbio.1000408

Smith, B.N., Ticozzi, N., Fallini, C., Gkazi, A.S., Topp, S., Kenna, K.P., Scotter, E.L., Kost, J., Keagle, P., Miller, J.W., Calini, D., Vance, C., Danielson, E.W., Troakes, C., Tiloca, C., Al-Sarraj, S., Lewis, E.A., King, A., Colombrita, C., Pensato, V., Castellotti, B., de Belleroche, J., Baas, F., ten Asbroek, A.L., Sapp, P.C., McKenna-Yasek, D., McLaughlin, R.L., Polak, M., Asress, S., Esteban-Pérez, J., Muñoz-Blanco, J.L., Simpson, M., D'Alfonso, S., Mazzini, L., Comi, G.P., Del Bo, R., Ceroni, M., Gagliardi, S., Querin, G., Bertolin, C., van Rheenen, W., Diekstra, F.P., Lauria, G., Duga, S., Corti, S., Cereda, C., Corrado, L., Sorarù, G., Morrison, K.E., Williams, K.L., Nicholson, G.A., Blair, I.P., Dion, P.A., Leblond, C.S., Rouleau, G.A., Hardiman, O., Veldink, J.H., van den Berg, L.H., Al-Chalabi, A., Pall, H., Shaw, P.J., Turner, M.R., Talbot, K., Taroni, F., García-Redondo, A., Wu, Z., Glass, J.D., Gellera, C., Ratti, A., Brown, R.H., Silani, V., Shaw, C.E., Landers, J.E., 2014. Exome-wide Rare Variant Analysis Identifies TUBA4A Mutations Associated with Familial ALS. Neuron 84, 324–331. https://doi.org/10.1016/j.neuron.2014.09.027

Soragni, E., Petrosyan, L., Rinkoski, T.A., Wieben, E.D., Baratz, K.H., Fautsch, M.P., Gottesfeld, J.M., 2018. Repeat-Associated Non-ATG (RAN) Translation in Fuchs' Endothelial Corneal Dystrophy. Invest Ophthalmol Vis Sci 59, 1888–1896. https://doi.org/10.1167/iovs.17-23265

Sorenson, E.J., Windbank, A.J., Mandrekar, J.N., Bamlet, W.R., Appel, S.H., Armon, C., Barkhaus, P.E., Bosch, P., Boylan, K., David, W.S., Feldman, E., Glass, J., Gutmann, L., Katz, J., King, W., Luciano, C.A., McCluskey, L.F., Nash, S., Newman, D.S., Pascuzzi, R.M., Pioro, E., Sams, L.J., Scelsa, S., Simpson, E.P., Subramony, S.H., Tiryaki, E., Thornton, C.A., 2008. Subcutaneous IGF-1 is not beneficial in 2-year ALS trial. Neurology 71, 1770–1775. https://doi.org/10.1212/01.wnl.0000335970.78664.36

Sreedharan, J., Blair, I.P., Tripathi, V.B., Hu, X., Vance, C., Rogelj, B., Ackerley, S., Durnall, J.C., Williams, K.L., Buratti, E., Baralle, F., de Belleroche, J., Mitchell, J.D., Leigh, P.N., Al-Chalabi, A., Miller, C.C., Nicholson, G., Shaw, C.E., 2008. TDP-43 mutations in familial and sporadic amyotrophic lateral sclerosis. Science 319, 1668–1672. https://doi.org/10.1126/science.1154584

Sridhar, S., Patel, B., Aphkhazava, D., Macian, F., Santambrogio, L., Shields, D., Cuervo, A.M., 2013. The lipid kinase PI4KIIIβ preserves lysosomal identity. The EMBO Journal 32, 324–339. https://doi.org/10.1038/emboj.2012.341

Staats, K.A., Hernandez, S., Schönefeldt, S., Bento-Abreu, A., Dooley, J., Van Damme, P., Liston, A., Robberecht, W., Van Den Bosch, L., 2013. Rapamycin increases survival in ALS mice lacking mature lymphocytes. Molecular Neurodegeneration 8, 31. https://doi.org/10.1186/1750-1326-8-31

Stevanin, G., Santorelli, F.M., Azzedine, H., Coutinho, P., Chomilier, J., Denora, P.S., Martin, E., Ouvrard-Hernandez, A.-M., Tessa, A., Bouslam, N., Lossos, A., Charles, P., Loureiro, J.L., Elleuch, N., Confavreux, C., Cruz, V.T., Ruberg, M., Leguern, E., Grid, D., Tazir, M., Fontaine, B., Filla, A., Bertini, E., Durr, A., Brice, A., 2007. Mutations in SPG11, encoding spatacsin, are a major cause of spastic paraplegia with thin corpus callosum. Nat Genet 39, 366–372. https://doi.org/10.1038/ng1980

Strong, M.J., 2010. The evidence for altered RNA metabolism in amyotrophic lateral sclerosis (ALS). J Neurol Sci 288, 1–12. https://doi.org/10.1016/j.jns.2009.09.029

Su, M.-Y., Fromm, S.A., Remis, J., Toso, D.B., Hurley, J.H., 2021. Structural basis for the ARF GAP activity and specificity of the C9orf72 complex. Nat Commun 12, 3786. https://doi.org/10.1038/s41467-021-24081-0

Su, M.-Y., Fromm, S.A., Zoncu, R., Hurley, J.H., 2020. Structure of the C9orf72 Arf GAP complex haploinsufficient in ALS and FTD. Nature 585, 251–255. https://doi.org/10.1038/s41586-020-2633-x

Sudria-Lopez, E., Koppers, M., de Wit, M., van der Meer, C., Westeneng, H.-J., Zundel, C.A.C., Youssef, S.A., Harkema, L., de Bruin, A., Veldink, J.H., van den Berg, L.H., Pasterkamp, R.J., 2016. Full ablation of C9orf72 in mice causes immune system-related pathology and neoplastic events but no motor neuron defects. Acta Neuropathol 132, 145–147. https://doi.org/10.1007/s00401-016-1581-x

Suh, E., Lee, E.B., Neal, D., Wood, E.M., Toledo, J.B., Rennert, L., Irwin, D.J., McMillan, C.T., Krock, B., Elman, L.B., McCluskey, L.F., Grossman, M., Xie, S.X., Trojanowski, J.Q., Van Deerlin, V.M., 2015. Semi-automated quantification of C9orf72 expansion size reveals inverse correlation between hexanucleotide repeat number and disease duration in frontotemporal degeneration. Acta Neuropathol 130, 363–372. https://doi.org/10.1007/s00401-015-1445-9

Suhr, O.B., Coelho, T., Buades, J., Pouget, J., Conceicao, I., Berk, J., Schmidt, H., Waddington-Cruz, M., Campistol, J.M., Bettencourt, B.R., Vaishnaw, A., Gollob, J., Adams, D., 2015. Efficacy and safety of patisiran for familial amyloidotic polyneuropathy: a phase II

multi-dose study. Orphanet Journal of Rare Diseases 10, 109. https://doi.org/10.1186/s13023-015-0326-6

Sullivan, P.M., Zhou, X., Robins, A.M., Paushter, D.H., Kim, D., Smolka, M.B., Hu, F., 2016. The ALS/FTLD associated protein C9orf72 associates with SMCR8 and WDR41 to regulate the autophagy-lysosome pathway. Acta Neuropathol Commun 4, 51. https://doi.org/10.1186/s40478-016-0324-5

Sun, C.N., Araoz, C., Lucas, G., Morgan, P.N., White, H.J., 1975. Amyotrophic lateral sclerosis. Inclusion bodies in a case of the classic sporadic form. Ann Clin Lab Sci 5, 38–44.

Swaminathan, A., Bouffard, M., Liao, M., Ryan, S., Callister, J.B., Pickering-Brown, S.M., Armstrong, G.A.B., Drapeau, P., 2018. Expression of C9orf72-related dipeptides impairs motor function in a vertebrate model. Hum Mol Genet 27, 1754–1762. https://doi.org/10.1093/hmg/ddy083

Swinnen, B., Bento-Abreu, A., Gendron, T.F., Boeynaems, S., Bogaert, E., Nuyts, R., Timmers, M., Scheveneels, W., Hersmus, N., Wang, J., Mizielinska, S., Isaacs, A.M., Petrucelli, L., Lemmens, R., Van Damme, P., Van Den Bosch, L., Robberecht, W., 2018. A zebrafish model for C9orf72 ALS reveals RNA toxicity as a pathogenic mechanism. Acta Neuropathol 135, 427–443. https://doi.org/10.1007/s00401-017-1796-5

Swinnen, B., Robberecht, W., 2014. The phenotypic variability of amyotrophic lateral sclerosis. Nat Rev Neurol 10, 661–670. https://doi.org/10.1038/nrneurol.2014.184

Tang, D., Sheng, J., Xu, L., Zhan, X., Liu, J., Jiang, H., Shu, X., Liu, X., Zhang, T., Jiang, L., Zhou, C., Li, W., Cheng, W., Li, Z., Wang, K., Lu, K., Yan, C., Qi, S., 2020. Cryo-EM structure of C9ORF72–SMCR8–WDR41 reveals the role as a GAP for Rab8a and Rab11a. Proc Natl Acad Sci U S A 117, 9876–9883. https://doi.org/10.1073/pnas.2002110117

Tang, X., Toro, A., T.G., S., Gao, J., Chalk, J., Oskarsson, B.E., Zhang, K., 2020. Divergence, Convergence, and Therapeutic Implications: A Cell Biology Perspective of C9ORF72-ALS/FTD. Molecular Neurodegeneration 15, 34. https://doi.org/10.1186/s13024-020-00383-7

Tao, Z., Wang, H., Xia, Q., Li, Ke, Li, Kai, Jiang, X., Xu, G., Wang, G., Ying, Z., 2015. Nucleolar stress and impaired stress granule formation contribute to C9orf72 RAN translation-induced cytotoxicity. Hum Mol Genet 24, 2426–2441. https://doi.org/10.1093/hmg/ddv005

Teyssou, E., Chartier, L., Amador, M.-D.-M., Lam, R., Lautrette, G., Nicol, M., Machat, S., Da Barroca, S., Moigneu, C., Mairey, M., Larmonier, T., Saker, S., Dussert, C., Forlani, S., Fontaine, B., Seilhean, D., Bohl, D., Boillée, S., Meininger, V., Couratier, P., Salachas, F., Stevanin, G., Millecamps, S., 2017. Novel UBQLN2 mutations linked to amyotrophic lateral sclerosis and atypical hereditary spastic paraplegia phenotype through defective HSP70-mediated proteolysis. Neurobiology of Aging 58, 239.e11-239.e20. https://doi.org/10.1016/j.neurobiolaging.2017.06.018

Theile, J.W., Cummins, T.R., 2011. Inhibition of Navβ4 Peptide-Mediated Resurgent Sodium Currents in Nav1.7 Channels by Carbamazepine, Riluzole, and Anandamide. Mol Pharmacol 80, 724–734. https://doi.org/10.1124/mol.111.072751

Therrien, M., Rouleau, G.A., Dion, P.A., Parker, J.A., 2013. Deletion of C9ORF72 Results in Motor Neuron Degeneration and Stress Sensitivity in C. elegans. PLoS One 8, e83450. https://doi.org/10.1371/journal.pone.0083450

Thompson, R.F., Walker, M., Siebert, C.A., Muench, S.P., Ranson, N.A., 2016. An introduction to sample preparation and imaging by cryo-electron microscopy for structural biology. Methods 100, 3–15. https://doi.org/10.1016/j.ymeth.2016.02.017

Thurston, T.L.M., Wandel, M.P., von Muhlinen, N., Foeglein, A., Randow, F., 2012. Galectin 8 targets damaged vesicles for autophagy to defend cells against bacterial invasion. Nature 482, 414–418. https://doi.org/10.1038/nature10744

Todd, P.K., Oh, S.Y., Krans, A., He, F., Sellier, C., Frazer, M., Renoux, A.J., Chen, K., Scaglione, K.M., Basrur, V., Elenitoba-Johnson, K., Vonsattel, J.P., Louis, E.D., Sutton, M.A., Taylor, J.P., Mills, R.E., Charlet-Berguerand, N., Paulson, H.L., 2013. CGG Repeat-Associated Translation Mediates Neurodegeneration in Fragile X Tremor Ataxia Syndrome. Neuron 78, 440–455. https://doi.org/10.1016/j.neuron.2013.03.026

Todd, T.W., McEachin, Z.T., Chew, J., Burch, A.R., Jansen-West, K., Tong, J., Yue, M., Song, Y., Castanedes-Casey, M., Kurti, A., Dunmore, J.H., Fryer, J.D., Zhang, Y.-J., Millan, B.S., Bautista, S.T., Arias, M., Dickson, D., Gendron, T.F., Sobrido, M.-J., Disney, M.D., Bassell, G.J., Rossoll, W., Petrucelli, L., 2020. Hexanucleotide Repeat Expansions in c9FTD/ALS and SCA36 Confer Selective Patterns of Neurodegeneration In Vivo. Cell Rep 31, 107616. https://doi.org/10.1016/j.celrep.2020.107616

Topp, J.D., Gray, N.W., Gerard, R.D., Horazdovsky, B.F., 2004. Alsin Is a Rab5 and Rac1 Guanine Nucleotide Exchange Factor*. Journal of Biological Chemistry 279, 24612–24623. https://doi.org/10.1074/jbc.M313504200

Tran, H., Almeida, S., Moore, J., Gendron, T.F., Chalasani, U., Lu, Y., Du, X., Nickerson, J.A., Petrucelli, L., Weng, Z., Gao, F.-B., 2015. Differential Toxicity of Nuclear RNA Foci versus Dipeptide Repeat Proteins in a Drosophila Model of C9ORF72 FTD/ALS. Neuron 87, 1207–1214. https://doi.org/10.1016/j.neuron.2015.09.015

Traub, L.M., Bannykh, S.I., Rodel, J.E., Aridor, M., Balch, W.E., Kornfeld, S., 1996. AP-2-containing clathrin coats assemble on mature lysosomes. Journal of Cell Biology 135, 1801–1814. https://doi.org/10.1083/jcb.135.6.1801

Tsai, P.-C., Liao, Y.-C., Chen, P.-L., Guo, Y.-C., Chen, Y.-H., Jih, K.-Y., Lin, K.-P., Soong, B.-W., Tsai, C.-P., Lee, Y.-C., 2018. Investigating CCNF mutations in a Taiwanese cohort with amyotrophic lateral sclerosis. Neurobiology of Aging 62, 243.e1-243.e6. https://doi.org/10.1016/j.neurobiolaging.2017.09.031

Tsukada, M., Ohsumi, Y., 1993. Isolation and characterization of autophagy-defective mutants of Saccharomyces cerevisiae. FEBS Lett 333, 169–174. https://doi.org/10.1016/0014-5793(93)80398-e

Tsun, Z.-Y., Bar-Peled, L., Chantranupong, L., Zoncu, R., Wang, T., Kim, C., Spooner, E., Sabatini, D.M., 2013. The folliculin tumor suppressor is a GAP for the RagC/D GTPases that signal amino acid levels to mTORC1. Mol Cell 52, 495–505. https://doi.org/10.1016/j.molcel.2013.09.016

Turco, E., Fracchiolla, D., Martens, S., 2020. Recruitment and Activation of the ULK1/Atg1 Kinase Complex in Selective Autophagy. J Mol Biol 432, 123–134. https://doi.org/10.1016/j.jmb.2019.07.027

Turner, M.R., Swash, M., 2015. The expanding syndrome of amyotrophic lateral sclerosis: a clinical and molecular odyssey. J Neurol Neurosurg Psychiatry 86, 667–673. https://doi.org/10.1136/jnnp-2014-308946

Ugolino, J., Ji, Y.J., Conchina, K., Chu, J., Nirujogi, R.S., Pandey, A., Brady, N.R., Hamacher-Brady, A., Wang, J., 2016. Loss of C9orf72 Enhances Autophagic Activity via

Deregulated mTOR and TFEB Signaling. PLoS Genet 12, e1006443. https://doi.org/10.1371/journal.pgen.1006443

Vaarmann, A., Kovac, S., Holmström, K.M., Gandhi, S., Abramov, A.Y., 2013. Dopamine protects neurons against glutamate-induced excitotoxicity. Cell Death Dis 4, e455–e455. https://doi.org/10.1038/cddis.2012.194

Valverde, D.P., Yu, S., Boggavarapu, V., Kumar, N., Lees, J.A., Walz, T., Reinisch, K.M., Melia, T.J., 2019. ATG2 transports lipids to promote autophagosome biogenesis. J Cell Biol 218, 1787–1798. https://doi.org/10.1083/jcb.201811139

van Blitterswijk, M., DeJesus-Hernandez, M., Niemantsverdriet, E., Murray, M.E., Heckman, M.G., Diehl, N.N., Brown, P.H., Baker, M.C., Finch, N.A., Bauer, P.O., Serrano, G., Beach, T.G., Josephs, K.A., Knopman, D.S., Petersen, R.C., Boeve, B.F., Graff-Radford, N.R., Boylan, K.B., Petrucelli, L., Dickson, D.W., Rademakers, R., 2013. Association between repeat sizes and clinical and pathological characteristics in carriers of C9ORF72 repeat expansions (Xpansize-72): a cross-sectional cohort study. The Lancet Neurology 12, 978–988. https://doi.org/10.1016/S1474-4422(13)70210-2

van Blitterswijk, M., Gendron, T.F., Baker, M.C., DeJesus-Hernandez, M., Finch, N.A., Brown, P.H., Daughrity, L.M., Murray, M.E., Heckman, M.G., Jiang, J., Lagier-Tourenne, C., Edbauer, D., Cleveland, D.W., Josephs, K.A., Parisi, J.E., Knopman, D.S., Petersen, R.C., Petrucelli, L., Boeve, B.F., Graff-Radford, N.R., Boylan, K.B., Dickson, D.W., Rademakers, R., 2015. Novel clinical associations with specific C9ORF72 transcripts in patients with repeat expansions in C9ORF72. Acta Neuropathol 130, 863–876. https://doi.org/10.1007/s00401-015-1480-6

van Blitterswijk, M., van Es, M.A., Hennekam, E.A.M., Dooijes, D., van Rheenen, W., Medic, J., Bourque, P.R., Schelhaas, H.J., van der Kooi, A.J., de Visser, M., de Bakker, P.I.W., Veldink, J.H., van den Berg, L.H., 2012. Evidence for an oligogenic basis of amyotrophic lateral sclerosis. Human Molecular Genetics 21, 3776–3784. https://doi.org/10.1093/hmg/dds199

van Es, M.A., Hardiman, O., Chio, A., Al-Chalabi, A., Pasterkamp, R.J., Veldink, J.H., van den Berg, L.H., 2017. Amyotrophic lateral sclerosis. The Lancet 390, 2084–2098. https://doi.org/10.1016/S0140-6736(17)31287-4

Van Mossevelde, S., van der Zee, J., Cruts, M., Van Broeckhoven, C., 2017. Relationship between C9orf72 repeat size and clinical phenotype. Current Opinion in Genetics & Development, Molecular and genetic bases of disease 44, 117–124. https://doi.org/10.1016/j.gde.2017.02.008

van Rheenen, W., Shatunov, A., Dekker, A.M., McLaughlin, R.L., Diekstra, F.P., Pulit, S.L., van der Spek, R.A.A., Võsa, U., de Jong, S., Robinson, M.R., Yang, J., Fogh, I., van Doormaal, P.T., Tazelaar, G.H.P., Koppers, M., Blokhuis, A.M., Sproviero, W., Jones, A.R., Kenna, K.P., van Eijk, K.R., Harschnitz, O., Schellevis, R.D., Brands, W.J., Medic, J., Menelaou, A., Vajda, A., Ticozzi, N., Lin, K., Rogelj, B., Vrabec, K., Ravnik-Glavač, M., Koritnik, B., Zidar, J., Leonardis, L., Grošelj, L.D., Millecamps, S., Salachas, F., Meininger, V., de Carvalho, M., Pinto, S., Mora, J.S., Rojas-García, R., Polak, M., Chandran, S., Colville, S., Swingler, R., Morrison, K.E., Shaw, P.J., Hardy, J., Orrell, R.W., Pittman, A., Sidle, K., Fratta, P., Malaspina, A., Topp, S., Petri, S., Abdulla, S., Drepper, C., Sendtner, M., Meyer, T., Ophoff, R.A., Staats, K.A., Wiedau-Pazos, M., Lomen-Hoerth, C., Van Deerlin, V.M., Trojanowski, J.Q., Elman, L., McCluskey, L., Basak, A.N., Tunca, C., Hamzeiy, H., Parman, Y., Meitinger, T., Lichtner, P., Radivojkov-Blagojevic, M., Andres, C.R., Maurel,

C., Bensimon, G., Landwehrmeyer, B., Brice, A., Payan, C.A.M., Saker-Delye, S., Dürr, A., Wood, N.W., Tittmann, L., Lieb, W., Franke, A., Rietschel, M., Cichon, S., Nöthen, M.M., Amouyel, P., Tzourio, C., Dartigues, J.-F., Uitterlinden, A.G., Rivadeneira, F., Estrada, K., Hofman, A., Curtis, C., Blauw, H.M., van der Kooi, A.J., de Visser, M., Goris, A., Weber, M., Shaw, C.E., Smith, B.N., Pansarasa, O., Cereda, C., Bo, R.D., Comi, G.P., D'Alfonso, S., Bertolin, C., Sorarù, G., Mazzini, L., Pensato, V., Gellera, C., Tiloca, C., Ratti, A., Calvo, A., Moglia, C., Brunetti, M., Arcuti, S., Capozzo, R., Zecca, C., Lunetta, C., Penco, S., Riva, N., Padovani, A., Filosto, M., Muller, B., Stuit, R.J., Blair, I., Zhang, K., McCann, E.P., Fifita, J.A., Nicholson, G.A., Rowe, D.B., Pamphlett, R., Kiernan, M.C., Grosskreutz, J., Witte, O.W., Ringer, T., Prell, T., Stubendorff, B., Kurth, I., Hübner, C.A., Leigh, P.N., Casale, F., Chio, A., Beghi, E., Pupillo, E., Tortelli, R., Logroscino, G., Powell, J., Ludolph, A.C., Weishaupt, J.H., Robberecht, W., Van Damme, P., Franke, L., Pers, T.H., Brown, R.H., Glass, J.D., Landers, J.E., Hardiman, O., Andersen, P.M., Corcia, P., Vourc'h, P., Silani, V., Wray, N.R., Visscher, P.M., de Bakker, P.I.W., van Es, M.A., Pasterkamp, R.J., Lewis, C.M., Breen, G., Al-Chalabi, A., van den Berg, L.H., Veldink, J.H., 2016. Genome-wide association analyses identify new risk variants and the genetic architecture of amyotrophic lateral sclerosis. Nat Genet 48, 1043–1048. https://doi.org/10.1038/ng.3622

Vance, C., Rogelj, B., Hortobágyi, T., De Vos, K.J., Nishimura, A.L., Sreedharan, J., Hu, X., Smith, B., Ruddy, D., Wright, P., Ganesalingam, J., Williams, K.L., Tripathi, V., Al-Saraj, S., Al-Chalabi, A., Leigh, P.N., Blair, I.P., Nicholson, G., de Belleroche, J., Gallo, J.-M., Miller, C.C., Shaw, C.E., 2009. Mutations in FUS, an RNA Processing Protein, Cause Familial Amyotrophic Lateral Sclerosis Type 6. Science 323, 1208–1211. https://doi.org/10.1126/science.1165942

Varga, R.-E., Khundadze, M., Damme, M., Nietzsche, S., Hoffmann, B., Stauber, T., Koch, N., Hennings, J.C., Franzka, P., Huebner, A.K., Kessels, M.M., Biskup, C., Jentsch, T.J., Qualmann, B., Braulke, T., Kurth, I., Beetz, C., Hübner, C.A., 2015. In Vivo Evidence for Lysosome Depletion and Impaired Autophagic Clearance in Hereditary Spastic Paraplegia Type SPG11. PLoS Genet 11, e1005454. https://doi.org/10.1371/journal.pgen.1005454

Velde, C.V., McDonald, K.K., Boukhedimi, Y., McAlonis-Downes, M., Lobsiger, C.S., Hadj, S.B., Zandona, A., Julien, J.-P., Shah, S.B., Cleveland, D.W., 2011. Misfolded SOD1 Associated with Motor Neuron Mitochondria Alters Mitochondrial Shape and Distribution Prior to Clinical Onset. PLOS ONE 6, e22031. https://doi.org/10.1371/journal.pone.0022031

Verde, F., Silani, V., Otto, M., 2019. Neurochemical biomarkers in amyotrophic lateral sclerosis. Current Opinion in Neurology 32, 747–757. https://doi.org/10.1097/WCO.0000000000000744

Vieira, R.T., Caixeta, L., Machado, S., Silva, A.C., Nardi, A.E., Arias-Carrión, O., Carta, M.G., 2013. Epidemiology of early-onset dementia: a review of the literature. Clin Pract Epidemiol Ment Health 9, 88–95. https://doi.org/10.2174/1745017901309010088

Viodé, A., Fournier, C., Camuzat, A., Fenaille, F., NeuroCEB Brain Bank, Latouche, M., Elahi, F., Le Ber, I., Junot, C., Lamari, F., Anquetil, V., Becher, F., Letournel, F., Vital, A., Chapon, F., Godfraind, C., Maurage, C.-A., Deramecourt, V., Meyronnet, D., Streichenberger, N., Maues de Paula, A., Rigau, V., Vandenbos-Burel, F., Duyckaerts, C., Seilhean, D., Sazdovitch, V., Milin, S., Christian Chiforeanu, D., Laquerrière, A., Lannes, B., 2018. New Antibody-Free Mass Spectrometry-Based Quantification Reveals That C9ORF72 Long

Protein Isoform Is Reduced in the Frontal Cortex of Hexanucleotide-Repeat Expansion Carriers. Frontiers in Neuroscience 12.

Wagner, T., Merino, F., Stabrin, M., Moriya, T., Antoni, C., Apelbaum, A., Hagel, P., Sitsel, O., Raisch, T., Prumbaum, D., Quentin, D., Roderer, D., Tacke, S., Siebolds, B., Schubert, E., Shaikh, T.R., Lill, P., Gatsogiannis, C., Raunser, S., 2019. SPHIRE-crYOLO is a fast and accurate fully automated particle picker for cryo-EM. Commun Biol 2, 1–13. https://doi.org/10.1038/s42003-019-0437-z

Waite, A.J., Bäumer, D., East, S., Neal, J., Morris, H.R., Ansorge, O., Blake, D.J., 2014. Reduced C9orf72 protein levels in frontal cortex of amyotrophic lateral sclerosis and frontotemporal degeneration brain with the C9ORF72 hexanucleotide repeat expansion. Neurobiology of Aging 35, 1779.e5-1779.e13. https://doi.org/10.1016/j.neurobiolaging.2014.01.016

Wang, C., Yeo, S., Haas, M.A., Guan, J.-L., 2017. Autophagy gene FIP200 in neural progenitors non–cell autonomously controls differentiation by regulating microglia. Journal of Cell Biology 216, 2581–2596. https://doi.org/10.1083/jcb.201609093

Wang, M., Wang, H., Tao, Z., Xia, Q., Hao, Z., Prehn, J.H.M., Zhen, X., Wang, G., Ying, Z., 2020. C9orf72 associates with inactive Rag GTPases and regulates mTORC1-mediated autophagosomal and lysosomal biogenesis. Aging Cell 19, e13126. https://doi.org/10.1111/acel.13126

Wang, Q., Lu, M., Zhu, X., Gu, X., Zhang, T., Xia, C., Yang, L., Xu, Y., Zhou, M., 2022. The role of microglia immunometabolism in neurodegeneration: Focus on molecular determinants and metabolic intermediates of metabolic reprogramming. Biomedicine & Pharmacotherapy 153, 113412. https://doi.org/10.1016/j.biopha.2022.113412

Wang, R., Yu, Z., Sunchu, B., Shoaf, J., Dang, I., Zhao, S., Caples, K., Bradley, L., Beaver, L.M., Ho, E., Löhr, C.V., Perez, V.I., 2017. Rapamycin inhibits the secretory phenotype of senescent cells by a Nrf2-independent mechanism. Aging Cell 16, 564–574. https://doi.org/10.1111/acel.12587

Wang, S.-J., Wang, K.-Y., Wang, W.-C., 2004. Mechanisms underlying the riluzole inhibition of glutamate release from rat cerebral cortex nerve terminals (synaptosomes). Neuroscience 125, 191–201. https://doi.org/10.1016/j.neuroscience.2004.01.019

Wang, T., Liu, H., Itoh, K., Oh, S., Zhao, L., Murata, D., Sesaki, H., Hartung, T., Na, C.H., Wang, J., 2021. C9orf72 regulates energy homeostasis by stabilizing mitochondrial complex I assembly. Cell Metab 33, 531-546.e9. https://doi.org/10.1016/j.cmet.2021.01.005

Wang, W., Wang, L., Lu, J., Siedlak, S.L., Fujioka, H., Liang, J., Jiang, S., Ma, X., Jiang, Z., da Rocha, E.L., Sheng, M., Choi, H., Lerou, P.H., Li, H., Wang, X., 2016. The inhibition of TDP-43 mitochondrial localization blocks its neuronal toxicity. Nat Med 22, 869–878. https://doi.org/10.1038/nm.4130

Wang, Y., Branicky, R., Noë, A., Hekimi, S., 2018. Superoxide dismutases: Dual roles in controlling ROS damage and regulating ROS signaling. J Cell Biol 217, 1915–1928. https://doi.org/10.1083/jcb.201708007

Wang, Y., Li, L., Hou, C., Lai, Y., Long, J., Liu, J., Zhong, Q., Diao, J., 2016. SNARE-mediated membrane fusion in autophagy. Semin Cell Dev Biol 60, 97–104. https://doi.org/10.1016/j.semcdb.2016.07.009

Warita, H., Itoyama, Y., Abe, K., 1999. Selective impairment of fast anterograde axonal transport in the peripheral nerves of asymptomatic transgenic mice with a G93A

mutant SOD1 gene. Brain Research 819, 120–131. https://doi.org/10.1016/S0006-8993(98)01351-1

Watanabe, K., Tanaka, M., Yuki, S., Hirai, M., Yamamoto, Y., 2018. How is edaravone effective against acute ischemic stroke and amyotrophic lateral sclerosis? J Clin Biochem Nutr 62, 20–38. https://doi.org/10.3164/jcbn.17-62

Watanabe, M., Dykes-Hoberg, M., Culotta, V.C., Price, D.L., Wong, P.C., Rothstein, J.D., 2001. Histological evidence of protein aggregation in mutant SOD1 transgenic mice and in amyotrophic lateral sclerosis neural tissues. Neurobiol Dis 8, 933–941. https://doi.org/10.1006/nbdi.2001.0443

Webster, C.P., Smith, E.F., Bauer, C.S., Moller, A., Hautbergue, G.M., Ferraiuolo, L., Myszczynska, M.A., Higginbottom, A., Walsh, M.J., Whitworth, A.J., Kaspar, B.K., Meyer, K., Shaw, P.J., Grierson, A.J., De Vos, K.J., 2016. The C9orf72 protein interacts with Rab1a and the ULK1 complex to regulate initiation of autophagy. EMBO J 35, 1656–1676. https://doi.org/10.15252/embj.201694401

Wei, H., Gan, B., Wu, X., Guan, J.-L., 2009. Inactivation of FIP200 Leads to Inflammatory Skin Disorder, but Not Tumorigenesis, in Conditional Knock-out Mouse Models *. Journal of Biological Chemistry 284, 6004–6013. https://doi.org/10.1074/jbc.M806375200

Wen, X., Tan, W., Westergard, T., Krishnamurthy, K., ShamamandriMarkandaiah, S., Shi, Y., Lin, S., Shneider, N.A., Monaghan, J., Pandey, U.B., Pasinelli, P., Ichida, J.K., Trotti, D., 2014. Antisense Proline-Arginine RAN dipeptides linked to C9ORF72-ALS/FTD form toxic nuclear aggregates that initiate in vitro and in vivo neuronal death. Neuron 84, 1213–1225. https://doi.org/10.1016/j.neuron.2014.12.010

Westergard, T., Jensen, B.K., Wen, X., Cai, J., Kropf, E., Iacovitti, L., Pasinelli, P., Trotti, D., 2016. Cell-to-Cell Transmission of Dipeptide Repeat Proteins Linked to C9orf72-ALS/FTD. Cell Reports 17, 645–652. https://doi.org/10.1016/j.celrep.2016.09.032

Westergard, T., McAvoy, K., Russell, K., Wen, X., Pang, Y., Morris, B., Pasinelli, P., Trotti, D., Haeusler, A., 2019. Repeat-associated non-AUG translation in C9orf72-ALS/FTD is driven by neuronal excitation and stress. EMBO Mol Med 11, e9423. https://doi.org/10.15252/emmm.201809423

Witzel, S., Maier, A., Steinbach, R., Grosskreutz, J., Koch, J.C., Sarikidi, A., Petri, S., Günther, R., Wolf, J., Hermann, A., Prudlo, J., Cordts, I., Lingor, P., Löscher, W.N., Kohl, Z., Hagenacker, T., Ruckes, C., Koch, B., Spittel, S., Günther, K., Michels, S., Dorst, J., Meyer, T., Ludolph, A.C., 2022. Safety and Effectiveness of Long-term Intravenous Administration of Edaravone for Treatment of Patients With Amyotrophic Lateral Sclerosis. JAMA Neurol 79, 1–11. https://doi.org/10.1001/jamaneurol.2021.4893

Wong, Y.C., Holzbaur, E.L.F., 2014. Optineurin is an autophagy receptor for damaged mitochondria in parkin-mediated mitophagy that is disrupted by an ALS-linked mutation. Proc Natl Acad Sci U S A 111, E4439-4448. https://doi.org/10.1073/pnas.1405752111

Writing Group, Edaravone (MCI-186) ALS 19 Study Group, 2017. Safety and efficacy of edaravone in well defined patients with amyotrophic lateral sclerosis: a randomised, double-blind, placebo-controlled trial. Lancet Neurol 16, 505–512. https://doi.org/10.1016/S1474-4422(17)30115-1

Wu, C.-H., Fallini, C., Ticozzi, N., Keagle, P.J., Sapp, P.C., Piotrowska, K., Lowe, P., Koppers, M., McKenna-Yasek, D., Baron, D.M., Kost, J.E., Gonzalez-Perez, P., Fox, A.D., Adams, J., Taroni, F., Tiloca, C., Leclerc, A.L., Chafe, S.C., Mangroo, D., Moore, M.J., Zitzewitz, J.A.,

Xu, Z.-S., van den Berg, L.H., Glass, J.D., Siciliano, G., Cirulli, E.T., Goldstein, D.B., Salachas, F., Meininger, V., Rossoll, W., Ratti, A., Gellera, C., Bosco, D.A., Bassell, G.J., Silani, V., Drory, V.E., Brown Jr, R.H., Landers, J.E., 2012. Mutations in the profilin 1 gene cause familial amyotrophic lateral sclerosis. Nature 488, 499–503. https://doi.org/10.1038/nature11280

Xi, Z., Zhang, M., Bruni, A.C., Maletta, R.G., Colao, R., Fratta, P., Polke, J.M., Sweeney, M.G., Mudanohwo, E., Nacmias, B., Sorbi, S., Tartaglia, M.C., Rainero, I., Rubino, E., Pinessi, L., Galimberti, D., Surace, E.I., McGoldrick, P., McKeever, P., Moreno, D., Sato, C., Liang, Y., Keith, J., Zinman, L., Robertson, J., Rogaeva, E., 2015. The C9orf72 repeat expansion itself is methylated in ALS and FTLD patients. Acta Neuropathol 129, 715–727. https://doi.org/10.1007/s00401-015-1401-8

Xi, Z., Zinman, L., Moreno, D., Schymick, J., Liang, Y., Sato, C., Zheng, Y., Ghani, M., Dib, S., Keith, J., Robertson, J., Rogaeva, E., 2013. Hypermethylation of the CpG Island Near the G4C2 Repeat in ALS with a C9orf72 Expansion. Am J Hum Genet 92, 981–989. https://doi.org/10.1016/j.ajhg.2013.04.017

Xiao, S., MacNair, L., McGoldrick, P., McKeever, P.M., McLean, J.R., Zhang, M., Keith, J., Zinman, L., Rogaeva, E., Robertson, J., 2015. Isoform-specific antibodies reveal distinct subcellular localizations of C9orf72 in amyotrophic lateral sclerosis. Ann Neurol 78, 568–583. https://doi.org/10.1002/ana.24469

Xu, Z., Poidevin, M., Li, X., Li, Y., Shu, L., Nelson, D.L., Li, H., Hales, C.M., Gearing, M., Wingo, T.S., Jin, P., 2013. Expanded GGGGCC repeat RNA associated with amyotrophic lateral sclerosis and frontotemporal dementia causes neurodegeneration. Proc Natl Acad Sci U S A 110, 7778–7783. https://doi.org/10.1073/pnas.1219643110

Yamakawa, M., Ito, D., Honda, T., Kubo, K., Noda, M., Nakajima, K., Suzuki, N., 2015. Characterization of the dipeptide repeat protein in the molecular pathogenesis of c9FTD/ALS. Hum Mol Genet 24, 1630–1645. https://doi.org/10.1093/hmg/ddu576

Yamamoto, T., Yuki, S., Watanabe, T., Mitsuka, M., Saito, K.I., Kogure, K., 1997. Delayed neuronal death prevented by inhibition of increased hydroxyl radical formation in a transient cerebral ischemia. Brain Res 762, 240–242. https://doi.org/10.1016/s0006-8993(97)00490-3

Yang, M., Liang, C., Swaminathan, K., Herrlinger, S., Lai, F., Shiekhattar, R., Chen, J.-F., 2016. A C9ORF72/SMCR8-containing complex regulates ULK1 and plays a dual role in autophagy. Sci Adv 2, e1601167. https://doi.org/10.1126/sciadv.1601167

Yeliseev, A., Zoubak, L., Gawrisch, K., 2007. Use of Dual Affinity Tags for Expression and Purification of Functional Peripheral Cannabinoid Receptor. Protein Expr Purif 53, 153–163. https://doi.org/10.1016/j.pep.2006.12.003

Yoshida, Y., Yasuda, S., Fujita, T., Hamasaki, M., Murakami, A., Kawawaki, J., Iwai, K., Saeki, Y., Yoshimori, T., Matsuda, N., Tanaka, K., 2017. Ubiquitination of exposed glycoproteins by SCFFBXO27 directs damaged lysosomes for autophagy. Proceedings of the National Academy of Sciences 114, 8574–8579. https://doi.org/10.1073/pnas.1702615114

Yu, L., McPhee, C.K., Zheng, L., Mardones, G.A., Rong, Y., Peng, J., Mi, N., Zhao, Y., Liu, Z., Wan, F., Hailey, D.W., Oorschot, V., Klumperman, J., Baehrecke, E.H., Lenardo, M.J., 2010. Termination of autophagy and reformation of lysosomes regulated by mTOR. Nature 465, 942–946. https://doi.org/10.1038/nature09076

Zamiri, B., Reddy, K., Macgregor, R.B., Pearson, C.E., 2014. TMPyP4 Porphyrin Distorts RNA G-quadruplex Structures of the Disease-associated r(GGGGCC)n Repeat of the C9orf72

Gene and Blocks Interaction of RNA-binding Proteins *. Journal of Biological Chemistry 289, 4653–4659. https://doi.org/10.1074/jbc.C113.502336

Zancanella, V., van Rooijen, K., van Vliet, R., Pereira, I., de Ruiter, A., Shtefaniuk, V., Kieper, S., Wartel, M., Dobrynin, G., Kovačević, J., Seron, M.V., Liu, Y., n.d. AAV-miQURE®-mediated targeting of hexanucleotide repeat expansion-containing transcripts in ALS C9orf72 mouse models.

Zhang, D., Iyer, L.M., He, F., Aravind, L., 2012. Discovery of Novel DENN Proteins: Implications for the Evolution of Eukaryotic Intracellular Membrane Structures and Human Disease. Front Genet 3, 283. https://doi.org/10.3389/fgene.2012.00283

Zhang, K., 2016. Gctf: Real-time CTF determination and correction. J Struct Biol 193, 1–12. https://doi.org/10.1016/j.jsb.2015.11.003

Zhang, K., Donnelly, C.J., Haeusler, A.R., Grima, J.C., Machamer, J.B., Steinwald, P., Daley, E.L., Miller, S.J., Cunningham, K.M., Vidensky, S., Gupta, S., Thomas, M.A., Hong, I., Chiu, S.-L., Huganir, R.L., Ostrow, L.W., Matunis, M.J., Wang, J., Sattler, R., Lloyd, T.E., Rothstein, J.D., 2015. The C9orf72 repeat expansion disrupts nucleocytoplasmic transport. Nature 525, 56–61. https://doi.org/10.1038/nature14973

Zhang, Yingying, Burberry, A., Wang, J.-Y., Sandoe, J., Ghosh, S., Udeshi, N.D., Svinkina, T., Mordes, D.A., Mok, J., Charlton, M., Li, Q.-Z., Carr, S.A., Eggan, K., 2018. The C9orf72-interacting protein Smcr8 is a negative regulator of autoimmunity and lysosomal exocytosis. Genes Dev 32, 929–943. https://doi.org/10.1101/gad.313932.118

Zhang, Yuan, Roland, C., Sagui, C., 2018. Structural and Dynamical Characterization of DNA and RNA Quadruplexes Obtained from the GGGGCC and GGGCCT Hexanucleotide Repeats Associated with C9FTD/ALS and SCA36 Diseases. ACS Chem Neurosci 9, 1104–1117. https://doi.org/10.1021/acschemneuro.7b00476

Zhang, Y.-J., Gendron, T.F., Grima, J.C., Sasaguri, H., Jansen-West, K., Xu, Y.-F., Katzman, R.B., Gass, J., Murray, M.E., Shinohara, M., Lin, W.-L., Garrett, A., Stankowski, J.N., Daughrity, L., Tong, J., Perkerson, E.A., Yue, M., Chew, J., Castanedes-Casey, M., Kurti, A., Wang, Z.S., Liesinger, A.M., Baker, J.D., Jiang, J., Lagier-Tourenne, C., Edbauer, D., Cleveland, D.W., Rademakers, R., Boylan, K.B., Bu, G., Link, C.D., Dickey, C.A., Rothstein, J.D., Dickson, D.W., Fryer, J.D., Petrucelli, L., 2016. C9ORF72 poly(GA) aggregates sequester and impair HR23 and nucleocytoplasmic transport proteins. Nat Neurosci 19, 668–677. https://doi.org/10.1038/nn.4272

Zhang, Y.-J., Jansen-West, K., Xu, Y.-F., Gendron, T.F., Bieniek, K.F., Lin, W.-L., Sasaguri, H., Caulfield, T., Hubbard, J., Daughrity, L., Chew, J., Belzil, V.V., Prudencio, M., Stankowski, J.N., Castanedes-Casey, M., Whitelaw, E., Ash, P.E.A., DeTure, M., Rademakers, R., Boylan, K.B., Dickson, D.W., Petrucelli, L., 2014. Aggregation-prone c9FTD/ALS poly(GA) RAN-translated proteins cause neurotoxicity by inducing ER stress. Acta Neuropathol 128, 505–524. https://doi.org/10.1007/s00401-014-1336-5

Zhao, X., Li, G., Liang, S., 2013. Several Affinity Tags Commonly Used in Chromatographic Purification. J Anal Methods Chem 2013, 581093. https://doi.org/10.1155/2013/581093

Zheng, S.Q., Palovcak, E., Armache, J.-P., Verba, K.A., Cheng, Y., Agard, D.A., 2017. MotionCor2: anisotropic correction of beam-induced motion for improved cryo-electron microscopy. Nat Methods 14, 331–332. https://doi.org/10.1038/nmeth.4193

Zhou, B., Geng, Y., Liu, C., Miao, H., Ren, Y., Xu, N., Shi, X., You, Y., Lee, T., Zhu, G., 2018. Characterizations of distinct parallel and antiparallel G-quadruplexes formed by two-

repeat ALS and FTD related GGGGCC sequence. Sci Rep 8, 2366. https://doi.org/10.1038/s41598-018-20852-w

Zhou, Q., Lehmer, C., Michaelsen, M., Mori, K., Alterauge, D., Baumjohann, D., Schludi, M.H., Greiling, J., Farny, D., Flatley, A., Feederle, R., May, S., Schreiber, F., Arzberger, T., Kuhm, C., Klopstock, T., Hermann, A., Haass, C., Edbauer, D., 2017. Antibodies inhibit transmission and aggregation of C9orf72 poly-GA dipeptide repeat proteins. EMBO Molecular Medicine 9, 687–702. https://doi.org/10.15252/emmm.201607054

Zhou, W., Ma, Dongrui, Sun, A.X., Tran, H.-D., Ma, Dong-liang, Singh, B.K., Zhou, J., Zhang, J., Wang, D., Zhao, Y., Yen, P.M., Goh, E., Tan, E.-K., 2019. PD-linked CHCHD2 mutations impair CHCHD10 and MICOS complex leading to mitochondria dysfunction. Human Molecular Genetics 28, 1100–1116. https://doi.org/10.1093/hmg/ddy413

Zivanov, J., Nakane, T., Forsberg, B.O., Kimanius, D., Hagen, W.J., Lindahl, E., Scheres, S.H., 2018. New tools for automated high-resolution cryo-EM structure determination in RELION-3. Elife 7, e42166. https://doi.org/10.7554/eLife.42166

Zu, T., Cleary, J.D., Liu, Y., Bañez-Coronel, M., Bubenik, J.L., Ayhan, F., Ashizawa, T., Xia, G., Clark, H.B., Yachnis, A.T., Swanson, M.S., Ranum, L.P.W., 2017. RAN Translation Regulated by Muscleblind Proteins in Myotonic Dystrophy Type 2. Neuron 95, 1292-1305.e5. https://doi.org/10.1016/j.neuron.2017.08.039

Zu, T., Liu, Y., Bañez-Coronel, M., Reid, T., Pletnikova, O., Lewis, J., Miller, T.M., Harms, M.B., Falchook, A.E., Subramony, S.H., Ostrow, L.W., Rothstein, J.D., Troncoso, J.C., Ranum, L.P.W., 2013. RAN proteins and RNA foci from antisense transcripts in C9ORF72 ALS and frontotemporal dementia. Proc Natl Acad Sci U S A 110, E4968–E4977. https://doi.org/10.1073/pnas.1315438110

Université de Strasbourg

**David PIETRI**

École Doctorale des Sciences de la Vie et de la Santé STRASBOURG

# Structure and function of the C9ORF72-SMCR8-WDR41 complex and its implication for Amyotrophic Lateral Sclerosis (ALS)

**Abstract**

Amyotrophic lateral sclerosis (ALS or Charcot disease) is the third most common neurodegenerative disease. The main genetic cause of ALS is an expansion of GGGGCC repeats in the *C9ORF72* gene which protein forms a complex with the SMCR8 and WDR41 proteins. To better understand its molecular functions, solving its structure was a main goal of my thesis. In parallel, we discovered that C9ORF72 regulates a newly described mechanism of biogenesis of newly-formed lysosomes, called autophagic lysosome reformation (ALR). This process has been extensively investigated during my thesis, in order to better understand its regulation, particularly for the regeneration of lysosomes in basal conditions and amino acid deprivation. My work reveals a new partner of the C9ORF72 complex as a novel function in lysosome biogenesis. These results could thus explain the dysfunction of lysosomes and neurodegeneration observed in ALS, which open new therapeutic ways for this devastating disease.

**Résumé**

La sclérose latérale amyotrophique (SLA ou maladie de Charcot) est la troisième maladie neurodégénérative la plus répandue. La principale cause génétique de la SLA est une expansion de répétitions GGGGCC dans le gène *C9ORF72*, dont la protéine forme un complexe avec les protéines SMCR8 et WDR41. Afin de mieux comprendre ses fonctions moléculaires, résoudre sa structure était un objectif principal de ma thèse. En parallèle, nous avons découvert que C9ORF72 régule un mécanisme nouvellement décrit de biogenèse de nouveaux lysosomes nommé reformation autophagique des lysosomes (ALR). Ce processus a largement été investigué dans cette thèse afin de mieux comprendre sa régulation, notamment pour la régénération des lysosomes en conditions basales et de privation d'acides aminés. Mon travail révèle un nouveau partenaire du complexe C9ORF72 et une nouvelle fonction de ce complexe dans la biogenèse des lysosomes. Ces résultats pourraient ainsi expliquer le dysfonctionnement des lysosomes et la neurodégénérescence observés dans la SLA, ce qui pourrait ainsi ouvrir de nouvelles voies thérapeutiques pour cette maladie dévastatrice.